# การประเมินเชิงทฤษฎีระบบร่วมเซลล์เชื้อเพลิงชนิดออกไซด์แข็งและเครื่องกังหันก๊าซที่ป้อนด้วยเอทานอล

นางสาวแดง แซ่เบ๊

วิทยานิพนธ์นี้เป็นส่วนหนึ่งของการศึกษาตามหลักสูตรปริญญาวิศวกรรมศาสตรดุษฎีบัณฑิต
สาขาวิชาวิศวกรรมเคมี ภาควิชาวิศวกรรมเคมี
คณะวิศวกรรมศาสตร์ จุฬาลงกรณ์มหาวิทยาลัย
ปีการศึกษา 2554

# THEORETICAL EVALUATION OF SOLID OXIDE FUEL CELL AND GAS TURBINE COMBINED SYSTEMS FED BY ETHANOL

Miss Dang Saebea

A Thesis Submitted in Partial Fulfillment of the Requirements
for the Degree of Doctor of Engineering Program in Chemical Engineering
Department of Chemical Engineering
Faculty of Engineering
Chulalongkorn University
Academic Year 2011

| | |
|---|---|
| Thesis Title | THEORETICAL EVALUATION OF SOLID OXIDE FUEL CELL AND GAS TURBINE COMBINED SYSTEMS FED BY ETHANOL |
| By | Miss Dang Saebea |
| Field of Study | Chemical Engineering |
| Thesis Advisor | Assistant Professor Amornchai Arpornwichanop, D.Eng. |

Accepted by the Faculty of Engineering, Chulalongkorn University in Partial Fulfillment of the Requirements for the Doctoral Degree

……Dean of the Faculty of Engineering
(Associate Professor Boonsom Lerdhirunwong, Dr.Ing.)

THESIS COMMITTEE

…….. Chairman
(Associate Professor Tharathon Mongkhonsi, Ph.D.)

……...Thesis Advisor
(Assistant Professor Amornchai Arpornwichanop, D.Eng.)

…….. Examiner
(Assistant Professor Soorathep Kheawhom, Ph.D.)

…….. Examiner
(Assistant Professor Apinan Soottitantawat, D.Eng.)

…….. External Examiner
(Assistant Professor Wanwilai Kraipech Evans, Ph.D.)

แดง แซ่เบ๊ : การประเมินเชิงทฤษฎีระบบร่วมเซลล์เชื้อเพลิงชนิดออกไซด์แข็งและเครื่องกังหันก๊าซที่ป้อนด้วยเอทานอล. (THEORETICAL EVALUATION OF SOLID OXIDE FUEL CELL AND GAS TURBINE COMBINED SYSTEMS FED BY ETHANOL) อ. ที่ปรึกษาวิทยานิพนธ์หลัก: ผศ.ดร. อมรชัย อาภรณ์วิชานพ, 211 หน้า.

งานวิจัยนี้นำเสนอการวิเคราะห์สมรรถนะของเซลล์เชื้อเพลิงชนิดออกไซด์แข็งที่ป้อนด้วยเชื้อเพลิงเอทานอล ในส่วนแรกของงานจะศึกษาถึงความเหมาะสมของการใช้เชื้อเพลิงเอทานอลสำหรับเซลล์เชื้อเพลิงชนิดออกไซด์แข็ง ซึ่งถูกเปรียบเทียบกับ เชื้อเพลิง ที่สามารถผลิตขึ้นใหม่ได้ (Renewable fuel) ได้แก่ไบโอ แก๊ส และกลีเซอรอล ผลที่ได้พบว่าการใช้เชื้อเพลิงเอทานอลจะทำให้ประสิทธิภาพทางไฟฟ้าและทางความร้อนของระบบมีค่ามากที่สุด นอกจากนี้ยังมีการปล่อยก๊าซคาร์บอนไดออกไซด์ออกจากระบบน้อยที่สุด เมื่อพิจารณาหลักทางเทอร์โมไดนามิกส์ของปฏิกิริยารีฟอร์มมิงด้วยไอน้ำของเอทานอลชี้ให้เห็นว่าปฏิกิริยานี้ต้องการดำเนินการที่สภาวะอุณหภูมิและอัตราส่วนของไอน้ำและเอทานอลที่สูงเพื่อได้ผลผลิตของไฮโดรเจนที่สูง การผลิตไฮโดรเจนของปฏิกิริยารีฟอร์มมิงด้วยไอน้ำของเอทานอลจะถูกพัฒนาด้วยการพิจารณาการทำงานร่วมกันของตัวดูดซับและเยื่อเลือกผ่าน ซึ่งพบว่าผลิตภัณฑ์ของไฮโดรเจนที่ได้เพิ่มสูงขึ้นที่อุณหภูมิในการดำเนินการต่ำลง และการใช้ตัวดูดซับก๊าซคาร์บอนไดออกไซด์ในการผลิตไฮโดรเจนยังช่วยให้แนวโน้มในการเกิดคาร์บอนลดลง สำหรับการพิจารณาการ ทำงานร่วมกัน ของเซลล์เชื้อเพลิงและกระบวนการรีฟอร์มมิงด้วยเอทานอล การรีไซเคิลก๊าซแอโนดไปยังรีฟอร์เมอร์สามารถลดพลังงานในส่วนของการให้ความร้อนแก่ไอน้ำและเพิ่มประสิทธิภาพทางไฟฟ้าของระบบได้ แต่อย่างไรก็ตาม เมื่อเซลล์มีอัตราการใช้เชื้อเพลิงภายในมาก การเพิ่มอัตราส่วนในการรีไซเคิลก๊าซแอโนดจะทำให้ประสิทธิภาพทางไฟฟ้าของเซลล์เชื้อเพลิงลดลง เพื่อเพิ่มกำลังไฟฟ้าของระบบในการผลิตกระแสไฟฟ้าของเซลล์เชื้อเพลิง ระบบของการทำงานร่วมกันระหว่างเซลล์เชื้อเพลิงชนิดออกไซด์แข็งและเครื่องกังหันก๊าซจึงถูกศึกษาในงานนี้ ผลในการศึกษาของงานนี้ชี้ให้เห็นว่าประสิทธิภาพทางไฟฟ้าของระบบจะมีค่าสูงขึ้นด้วยการเพิ่มความดันในช่วง 2-6 บาร์ แต่อย่างไรก็ตาม ความร้อนที่ออกจากเครื่องกังหันก๊าซไปใช้ในหน่วยต่างๆ ลดลง ดังนั้นในงานนี้จึงเสนอระบบการผลิตกระแสไฟฟ้าด้วยการทำงานร่วมกันของเซลล์เชื้อเพลิงชนิดออกไซด์แข็งและเครื่องกังหันก๊าซโดยรีไซเคิลก๊าซแคโทดบางส่วนกลับเข้าไปใช้ในเซลล์เพื่อต้องการพลังงานที่ใช้จากภายนอกลดลงสำหรับการให้ความร้อนแก่อากาศ ซึ่งเป็นหน่วยที่ต้องการพลังงานจากภายนอกมากที่สุด ผลที่ได้พบว่าระบบที่ทำงานร่วมกันของเซลล์เชื้อเพลิงและเครื่องกังหันก๊าซที่รีไซเคิลก๊าซแคโทดสามารถดำเนินการได้โดยไม่อาศัยความร้อนจากภายนอก สำหรับการศึกษาการจัดการความร้อนภายในระบบที่ทำงานร่วมกันของเซลล์เชื้อเพลิงและเครื่องกังหันก๊าซถูกศึกษาในส่วนสุดท้ายของงาน โดยพิจารณาสองโครงสร้าง ซึ่งระบบแรกใช้เครื่องแลกเปลี่ยนความร้อนที่อุณหภูมิสูง และระบบที่สองใช้การรีไซเคิลก๊าซแคโทดบางส่วนจากเซลล์เชื้อเพลิง ผลที่ได้ชี้ให้เห็นว่าระบบที่สองจะให้ประสิทธิภาพสูงสุด

ภาควิชา……วิศวกรรมเคมี…….. ลายมือชื่อนิสิต.....
สาขาวิชา……วิศวกรรมเคมี……. ลายมือชื่อ อ.ที่ปรึกษาวิทยานิพนธ์หลัก…….....
ปีการศึกษา …2554……

# # 5071810021 : MAJOR CHEMICAL ENGINEERING
KEYWORDS : SOLID OXIDE FUEL CELL / ETHANOL / GAS TURBINE / SIMULATION

DAND SAEBEA : THEORETICAL EVALUATION OF SOLID OXIDE FUEL CELL AND GAS TURBINE COMBINED SYSTEMS FED BY ETHANOL. ADVISOR: ASST. PROF. AMORNCHAI APPORNWICHANOP, 211 pp.

This research presents the performance analysis of a solid oxide fuel cell (SOFC) system fuelled by ethanol. The suitability of using ethanol for SOFC system is compared with other attractive renewable fuels, i.e., biogas and glycerol. The simulation results show that the SOFC system fuelled by ethanol provides the highest electrical and thermal efficiencies and less emission of carbon dioxide. The thermodynamic analysis of ethanol steam reforming indicates that high temperature and steam-to-carbon ratio are preferred operating conditions so as to obtain high hydrogen yield. The hydrogen production of ethanol steam reforming is improved when an adsorption-membrane hybrid system is considered. It is found that a higher hydrogen product can be obtained at a lower operating temperature and that the formation of carbon is likely to be reduced when a carbon dioxide adsorption is combined with the hydrogen production. Considering the integration of the ethanol steam reformer and SOFC, the recycle of anode exhaust gas to the reformer can reduce the energy required for preheating steam and enhance the electrical efficiency of the system. However, when SOFC is operated at high fuel utilization, an increase in the recirculation ratio of anode exhaust gas degrades the SOFC electrical efficiency. To improve the performance of SOFC system, a hybrid SOFC system with a gas turbine (GT) is also studied. The results show that the electrical efficiency of the SOFC-GT hybrid system raises with increasing the operating pressure (2-6 bar); however, the heat obtained from GT exhaust gas is reduced, thereby the SOFC-GT hybrid system cannot be operated at an energetically self-sustaining condition. Thus, the pressurized SOFC-GT hybrid system with a cathode exhaust gas recirculation is proposed with the aim to minimize the requirement of an external heat for air preheating, which is a major unit that requires the external heat. The results show that the SOFC-GT hybrid system with recycling cathode-exhaust gas can be run at the energetically self-sustaining condition. It is also found that a high cathode-exhaust gas recirculation ratio decreases SOFC electrical efficiency. Finally, a heat recovery of the SOFC-GT hybrid system is studied. Two designs of the SOFC system with uses of a high-temperature recuperative heat exchanger and a recirculation of cathode exhaust gas are compared. The results indicate that the SOFC system with cathode gas recirculation can achieve higher system efficiency and specific work.

Department : Chemical Engineering Student's Signature .....

Field of Study : Chemical Engineering Advisor's Signature .....

Academic Year : 2011

# ACKNOWLEDGEMENTS

I would first like to sincerely thank Assistant Professor Amornchai Arpornwichanop for his understanding, patience and guidance on attitude toward work-life balance during my Ph.D. study. His generous support and enthusiasm causes me to be successful. It has been a great experience for me to work with him.

I would also like to thank the member of my thesis committee, Associate Professor Tharathon Mongkhonsi, Assistant Professor Wanwilai Kraipech Evans, Assistant Professor Soorathep Kheawhom and Dr. Apinan Soottitantawat for their time and useful comments on this work.

I am very grateful to Professor Aristide F. Massardo and Assistant Professor Loredana Magistri who give a chance for me to join their group, for their support and advice during my visit to the Thermochemical Power Group (TPG), University of Genoa, Italy. Additionally, I would like to thank all the staff in the TPG for their helpful, suggestion, generosity and friendship to me.

I would like to thank the Office of the Higher Education Commission, Thailand for their grant support under the program “Strategic Scholarships for Frontier Research Network for the Joint Ph.D. Program Thai Doctoral Degree” for this research. Support from the Thailand Research Fund, the Graduate School of Chulalongkorn University (Conference Grant for Ph.D. Student) and the Computational Process Engineering Research Group, the Special Task Force for Activating Research (STAR), Chulalongkorn University Centenary Academic Development Project is also gratefully acknowledged.

I would also like to thank all the member of the Control and Systems Engineering Research Laboratory, Department of Chemical Engineering, Chulalongkorn University. In particular, I am very thankful to Dr. Yaneeporn Patcharavorachot, Suthida, Anon, Lida and Narissara for their moral support, advice and nice friendship. Finally, and most importantly, I would like to thank my grandmother, parents, sisters and brothers for their love and encouragement that push me to attempt doing this research even I face with problems. I cannot completely achieve a success without the support from my family.

# CONTENTS

PAGE

CHAPTER PAGE

CHAPTER PAGE

CHAPTER PAGE

CHAPTER PAGE

CHAPTER PAGE

CHAPTER PAGE

CHAPTER PAGE

# LIST OF TABLES

**PAGE**

**PAGE**

# LIST OF FIGURES

PAGE

PAGE

PAGE

PAGE

PAGE

PAGE

# NOMENCLATURES

| | |
|---|---|
| $a_c$ | Activity coefficient of carbon **[-]** |
| $A_c$ | Cell active area **[**$m^2$] |
| $C_i$ | Molar concentration of component *i* **[**mol $m^{-3}$] |
| $D_{eff,anode}$ | Effective gaseous diffusivity through the anode [$m^2$ $s^{-1}$] |
| $D_{eff,cathode}$ | Effective oxygen diffusivity through the cathode [$m^2$ $s^{-1}$] |
| $E^{OCV}$ | Open-circuit voltage [V] |
| $E^0$ | Open-circuit voltage at the standard pressure [V] |
| $E_{act}$ | Activation energy for reforming reaction **[**kJ $mol^{-1}$] |
| $E_{anode}$ | Activation energies of the anode [kJ $mol^{-1}$] |
| $E_{cathode}$ | Activation energies of the cathode [kJ $mol^{-1}$] |
| $F$ | Faraday constant [C $mol^{-1}$] |
| $\dot{h}$ | Enthalpy [kJ $mol^{-1}$] |
| $h_a$ | Air channel height [m] |
| $h_f$ | Fuel channel height [m] |
| $\Delta H^\circ$ | Standard enthalpy change of reaction [kJ $mol^{-1}$] |
| $H_i^{Vap}$ | Enthalpy of vaporization of component *i* [kJ $mol^{-1}$] |
| $j$ | Current density [A $m^{-2}$] |
| $j_{0,anode}$ | Exchange current density at the anode [A $m^{-2}$] |

# NOMENCLATURES

| | |
|---|---|
| $j_{0,cathode}$ | Exchange current density at the cathode [A $m^{-2}$] |
| $k_{act}$ | Pre-exponential constant for reforming reaction [mol $s^{-1}$ $m^{-2}bar^{-1}$] |
| $k_{anode}$ | Pre-exponential factor of the anode [A $m^{-2}$] |
| $k_{cathode}$ | Pre-exponential factor of the cathode [A $m^{-2}$] |
| $k_{WGSR}$ | Pre-exponential constant for reforming reaction [-] |
| $K_b$ | Equilibrium constant for Boudouard reaction [$bar^{-1}$] |
| $K_{eq}$ | Equilibrium constants |
| $L$ | Cell length [m] |
| $LHV_{C_2H_5OH}$ | Low heating value of ethanol [mol $s^{-1}$] |
| $n$ | Number of electrons transferred |
| $\dot{n}$ | Molar flow rate [mol $s^{-1}$] |
| $p_i$ | Partial pressures of the component i [bar] |
| $P_{sofc}$ | Electrical power output from SOFC [W] |
| $P_{gt}$ | Electrical power output from GT [W] |
| Q | Thermal energy [kJ $s^{-1}$] |
| $Q_{rec}$ | Amount of thermal energy from the SOFC system [kJ $s^{-1}$] |
| $Q_{use}$ | Total amount of thermal energy used in system [kJ $s^{-1}$] |
| $\Re$ | Gas constant [kJ $mol^{-1}$ $K^{-1}$] |

# NOMENCLATURES

| | |
|---|---|
| $R_j$ | Rate of reaction $\boldsymbol{j}$ [mol $m^{-2}s^{-1}$] |
| $R_{ohm}$ | Total internal resistance $[\Omega\ m^2]$ |
| $T$ | Temperature [K] |
| $T_C$ | Critical temperature [K] |
| $u_a$ | Fuel velocity at fuel channel [m $s^{-1}$] |
| $u_f$ | Fuel velocity at fuel channel [m $s^{-1}$] |
| $V$ | Operating cell voltage [V] |
| $W$ | Cell width [m] |
| $U_a$ | Air utilization factor [-] |
| $U_f$ | Fuel utilization factor [-] |
| $y_i$ | Mole fraction of component $i$ [-] |
| $\dot{z}$ | Amount of hydrogen consumed by the electrochemical reaction [mol $s^{-1}$] |

***Greek symbols***

| | |
|---|---|
| $\alpha$ | Transfer coefficient [-] |
| $\varepsilon_{REC}$ | Heat exchanger effectiveness [%] |
| $\phi_i$ | Fugacity coefficient of component $i$ [-] |
| $\eta_{act}$ | Activation overpotentials [V] |

# NOMENCLATURES

| | |
|---|---|
| $\eta_{cell}$ | Efficiency of solid oxide fuel cell [%] |
| $\eta_{conc}$ | Concentration overpotentials [V] |
| $\eta_{el,\ system}$ | Electrical efficiency [%] |
| $\eta_g$ | Generator efficiency [%] |
| $\eta_m$ | Mechanical efficiency [%] |
| $\eta_{ohmic}$ | Ohmic loss [V] |
| $\eta_p$ | Pump efficiency [%] |
| $\eta_{invert}$ | Dc-ac inverter efficiency [%] |
| $\eta_{system}$ | System efficiency [%] |
| $\lambda_{air}$ | Excess air ratio **[-]** |
| $\dot{\lambda}_i$ | Specific latent heat of component component $i$ [kJ $mol^{-1}$] |
| $v_i$ | Stoichiometric coefficient of component $i$ [-] |
| $\rho_i$ | Densityof component $i$ [kg $m^{-3}$] |
| $\sigma_{anode}$ | Electronic conductivity of the anode [$\Omega^{-1}m^{-1}$] |
| $\sigma_{cathode}$ | Electronic conductivity of cathode [$\Omega^{-1}m^{-1}$] |
| $\sigma_{electrolyte}$ | Ionic conductivity of the electrolyte [$\Omega^{-1}m^{-1}$] |
| $\tau_{anode}$ | Thickness of anode [m] |
| $\tau_{cathode}$ | Thickness of cathode [m] |
| $\tau_{electrolyte}$ | Thickness of electrolyte [m] |

# NOMENCLATURES

***Superscript***

| | |
|---|---|
| ◦ | standard condition |
| in | Feed inlet condition |
| out | Feed outlet condition |

***Subscripts***

| | |
|---|---|
| a | air channel |
| ab | afterburner |
| ac | alternating current |
| an | anode side |
| avg | average |
| c | compressor |
| ca | cathode side |
| conc | concentration overpotentials |
| cool | cooling stream |
| dc | direct current |
| elec | electrochemical reaction |
| f | fuel channel |
| gt | gas turbine |

# NOMENCLATURES

| | |
|---|---|
| hot | hot stream |
| *i* | chemical component |
| is | isentropic |
| *j* | reaction |
| mix | mixer |
| ohm | ohmic loss |
| ph | preheater |
| pum | pump |
| r | reformer |
| sofc | solid oxide fuel cell |
| SR | steam reforming reaction |
| t | turbine |
| TPB | three-phase boundary |
| vap | vaporizer |
| WGS | water gas shift reaction |

# CHAPTER I

# INTRODUCTION

## 1.1 Introduction

Nowadays the consumption of electrical energy deriving from combustion of fossil fuel has been increased. It is known that the burning of fossil fuel produces air pollutants (especially greenhouse gases such as $CO_2$), resulting in global warming and climate change. Therefore, it should find other power generation technologies that are environmental friendly and high efficient instead of the conventional combustion system. Fuel cells have been identified as an alternative method to generate power with high efficiency and environmental friendliness when compared to a conventional combustion-based process. Among the various types of fuel cells, the solid oxide fuel cell (SOFC) is the most promising fuel cell technology, as it can be used in a wide range of commercial applications. The high operational temperature of the SOFC (1073–1273 K) results in many advantages; for example, the high-temperature waste heat from a SOFC can be recovered for use in other heat-demanding units in the SOFC system. In addition, different fuels (e.g., methane, methanol, biogas, etc.) can be directly fed to the SOFC due to the possibility for operation with internal reforming (Patcharavorachot et al., 2008).

SOFCs can produce electricity from chemical conversion of a hydrogen and oxygen via an electrochemical reaction. Natural gas is mostly used as a fuel in hydrogen production for SOFC systems. Since it is a limited energy resource, renewable fuels have been received much attention in hydrogen production (Hatza et al., 2008; Levin and Chahine, 2010; Brouwer, 2010). Moreover, SOFC applications for remote areas, island and auxiliary power unit (APUs) require fuels that is convenient for transportation (Santin et al., 2009). In comparison with other feedstock, ethanol is considered an attractive liquid fuel as it can be produced

renewably via a biomass fermentation process and has relatively high hydrogen content. Moreover, it is easy to store, handle and transport in a safe way due to its lower toxicity and volatility. Douvartzides et al. (2003) presented thermodynamic and economic analyses of the use of various fuels, namely, methane, methanol, ethanol and gasoline for electricity generation from SOFCs. The results showed that the use of ethanol to produce hydrogen for SOFCs is a very promising option. Additionally, glycerol and biogas are also promising renewable fuels. Glycerol is by-product from biodiesel production processor while biogas is produced from an anaerobic digestion process of municipal solid waste. Both fuels are likely to increase and be available in future. The suitability of ethanol as fuel for SOFC system should be considered by comparing with other attractive renewable fuels, i.e., glycerol and biogas.

When ethanol is considered the primary fuel for fuel cells, it is possible to be internally reformed into a hydrogen-rich gas (synthesis gas) within a fuel cell stack (referred to as an internal reforming SOFC, or IR-SOFC) because the operating temperature of the SOFC is in the same range as that of the reforming reactions. IR-SOFC presently attracts research interests because it offers the simplest and most cost-effective design for an SOFC system. During IR-SOFC operation, heat released from an exothermic electrochemical oxidation is employed for the reforming of fuel to generate hydrogen (Kendall and Singhal, 2003). However, it was reported that the direct feed of ethanol to the SOFC stack is not appropriate due to the easy degradation of the Ni/YSZ catalyst at the anode by carbon formation, which leads to the loss of fuel cell performance and poor durability (Laosiripojana and Assabumrungrat, 2007). Another major problem with IR-SOFC is an increased temperature gradient along the length of the anode due to the strongly endothermic cooling effect of the steam reforming reaction at the cell inlet. This can result in the cracking of the anode and electrolyte materials. In order to avoid these problems, the implementation of an external reforming system is a potentially better option because the higher content of hydrogen that is obtained from the conversion of ethanol via a steam reforming process can be introduced to the SOFC stack (Cocco and Tola, 2008). Nevertheless, because the steam reforming reaction involves a highly endothermic reaction, the SOFC system with external reforming requires a high external heat source for fuel processor and efficient energy management.

Ethanol can be reformed to hydrogen by several methods, namely, steam reforming, partial oxidation, autothermal reforming, and dry reforming. Each reforming process has its own advantages, depending on its applications. Considering the yield of hydrogen product ion, the steam reforming process provides higher hydrogen production yield than other reforming processes (Rabenstein and Hacker, 2008). Ethanol steam reforming has been widely investigated based on thermodynamic (Tsiakaras et al., 1998; Comas et al., 2004a) and experimental studies (Cavallaro et al., 2003; Comas et al., 2004b). Thermodynamic studies indicated that at atmospheric pressure, the steam reforming of ethanol can achieve high hydrogen production at temperatures higher than 1000 K because it is limited by the thermodynamic equilibrium of the reversible reforming reaction (Tsiakaras et al., 1999). As a result, the operation of ethanol steam reforming consumes high energy. To enhance SOFC performance, the problem on purifying hydrogen is another issue in hydrogen production for fuel cell. Consequently, a new concept for the production of hydrogen with lower operating and capital costs compared to a conventional reforming process is desired. The performance improvement of the steam methane reforming (SMR) by removing hydrogen and carbon dioxide by selective permeation through membrane or carbon dioxide acceptor added in system is of great interest (Barelli et al., 2009). It can improve the extent of reaction and produce a higher pure hydrogen at the same time. Previous studies showed that the operating temperature can be reduced when the methane steam reforming is carried out in a hydrogen-permeable membrane reactor or a carbon dioxide acceptor (Ding et al., 2000; Tong and Matsumura, 2006; Harrison, 2009). It is interesting to take both principles in producing hydrogen as fuel for SOFC from ethanol steam reforming to find out the suitable process and the possibility of combining the carbon dioxide removal and the hydrogen separation together.

In general, an ethanol steam reformer needs to be operated at a higher steam-to-ethanol ratio and an operating temperature over 550 K (Garcia et al., 1991; Rabensteinl and Hacker, 2008; Silva et al., 2009) to prevent carbon deposition. Therefore, high heat is required for preheating steam in a fuel processor. Generally, the exhaust gas from the anode channel is composed of more steam that is generated by the electrochemical reaction and the amount of steam in the exhaust gas depends

on a fuel utilization within fuel cell. It has been known that SOFCs operated at high fuel utilization can provide high electrical efficiency. However, at high fuel utilization, more hydrogen is consumed by the electrochemical reactions, and the fuel stream at the SOFC fuel channel is thus diluted by steam. A hydrogen deficiency due to the unbalanced fuel flowing through the SOFC causes a larger buildup of nickel oxide as well as corrosion on the carbon plate (Nehter, 2007; Nishikawa et al., 2008). Therefore, it is reasonable to operate the SOFC at moderate fuel utilization. Under this condition, the SOFC can produce electrical power together with a high-temperature exhaust gas that contains useful remaining fuel (i.e., hydrogen and carbon monoxide). Typically, the exhaust gases from fuel and air channels are burnt in an afterburner to produce more heat, which is used to preheat the fuel stream and supplied to the steam reformer. Although the combustion of exhaust gases can increase the thermal efficiency of the SOFC system, the fuel stream is utilized inefficiently. To improve the overall SOFC performance, a SOFC system with anode exhaust gas recycling has been proposed in the literatures (Granovskii et al., 2007; Shekhawat et al., 2007). Jia et al. (2011) proposed the internal reforming SOFC power system with anode gas recycle. With the proposed system, the remaining fuel from the exhaust gas can be reused and the steam produced by the electrochemical reaction can be further used as a reagent for steam reforming and thus the requirement for fresh steam can be reduced.

To further improve the electrical efficiency of SOFC systems, a high-quality exhaust gas of SOFC can be also utilized in other systems, i.e., gas turbine (GT) or steam turbine (ST). Steam turbine cannot be combined with a SOFC using the direct thermal coupling scheme. Due to the use of a gas-based working fluid, gas turbine is a favorable candidate for SOFC integration (Zhang et al., 2010). A SOFC-GT plant has been regarded as a promising power plant (Leucht et al, 2011). The SOFC-GT hybrid system can theoretically have the overall electrical efficiency of up to 70% (Kandepu et al., 2007), because it is high fuel-to-end efficiency. Although SOFC-GT hybrid system achieves higher electrical efficiency, the coupling of SOFC and gas turbine is rather complex due to different conditions of both the operation (Calise et al., 2006; Park et al., 2009; Motahar and Alemrajabi, 2009). Therefore, an appropriate operation and design configuration is required for the SOFC-GT hybrid system.

## 1.2 Research Objective

The aim of this study is concentrated on the performance analysis and design of a SOFC-GT hybrid system integrated with ethanol reforming process.

## 1.3 Scope of research

The integration of the SOFC and gas turbine fuelled ethanol is considered to improve the electrical and thermal efficiency of the power system. The scope of work is as follows:

1. To analyze a suitability of ethanol supplied for hydrogen production in SOFC system compared with other renewable, i.e., glycerol and biogas.

2. To improve the performance of an ethanol steam reforming process by coupling with a carbon dioxide adsorption and/or a hydrogen-selective membrane for hydrogen production.

3. To analyze a SOFC system with an ethanol reforming process with/without the recycle of anode-off gas.

4. To investigate the performance of a SOFC and gas turbine hybrid system and study the effect of recycling the cathode exhaust gas on a pressurized SOFC-GT hybrid system.

5. To design a heat recovery of the pressurized SOFC-GT hybrid system.

# CHAPTER II

# LITERATURE REVIEWS

This chapter presents overview of solid oxide fuel cells (SOFCs). The studies of SOFC design are presented in early part. Research studies of the model development are considered in Section 2.2. Then, hydrogen products derived from ethanol in various reactions and SOFC integrated with reforming process as well as fuel cell system analysis are discussed in Section 2.3. Additionally, the hydrogen production through sorption-enhanced steam reforming and membrane technology is presented in Section 2.4. Finally, a SOFC system integrated with other systems to develop thermal efficiency of system is discussed in Section 2.5 and 2.6.

## 2.1 SOFC design

In general, SOFC operated at high-temperature between 1073 and 1273 K cause to be difficult to find materials of SOFC fabrication since materials used in SOFC structure have to tolerate at high temperature. Nowadays, a number of research groups concentrate on finding materials to reduce SOFC operating temperature. Comparison of different materials for electrolyte is made from yttria-stabilized zirconia (YSZ) and gadolinia-doped ceria (CGO) for planar SOFC. The YSZ-electrolyte can be used to obtain a high power density than the CGO-electrolyte solid oxide fuel cells for the intermediate temperature (Pramuanjaroenkij et al., 2008). In addition, the problem of reduced temperature operation is an increase of internal resistance of cell. In particular, it is the ohmic loss because of reducing ionic conductivity of the electrolyte. Therefore, the electrolyte should reduce thin of electrolyte to reduce the ohmic loss. Some of researchers analyze the performance of a planar SOFC with different support structures, i.e., electrode (anode and cathode) and electrolyte-supported structures operated at an intermediate temperature. The simulation results found that an anode-supported SOFC is superior to an electrolyte- and cathode-supported SOFC (Patcharavorachot et al., 2008; Ni et al., 2009).

For the conventional electrolyte of SOFC, there are two types namely oxygen ion-conducting electrolyte (SOFC-$O^{2-}$) and proton conducting electrolyte (SOFC-$H^{+}$). The advantageous of use of proton conducting electrolyte is the possibility of complete fuel utilization when $H_2O$ is produced in the cathode. For an SOFC-$O^{2-}$, $H_2O$ produced in the anode channel dilutes the concentration of $H_2$ at the anode and raises the issue of gas separation. The various research investigated the comparison of SOFC performance with two types of solid electrolytes. Their results showed that SOFC-$H^{+}$ presents superior theoretical performance over the SOFC-$O^{2-}$ electrolyte; however, the actual performance of the SOFC-$O^{2-}$ becomes significantly better than that of SOFC-$H^{+}$ because SOFC-$H^{+}$ occurs highly total resistance (Jamsak et al., 2007; Ni et al., 2008).

## 2.2 SOFC modeling

The physical properties or reaction kinetic can be estimated by fitting performance data from small-size or laboratory-scale. Mathematical models are more important tools in understanding and examining effects of various designs and operating parameters on SOFC performance since the study of larger cell and SOFC system design are complexity and limitation for experiment. Therefore, mathematical tools are able to help in the study and development of SOFC to optimize designs and select optimal operating conditions. In general, SOFC model composes of mass and energy balances, and an electrochemical model.

### 2.2.1 Electrochemical model

The electrochemical model is significant model presenting the SOFC characteristics. The various overpotentials leading to voltage loss occur within cell, i.e., activation, ohmic and concentration overpotentials. The cathode activation and ohmic overpotentials represent the major losses within cell (Aguiar et al., 2004; Patcharavorachot et al., 2008).

The ohmic overpotentials can be described by Ohm's law, which is functional with the current density and cell resistances (Kendall and Singhal, 2003). The ohmic overpotentials depend on a cell material property. The major ohmic overpotentials in cell occur at the electrolyte. The commercials electrolyte for SOFC is YSZ

electrolyte. The resistivity of Ni-YSZ electrolyte and conductivity are determined to the empirical correlations, which is various forms (Bessette, 1994; Ferguson et al., 1996; Motloch, 1998). The comparison of various resistivity forms was studied by Hernandez-Pacheco et al. (2004). It was proved that the correlations at medium temperature ($\approx 873K$) are an almost perfect agreement and a small discrepancy at high temperature at higher than 1173 K. The most of equation used for calculating the ohmic overpotentials considers the anode/electrolyte/cathode resistance (Khaleel et al., 2004; Aloui et al., 2007; Mahcene et al., 2011) while some researchers specify a constant value (Qi et al., 2005; Hajimolana and Soroush, 2009).

The activation overpotentials are the results of the kinetics involved with the electrochemical reaction. These losses are significant at high current density and become lower at low current density (Aguiar et al., 2004). There are many types of model for expressing activation overpotentials namely the Bulter-Volmer equation, Tafel equation, and linear equation. Activation overpotentials are normally expressed from the Bulter-Volmer equation. However, the Bulter-Volmer equation is a rather complicated form so it can change to simplified forms which depend on the value of activation polarization in cell. The activation polarization can be expressed to Tafel expression at high activation overpotentials due to be much small in the second term of the Bulter-Volmer equation when it compared to the first term (Hajimolana et al., 2011) whereas it can be expressed as Taylor series to the linear current-potential relation at low activation polarization. Chan et al. (2001) compared the Tafel equation and the linear current-potential equation with the Burtler-Volmer equation at 1073 K. It was illustrated that the Tafel equation can be used as lower operating voltage of 0.28 and the linear relation can be used as higher operating voltage of 0.1 when it is allowed error of 5%. The most widely used semi-empirical correlations are Achenbach's, Hendriksen's and Karoliussen's correlations. The comparison of these correlations and the Butler-Volumer equation was investigated by Hernandez-Pacheco et al. (2004). Their results showed that the empirical expressions were reasonably accurate between 1173 and 1273 K. However, the operation of cell over this temperature range, the numerical values of these correlations are unrealistic results. Therefore, the Butler-Volmer equation was recommended for predicting the activation overpotentials because there is no reason to sacrifice accuracy for simplified relations.

For concentration overpotentials, it occurs from reduction of reactant gas concentrations or reduction of partial pressures of the reactant gas that are relative to mass transport through electrode. The flow of reactant gases through electrode is low velocity so the diffusion dominates on transport process. The number of researcher investigated the mass transport in porous electrode in various approaches. Three approaches are usually used for investigation of mass transport; that are the Fick's Low, Knudsen diffusion and Stefan-Maxwell model (Pramuanjaroenkij et al., 2008). Models for mass transport inside a porous SOFC developed based on these approaches to predict the concentration overpotentials were investigated by Suwanwarangkul et al. (2003). All models were validated with experimental data by considering three parameters i.e., current density, reactant concentration and pore size. Their results showed that otherwise, the Stefan–Maxwell model (SMM) is a satisfactorily appropriate model for the $H_2$–$H_2O$ system while Fick's model is suitable for the CO–$CO_2$ system. However, the most appropriate model for $H_2$- $H_2O$ and CO-$CO_2$ system is the dusty-gas model because this approach can calculate the complicated flux ratio and it takes into account Knudsen diffusion effect as well as Graham's law of diffusion.

### 2.2.2 Mass and energy model

The main model is divided to two classifications; that is micro- and macro modeling. Micro models are used to consider behaviors in cell component expanding the functional or electrochemical active layer of the electrode while macro models are used to consider the macroscopic or overall operational behaviors of SOFCs. In this study, macro models are applied for analysis. There are two approaches namely zero-dimensional and one-dimensional analysis.

#### 2.2.2.1. Zero-dimensional model

The zero-dimensional model is simplest one and the requirement of fast computation because it does not analysis the effect of variation dimension based on suitable assumptions and practical information. This model can reduce complex computation. In zero-dimensional model, fuel cell behavior the stirrer reactor that is counted as a single unit of system. Zero-dimensional models are often used to analyze

the whole system by concentrating in terms of power, heat and input requirements in order to analyze the performance which disregard the variation of the physical-chemical. There are two categories of zero-dimensional model that are the empirical model and box model (Wang et al., 2011). The empirical model is used in more complex systems. The performance of fuel cell derives the model simulation from experimentally data called that state-of-the-art. The box model is the thermodynamic model and it is usually employed for analysis of fuel cell system based energy systems, e.g. SOFC-CHP (combined heat and power system), SOFC-GT (combined SOFC and gas turbine system) (Bove and Ubertini, 2006).

Cali et al. (2006) and (2007) studied the SOFC CHP 100 kWe by using zero-dimensional model. The mathematical model has been calibrated with the results acquired during the first CHP100 demonstration at EDB/ELSAM in Westerwoort. The considered factors (fuel utilization, air utilization, air temperature at generator inlet) have main significant effect on the voltage. Analysis accounts for the effects of parameters on stack electric power, thermal recovered power, single cell voltage, cell operative temperature, consumed fuel flow and steam-to-carbon ratio. In study of the effect factors on SOFC performance, the optimal condition was found for the SOFC CHP 100 kWe. Each main effect and interaction effect of parameters is shown with particular attention on generated electric power and stack heat recovered.

The development of a thermodynamic model of SOFC-GT hybrid system with using zero-dimensional approach was considered by Akkaya et al. (2008). The steam reforming reaction in cell is assumed as chemical equilibrium. The SOFC-GT system model was validated with experimental results from Siemens Westinghouse (George, 2000; Song et al., 2005) and the presented model results is found to be in an acceptable range (maximum 3%). This simplified zero-dimensional approach was used in order to save computational time while maintaining an acceptable accuracy in the overall plant performances evaluation. These models are able to express the inlet and outlet condition of mass and energy and exergy in each component which takes it to analyze the performance of system. The other literatures study the performance of SOFC-GT hybrid system by using zero-dimensional model (Costamagna et al., 2001; Calise et al., 2006; Rokni, 2010).

### 2.2.2 One-dimensional model

In one-dimensional model, one geometric dimension is considered. The assumption of physical variation along the other two directions is negligible. For planar SOFC, the gas flow direction following along the gas channel is determined. Although the one dimensional model is simpler model than two and three dimensional models for consideration of phenomena in cell, the use of one-dimensional model must consider the type of flow. It is noted that cross flow planar SOFCs cannot be simulated by mean of one dimensional model.

The one-dimensional model of anode-supported intermediate temperature reforming planar solid oxide fuel cell stack was developed by Aguiar et al. (2004). The developed model consists of mass and energy balances, and an electrochemical model that relates the fuel and air gas composition and temperature to voltage, current density, and other relevant fuel cell variables. These models can express the impact of changes in fuel and air inlet temperatures, fuel utilization, average current density, and flow configuration on performance of the cell at the steady-state condition. It was found that SOFC operation under counter-flow of the fuel and air gas streams has been shown to lead to steep temperature gradients and uneven current density distributions.

Iora et al. (2005) presented the comparison of two intermediate temperature direct internal reforming (DIR) solid oxide fuel cell (SOFC) models: one where the flow properties (pressure, gas stream densities, heat capacities, thermal conductivities, and viscosity) and gas velocities are taken as constant throughout the system, based on inlet conditions, and one where this assumption is removed to focus on the effect of considering the variation of local flow properties on the prediction of the fuel cell performance. The results show that, although the error incurred in the prediction of the flow properties in the first model is significant, there is good agreement between both models in terms of the overall cell performance. However, the discrepancies between the two models increase, especially in the fuel channel, when higher current density values are assigned to the cell.

The methane ($CH_4$) directly internal reforming solid oxide fuel cells model considering methane steam reforming and water gas shift reaction was introduced by Ni et al. (2009). Parametric analyses showed that all the overpotentials decreased with

increasing temperature. This finding is different from previous analyses on $H_2$ fed SOFCs, in which the concentration overpotentials is found slightly increasing with increasing temperature. Furthermore, they investigated the electrode's microstructural effects on the performance of $CH_4$ fed SOFCs. It is found that the increase in electrode porosity or pore size decreases concentration overpotentials whereas it increases activation overpotentials of $CH_4$ fed SOFCs. At low current densities, low porosity and pore size are desirable to reduce the electrode total overpotentials as concentration overpotentials is insignificant compared with activation overpotentials. At high current densities, the total overpotentials can be minimized at optimal porosities and pore sizes.

Moussa et al. (2009) studied power density and hydrogen consumption in a co-flow planar solid oxide fuel cell according to the inlet functional parameters such as operational temperature, the operational pressure, the flow rates and the mass fractions of the species. They also investigated the effect of the cell size. The results of a zero and a one-dimensional numerical electro-dynamic model predict the remaining quantity of the fed hydrogen at the output of the anode flow channel as a function of the inlet functional parameters, the geometrical configuration of the cell and several operating cell voltages values.

For tubular SOFC, the kept dimension is usually the tube axis which coincides with the direction of the fuel and oxidant flow. A one dimensional model of a single tubular solid oxide fuel cell (SOFC) unit using the control volume (CV) approach was presented by Xue et al. (2005). The effects of heat transfer, species transportation, and electrochemical reaction are taken into account in a collective manner. The developed model is validated to experimental results such as the polarization curve and power density, which shows good agreement. This model is used to study the spatial distributions of a series of state variables under both steady-state and transient operations and evaluate the system dynamic behavior.

Jiang et al. (2006) presented an improved one-dimensional dynamic model of a tubular SOFC stack to consider the simulation of system with using the virtual test bed (VTB) simulation environment based on the electrochemical and thermal modeling, accounting for the voltage losses and temperature dynamics. This model is able to express the influence of operating parameters: pressure ratio, temperature,

mass flow rate, external reforming degree and stream to carbon (S/C) ratio as well as the cell geometric parameters: cell diameter and cell length on SOFC performance. Moreover, the one dimensional models of tubular SOFC were presented by Haynes et al. (2000), by Magistri et al. (2004) and by Li and Suzuki (2004).

Additionally, some researches focused on new methods to provide an easy solution for studying of SOFCs. The minimum Gibbs free energy (MGFE) method to be used instead of the complicated mathematical models of the SOFC's dynamic characteristics is presented by Xi et al. (2007). MGFE method is exploited to simplify the calculation of the mass balance dynamics of the fuel flow in the SOFC in an effort to develop a control oriented model achieves an appropriate trade-off between model accuracy and simplicity. This study concluded that the accuracy of the reduced-order model is acceptable at normal conditions for both steady-state and transient operation, but errors of model are only observed in steady-state responses at extreme conditions, where the inlet fuel has a high fraction of $CH_4$ and the fuel cell has low fuel utilization, and in transient when the inputs change at high frequency. Then, Wang et al. (2008) developed one-dimensional mathematical model for direct internal reforming solid oxide fuel cell (DIR-SOFC) by using volume–resistance (*V–R*) characteristic modeling technique in order to reduce complication of system with heat and mass transfer as well as electrochemical reactions. Based on the *V–R* modeling technique and the modular modeling idea, ordinary differential equations meeting the quick simulation are obtained from partial differential equations. The results indicate that the *V–R* characteristic modeling technique is valuable and viable in the SOFC system, and the model can be used in the quick dynamic and real-time simulation.

## 2.3. Ethanol fuel for SOFC

### 2.3.1 Hydrogen production from ethanol

Hydrogen is ultimate energy carrier in the electrochemical reactions of fuel cell. It achieves the highest of cell performance. However, it is improbable to be used in the near term, because of the difficulties in hydrogen store and the lack of a widespread distribution network. Therefore, numerous researches have studied using liquid hydrocarbon as fuel, such as methanol and ethanol (Cai et al., 2010). When comparing the two fuels, methanol has more the effect of health concerns than

ethanol because it is high volatility. Ethanol is considered to be promising candidate as a source for renewable hydrogen with several advantages, since it can be produced from the fermentation of biomaterial, such as biomass or renewable raw materials, including energy plants, organic fraction of municipal solid waste, waste materials from ago-industries or forestry residue materials, etc. (Ni et al., 2007). Moreover, ethanol used to produce hydrogen is not necessary to pure ethanol because water is also feed stock reacted with ethanol to product hydrogen fuel. Therefore, the using ethanol as raw material for product hydrogen should find the suitable separate process in order to high efficiency for system and cost-effective. At present, some research has concentrated on using crude ethanol for hydrogen product without separate water process (Akande et al., 2006). The components of crude ethanol can be shown in Table 2.1. The crude ethanol can produce hydrogen directly, since it is easy to product and free sulfur. Moreover, excess water in ethanol can favor further forward reaction and hydrogen product increase. However, hydrogen product from crude ethanol is diluted from excess water, so it should be separated water from hydrogen product by cooling.

**Table 2.1** Composition of crude ethanol (Akande et al., 2006)

| **Crude ethanol components** | **Volume %** | **Mole % on a water free basis** |
|---|---|---|
| Ethanol | 12.0 | 88.42 |
| Lactic acid | 1.0 | 5.71 |
| Glycerol | 1.0 | 5.87 |
| Maltose | 0.001 | 0.001 |
| Water | 86 | - |

Ethanol can be converted into hydrogen from different reforming technologies such as steam reforming, partial oxidation, autothermal reforming and

dry reforming. A number of publications have interested to be appropriate of each reforming technology to convert ethanol into hydrogen. Rabensteinl and Hacker (2008) investigated a thermodynamic analysis of the hydrogen production from ethanol by steam-reforming, partial-oxidation and combined auto-thermal reforming as a function of steam-to-ethanol ratio (0.00–10.00), oxygen-to-ethanol ratio (0.00–2.50) and temperatures (200–1000 °C) at atmospheric pressure. Partial-oxidation shows a low hydrogen yield and the avoidance of coke formation also demands the operation at high temperatures or high O/E ratios. Further, nitrogen dilution increases strongly with O/E ratios. Although auto-thermal reforming operation reduces the coke-formation and energy demand for the reforming process, steam-reforming achieves the highest hydrogen-yield and the energy used in the reforming process per hydrogen production is lowest. Their results concluded that the steam reforming is suitable process for hydrogen production with ethanol fuel.

The ethanol steam reforming has been widely studied both experimental and thermodynamic analysis. A thermodynamic analysis of hydrogen production from ethanol by the steam reforming at temperature more than 550 K and atmospheric pressure is carried out by Garcia et al. (1991). The result showed that a water to ethanol feed ratio > 2 is necessary in order to obtain hydrogen and prevent the carbon formation. Then, Vasudeva et al. (1996) studied steam reforming of ethanol for hydrogen production by using thermodynamic analysis method. The results of computation are compared with the previously published data of Garcia and Laborde. In addition, the computation is extended to high water-to-ethanol ratios to apply to dilute stream produced during the fermentation of molasses.

For studies of ethanol steam reforming with experimental analysis, Therdthianwong et al. (2001) studied the temperature effect on thermal cracking of ethanol. The results indicated that the conversion of ethanol achieve 97.7% when operate at temperature of 923 K. Liguras et al. (2003) investigated catalytic performance of the active metallic phase (Rh, Ru, Pt, Pd) and the nature of the support ($Al_2O_3$, MgO, $TiO_2$) for ethanol steam reforming in the temperature range of 873-1125 K. Their result showed that Rh is the most active and selective toward hydrogen formation. $Rh/Al_2O_3$ catalyst for ethanol steam reforming can complete conversion of ethanol at 1073 K. Additionally, the ethanol steam reforming over a commercial

alumina supported palladium catalyst for hydrogen production was investigated by Goula et al. (2003). The operating temperature close to 923 K can obtain hydrogen selectivities up to 95%.

Considering component of product, the main products are $H_2$, CO, $CH_4$ and $CO_2$ for most of catalysts. However, minor amounts by-products, such as $CH_3CHO$, $C_2H_4$, and $C_2H_6$ were also observed for using some catalyst (Biswas et al., 2007). Cavallaro et al. (2000) studied ethanol steam reforming on $Rh/Al_2O_3$ catalysts. The results showed that the increment of Rh content in catalyst is able to a progressive increase in $CH_4$, CO and $CO_2$ while ethylene, ethanol, and acetaldehyde disappear gradually from outlet gases stream. Further, coke formation of ethanol steam reforming is hindered with high operating temperature (973 K) and steam to carbon ratio (4.2:1). The carbon deposition of ethanol steam reforming over nickel supported on $\gamma$-$Al_2O_3$ was investigated by Fatsikostas et al. (2004). Their results indicated that the presence of lanthana on catalyst, the operation at high temperature, and high steam to ethanol ratio prevent on carbon deposition.

### 2.3.2 Reforming process for SOFC

SOFC is operated at high temperature so it can operate with the external reforming, direct internal reforming, and indirect internal reforming. The operating parameters of reforming process affect directly SOFC performance. Some of the researches have studied the effect of various operating parameters of the external or internal reforming of liquid fuel in SOFC.

Thermodynamic and economic analysis of various fuels for electricity generation of SOFC system was presented by Douvartzides et al. (2004). Their results showed that efficiency of ethanol as the second most valuable fuel option for SOFC after natural gas. The analysis reveals the cost relations between each fuel scenario and focuses upon the measures required so as the ethanol scenario to break through the threshold of economic viability.

Tsiakaras et al. (2001) studied a thermodynamic equilibrium product of ethanol a) steam reforming b) $CO_2$ reforming and c) partial oxidation before feeding into SOFC in order to produce electrical power. Thermodynamic point of view showed that theoretical maximum of the ethanol fueled SOFC efficiency is very high

in the temperature interval between 800-1200 K, and the most attractive system of ethanol preliminary transformation is steam reforming.

The possible ethanol with steam as a direct feed to Ni/YSZ anode of DIR-SOFC was investigated by Laosiripojana and Assabumrungrat (2007). They claimed that ethanol cannot be used as the direct fuel for DIR-SOFC operation (with Ni/YSZ anode) even at high steam content and high operating temperature due to the easy degradation of anode material. From the incomplete of ethanol steam reforming over Ni/YSZ produces ethane and ethylene. These formations are the major reason for the high rate of carbon formation as these components act as very strong promoters for carbon formation.

Douvartzides et al. (2003) carried out an energy-exergy analysis of a SOFC-based power plant fuel fed by ethanol in order to optimize the operational condition. A certain plant configuration was contemplated, equipped with an external steam reformer, an afterburner, a mixer and two heat exchangers (preheats).

Arteaga et al. (2008) studied a bioethanol processing system to feed a 200 kW solid oxide fuel cell. The performance pseudo-homogeneous model of the reactor, consisting of the catalytic ESR using a $Ni/Al_2O_3$ catalyst, has been developed based on the principles of classical kinetics and thermodynamics through a complex reaction scheme and a Lagmuir-Hishelwood kinetic pattern. The resulting model is employed to evaluate the effect of several designs and operation parameters on the process such as tube diameter, catalyst pellets diameter, temperature, space time and water/ethanol molar ratio.

### 2.4 Sorption-enhanced reforming and membrane technology

The steam reforming reaction of hydrocarbon fuels for hydrogen production are limited equilibrium, which cause that these processes are operated at the severe condition so as to achieve the high-yield production. Among the published work has been concentrated on this solution to improve performance of hydrogen production demonstrated theoretically and experimentally by removing hydrogen and carbon dioxide from the reaction in order that an equilibrium system drives forward reaction.

### 2.4.1 Membrane technology

For hydrogen removal, a palladium-based membrane reactor has been applied to diversely hydrogen-generating reactions. Hydrogen is removed by permeating membrane from steam reforming reaction zone. The conventional steam reforming of hydrocarbon fuels is operated at high temperature such as methane, biogas and ethanol. Chen et al. (2008) investigated the influences of reaction temperature on high performance Pd composite applied to construct a membrane reactor for methane steam reaction by using Ni-base catalyst. The results showed that the operating temperature for methane steam reforming in membrane reactor could be lowered than the conventional unit. Methane conversion is much higher than thermodynamic control and CO selectivity much lower than thermodynamic control values because the permeance of Pd membrane was high and kinetics of catalyst fast. The steam reforming in Pd alloy membrane reactor can not only reduce the operating temperature, but it is also such high endurance as 1600 h and 30 start-stops (Roy et al., 1998).

Some research focuses on study the steam reforming from ethanol fuel by using the membrane reactor. Papadias et al. (2010) studied high-pressure steam reforming of ethanol for the production of hydrogen needed to refuel the high-pressure tanks of fuel cell vehicles. These experiments are carried out in the membrane-micro-reactor by using the Pd-alloy membrane**.** These tests confirmed that hydrogen extraction increases the hydrogen yields. Analysis of the results indicates that the experimental membrane reactor was limited by the very low hydrogen flux through the membrane. However, the catalyst is sufficiently active and using a membrane with a higher hydrogen flux (and combination of reaction conditions of 650 $^{\circ}$C and S/C =3) can produce sufficient hydrogen to meet efficiency targets of 72%. The different catalyst between a Pt-base and Ni-base catalyst for carrying out the ethanol steam reforming by using Pd-Ag membrane reactor in the temperature range 400-450 °C was studied by Tosti et al. (2008). From their results, they found that the Ni-base catalyst is higher catalyst activity in terms of hydrogen yield than Pt-base catalyst at low $H_2O/C_2H_5OH$, while for higher $H_2O/C_2H_5OH$ feed flow ratios the sequence is Ni = Pt. However, the Ni-based catalyst is more interesting than Pt-based catalyst because the Ni-based catalyst is cheap. Moreover, the operating parameters of

the ethanol steam reforming in Pd-Ag reactor such as the pressure inside the membrane on hydrogen production the sweep gas mode (co-current and counter-current) and the spatial velocity is investigated with experiment (Tosti et al., 2010).

Some literatures investigated the ethanol steam reforming in Pd membrane reactor by model simulation in order to study the effect of various parameters on hydrogen yield and system performance. Gallucci et al. (2007) studied the ethanol steam-reforming reaction for the production of synthesis gas by using a membrane reactor in which the hydrogen production is increased by removing the hydrogen produced from the reaction mixture through a highly selective (100%) palladium-based membrane. Their simulation results showed that membrane reactor is possible to obtain both higher conversions of ethanol and higher hydrogen selectivities compared to those obtained in a traditional reactor when operating at the same experimental conditions. After that, Gallucci et al. (2008) simulated a dense Pd-based membrane reactor for carrying out the methane, the methanol and the ethanol steam reforming reactions for pure hydrogen production. This modeling work showed that the use of the membrane reactor in the ethanol steam reforming reaction gives an increase of the ethanol conversion (30%) and a relatively high increase of the hydrogen yield.

### 2.4.2 $CO_2$ absorption technology

In case of carbon dioxide removal, sorption enhanced reaction process by a mixture of steam reforming catalyst and carbon dioxide absorbent is generally used to scavenge carbon dioxide from reaction. Harrison (2009) studied the addition of a calcium-based sorbent to a standard methane reforming catalyst in order to alters the equilibrium and permits both the reforming and water-gas shift reactions to approach completion in a single step at a temperature approximately 200 K lower than currently used. This results showed that in the suitable conditions possible greater than 95% and the product may contain 98+% $H_2$ (dry basis) and only ppm levels of CO and $CO_2$. Additionally, Cormos et al. (2008) investigated the technical aspects of innovative hydrogen production concepts based on coal gasification with $CO_2$ capture in the gasifier instead of using nitrogen as a transport gas for the coal and a pressure

limitation of this type of design. This method can enhance hydrogen purity and pressure.

The most common sorbents of $CO_2$ from nature used are Calcium carbonate ($CaCO_3$), Dolomyte ($CaCO_3xMgCO_3$), Huntile and Hidrotalcite as well as synthesis ones namely Lithium orthosilicate ($Li_4SiO_4$) and Lithium zirconate ($LiZrO_3$). Johnsen et al. (2007) studied the performance of a dolomite and a limestone with a commercial reforming catalyst. The both of absorbents were compared based on the air jet attrition index (AJI). The dolomite showed the poorest resistance to attrition, likely due to the extra pore volume caused by calcination of $MgCO_3$. The degree of loss of fines from the catalyst was significant that point to the need to develop catalysts suited to fluidized bed operation. Co-fluidization of the harder catalyst and the dolomite did not lead to additional attrition of the dolomite. Martavaltzi et al. (2010) presented the development of a new hybrid material, $NiO–CaO–Ca_{12}Al_{14}O_{33}$, which functions simultaneously as reforming catalyst and $CO_2$ sorbent for application in enhanced steam reforming process in order to overcome the complex problem related with handing of two solid between catalyst and $CO_2$ sorbent. The production from use this hybrid material show $H_2$ (90%) and poor in $CO_2$ (2.8%) and CO (2%).

Moreover, some research studied adsorption-enhanced steam reforming of hydrocarbon fuels so as to produce hydrogen by model simulation. The adsorption-enhanced steam reforming of glycerol for hydrogen production on the hydrogen yield and carbon formation by thermodynamic analysis is investigated by Chen et al. (2009). Their analyses suggested that the temperature of steam glycerol reforming in presence of $CO_2$ adsorbent is lower than reforming without $CO_2$ adsorption about 100 K. In addition, steam glycerol reforming in presence of $CO_2$ adsorbent can reduce the lower limit of the water to glycerol feed ratio for carbon formation. The steam reforming with $CO_2$ adsorption is not only reduces the lower operating temperature, it is also inhibits carbon deposition at low and moderate temperatures (Silva et al, 2011).

For the operation of the sorption enhanced steam reforming process, Wang et al. (2010) studied the sorption enhanced steam methane reforming (SE-SMR) and the sorbent regeneration processes with CaO based sorbent in fluidized bed reactors. The effects of pressure and steam-to-carbon ratio on the reactions are studied. High

pressure and low steam-to-carbon ratio will decrease the conversion of methane. But the high pressure makes the adsorption of $CO_2$ faster. The methane conversion and heat utility are enhanced by CO2 adsorption. The adsorption rate of $CO_2$ is fast enough compared with the SMR rate. In regeneration process, higher temperature makes the release of $CO_2$ faster, but the rate is severely restrained by the increased $CO_2$ concentration in gas phase. Regeneration rate and capacity of sorbents are important factors in selecting the type of reactors for SE-SMR process.

### 2.4.3 Hybrid membrane and $CO_2$ absorption technology

The published works recently have concentrated on hybrid of both principles between membrane reactor and adsorption in producing hydrogen. Chena et al. (2008) studied a fluidized bed membrane reactor with in situ or ex situ hydrogen and/or $CO_2$ removal for production of pure hydrogen by steam methane reforming by analysis from thermodynamic equilibrium and kinetic reactor. Theirs results showed that sorbent enhancement combined with membranes could provide very high hydrogen yields.

Harale et al. (2007) presented experimental investigations of the HAMR for the water-gas-shift (WGS) reaction using layered double hydroxides as adsorbents for $CO_2$ and nanoporous $H_2$-selective carbon molecular sieve membranes. Moreover, they present the WGS-HAMR experiments and discuss fitting the results to the model. The experimental studies indicated that the HAMR system is of potential interest to pure hydrogen production and good agreement with the model predictions without any adjustable parameters. Then, they (2010) studied optimization of selection and design of HAMR for continuous operation for fuel-cell applications with both experimentally and through modeling methods. The ability of membrane, catalyst and adsorbent to operate stably under a cyclic operation was tested experimentally in a four-cycle experiment. The HAMR was shown to operate stably without any apparent decline in performance. The reactor system was shown capable of attaining high conversions, and a high purity hydrogen product.

A novel pilot fluidized-bed membrane reformer (FBMR) with permselective palladium reactor and a mixture of calcium oxide (CaO)/limestone ($CaCO_3$) and a Ni-

alumina catalyst for methane steam reforming reaction was investigated by Andres et al (2011). Their results showed that a mole of CaO is able to adsorb a maximum of 0.19 mol of $CO_2$ during carbonation and the maximum carbon capture efficiency was 87%. The reformer operated for up to 30 min without releasing $CO_2$ and for up to 240 min with some degree of $CO_2$ capture. It was demonstrated that the use of $CO_2$ adsorption in situ reformer can significantly improve the productivity of the reforming process and enhance purity of hydrogen production at 99.99%. The experimentally at the pilot scale showed the possibility of continuous operation with recirculation of solids, as well as by a simulation at industrial scale, with a predicted overall thermal efficiency of 78%.

### 2.4.4 Membrane or/and $CO_2$ absorption technology combined with power generation process

The membrane and the $CO_2$ sorption technologies are applied for power generation processes in order to get rid of $CO_2$ from system and increase the system performance. Tarun et al. (2007) found out the best operating conditions that minimize the energy penalty associated with $CO_2$ capture while maximizing $H_2$ production. The two $CO_2$ capture schemes evaluated in this study include a membrane separation process and the mono ethanol amine (MEA) absorption process. The process simulation results show that both $CO_2$ capture processes, the membrane process and the MEA absorption process, are comparable in terms of energy penalty and $CO_2$ avoided when both are operated at conditions where lowest energy penalty exists.

Sangtongkitcharoen et al. (2008) presented the performance analysis of a methanol-fueled SOFC system incorporated with a palladium membrane reactor to extract pure hydrogen from the reformed gas and fed to the anode of the SOFC unit, which could increase the maximum power density of the SOFC about 12.6% from the system with the conventional reformer. Moreover, some research analyzed performance of the integrated systems of calcium oxide (CaO)-carbon dioxide ($CO_2$) capture unit and fuel cell. Vivanpatarakij et al. (2009) studied the effect of location of CaO-$CO_2$ capture unit integrated with SOFC in system (i.e., CaO-Before-SOFC; CBS, CaO-After-SOFC; CAS and CaO-After-Burner; CAB). They found that all

SOFC–CaO systems can reduce the $CO_2$ emission; however, only the CaO-After-SOFC can improve performance of SOFC. Jose et al. (2004) investigated potential advantages of the presence of CaO as $CO_2$ sorbent in steam reforming include higher energy efficiency, higher hydrogen production and lower CO content in reformer gas exit to using in PEMFC.

**2.5 Fuel cell system analysis**

In general, SOFC system composes of the SOFC stack, fuel processing, and off-gas treatment. The significant advantage of SOFC is that operate at high temperature which is caused high quality exhaust gas of SOFC. It can utilize within system to increase the total energy system efficiency. A number of researchers study manangement heat in SOFC system.

Colpan et al. (2006) proposed a model for direct internal reforming SOFC (DIR-SOFC) and studied the effect of recirculation ratio of the anode exit gas into direct internal reforming SOFC (DIR-SOFC) in order to supply steam in initiating the chemical reactions and preventing carbon deposition. However, as recircuration ratio increase, power output and electrical efficiency decrease.

The thermodynamic model of a tubular SOFC module fed by methane, which consists of mixer, pre-reformer, internal reforming fuel cell group, afterburner and internal pre-heater components were developed by Akkaya et al. (2008). This study based on performance criteria (exergy efficiency, exergetic performance coefficient, exergy output and exergy destruction rate) to investigate the effect of operating parameters such as current density, fuel utilization factor and operating pressure. They claimed that the developed thermodynamic model is expected to provide not only a convenient tool to determine the module exergetic performances and component irreversibility but also an appropriate basis to design complex hybrid power generation plants.

Musa et al. (2008) studied performances of both high temperature (HT) and intermediate temperature (IT) SOFC. Furthermore, they compared two types of combined cycles: a combined cycle consisting of a two-staged combination of IT-SOFC and HT-SOFC and another consisting of two stages of IT-SOFC. Their

simulation results show that a combined cycle of two-staged IT-SOFC is more efficient than single-staged HT/SOFC and IT/SOFC.

Hernandez et al. (2009) designed an integrated process for sustainable electrical energy production from bio-ethanol simulated by Aspen–HYSYS software. They developed an integrated process by using the exhausted gas of outlet stream from SOFC anode to pre-heat air, ethanol, and water, or the exhausted gas from SOFC anode was divided in two streams where one of them was recycled to be mixed with water fed to the system and other is fed to combustion stage.

In addition, an exhaust gas from SOFC is used to drive absorption chiller (AC) to enhancing the energy utilization efficiency of a total energy system, which is proposed by Yu et al. (2009). The results showed that the cooling efficiency increases caused increment of current density, on the contrary the electrical efficiency and total efficiency decreased at the same condition. Then, Arteaga-Perez et al. (2009) carried out the simulation and heat integration of SOFC combined with an ethanol steam reforming system. They proposed design process so as to obtain a high efficiency and to avoid the use of any external source of energy.

### 2.6 SOFC-GT system analysis

The SOFC system can increase the electrical efficiency system by SOFC combined with gas turbine process because the SOFC operates at high temperature. In SOFC-GT hybrid system, the exhaust gas from SOFC is fed into afterburner so as to burn the residual fuel and then it is sent to turbine in order to produce the electricity, which can increase the system electrical efficiency. The SOFC hybrid gas turbine system was firstly proposed by National Fuel cell Research Center in Irvine, California. This system designed and built by Siemens-Westinghouse Power Corporation (SWPC). This system is the 220 kW hybrid system with 200 kW from the SOFC and 20 kW from the micro turbine generator (Samuelsen, 2004). This system tested at NFCRC. It can operate for 900 h and achieved 53 % efficiency. Moreover, Lim et al. (2008) designed and constructed an atmospheric and pressurized 5 kW class SOFC power generation system with a pre-reformer for the fuel cell/gas turbine hybrid system. In the hybrid mode of operation at 3.5atm (abs.), the SOFC stack combined with an LNG pre-reformer and a micro-gas turbine, produces 5.1 kW and 33.2% fuel utilization. Their results showed that

they have confirmed the success of our design and fabrication technologies for a pressurized anode-supported planar SOFC system combined with a micro-gas turbine.

However, the SOFC-GT hybrid system should be still studied and developed. The build of this system to study and design is complicated and high cost. Further, the experiment approach is limited to the system characteristic such as size and configuration and it is not a general approach. The study of SOFC-GT hybrid system by using the mathematic model is attractively another option. The model of SOFC-GT system is able to show the system characteristic by including the detailed cell and component in system. This method is a relatively easy and evaluated variation of system configuration and size. Therefore, a number of literatures have studied SOFC and gas turbine hybrid system by model simulation. The studies of fuel cell and gas turbine hybrid system with build real plant and that with analysis of model simulation for the investigation are concluded in Table 2.2 and 2.3, respectively.

SOFC-GT hybrid system by model simulation in literatures has been studied in various ways such as analyzing the effect of parameters on the system performance, designing the system and controlling the system. Some researcher focuses on the effect of operating parameters on system performance by analyzing from the energy and exergetic performance. The results of exergetic performance analysis based on the developed model will contribute some original information on the role of the considered operating variables and will be beneficial in design of the hybrid systems. Akkaya et al. (2009) studied a tubular SOFC module fed by methane which analyzes from thermodynamical model. Their results of the analysis showed that most of the exergy entering the tubular SOFC module is converted to the product electricity and rejected from module as heat of exhaust gases. The most important exergy destruction rates in the components are associated with fuel cell group and afterburner, respectively. Note that the heat rejected from the module has significant exergy amount due to high exhaust temperature, and can be therefore beneficial for cogeneration or hybrid application. Moreover, they (2008) considered a thermodynamic model of solid oxide fuel cell/gas turbine combined heat and power (SOFC-GT CHP) system under steady-state operation using zero-dimensional approach. The exergetic performance coefficient (EPC) as a new criterion is

**Table 2.2 Summary of experimental studies on fuel cell/GT hybrid systems**

| Author | Plant size | Fuel cell type | System type | Supplied fuel | Efficiency |
|---|---|---|---|---|---|
| Siemens-Westinghouse (Veyo et al., 2003) | 220 kW SOFC:200 kW GT:20 kW | Cathode-supported tubular SOFC | Pressurized SOFC-micro gas turbine hybrid system (two shaft type) | Natural gas | 57% |
| Agnew et. al. (2006) | - | Planar SOFC | Pressurized SOFC-GT hybrid system | Natural gas | |
| Lim et. al. (2008) | 5 kW | Anode-supported planar SOFC | Pressurized SOFC-micro gas turbine hybrid system | Liquefied natural gas | - |
| DOE/NETL and FuelCell Energy (FCE) | 300 kW | MCFC | Atmospheric MCFC-micro gas turbine hybrid system | Natural gas | 52% |
| FutureGen (SECA industrial team participants) | 280 kW | Fuel cell | Direct fuel cell/turbine hybrid system | Coal | 52% |

**Table 2.3 Summary of simulation studies on fuel cell/GT hybrid systems**

| Author | Plant size | SOFC model | System type | Supplied fuel | Efficiency |
|---|---|---|---|---|---|
| Costamagna et al (2001) | ~300 kW<br>SOFC:240 kW<br>MGT: 50 kW | Tubular SOFC | Recuperated Micro gas turbine with high temperature SOFC | Methane | 60% |
| Palsson et al., 2000 | 500kW<br>SOFC:311 kW<br>GT:173 kW | Planar SOFC | Pressurized SOFC-GT hybrid system with GT reheat and air compression inter-cooling | Methane | <65% |
| Akkaya et al, 2008 | 220 kW<br>SOFC:176 kW<br>MGT: 47 kW | Tubular SOFC | Pressurized SOFC-MGT hybrid system | Methane | 58.7 % |
| Lisbona et al, 2008 | 400 MW<br>SOFC:203.11 MW<br>GT: 221.83 MW | Tubular SOFC | SOFC-GT hybrid system integrated with enhanced coal gasification heated by unmixed combustion | Coal | <73% |
| Franzoni et al, 2008 | 1.50 MW | Tubular SOFC | Pressurized hybrid SOFC system with CO2 separation | Natural gas | <50% |

investigated in this study with regard to main design parameters such as fuel utilization, current density, recuperator effectiveness, compressor pressure ratio and pinch point temperature, aiming at achieving higher exergy output with lower exergy loss in the system. Additionally, Haseli et al. (2008) investigated the effects of various performance parameters such as the compression ratio, and turbine inlet temperature, on the thermal and exergy efficiency of a SOFC combined gas turbine power system. From the simulated results, both thermal and exergy efficiencies are reduced with increasing the turbine inlet temperature.

A full load and partial load analysis of SOFC-GT power plant is presented by Calise et al. (2006). The plant basically consists of: an air compressor, a fuel compressor, several heat exchangers, a radial gas turbine, mixers, a catalytic burner, an internal reforming tubular SOFC stack, bypass values, an electrical generator, an electrical generator and an inverter. In this work, they consider parameter such as: air mass flow rate, fuel mass flow rate, combustor bypass, gas turbine bypass, to avoid the use of a variable speed control system. Results showed that the most efficient part-load strategy corresponded to a constant value of fuel to air ratio. On the other hand, a lower value of net electrical power could be achieved reducing fuel flow rate, at constant air flow rate.

The system efficiency varies depending on system configurations and design conditions. The design of SOFC-GT hybrid system is presented in diverse publications. Motahar et al. (2009) presented the comparison of the conventional SOFC-GT hybrid system with retrofitted system by steam injection, which use hot gas turbine exhaust gases heat in a heat recovery steam generator to produce steam and inject it into gas turbine. Their process based on a steady-state model, exergy flow rates are calculated for all components and a detailed exergy analysis is performed. Their results show that steam injection decreases the wasted exergy from the system exhaust and boosts the exergetic efficiency by 12.11%. Also, 17.87% and 12.31% increase in exergy output and the thermal efficiency, respectively. Park et al. (2009) examined two different configurations (pressurized system and ambient pressure system) by concentrating on the effect of injecting steam on the recovering heat from the exhaust gas and system performance. The results showed that the pressurized system hardly takes advantage of the steam injection in terms of system efficiency.

On the other hand, the steam injection contributes to the efficiency improvement of the ambient pressure system in some design conditions. In particular, a higher pressure ratio provides a better chance of efficiency increase due to the steam injection.

Another design option is to reforming method for generating hydrogen from the conventional fuel (natural gas) in SOFC-GT hybrid system. Yang et al. (2006) analyzed two types of hybrid system configurations with internal and external reforming by examining the effect of matching between the fuel cell temperature and the turbine inlet temperature on the hybrid system performance. The system with internal reforming gives better efficiency and power capacity for all design conditions than the system with external reforming under the same constraints. Its efficiency gain over the SOFC only system is considerable, while that of the system with external reforming is far less. Further, the hybrid SOFC-GT system by comparing between SOFC at intermediate and low temperature (IT/LT, 300-800°C) was studied by Zhe et al. (2009). They found that the electrical efficiency and the total efficiency of intermediate temperature SOFC hybrid system can be about 60 % and 80 % higher than efficiency of low temperature.

## 2.7 Conclusion

As mentioned above, the SOFC power plant is promising technology to generate electricity in the future. SOFC have been studied from both experiment and model simulation. The most of SOFC analysis was studied with mathematical modeling because SOFC system design is complexity and limitation for experiment. SOFC models based on three parts were proposed i.e., mass balance, energy balance and electrochemical. The zero and one dimensional models of SOFC are suitable for adoption with analysis of SOFC system. The main components of SOFC system are fuel processor, power generation, afterburner and auxiliary air compressor. A number of researchers presently focus on use of renewable fuels for SOFC system instead of fossil fuel. Among all possible renewable fuels, ethanol has been considered as an attractive green fuel. The development of fuel processor is also important on SOFC efficiency. The Pd-based membrane reactor or $CO_2$ sorbents technologies can improve hydrogen production, which remove hydrogen or carbon dioxide from

system and consequently limited equilibrium reaction drive forward. The majority of publications proposed these technologies with methane steam reforming. Thus, this is possibly combination of both technologies and adapted with ethanol steam reforming in order to enhance hydrogen production and efficient SOFC. In study on the integration of SOFC and ethanol steam reformer, the operating parameters of reformer i.e., steam-to-carbon, pressure, temperature directly affect SOFC performance. Moreover, SOFC operated at high temperature is capable to combine with gas turbine so as to enhance system efficiency. Nonetheless, the operation of SOFC integrated with gas turbine is quite complicated due to difficult matching between operations of both units. The suitable hybrid between solid oxide fuel cell with gas turbine still challenge in present.

# CHAPTER III

# THEORY

This chapter presents the main principles of this thesis. There are as following: first, presenting the description general basic concepts of fuel cells, such as principle, type, system and advantage of fuel cell; secondly, presenting the details of solid oxide fuel cell (SOFCs) which is the fuel cell type of interest in this thesis; thirdly, fuel processing for SOFC by describing reforming configuration and the development of the hydrogen product through sorption-enhanced steam reforming and membrane technology; fourthly, SOFC system configurations; finally, principle for SOFC hybrid systems.

## 3.1 Fuel Cell

Fuel cells are very promising power generation with high efficiency, flexibility of size, quiet operation and low emissions. Fuel cells are not restricted by Carnot's theorem limitations. The overall energy conversion efficiency is higher than what obtained by conventional combustion engines. Moreover, because combustion is avoided, fuel cells produce power with minimal pollutants. Fuel cell components and characteristics are similar to battery. However, fuel cell does not require recharging which is an energy conversion device that theoretically has the capability of producing electrical energy for as long as the fuel and oxidant are supplied to the electrodes.

### 3.1.1. Principle of fuel cells

Fuel cells are electrochemical devices which convert the chemical energy stored in fuel to electric energy directly by electrochemical reaction between fuel (hydrogen) and oxidant (oxygen or air). The basic physical structure or building block of a fuel cell consists of an electrolyte layer sandwiched between a porous anode and cathode. A schematic presentation of a fuel cell with the reactant/product gases and the ion conduction flow directions through the cell is shown in Figure 3.1. In fuel cell

operation, gaseous fuels are continuously fed to the anode (negative electrode) compartment and an oxidant (i.e., oxygen from air) is continuously fed to the cathode (positive electrode) compartment; the electrochemical reactions take place at the electrodes to produce an electric current.

### 3.1.2 Type of fuel cells

Types of fuel cell are in different stages of development. They can be classified by use of diverse categories, depending on the combination of type of fuel and oxidant, the type of electrolyte and the operating temperature. The most common classification of fuel cells is by the type of electrolyte used in the cells and includes: 1) Proton exchange membrane (polymer) electrolyte fuel cell (PEMFC), 2) Alkaline fuel cell (AFC), 3) Phosphoric acid fuel cell (PAFC), 4) Molten carbonate fuel cell (MCFC), 5) Solid oxide fuel cell (SOFC).

These fuel cells are listed in the order of approximate operating temperature, ranging from ~80 °C for PEMFC, ~100 °C for AFC, ~200 °C for PAFC, ~650 °C for MCFC, and 800 °C to 1000 °C for SOFC. The operating temperature and useful life of a fuel cell dictate the physicochemical and thermomechanical properties of materials used in the cell components i.e., electrodes, electrolyte, interconnect, current collector, etc. The operating temperature also plays an important role in dictating the type of fuel that can be utilized in a fuel cell. The low-temperature fuel cells with aqueous electrolytes are, in most practical applications, restricted to hydrogen as a fuel. In high-temperature fuel cells, CO and even $CH_4$ can be used because of the inherently rapid electrode kinetics and the lesser need for high catalytic activity at high temperature.

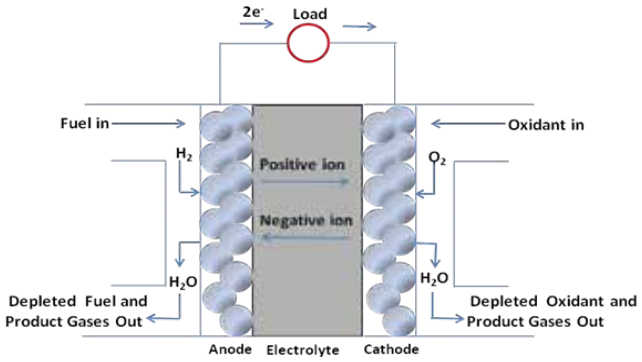


**Figure 3.1** The Schematic of Individual Fuel cell

In low-temperature fuel cells (PEMFC, AFC, PAFC), protons or hydroxyl ions are the major charge carriers in the electrolyte, whereas in the high-temperature fuel cells, MCFC and SOFC, carbonate ions and oxygen ions are the charge carriers, respectively. Advantage and disadvantage of the various cells are shown in Table 3.1. Moreover, major differences of the various cells are shown in Table 3.2.

**Table 3.1** Advantages and disadvantages of different types of fuel cell (Kendall and Singhal, 2003)

| Fuel cell | Application | Advantage | Disadvantage |
|---|---|---|---|
| **PEMFC** | - Electric utility<br>- Portable power<br>- Transportation | - Solid electrolyte reduces corrosion & management problems<br>- Quick start | - Low temperature require expensive catalysts<br>- High sensitivity to fuel impurities |
| **AFC** | - Military<br>- Space | - Cathode reaction faster in alkaline electrolyte so high performance | - Expensive removal of from fuel and air streams required |
| **PAFC** | - Electric utility<br>- Transportation | - Up to 85% efficiency in cogeneration of electricity and heat<br>- Can use impure $H_2$ as fuel | - Requires platinum catalyst<br>- Low current and power<br>- Large size/weight |
| **MCFC** | - Electric utility | - High efficiency<br>- Can use a variety of fuels and catalysts | - High temperature enhance corrosion and breakdown cell components |
| **SOFC** | - Electric utility | - High efficiency<br>- Can use a variety of fuels and catalysts<br>- Solid electrolyte reduces corrosion | - High temperature enhance corrosion and breakdown cell components |

**Table 3.2** Important characteristics of fuel cells (Stolten, 2010)

| | **PEMFC** | **AFC** | **PAFC** | **MCFC** | **SOFC** |
|---|---|---|---|---|---|
| Electrolyte | Hydrated Polymeric Ion Exchange Membranes | Mobilized or Immobilized Potassium Hydroxide in asbestos matrix | Immobilized Liquid Phosphoric Acid in SiC | Immobilized Liquid Molten Carbonate in $LiAlO_2$ | Perovakites (Ceramics) |
| Electrodes | Carbon | Transition metals | Carbon | Nickel and Nickel Oxide | Perovakite and perovakite/metal cermet |
| Catalyst | Platinum | Platinum | Platinum | Electrode material | Electrode material |
| Interconnect | Carbon or metal | Metal | Graphite | Stainless steel or Nickel | Nickel, ceramic, or steel |
| Operating Temperature | 40-80 °C | 65-220 °C | 205 °C | 650 °C | 600-1000 °C |
| Charge Carrier | $H^+$ | $OH^-$ | $H^+$ | $CO_3^-$ | $O^{2-}$ |
| External Reformer for hydrocarbon fuels | Yes | Yes | Yes | No. for some fuels | No. for some fuels and designs |
| External shift conversion of CO to hydrogen | Yes, plus purification to remove trace CO | Yes, plus purification to remove CO and $CO_2$ | Yes | No | No |
| Prime Cell Components | Carbon-based | Carbon-based | Graphite-based | Stainless-based | Ceramic |
| Product Water Management | Evaporative | Evaporative | Evaporative | Gaseous Product | Gaseous Product |
| Product Heat Management | Process Gas + Liquid Cooling Medium | Process Gas + Electrolyt e Circulation | Process Gas + Liquid cooling medium or steam generation | Internal Reforming + Process Gas | Internal Reforming + Process Gas |
| Size (MW) | 0.25 | Very small | 11 | 2 | 1-2 |
| Efficiency (%) | <40 | >60 | 40-45 | 50-60 | 50-60 |

## 3.2 Solid Oxide Fuel Cell (SOFC)

The main characteristics of the solid oxide fuel cell are its solid-phase oxygen-ion conducting electrolyte and its high operation temperature. Due to the latter, it is less vulnerable for carbon and fuel impurities and suitable for combination with bottoming thermodynamic cycles.

### 3.2.1 Advantage of SOFC

The unique working temperature and the structure of SOFC give it the following advantages:

1) High efficiency compared direct combustion power generator.

2) Suitable for hydrogen fuels as well as hydrocarbon fuels, makes it compatible with current energy infrastructure. Hydrogen provides a potential clean energy solution for large-scale deployment.

3) Environment friendly: unlike batteries usually containing elements harmful to health, the materials in SOFC have less impact to the environment.

4) Easy to operate and maintain, because of no liquid electrolyte.

5) Inexpensive catalysts, due to high operating temperature.

6) No moving parts, so no vibration and less noise.

7) Increasing overall efficiency by SOFC operation as auxiliary power unit to utilize the heat generated.

8) Suitable for large, high power applications, such as power generation stations.

### 3.2.2 SOFC features

The SOFC unit has a three-layer sandwich structure: two porous electrode, anode and cathode, serving as the chemical reaction, and the electrolyte, serving as the diffusion layer of oxygen ions but electrically nonconductive. A typical SOFC structure is shown in Figure 3.2. The anode and cathode should be porous to allow the diffusion of oxygen ions. A single SOFC unit cannot provide enough power; therefore, the interconnection between stacks of cells is required.

In SOFC operation, oxygen or air is reduced to oxygen ions at the cathode:

$$\frac{1}{2}O_2 + 2e^- \rightarrow O^{2-} \quad (3.1)$$

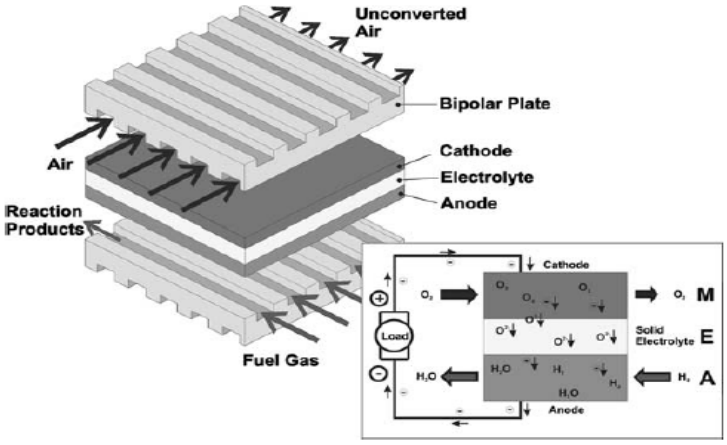


**Figure 3.2** Schematic representation of a Solid Oxide Fuel Cell (Henne, 2007)

The cathode has to be porous to allow oxygen to flow through it to the electrolyte. It also must have low resistivity to conduct electrons. It is required that the cathode material has excellent electronic conductivity as well as thermal stability. Therefore, noble metals and electronic conductive oxides are used as cathode materials.

At the anode, the oxidation reaction occurs when fuel reacts with the oxygen ions to generate electricity and water:

$$O^{2-} + H_2 \rightarrow H_2O + 2e^- \quad (3.2)$$

The function of electrolyte is to separate cathode and anode electronically so the electrons are “forced” to flow through external circuit. At the same time, the electrolyte must allow the oxygen ions to diffuse through it. The electrolyte usually determines the operating temperature of the fuel cell. It also allows the flow of charged ions from one electrode to the other to maintain the overall electrical charge balance.

From the mechanical support point of view, SOFCs can be divided into two main groups: the electrolyte-supported and electrode-supported SOFC. Usually the support layer is the thickest to provide enough mechanical strength for the cell.

The SOFC voltage potential depends on a considerable number of parameters:

- Operating temperature and pressure
- Anode, cathode, electrolyte, and interconnection thicknesses
- Fuel cell material
- Fuel cell geometry
- Fuel cell length
- Fuel utilization factor
- Fuel and air composition
- Current density
- Geometric configuration (i.e. flat plate, tubular, monolithic, etc.)

### 3.2.3 SOFC characteristics

The theoretical maximum voltage produced by a fuel cell can be measured if no current is produced and is hence often termed “Open Circuit Voltage” (OCV). In cell operation, the voltage will drop to zero or even below zero if a voltage is put on the cell. The operating voltage is decreased from its open circuit voltage due to the losses associated with the current production as seen in Figure 3.3. The major losses are called polarization, or overpotential, or overvoltage. The dependency of these losses on temperature, current density and species concentrations mainly determine the characteristics of a fuel cell. Three main mechanisms of voltage losses exist:

a) Ohmic losses

Ohmic losses occur due to the electrical resistance the charge has to overcome when traveling across the different materials or interfaces. The resistance along the flow of ions in the electrolyte and resistance to flow of electrons through the electrode and current collectors are all factor which cause the energy loss. This potential loss can be described by Ohm’s law, this behavior is linear between voltage drop and current density.

b) Activation overpotentials

Activation overpotentials are the voltage drop due to the sluggishness of reactions occurring at the electrode-electrolyte interfaces which is associated with

the energy intensive activities of the making and breaking of chemical bonds at the electrodes. The amount of energy needed for these activities of breaking and forming of chemical bonds comes from the fuel, and thus reduces the overall energy the cell can produce. If the reaction rate increases (i.e. high current density), the fuel flow rate must also increase which increases the kinetics and thus lowers the energy required to break bonds. Therefore when the current requirement is low, the overall cell polarization is dominated by the activation losses. Other factors, which lower the activation polarization, are increasing temperature, active area of the electrode, and activity of electrodes by the use of suitable catalyst (Angrist, 1965).

c) Concentration overpotentials

Concentration overpotentials are resistance to mass transport through the electrodes and interfaces caused by the decreasing of the substance in the reaction. This usually occurs at high current densities because the rate of hydrogen consumption at reaction sites is higher than that of diffusion of the reactants/products through the electrolyte to/from the reaction sites. The scarcity of hydrogen at the reaction sites effectively reduces the electrode activity, leading to a corresponding loss in output voltage. This polarization is also affected by the physical restriction of the transfer of a large atom, oxygen, to the reaction sites on the cathode side of the fuel cell. Concentration overpotentials can be reduced by increasing the gas pressure and fuel concentration, using high surface area electrodes, or using thinner electrodes which shortens the path of the gas to the reaction sites.

**Table 3.3** Materials used for SOFC components (Sammes et al., 2006)

| Component | composition | Specific conductivity (S/m) at SOFC running temperature | Conductivity depends upon |
|---|---|---|---|
| Anode | Ni/YSZ cermet | 400-1000 | Particle size ratio Ni content |
| Cathode | $Sr_xLa_{1-x}MnO_{3-\delta}$ | 6-60 | Cathode Porosity Sr content |
| Electrolyte | $Y_2O_3$-$ZrO_2$ | 10-15 | Electrolyte Density |

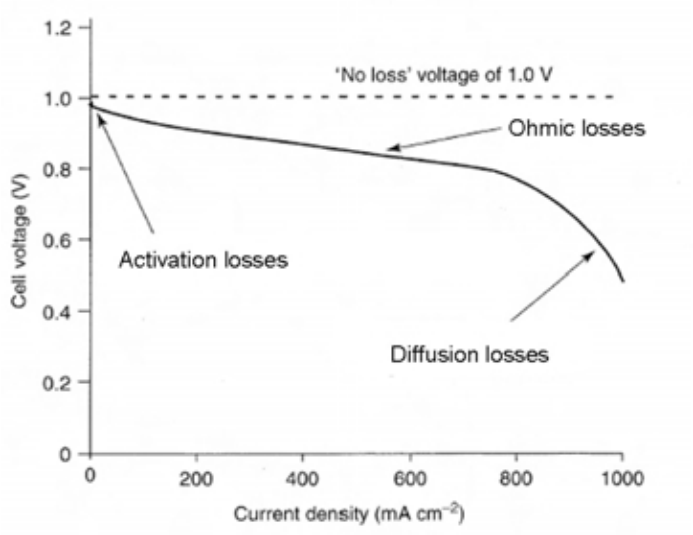


**Figure 3.3** Current-Voltage characteristics of fuel cell

### 3.2.4 SOFC materials

Due to the high operating temperature, and to the all-solid state nature of the components, the thermal expansion of each material composing the stack must be as close as possible, in order to avoid mechanical fracture and material delimitation. Other desired characteristics include chemical stability under the relative operational conditions, high electrical conductivity for the electrodes and electrical interconnects, high ionic conductivity and almost zero electrical conductivity for the electrolyte, and low cost. The choice of materials is usually the result of a compromise between the above characteristics, and, at the present, a variety of materials are being investigated. There are, however, some materials that are considered 'traditional' for SOFC, due to the large number of applications in the last few years.

### 3.2.5 SOFC configurations

The three main SOFC arrangements are: tubular, planar and monolithic. These arrangements differ in their complexity, sealing methods, losses, and power density. The highest power density is achieved with the monolithic design, which looks like a corrugated card box in its cross section. However, difficulties with the sealing and thermally induced tensions, which cause the breaking of the cell, favor the tubular, planar or the combination of the two arrangements.

### 3.2.5.1 Tubular design

Siemens Westinghouse Power Corporation first developed the tubular design of a solid oxide fuel cell. Figure 3.4 shows the schematic and stacking arrangement. The cell unit is in the form of a hollow cylindrical tube closed at one end. Air channel, cathode, electrolyte, anode, and fuel channel are arranged in layers from the center to the periphery. In this design, thin layers of electrolyte and anode are deposited on a cathode tube. The tube is produced by extrusion and sintering. A strip of interconnect is tightly attached to the cathode and the other end of it is in contact with the anode of the adjacent cell unit. Air is supplied in the inner tube and fuel to the free side of the anode.

Tubular configuration allows the cell to overcome most of the current drawbacks. In particular sealing is required only at the tube ends, thus reducing the sealing problems. Secondly, the cylindrical geometry allows a reduction of the shear stress, thus enabling a cell with better mechanical properties. However, the tubular design has some disadvantages as follows:

1) Low volumetric power density, compared to the planar configuration.
2) High manufacturing costs.

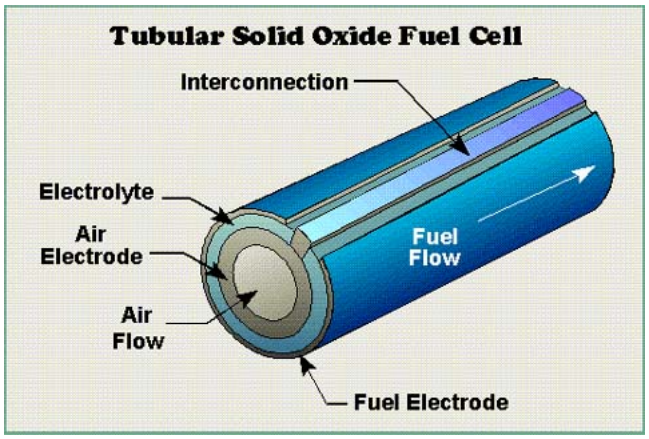


**Figure 3.4** Schematic representation of a tubular SOFC (http://americanhistory.si.edu/fuelcells/so/sox1.htm).

### 3.2.5.2 Planar Design

In this configuration, the electrodes, the electrolyte and the current collectors are present as a flat planar geometry, and are arranged in the ‘typical’ sandwich

configuration (Figure 3.5). This configuration is quite simple, relatively easy and inexpensive to construct, and the associated power density can be relatively high.

Disadvantages of the flat planar SOFCs can be list as below:

1) The different thermal expansion of the components can lead to cracking problems and thus, the maximum active surface is usually limited to some hundred $cm^2$ and the scale-up to multi MW system is possible only through a modular approach.
2) There is high contact resistance between electrolyte and electrodes, due to the geometrical configuration and the all solid state components. The non-perfect manufacturing of the current collectors and the electrodes, in fact, leads to non-uniform contact between the two adjacent parts. Although an external pressure can increase the contact area, cracking problems limit the maximum external load.

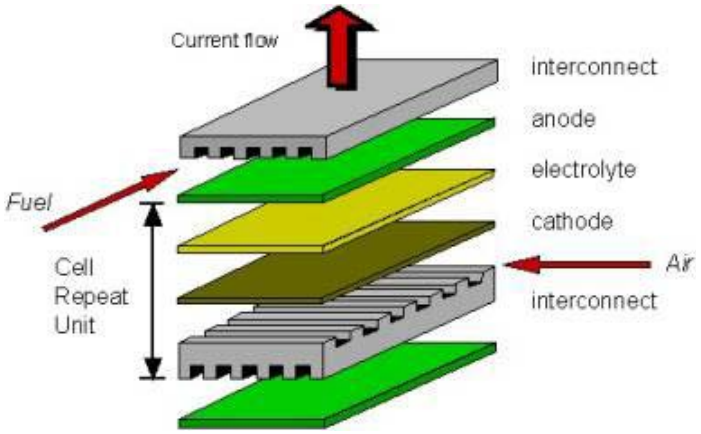


**Figure 3.5** Flat Plate SOFC Unit (Craig Fisher) (http://people.bath.ac.uk/cf233/sofc.html).

### 3.2.5.3 Monolithic Design

The monolithic SOFC is the most evolved of flat planar configuration (Figure 3.6). It consists of corrugated thin cell components. The result is that the volumetric power density is very high. On the other hand, the structure is more complex to be realized, as well as the manifold system, compared to the flat planar.

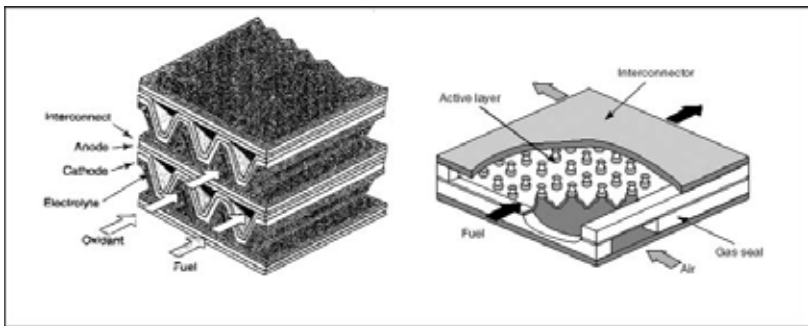


**Figure 3.6** Schematic cross section of a monolithic SOFC (Blum et al., 2005)**.**

### 3.2.6 Flow configurations in SOFC

SOFCs have three basic flow cases: 1) Co-flow where air and fuel parallel and in the same direction, 2) Cross-flow where air and fuel flow perpendicular to each other, 3) Counter-flow where air and fuel flow parallel but in opposite directions as shown in Fig. 3.7. In a planar SOFC design, the co-flow arrangement is the most favorable design in terms of thermal stresses where as the counter flow is the least favorable in terms of thermal gradient.

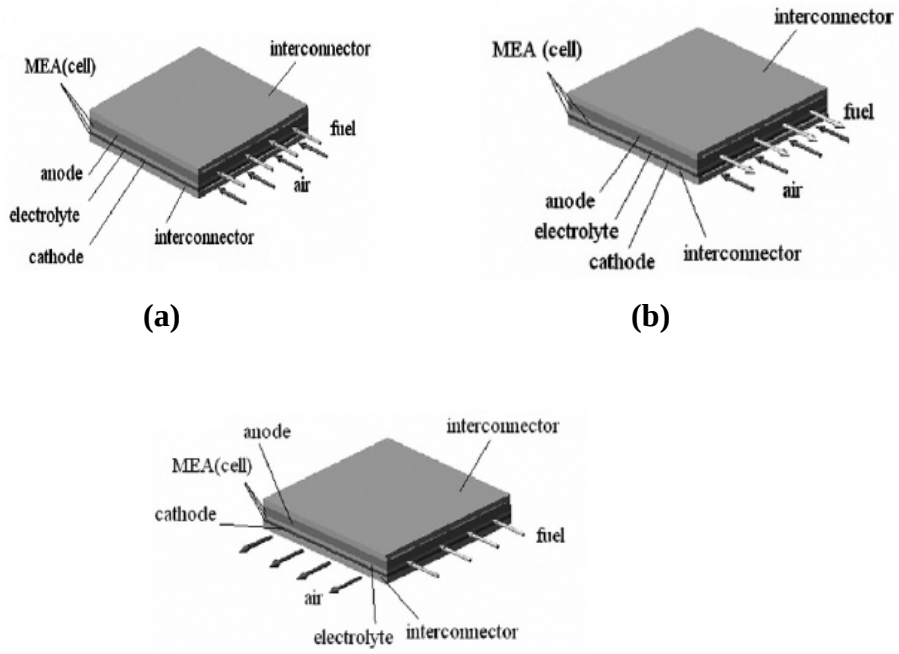


**Figure 3.7** Sketch for flow configurations; (a) co-flow; (b) counter-flow; (c) cross-flow (Rahimpour and Lotfinejad, 2008).

### 3.2.7 Intermediate temperature SOFC

The conventional SOFCs operated at high temperature ~1273 K encounter some problems associated with fabrication cost and cell durability. Operation of the SOFC at a reduced temperature in range of 873 to 1073 K (referred to 'intermediate-temperature solid oxide fuel cell: IT-SOFC') can overcome these problems and bring additional benefits as follow:

- Low cost metallic materials e.g. ferritic stainless steels can be used as interconnect and construction materials. This makes both the stack and balance of plant cheaper and more robust. (Balance of Plant is widely assumed to constitute 50% of the cost of the SOFC system). Using ferritic materials also significantly reduces the above-mentioned problems associated with Chromium.
- The start up and shut down procedures are potentially more rapid.
- The design and materials requirements of the balance of plant are simplified.
- The corrosion rates of fuel cell stack reduce.

## 3.3 Fuel processing for SOFC

Fuel cell can produce the electricity by the electrochemical reaction between hydrogen and oxygen. Hydrogen can be derived from hydrocarbon fuels such as natural gas, biogas, alcohol fuels or coal by reforming. In fuel processors for SOFC, there are diverse configurations and reforming processor which are presented in this section. Moreover, this section also presents the principles of carbon dioxide adsorption and membrane reactor in reforming reaction, which are technologies of improvement for reforming processors

### 3.3.1 Reforming configurations

Three different reforming configurations for SOFC are possible: (i) external reforming (ER), (ii) indirect internal reforming (IIR), and (iii) direct internal reforming (DIR). These configurations are conceptually illustrated in Figure 3.8.

a) External reforming

External reforming is a separate chemical reactor that is typically combined with catalysts and steam to break down the carrier fuel into $H_2$. Thus, external reforming produces hydrogen or synthesis gas before supplying in fuel cell. This process can remove impurities and poisons from the carrier stream before use which lead to achieve efficient operation of SOFC and prevent cell degradation. Nevertheless, chemical processes may require external heat source such as a burner or hot waste gas.

b) Indirect internal reforming

Indirect internal reforming physically separates catalyst reforming the hydrocarbon fuel to synthesis gas, is integrated within the SOFC stack upstream of the anode, making use of the cell-stack heat release either by radiation heat transfer or by direct physical contact between the cell hardware and the reforming unit which provide a convenient and efficient setting for energy transfer between heat source and heat sink and simultaneously lowering the air cooling requirements of the SOFC.

c) Direct internal reforming

Direct internal reforming, the hydrocarbon fuel-steam mixture is admitted directly into the anode compartment and the fuel is reformed on the porous, nickel-based anode layer. The anode must fulfill three roles; firstly as a hydrocarbon reforming catalyst, catalysing the conversion of hydrocarbons to hydrogen and carbon monoxide; secondly as an electrocatalyst responsible for the electrochemical oxidation of $H_2$ and CO to water and $CO_2$, respectively; and finally as an electrically conducting electrode. Direct reforming of the fuel on the anode offers the simplest and most cost-effective design for an SOFC system and in principle provides the greatest system efficiency with least loss of energy. In direct reforming, high-efficiency results from utilizing the heat from the exothermic electrochemical oxidation reaction to reform the hydrocarbon fuel, which is a strongly endothermic reaction. A further advantage of direct internal reforming is that by consuming the hydrogen to form steam, which can then reform more of the hydrocarbon fuel, the electrochemical reactions help drive the reforming reaction to completion.

Although internal reforming operation achieves high efficiency, it has several problems. Disadvantage of internal reforming are:

- It gives rise to a sharp endothermic cooling effect at the cell inlet, generating inhomogeneous temperature distributions and a steep temperature gradient along the length of the anode, which is very difficult to control and can result in cracking of the anode and electrolyte materials.
- The susceptibility of the nickel anode to catalyst cause the pyrolysis of methane and higher hydrocarbons resulting in deleterious carbon deposition and subsequent build-up of deactivating carbon, and leads to rapid deactivation of the cell.
- Sintering of the nickel anode particles results in a significant reduction in the catalytic activity of the anode and a loss in cell performance because of high steam partial pressures with hydrocarbon reforming directly on the anode

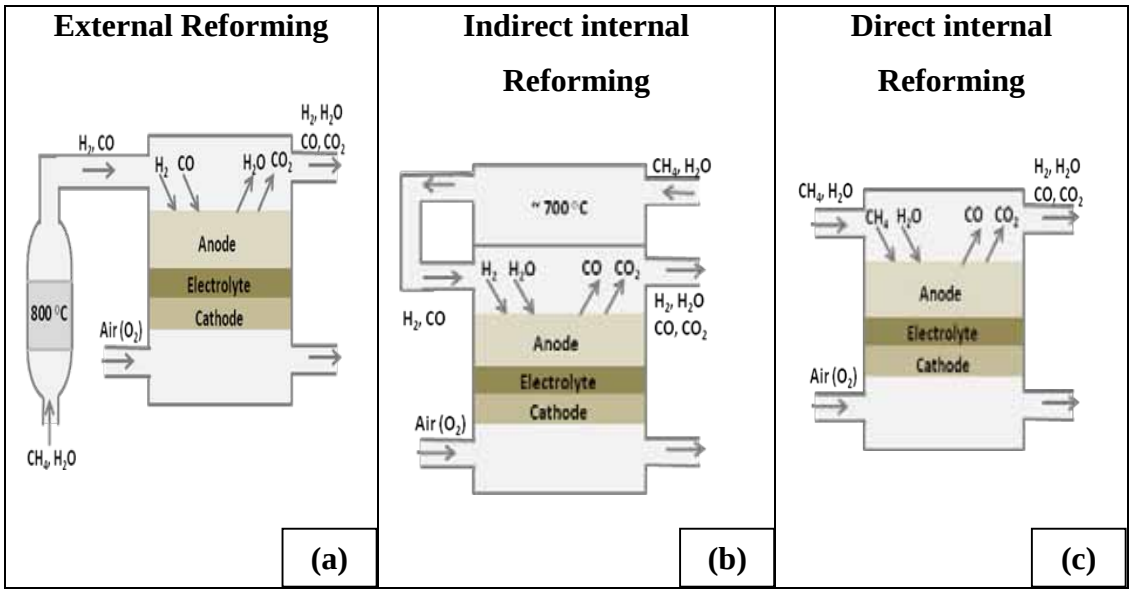


**Figure 3.8** Schematic representation of three different reforming configurations is possible: (a) external reforming (ER), (b) indirect internal reforming (IIR), and (c) direct internal reforming (DIR).

### 3.3.2 Fuel reforming processor

Fuel processing technologies convert a hydrogen containing material such as gasoline, ammonia, or methanol into a hydrogen rich stream. There are three primary techniques used to produce hydrogen from hydrocarbon fuels: steam reforming, partial oxidation (POX), and autothermal reforming (ATR). Each reaction is different reagent reacted with hydrocarbon. Table 3.4 summarizes the advantages and challenges of each process.

a) Steam reforming

Steam reforming is steam as reagent reacted with hydrocarbon. Endothermic steam reforming of hydrocarbons requires an external heat source.

$$C_mH_n + mH_2O = mCO + (m + \frac{1}{2}n)H_2 \quad (3.1)$$

b) Partial oxidation

Partial oxidation converts hydrocarbons to hydrogen by partially oxidizing (combusting) the hydrocarbon with oxygen. The heat is provided by the ‘‘controlled’’ combustion. It does not require a catalyst for operation and is more sulfur tolerant than the other processes. The process occurs at high temperatures with some soot formation.

$$C_mH_n + \frac{1}{2}mO_2 = mCO + \frac{1}{2}H_2 \quad (3.2)$$

c) Autothermal reforming

Autothermal reforming uses the partial oxidation to provide the heat and steam reforming to increase the hydrogen production resulting in a thermally neutral process. Autothermal reforming is typically conducted at a lower pressure than POX reforming. Since POX is exothermic and ATR incorporates POX, these processes do not need an external heat source for the reactor.

$$C_mH_n + \frac{1}{2}mH_2O + \frac{1}{4}mO_2 = mCO + (\frac{1}{2}m + \frac{1}{2}n)H_2 \quad (3.3)$$

### 3.3.3 Advanced hydrogen production technology

#### 3.3.3.1 Sorption enhanced reforming using $CO_2$ sorption

To develop new steam reforming processes**,** the sorption-enhanced steam reforming method is promising with addition of sorbents mixed catalyst in reactor. In this processor, carbon dioxide gases are separated during reactions which enhance the reactions. An innovative plant solution for hydrogen production, developed through the sorption-enhanced steam reforming process implementation.

The main criteria used to estimate the potentiality of a sorbent for sorption-enhanced steam reforming are:

- high reaction rate in the range of temperature 450–650 °C
- stability of the performances relative to their use in production/regeneration cycles
- low temperature interval between carbonation and calcination
- low cost
- high adsorption ability

Calcium carbonate and dolomite are inexpensive, easy to find and characterized by high adsorption ability. Otherwise, the sorbents, constituted mainly by inert, need a greater energy amount for their regeneration. CaO is capable of scavenging $CO_2$ to very low concentrations at moderate temperatures (450–750 °C) and at atmospheric pressure. CaO is low cost and abundant because it can be derived from a range of naturally occurring precursors including limestone, dolomite and calcium hydroxide. $CO_2$ is captured in the form of $CaCO_3$, a common and stable solid species, according to the following equation:

*Carbonation*:

$$CaO(s)+CO_2(g) \rightarrow CaCO_3(s) \qquad \Delta H^0_{923} = -170.5 \text{ kJ mol}^{-1} \text{ (exothermic)} \quad (3.28)$$

When the sorbent reaches its ultimate conversion, it can be regenerated to produce CaO and $CO_2$ by heating to 700–950 °C, depending on the $CO_2$ partial pressure.

$$CaCO_3(s) \rightarrow CaO(s)+CO_2(g) \qquad \Delta H^0_{923} = 170.5 \text{ kJ mol}^{-1} \text{ (endothermic)} \quad (3.29)$$

**Table 3.4** Comparison of different reforming processes

| Technology | Efficiency | Heat of reaction | Application | Advantages | Disadvantages |
|---|---|---|---|---|---|
| Steam reforming | 70-80% | Endothermic | Commercial | - Most extensive industrial experience<br>- Oxygen not required<br>- Lowest process temperature<br>- Best $H_2$/CO ratio for H2 production | - Highest air emissions |
| Partial oxidation | 60-75% | Exothermic | Commercial | - Decreased desulfurization requirement<br>- No catalyst required<br>- Low methane slip | - Low $H_2$/CO ratio<br>- Very high processing temperatures<br>- Soot formation/handing adds process complexity. |
| Autothermal reforming | 60-75% | thermally neutral | Near term | - Lower process temperature than POX<br>- Low methane slip | - Limited commercial experience<br>- Requires air or oxygen |

Although the regeneration process requires the input of energy, the heat generated by the exothermic absorption reaction partially off sets this penalty. The input of heat necessary for sorbent regeneration may be provided directly or indirectly, e.g. directly by the combustion of unconverted char or a fraction of the $H_2$ within the regeneration reactor, or indirectly, by utilizing an external heat source. However, we note that indirect heating is preferable in order to avoid the dilution of a pure stream of $CO_2$, which can then be used or sequestered as required. If the production of a highly concentrated stream of $CO_2$ is a key objective, higher calcination temperatures are necessarily (~ 950 ˚C) due to thermodynamic limitations.

### 3.3.3.2 Membranes reactor for steam reforming

In a membrane reactor, the separation properties of membrane are utilized to enhance the performance of a catalytic system for steam reforming reaction. For membrane reactor of steam reforming process as shown in the Figure 3.9, hydrogen as product of steam reforming is selectively removed from the reactor. By selective withdrawal of hydrogen from the reaction mixture, the chemical equilibrium of reactions is shifted towards the products, resulting in an increase in the conversion of hydrocarbon fuel to hydrogen and carbon monoxide. The thermodynamic equilibrium restrictions can be overcome with use of membrane reactor. Additionally, the membrane reactor offers high purity hydrogen product and the possibility of operation under less severe condition of reactions in terms of temperature and pressure.

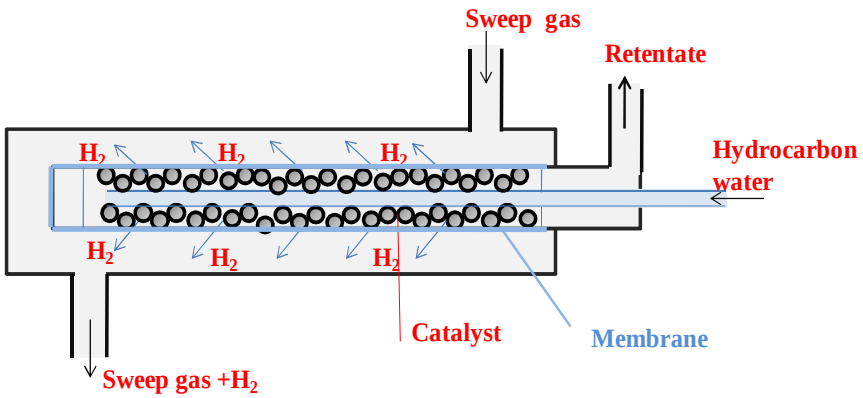


**Figure 3.9** Schematic diagram of a membrane reactor.

Palladium-based membrane reactor is promising and suitable for steam reforming reaction of hydrocarbon necessary in operation at high temperature. This kind of membrane is made of palladium alloy, which allows only hydrogen to permeate. Installing reforming catalysts and the membrane modules in the same reactor, simultaneous generation and separation of hydrogen is achieved. This not only makes the reactor drastically compact, but also drastically lowers the reaction temperature thanks to the breakage of chemical equilibrium. However, in the case of membrane made of palladium alloy, the reaction temperature can be lowered to 773–923 K, which enhances high thermal efficiency and hydrogen separation unit can be eliminated.

For dense Pd-based membrane reactor principle, hydrogen transport through dense Pd-based membranes may be divided into a series of different stages:

- Diffusion of hydrogen to the metal surface on the feed side of the membrane.
- Adsorption of hydrogen on the surface.
- Splitting of hydrogen molecules and incorporation into the metal.
- Diffusion of protons in the lattice and of electrons in the electron bands.
- Regeneration of hydrogen molecules on the permeate side surface.
- Desorption of the hydrogen molecule.
- Diffusion of the $H_2$ molecule from the surface, assuming a porous support.

It is noted that when a dense metal support is employed, the transport will include lattice diffusion in the support as well.

### 3.4 SOFC-GT hybrid system

SOFC operate at high temperature so heat from SOFC can be recovered to use in other units of an SOFC system with combined heat and power. There are two possibilities (or configurations) considered for the SOFC based system: that is Brayton (gas) regenerative cycle and Rankine (steam) cycle. The Rankine cycle is essentially a heat engine with a vapor power be combined with a SOFC using the direct thermal coupling scheme. The commonly used working fluid is water, and the system operates in the liquid–vapor mode. Thus, the Rankine cycle cannot be combined with a SOFC using the direct thermal coupling scheme. Due to the use of a

gas-based working fluid, the Brayton cycle is a favorable candidate for SOFC integration (Zhang, et al., 2010).

### 3.4.1 Basic gas turbine operation

A gas turbine cycle is based on the Brayton cycle, which is a simple series of compression, combustion, and expansion processes. The main components of the cycle are a compressor, a combustor, and a gas turbine. The number of components is not limited to three as the cycle may consist of several compressors and turbines (expanders). The simple-cycle gas turbine, a schematic diagram for a simple-cycle gas turbine, for power generation, is shown in Figure 3.10. Gas turbine cycle can express as following:

- Air entering the compressor at point 1 is compressed to some higher pressure. No heat is added, however, compression raises the air temperature so that the air at the discharge of the compressor is at higher temperature and pressure
- Air leaves the compressor and enters the combustion chamber at point 2, where fuel is injected and combustion occurs. The combustion process occurs at essentially constant pressure. Although high local temperature are reached within the primary combustion zone (approaching stoichiometric conditions), the combustion system is designed to provide mixing, burning, dilution and cooling. Thus, by the time the combustion mixture leaves the combustion system.
- Mixed gases from combustor enter the turbine at point 3. In the turbine section of the gas turbine, the energy of the hot gases is converted into work.

Gas turbines are largely used within power production and the power range goes from 70 kW to 330 MW. Electrical efficiency depends on the component design as well as the cycle layout and size of the plant. Usually, electrical efficiency is between 30 and 40%, but it can be further improved by adding a bottoming cycle, such as a steam turbine. Electrical efficiency for a large power plant combining gas- and steam turbines is nearly 60%.

Advantages of Brayton cycle are as follows:

- Simple cycle arrangement, minimum number of components used.
- Relatively low compressor and turbine pressure ratios, simple machines.
- Relatively low fuel cell operating pressure, hence avoiding the problems caused by the anode/cathode pressure differential, and high pressure housing and piping.
- Relatively low turbine inlet temperatures, perhaps 1065 $^{0}$C for the SOFC. Turbine rotor blade cooling may not be required.
- No internal heat transfer surface required for the heat removal.
- Fuel conversion in cells is maximized, taking full advantage of fuel cell efficiency.
- Adaptability to small scale power generation systems.
- Industrial compressor and turbine equipment can be adapted for this application.

Disadvantages of Brayton cycle are as follows:

- Tailoring of a compressor and the turbine equipment to the fuel cell temperature and cycle operating pressure.
- Large gas to gas exchanger for high temperature heat recuperation required.
- Efficiency and work output of the cycle sensitive to the cell, compressor and turbine efficiencies; pressure losses; and temperature differentials.

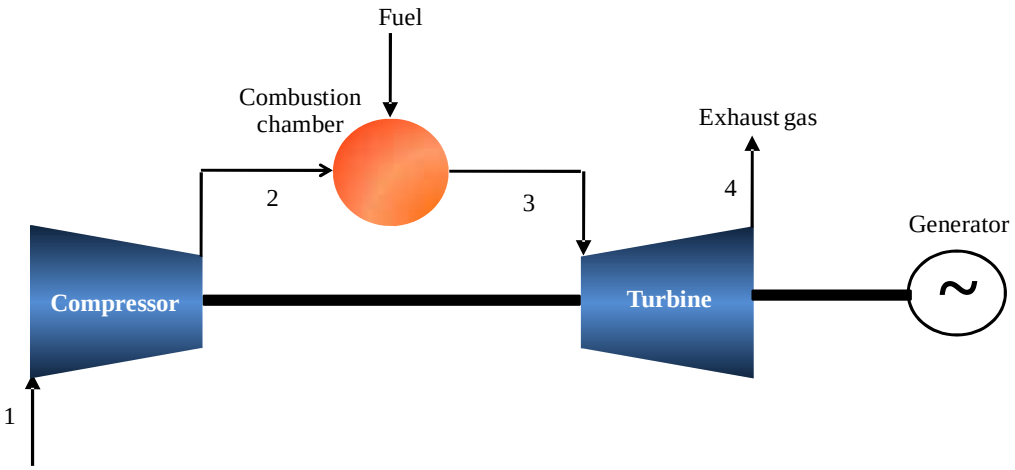


**Figure 3.10** Gas turbine process.

### 3.4.2 SOFC-GT hybrid design

A gas turbine can be directly or indirectly connected to the SOFC. Details are shown below.

- In an indirect integration between SOFC and gas turbine, as seen in Figure 3.11, air from the compressor is heated by the fuel cell exhaust through a heat exchanger before feeding to the combustor of the gas turbine and the SOFC can operate under atmospheric conditions. Although, it reduces the sealant requirement in the SOFC stack, the heat exchanger has to operate at very high temperatures and pressure differences. The material requirements in the indirect integration are really an issue and hence, it is not generally used.
- In a direct integration of a solid oxide fuel cell and a gas turbine system, as seen in Figure 3.12, the combustion chamber of the gas turbine engine has been replaced with an SOFC and an afterburner. The pressurized stream from the compressor goes into the SOFC. The exhaust from the SOFC goes to the afterburner and the resulting high temperature and pressure exhaust enters into the turbine. In this case, the SOFC operates at high pressure, which further improves its performance. Moreover, heat exchangers are added after the turbine exhaust to further utilize the waste heat in preheating of the streams entering the SOFC stack.

### 3.4.3 Advantages of SOFC-GT hybrid system

The integration of existing or specifically designed turbomachines into the hybrid system is expected to (Traverso, et al., 2010):

- To recover energy from the fuel cell exhaust gases, since they are at high temperature and, for pressurised stack, at high pressure.
- To pressurise the stack itself.
- To generate extra electrical power (up to 25% of the fuel cell power) to increase the system performance from the point of view of the efficiency, the specific power and the costs.

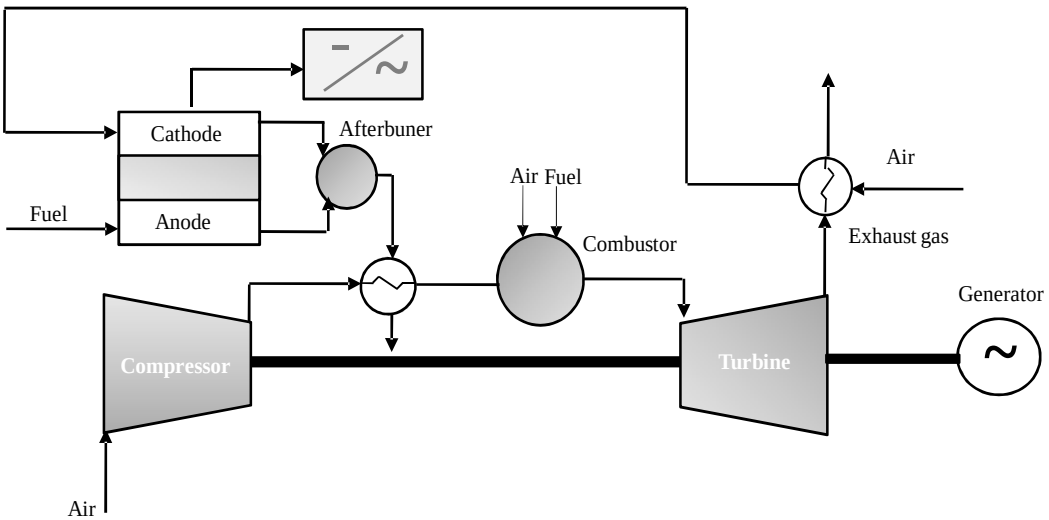


**Figure 3.11** An indirect integration of a solid oxide fuel cell and a gas turbine system.

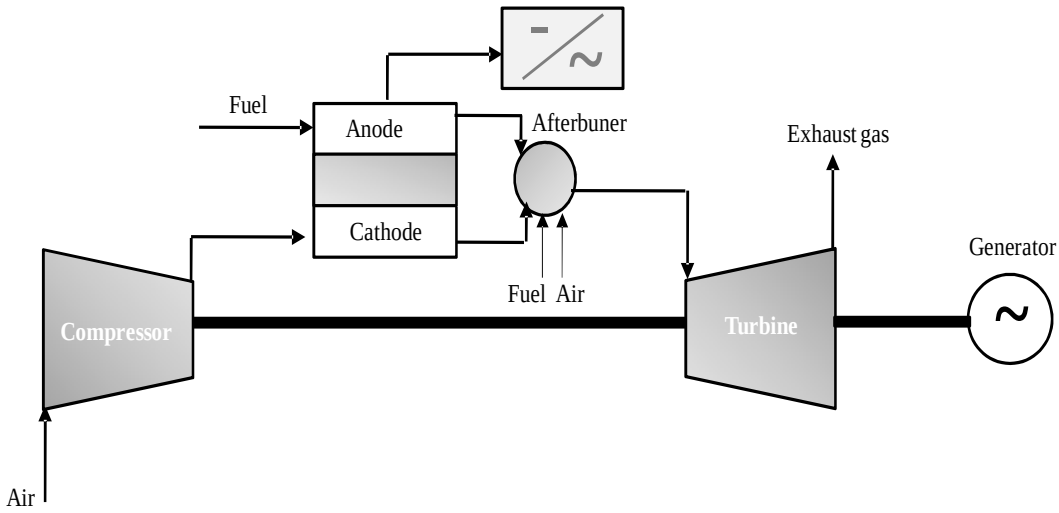


**Figure 3.12** A direct integration of a solid oxide fuel cell and a gas turbine system.

### 3.4.4 SOFC-GT system configuration

In reliable operation of solid oxide fuel cell, the fuel supply of the right quality, sufficient heat integration and effective system control are required in SOFC system.

a) Fuel and fuel processing
   - SOFCs are highly fuel flexible which are not only able to operate on purely hydrogen but also fuels containing carbon.
   - The fuel processor for the SOFC may include a preheating/vaporization unit, cracking/prereforming unit for mitigating carbon deposition problem in the reforming system, reformer, and energy and water recuperators.
   - Pre-reformer: any fuels are partially converted in hydrogen and carbon monoxide in reformer prior to entering the stack to avoid carbon deposition which might lead to damage cell. The mostly SOFC application have a pre-reformer before feeding fuel to cell.

b) Power generation
   - A fuel cell produces direct current (DC), and if connected to the electrical grid, the current must be transformed into alternating current (AC). This may be done in a DC/AC converter, which usually has an almost constant conversion efficiency of 95%. The converter must be designed for synchronisation with the grid, and it is advantageous if it facilitates fuel cell voltage control.
   - Mechanical work produced by a gas turbine is usually transformed into electrical current by an electrical generator. If the shaft speed is constant and runs with the same frequency as the grid, the generator may be directly connected to the grid. If the turbine shaft speed corresponds to half the grid frequency, a double spool alternator may be used. If not, either a gear box or an AC/AC-transformer must be included. Most generators have an energy efficiency of approximately 95%.
   - A SOFC-GT-cycle will produce both alternating and direct current. The two of them may either be independently connected to the grid by suitable power electronics, or the current may be connected to the same bus in order to make the system appear as a single power source to the grid. The latter may be achieved if a rectifier (AC/DC) is applied to

convert AC from the gas turbine generator into DC with the same voltage as the SOFC. Such a system would facilitate a common DC bus for the SOFC and GT and only one DC/AC converter is needed. However, there are many ways of assembling a power electronics system for a SOFC-GT cycle, and the preferred system would also depend on system configuration, size and operation mode of the plant.

c) Afterburner

- After-burner: Combustor where fuel in anode off-gas flow mixed with remaining oxygen in cathode off-gas is burnt. It produces a supplementary heat source to be used in and outside the system.
- Careful design is needed in case of the first approach, as radiation from the hot flames may cause large thermal gradients in the cell materials. In that respect, it may seem more convenient to include a separate afterburner. A separate afterburner may also promote supplementary firing for the gas turbine in a SOFC-GT cycle.

d) Auxiliary air compressor

- Excess air is needed during emergency shut downs or regular shut downs. The purpose of the auxiliary air compressor is to protect the air side of the fuel cell. For safety reasons compressed air is supplied to a storage tank, which facilitates immediate supply of compressed air in case of an emergency shutdown. The auxiliary air compressor can be an off-shelf regular dual fuel internal combustion engine driven compressor.

# CHAPTER IV

# MODELLING OF SOFC SYSTEMS

Mathematical models are more important tools in understanding and examining effects of various designs and operating parameters on SOFC performance, since SOFC system analysis are complexity and limitation of experiment. Therefore, mathematical tool is able to help in SOFC development so as to select optimal designs and operating conditions. This chapter presents mathematical models and configuration of SOFC and other unit operations in system; e.g., turbine, compressor, fuel processor, vaporizer, pre-heater, combustor and pump. Section 4.1 shows the configuration and model equations used for simulating SOFC. Zero- and one-dimensional SOFC model is used in evaluation as given in this chapter. Additionally, the validation of zero- and one-dimensional SOFC model is presented in this section. The fuel professor for ethanol steam reforming reaction of system among conventional reformer, membrane reactor, adsorptive reactor and adsorption-membrane hybrid system considered thermodynamic analysis are presented in Section 4.2. Section 4.3 and Section 4.4 describe model of gas turbine and the other units in system, respectively. Finally, the key parameters used to evaluate the performance are explained in Section 4.5.

## 4.1 SOFC model

In this section, the SOFC model and cell configuration are considered. SOFC model consists of three main parts; i.e. the electrochemical model, mass balance and energy balance in cell. The electrochemical model presents characteristic cell and evaluation of cell performance while the variations of gases and the control of cell temperature because of the reaction occur in cell are explained from mass and energy balance. The simulation models of SOFC are classified into two levels of consideration that are; zero- and one-dimensional analysis. For zero-dimensional model, the electrochemical performance evaluation and mass balance of cell are not considered cell dimension. In one-dimensional model, the electrochemical

performance evaluation and mass balance take into consideration of dimension along cell length which is more accurate than zero-dimensional model.

### 4.1.1 Model Configuration

In this work, the planar SOFC stack is selected to operate at the intermediate temperature SOFCs which use metal-ceramic and stainless steel interconnects as materials for cell. In cell characteristic configuration, an electrochemically active tri-layer cell composed of the anode, electrolyte and cathode (PEN structure) is between the fuel and air channels. A typical SOFC electrolyte is yttria-stabilised zirconia (YSZ) which only allows the oxygen ions to pass through at elevated temperature. The cathode is strontium doped lanthanum maganite mixed with YSZ in from of a composite ($LaSrMnO_3$/YSZ) and the anode is nickel/zirconia (Ni/YSZ). For SOFC designs, the anode-supported SOFC is considered in this study. The anode is the thickest component in cell as the support structure. The cell geometry used in calculation is given in Table 4.1.

**Table 4.1** Dimension of a planar SOFC (Aguiar et al., 2004)

| **Element** | **Size** |
|---|---|
| $L$ | 0.4 m |
| $W$ | 0.1 m |
| $h_{\mathrm{f}}$ | 1 mm |
| $h_{\mathrm{a}}$ | 1 mm |
| $\tau_{\mathrm{anode}}$ | 500 $\mu$m |
| $\tau_{\mathrm{cathode}}$ | 50 $\mu$m |
| $\tau_{\mathrm{electrolyte}}$ | 20 $\mu$m |

### 4.1.2 Electrochemical model

#### 4.1.2.1 Reversible open-circuit voltage

The theoretical open-circuit voltage or the reversible cell voltage computed by the difference between the thermodynamic potentials of the electrode reactions can be expressed by the Nernst equation:

$$E^{\mathrm{OCV}} = E^{0} - \frac{RT}{2F}\ln\left(\frac{P_{\mathrm{H_2O}}}{P_{\mathrm{H_2}} P_{\mathrm{O_2}}^{0.5}}\right) \quad (4.1)$$

where $E^0$ is the open-circuit voltage at standard pressure and is a function of the operating temperature, expressed as:

$$E^{0} = 1.253 - 2.4516\times10^{-4} T(K) \quad (4.2)$$

The operating cell voltage or actual fuel cell voltage ($V$) is always lower than its open-circuit voltage due to the internal voltage losses encountered in real fuel cell operation (Equation (4.3)). There are three dominant voltage losses, which are the function of the temperature, current density and substance concentrations; ohmic loss ($\eta_{\mathrm{ohm}}$); concentration overpotentials ($\eta_{\mathrm{conc}}$) and activation overpotentials ($\eta_{\mathrm{act}}$).

$$V = E - \eta_{\mathrm{ohm}} - \eta_{\mathrm{conc}} - \eta_{\mathrm{act}} \quad (4.3)$$

#### 4.1.2.2 Overpotentials

**Ohmic overpotential**

Ohmic losses ($\eta_{\mathrm{ohm}}$) occur due to the resistance to the flow of ions in the electrolyte and the resistance to the flow of electrons through the electrodes and current collectors. This loss is linearly correlated with the voltage drop and current density (Equation (4.4)).

$$\eta_{\mathrm{ohm}} = jR_{\mathrm{ohm}} \quad (4.4)$$

where $R_{\mathrm{ohm}}$ is the internal resistance, which depends on the conductivity and thickness of the individual layers as shown below:

$$R_{\mathrm{Ohm}} = \frac{\tau_{\mathrm{anode}}}{\sigma_{\mathrm{anode}}} + \frac{\tau_{\mathrm{electrolyst}}}{\sigma_{\mathrm{electrolyst}}} + \frac{\tau_{\mathrm{cathode}}}{\sigma_{\mathrm{cathode}}} \quad (4.5)$$

where $\tau_{\mathrm{anode}}$, $\tau_{\mathrm{cathode}}$ and $\tau_{\mathrm{electrolyte}}$ are the thickness of the anode, cathode and electrolyte layers, respectively. $\sigma_{\mathrm{anode}}$ and $\sigma_{\mathrm{cathode}}$ are the electronic conductivity of the anode and cathode, respectively, and $\sigma_{\mathrm{electrolyte}}$ is the ionic conductivity of the electrolyte. The values of the electronic conductivity in cell component are given in Table 4.2 (Petruzzi et al., 2003).

**Table 4.2** Conductivities of each cell component (Ferguson et al., 1996)

| Parameter | Value |
|---|---|
| $\sigma_{\text{anode}}$ $(\Omega^{-1}\ \text{m}^{-1})$ | $\frac{9.5\text{x}10^{7}}{T}\exp(\frac{-1150}{T})$ |
| $\sigma_{\text{cathode}}$ $(\Omega^{-1}\ \text{m}^{-1})$ | $\frac{4.2\text{x}10^{7}}{T}\exp(\frac{-1200}{T})$ |
| $\sigma_{\text{electrolyte}}$ $(\Omega^{-1}\ \text{m}^{-1})$ | $33.4\text{x}10^{3}\exp(\frac{-10300}{T})$ |

**Concentration overpotential**

The concentration overpotentials ($\eta_{\text{conc}}$) are caused by a decrease in the substances at the surface of the electrodes due to the resistance to mass transport. These overpotentials become significant at high current densities because the rate of hydrogen consumption at the reaction sites is higher than that of diffusion of the reactant through the porous electrode to the reaction sites (Aguiar et al., 2004; Patcharavorachot et al., 2008). These overpotentials can be expressed as:

$$\eta_{\text{conc}} = \eta_{\text{conc,anode}} + \eta_{\text{conc,cathode}} \tag{4.6}$$

$$\eta_{\text{conc,anode}} = \frac{RT}{2F}\ln\left(\frac{p_{\text{H}_2\text{O,TPB}}\, p_{\text{H}_2,\text{f}}}{p_{\text{H}_2\text{O,f}}\, p_{\text{H}_2,\text{TPB}}}\right) \tag{4.7}$$

$$\eta_{\text{conc,cathode}} = \frac{RT}{4F}\ln\left(\frac{p_{\text{O}_2,\text{a}}}{p_{\text{O}_{2,\text{TPB}}}}\right) \tag{4.8}$$

The partial pressures of $H_2$, $H_2O$, and $O_2$ at the three-phase boundaries can be determined by using a gas transport model in porous media as shown in the following expressions:

$$p_{\text{H}_2,\text{TPB}} = p_{\text{H}_2,\text{f}} - \frac{RT\tau_{\text{anode}}}{2FD_{\text{eff,anode}}}\, j \tag{4.9}$$

$$p_{\text{H}_2\text{O,TPB}} = p_{\text{H}_2\text{O,f}} + \frac{RT\tau_{\text{anode}}}{2FD_{\text{eff,anode}}}\, j \tag{4.10}$$

$$p_{O_2,TPB} = P - \left(P - p_{O_2,a}\right)\exp\left(\frac{RT\tau_{cathode}}{4FD_{eff,cathode}P}\,j\right) \tag{4.11}$$

where $P$ is the operating SOFC pressure, $D_{eff,anode}$ is the effective gaseous diffusivity through the anode (considered to be a binary gas mixture of $H_2$ and $H_2O$) and $D_{eff,cathode}$ is the effective oxygen diffusivity through the cathode (considered to be a binary gas mixture of $O_2$ and $N_2$). The effective diffusivity for both cathode and anode is given in Table 4.3 (Kim et al., 1999; Virkar et al., 2000; Chan et al., 2001).

**Table 4.3** Values of cathode and anode effective diffusivities

| **Parameter** | **Value** |
|---|---|
| $D_{eff,anode}$ ($m^2\ s^{-1}$) | $3.66x10^{-5}$ |
| $D_{eff,cathode}$ ($m^2\ s^{-1}$) | $1.37x10^{-5}$ |

**Activation overpotential**

The activation overpotentials ($\eta_{act}$) are caused by the sluggishness of the electrochemical reaction at the electrode surfaces. The activation overpotentials can be determined by the non-linear Butler–Volmer equation as follows:

$$j = j_{0,anode}\left[\frac{p_{H_2,TPB}}{p_{H_{2,f}}}\exp\left(\frac{\alpha nF}{RT}\eta_{act,anode}\right) - \frac{p_{H_2O,TPB}}{p_{H_2O,f}}\exp\left(-\frac{(1-\alpha)nF}{RT}\eta_{act,anode}\right)\right] \tag{4.12}$$

$$j = j_{0,cathode}\left[\exp\left(\frac{\alpha nF}{RT}\eta_{act,cathode}\right) - \exp\left(-\frac{(1-\alpha)nF}{RT}\eta_{act,cathode}\right)\right] \tag{4.13}$$

where $\alpha$ is the transfer coefficient which is usually taken to be 0.5 (Chan et al., 2001; Aguiar et al., 2004) $n$ is the number of electrons transferred in the single elementary rate-limiting reaction step represented by the Butler–Volmer equation, $j_{0,cathode}$ and $j_{0,anode}$ are the exchange current density of anode and cathode which depends on the operating temperature as shown in Equation (4.14)-(4.15), respectively.

$$j_{0,\text{cathode}} = \frac{RT}{nF} k_{\text{cathode}} \exp\left(-\frac{E_{\text{cathode}}}{RT}\right) \quad (4.14)$$

$$j_{0,\text{anode}} = \frac{RT}{nF} k_{\text{anode}} \exp\left(-\frac{E_{\text{anode}}}{RT}\right) \quad (4.15)$$

where $E_{\text{cathode}}$ and $E_{\text{anode}}$ represent the activation energies of the cathode and anode exchange current densities, respectively, and $k_{\text{cathode}}$ and $k_{\text{anode}}$ denote the pre-exponential factors of the exchange current density of cathode and anode, respectively. The value of all parameters is used in the calculation of the exchange current density in Table 4.4 (Jiang et al., 1999 and Holtappels et al., 1999).

**Table 4.4** Values of the parameters used for activation overpotential

| **Parameter** | **Value** |
|---|---|
| $E_{\text{anode}}$ (kJ mol$^{-1}$) | 140 |
| $E_{\text{cathode}}$ (kJ mol$^{-1}$) | 137 |
| $k_{\text{cathode}}$ ($\Omega^{-1}$m$^{-2}$) | 2.35x10$^{11}$ |
| $k_{\text{anode}}$ ($\Omega^{-1}$m$^{-2}$) | 6.54 x 10$^{11}$ |

### 4.1.3 Mass balance

The synthesis gas obtained from the ethanol steam reformer consists of $CH_4$, $H_2$, $H_2O$, CO, and $CO_2$ and is fed to a fuel channel of the SOFC. Because the SOFC is operated at high temperatures, a steam reforming reaction of methane (Equation (4.16)) and a water gas shift reaction (Equation (4.17)) can occur within the SOFC stack. Furthermore, the use of Ni–cermet as the anode can provide sufficient activity for the steam reforming reaction.

Steam reforming: $CH_4 + H_2O \rightarrow CO + 3H_2$ (4.16)

Water gas shift: $CO + H_2O \leftrightarrow CO_2 + H_2$ (4.17)

Hydrogen is produced from the ethanol steam reformer as well as from the methane reforming and water gas-shift reactions on the anode side and is consumed by the oxidation reaction (Equation (4.18)) to generate steam and electrons. Oxygen in the air that is fed at the cathode side is reduced to oxygen ions (Equation (4.19))

that migrate through the electrolyte. The overall electrochemical reaction occurring within the SOFC is shown in Equation 4.20. The electrons flow from the anode to the cathode to produce direct-current electricity.

Cathode: $0.5O_2 + 2e^- \rightarrow O^{2-}$ (4.18)

Anode: $H_2 + O^{2-} \rightarrow H_2O + 2e^-$ (4.19)

Overall: $H_2 + 0.5O_2 \rightarrow H_2O$ (4.20)

It is noted that the electrochemical reaction of carbon monoxide is neglected since the real mechanism for the consumption of carbon monoxide within anode compartment is not clear at present (Kendell and Singhal, 2003).

#### 4.1.3.1 Zero-dimensional analysis

In this model, the molar flow rates of each component at the SOFC outlet can be determined based on thermodynamics analysis. Eguchi et al. (2002) investigated the shift reaction at Ni–cermet anodes. Their results showed that the conversions are always close to the equilibrium compositions. The equilibrium constants of all the reactions can be determined form the Van't Hoff equation (Equation (4.21)) as

$$\frac{d \ln K}{dT} = \frac{\Delta H^{\circ}}{RT^2} \tag{4.21}$$

where $K$, $T$ and $R$ represent, respectively, the equilibrium constant, the operating temperature and the gas constant, and $\Delta H^{o}$ is the heat of reaction.

As all the reactions take place in the gas phase, the equilibrium constant can be expressed in terms of pressure and composition as follows:

$$\prod_i (y_i \phi_i)^{v_i} = \left( \frac{P}{P^0} \right)^{-v} K \tag{4.22}$$

with

$$v = \sum_i v_i \text{ and } y_i = \frac{n_i}{\sum_i n_i} \tag{4.23}$$

where $P$, $P^0$, $y_i$ and $v_i$ are the total pressure, the pressure at standard condition (1 bar), the mole fraction of the component $i$, and the stoichiometric coefficient, respectively, and $\phi_i$ is the fugacity coefficient of the component $i$.

The molar flow rates of each component at the SOFC outlet can be determined based on the reaction equilibrium. The relationships between the thermodynamic equilibrium constants and gaseous components for the steam reforming and water gas shift reactions in the SOFC stack are shown in Equations (4.24) and (4.25), respectively.

$$K_{\text{eq,SM}} = \frac{p_{\text{CO,an}}\, p_{\text{H}_2\text{,an}}^3}{p_{\text{CH}_4\text{,an}}\, p_{\text{H}_2\text{O,an}}} \tag{4.24}$$

$$K_{\text{eq,WGS}} = \frac{p_{\text{CO}_2\text{,an}}\, p_{\text{H}_2\text{,an}}}{p_{\text{CO,an}}\, p_{\text{H}_2\text{O,an}}} \tag{4.25}$$

when $p_{\text{i,sofc}}$ is the partial pressure of species $i$ at outlet SOFC.

In case of the calculation of the molar flow rates at the SOFC outlet, moles of hydrogen are deducted from being consumed in the electrochemical reaction ( $\dot{z}$ ).
The current density (*j*) generated by the fuel cell involves the decrease of hydrogen by the electrochemical reaction at the anode side (Equation (4.26)):

$$j = \frac{2.F.\dot{z}}{A_{\text{c}}} \tag{4.26}$$

where $F$ is Faraday constant and $A_{\text{c}}$ is the cell activation area.

The outlet molar flow rate of each gas from SOFC is given by following expressions:

For anode's components

$$n_{\text{EtOH,an}}^{\text{out}} = n_{\text{EtOH,an}}^{\text{in}} \tag{4.27}$$

$$n_{\text{CH}_4\text{,an}}^{\text{out}} = n_{\text{CH}_4\text{,an}}^{\text{out}} + x_{1,\text{an}} \tag{4.28}$$

$$n_{\text{CO}_2\text{,an}}^{\text{out}} = n_{\text{CO}_2\text{,an}}^{\text{in}} + x_{2,\text{an}} \tag{4.29}$$

$$n_{\text{CO,an}}^{\text{out}} = n_{\text{CO,an}}^{\text{in}} + x_{1,\text{an}} - x_{2,\text{an}} \tag{4.30}$$

$$n_{\text{H}_2\text{,an}}^{\text{out}} = n_{\text{H}_2\text{,an}}^{\text{in}} + 3x_{1,\text{an}} + x_{2,\text{an}} - \dot{z} \tag{4.31}$$

$$n_{\text{H}_2\text{O,an}}^{\text{out}} = n_{\text{H}_2\text{O,an}}^{\text{in}} - x_{1,\text{an}} - x_{2,\text{an}} + \dot{z} \tag{4.32}$$

$$n_{\text{total,an}}^{\text{out}} = \sum_{i=1}^{6} n_{\text{i,an}}^{\text{out}} \tag{4.33}$$

For cathode's components

$$n_{\mathrm{O_2,ca}}^{\mathrm{out}} = n_{\mathrm{O_2,ca}}^{\mathrm{out}} - 0.5\dot{z} \tag{4.34}$$

$$n_{\mathrm{N_2,ca}}^{\mathrm{out}} = n_{\mathrm{N_2,ca}}^{\mathrm{in}} \tag{4.35}$$

$$n_{\mathrm{total,ca}}^{\mathrm{out}} = \sum_{i=1}^{2} n_{\mathrm{i,ca}}^{\mathrm{out}} \tag{4.36}$$

where $n_{\mathrm{EtOH,an}}^{\mathrm{out}}$, $n_{\mathrm{CH_4,an}}^{\mathrm{out}}$, $n_{\mathrm{CO_2,an}}^{\mathrm{out}}$, $n_{\mathrm{CO,an}}^{\mathrm{out}}$, $n_{\mathrm{H_2,an}}^{\mathrm{out}}$ and $n_{\mathrm{H_2O,an}}^{\mathrm{out}}$ represent moles of ethanol, methane, carbon monoxide, carbon dioxide, hydrogen and steam in anode channel and $n_{\mathrm{O_2,ca}}^{\mathrm{out}}$, $n_{\mathrm{N_2,ca}}^{\mathrm{out}}$ represent moles of oxygen and nitrogen respectively.

#### 4.1.3.2 One-dimensional analysis

In this study, the flow direction of species gas in the SOFC stack is selected as *x*-direction while the *y*- and *z*- direction are the cell height and width direction, respectively, as shown in Figure 4.1. For one-dimensional model, the variation of species gas along the flow direction is considered while those in the vertical and transverse direction are ignored.

The steam reforming (Equation (4.16)) and water gas shift reactions (Equation (4.17)) taken place on anode side in this model explains from kinetic rate. The kinetic of methane reforming on nickel cermet SOFC anode developed from Achenbach et al. (1994) and Belyaev et al. (1995) is written as

$$R_{\mathrm{SR}} = k_{\mathrm{act}}\, p_{\mathrm{f,CH_4}} \exp\left(\frac{-E_{\mathrm{act}}}{RT_{\mathrm{f}}}\right) \tag{4.37}$$

For the water gas-shift reaction, an equilibrium-limited shift reaction rate expression is used because it is considered that occurs at equilibrium in the fuel channel. The rate expression of water gas shift is first order in carbon monoxide and with an arbitrarily high pre-exponential factor ($k_{\mathrm{WGSR}}$) (Aguiar et al., 2004; Haberman et al., 2004), given by

$$R_{\mathrm{WGS}} = k_{\mathrm{WGSR}}\, p_{\mathrm{f,CO}} \left(1 - \frac{p_{\mathrm{f,CO_2}}\, p_{\mathrm{f,H_2}}}{K_{\mathrm{eq}}\, p_{\mathrm{f,CO}}\, p_{\mathrm{f,H_2O}}}\right) \tag{4.38}$$

The kinetic parameters used in the rate equations for steam reforming and the water gas-shift reactions are summarized in Table 4.5.

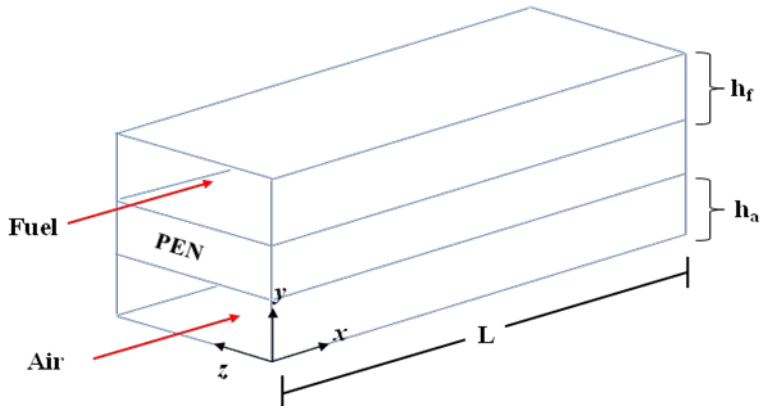


**Figure 4.1** Flow direction of air and fuel in planar solid oxide fuel cell.

**Table 4.5** Kinetic parameters for rate equations

| **Reaction** | **Parameter** | **Value** |
|---|---|---|
| Steam reforming reaction | $k_{act}$ (mol $s^{-1}$ $m^{-2}$$bar^{-1}$) | 4274 |
| | $E_{act}$ (kJ $mol^{-1}$) | 82 |
| Water gas shift reaction | $k_{WGSR}$ (-) | 0.01 |
| | $K_{eq}$ (-) | $\exp\left(\frac{4276}{T_f}-3.961\right)$ |

The solid oxide fuel cell products the electricity through the electrochemical reaction. The relation between variation of reactant fluxes and the electricity produced from cell can be explained Faraday's law. According to this law, the amount of hydrogen and oxygen consumed, the amount of water produced can be determined the local electrical current density produced in the cell, as expressed in Equation (4.39).

$$R_k = \frac{j}{2F} \tag{4.39}$$

The reformed gas is fed into fuel channel and the air is fed air channel. Thus, the fuel channel consists of $CH_4$, $H_2O$, CO, $H_2$, and $CO_2$ while in the air channel the chemical species are $O_2$ and $N_2$. The component concentrations in fuel and air channel along the axial direction can be described from the differential equations, which can be written as follows.

Fuel channel: ($i$ = $CH_4$, $H_2O$, CO, $H_2$, and $CO_2$)

$$\frac{dC_{\mathrm{EtOH,an}}}{dx} = 0 \tag{4.40}$$

$$\frac{dC_{\mathrm{CH_4,an}}}{dx} = \frac{1}{u_{\mathrm{f}} h_{\mathrm{f}}}\left(-R_{\mathrm{SR}}\right) \tag{4.41}$$

$$\frac{dC_{\mathrm{CO_2,an}}}{dx} = \frac{1}{u_{\mathrm{f}} h_{\mathrm{f}}}\left(R_{\mathrm{WGS}}\right) \tag{4.42}$$

$$\frac{dC_{\mathrm{CO,an}}}{dx} = \frac{1}{u_{\mathrm{f}} h_{\mathrm{f}}}\left(R_{\mathrm{SR}} - R_{\mathrm{WGS}}\right) \tag{4.43}$$

$$\frac{dC_{\mathrm{H_2,an}}}{dx} = \frac{1}{u_{\mathrm{f}} h_{\mathrm{f}}}\left(3R_{\mathrm{SR}} + R_{\mathrm{WGS}} - R_{elec}\right) \tag{4.44}$$

$$\frac{dC_{\mathrm{H_2O,an}}}{dx} = \frac{1}{u_{\mathrm{f}} h_{\mathrm{f}}}\left(R_{\mathrm{WGS}}\right) \tag{4.45}$$

$$C_{\mathrm{i,an}}\Big|_{x=0} = C^{0}_{\mathrm{i,an}} \tag{4.46}$$

Air channel: ($i$ = $O_2$ and $N_2$)

$$\frac{dC_{\mathrm{O_2,ca}}}{dx} = \frac{1}{u_{\mathrm{a}} h_{\mathrm{a}}}(-0.5R_{elec}) \tag{4.47}$$

$$\frac{dC_{\mathrm{N_2,ca}}}{dx} = 0 \tag{4.48}$$

$$C_{i,\mathrm{a}}\Big|_{x=0} = C^{0}_{i,\mathrm{a}} \tag{4.49}$$

where $C_{\mathrm{i,an}}$ is the concentration of species i , $u_{\mathrm{f}}$ and $u_{\mathrm{a}}$ are the inlet velocity of fuel and air respectively as well as $h_{\mathrm{f}}$ and $h_{\mathrm{a}}$ are the height of fuel and air channel respectively.

In this SOFC model, it is assumed which is the distributed model, so the average current density ( $j_{\mathrm{avg}}$ ) can be calculated by

$$j_{\mathrm{avg}} = \frac{1}{L}\int_{0}^{L} I(z)dz \tag{4.50}$$

### 4.1.4 Energy balance

In this study, the SOFC is assumed to operate under adiabatic condition; therefore, flowing excess air through the SOFC is required to control cell operating temperature, as shown Figure 4.2. The amount of excess inlet airflow fed into solid oxide fuel cell can be calculated from energy balance around the control volume enclosing the fuel cell given as:

$$(\sum_{i} \dot{n}_{\mathrm{i,an}}^{\mathrm{in}} \dot{h}_{\mathrm{i,an}}^{\mathrm{in}}) + (\sum_{i} \dot{n}_{\mathrm{i,ca}}^{\mathrm{in}} \dot{h}_{\mathrm{i,ca}}^{\mathrm{in}}) - (\sum_{o} \dot{n}_{\mathrm{i,an}}^{\mathrm{out}} \dot{h}_{\mathrm{i,an}}^{\mathrm{out}}) - (\sum_{o} \dot{n}_{\mathrm{i,ca}}^{\mathrm{out}} \dot{h}_{\mathrm{i,ca}}^{\mathrm{out}}) - P_{\mathrm{sofc}} = 0 \tag{4.51}$$

where $\dot{n}_i$ is molar flow rate of species $i$ and $\dot{h}_i$ is the enthalpy of species $i$ which is determined in Equation (4.50)

$$\dot{h} = h^0 + \int_{298}^{T_{sofc}} C_{\mathrm{p}} dT \tag{4.52}$$

where $h^0$ is the enthalpy at standard condition (temperature of 298 K and pressure of 1atm)

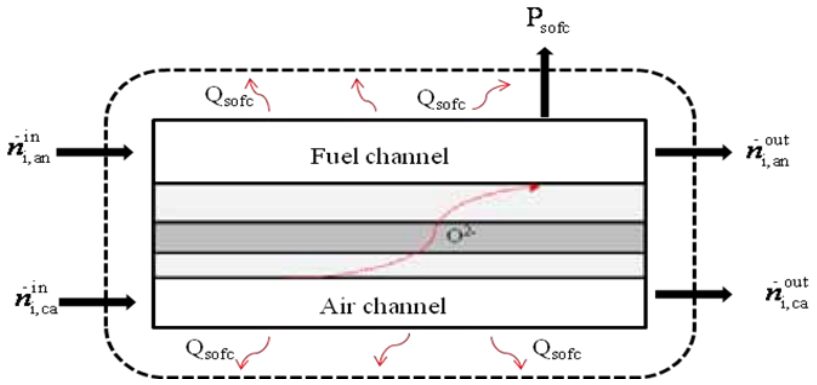


**Figure 4.2** Control volume of energy balance in solid oxide fuel cell.

### 4.1.5 SOFC performance parameters

Fuel utilization ratio is the amount of hydrogen that is reacted in electrochemical reaction to the amount of hydrogen in the inlet stream, as expressed in Equation (4.53).

$$U_{\mathrm{f}} = \frac{\dot{n}_{\mathrm{H_2,utillized}}}{\dot{n}_{\mathrm{H_2,inlet}}} \tag{4.53}$$

where $\dot{n}_{\mathrm{H_2,utillized}}$ is the hydrogen molar flow consumed in the electrochemical reaction

and $\dot{n}_{H_2,inlet}$ is the inlet molar flow rate of hydrogen fed into solid oxide fuel cell. It should be noted that if the fuel is reformed internally at the anode catalyst, hydrogen produced by the reforming reaction(s) should be added to the term $\dot{n}_{H_2,inlet}$.

Air utilization ratio is the amount of oxygen that is reacted in electrochemical reaction to the amount of oxygen in the inlet stream, as expressed in Equation (4.54)

$$U_a = \frac{\dot{n}_{O_2,utillized}}{\dot{n}_{O_2,inlet}} \tag{4.54}$$

where $\dot{n}_{O_2,utillized}$ is the oxygen molar flow consumed in the electrochemical reaction and $\dot{n}_{O_2,inlet}$ is the inlet molar flow rate of hydrogen fed into solid oxide fuel cell.

Excess air coefficient is the amount of the oxygen in the inlet stream to the amount of oxygen that is needed for a stoichiometry of electrochemical reaction, as follow in Equation (4.55)

$$\lambda_{air} = \frac{2\dot{n}_{O_2,inlet}}{\dot{n}_{H_2,inlet}} \tag{4.55}$$

For the relation among fuel utilization, air utilization ratio and excess air coefficient, Equation (4.53) to Equation (4.55) are combined into Equation (4.56)

$$U_f = U_a \lambda_{air} \tag{4.56}$$

For practical, the electrical power output ($P_{sofc,dc}$) is obtained when a reasonably current is drawn from the cell, which is defined as

$$P_{sofc,dc} = j \times V \tag{4.57}$$

Electrical power generated from SOFC is direct current (DC) which is converted to alternating current (AC) in inverter. The dc-ac inverter efficiency is specified as 94% (Akkaya et al., 2008) so the alternating current from SOFC can be determined in Equation (4.58)

$$P_{sofc,ac} = P_{sofc,dc} \times \eta_{invert} \tag{4.58}$$

The efficiency of solid oxide fuel cell means that the value ratio of the electrical energy converted from the energy content of the hydrogen, which represents thermal energy of fuel fed into cell namely methane, carbon monoxide and hydrogen. The efficiency of solid oxide fuel cell can be expressed Equation (4.59)

$$\eta_{\text{cell}} = \frac{P_{\text{cell}}}{(y^{\text{in}}_{\text{H}_2,\text{an}} LHV_{\text{H}_2} + y^{\text{in}}_{\text{CO,an}} LHV_{\text{CO}} + y^{\text{in}}_{\text{CH}_4,\text{an}} LHV_{\text{CH}_4}) \dot{n}^{\text{in}}_{\text{total,an}}} \tag{4.59}$$

where $LHV_i$ is low heating value and $y_i^{\text{in}}$ is mole fraction of component $i$

The corresponding cell voltage then determines the fuel cell efficiency. Decreasing the current density increases the cell voltage, thereby increasing the fuel cell efficiency. The trade-off is that as the current density is decreased, the active cell area must be increased to obtain the requisite amount of power. Thus, designing the fuel cell for higher efficiency increases the capital cost, but decreases the operating cost.

### 4.1.6 Calculation procedure

The simulation of mathematical models in this work was performed by programming codes in MATLAB 7.0, which can solve the formulated nonlinear and order differential equations. The procedures of calculation between zero-dimensional and one-dimensional model are different.

#### 4.1.6.1 Zero-dimensional model

The flow diagram of numerical solution for calculating the SOFC performance with using zero-dimensional model is shown in Figure 4.3. This model can determine the current density at the cell voltage and the suitable excess air ratio required for SOFC. The value of cell geometry and material properties as well as the operating conditions i.e., fuel and air composition, operating temperature, pressure, fuel utilization, cell voltage and inlet air temperature are specified. In the first of this procedure, the inlet molar flow rate of fuel and excess air ratio are presumed in order to calculate the amount of hydrogen consumed in the electrochemical reaction and the current density. The rate of consumption of hydrogen can calculate from fuel utilization in Equation (4.53), which transform into Equation (4.60).

$$\dot{z} = U_{\text{f}} (4\dot{n}_{\text{CH}_4} + \dot{n}_{\text{H}_2} + \dot{n}_{\text{CO}}) \tag{4.60}$$

The anode and cathode outlet molar flow rate of species gas are calculated. Afterwards, the open-circuit voltage, ohmic, concentration and activation overpotentials are evaluated by employing the sets of equation given in Section 4.1.2.

The actual voltage (Equation 4.3) and power density (Equation 4.57) are found. The iterative procedure is required when the values of actual voltage and inlet air temperature calculated do not match with the design condition. Thus, the inlet molar flow rate of fuel and the air excess ratio are guess again.

#### 4.1.6.2 One-dimensional model

For one-dimensional model, the flow diagram of numerical solution for calculating the SOFC performance is shown in Figure 4.4. The cell geometry, material properties, operating temperature, pressure, cell voltage are initially input into program. In this model, the average current density and excess air ratio at the required value of the fuel utilization and inlet air temperature are found. The calculation of this model begins with guessing the inlet molar flow rate of fuel and excess air ratio. The molar flow rate of various species gases at anode and cathode, open-circuit voltage, current density, ohmic, concentration, and activation overpotentials that are function of distance along cell length are calculated based on the electrochemical and the mass balance model in Section 4.1.2 and Section 4.1.3.2. The average current density and fuel utilization of cell can be considered in Equation (4.54) and Equation (4.57) while the inlet air temperature is calculated in Equation (4.51) and Equation (4.52). The iterative run is performed until matching between the value of the fuel utilization and inlet air temperature calculated and designed.

### 4.1.7 Model validation

The SOFC model was verified with the experimental data of Zhao and Virkar (2005) to ensure its reliability. The values of the operating parameters used for model validation are presented in Table 4.6. The comparison of the model prediction with the experimental data regarding the operating voltage of the SOFC at different current densities and operating temperatures is shown in Figure 4.5. It can be seen that the model prediction shows a good agreement with the experimental data of the SOFC operated under the temperature range used in this study. The model parameters may differ from the experiment as they are taken from different sources and this factor causes the error between the model prediction and experimental data; however, this error can be reasonably acceptable.

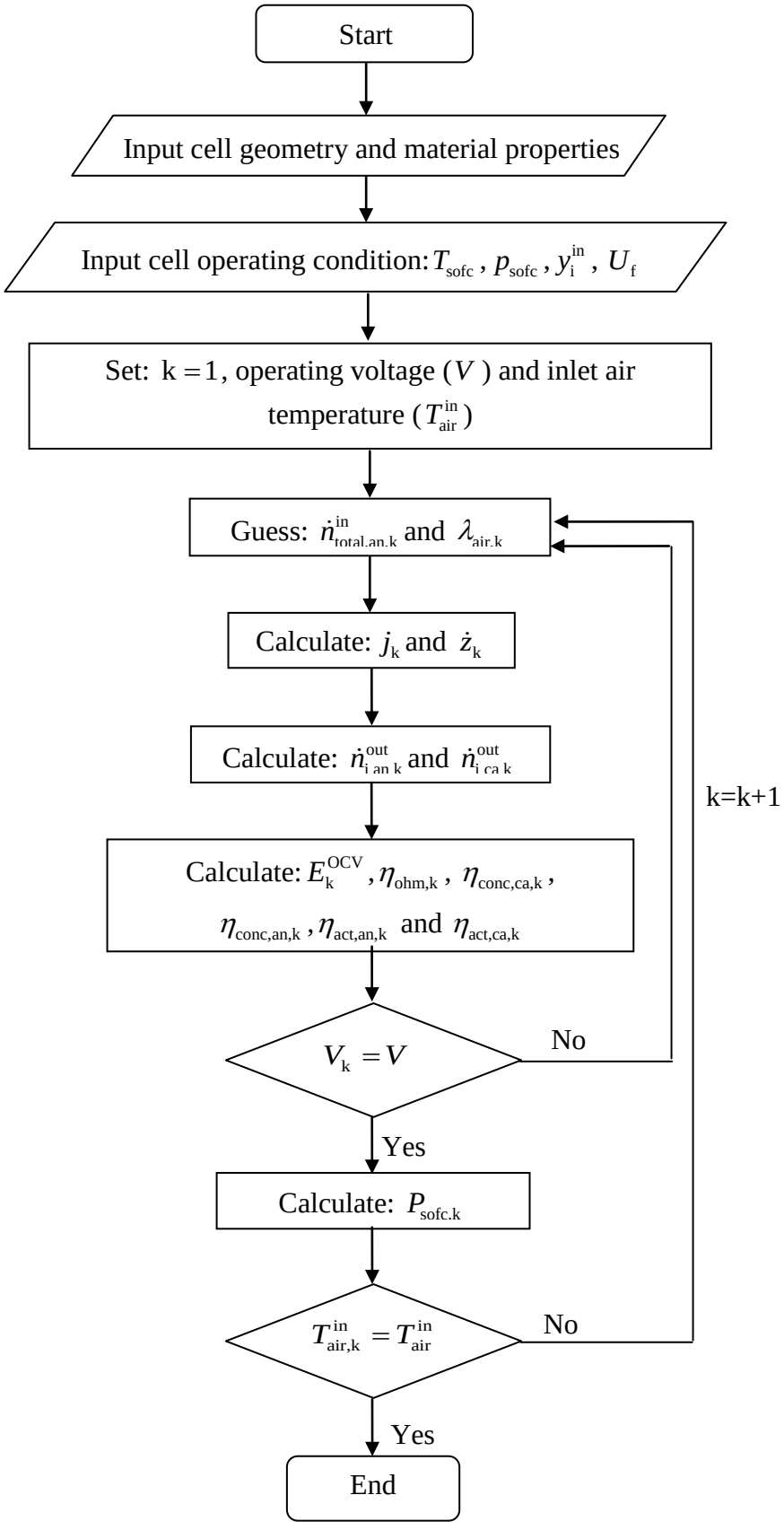


**Figure 4.3** Numerical solution of a zero-dimensional model of SOFC.

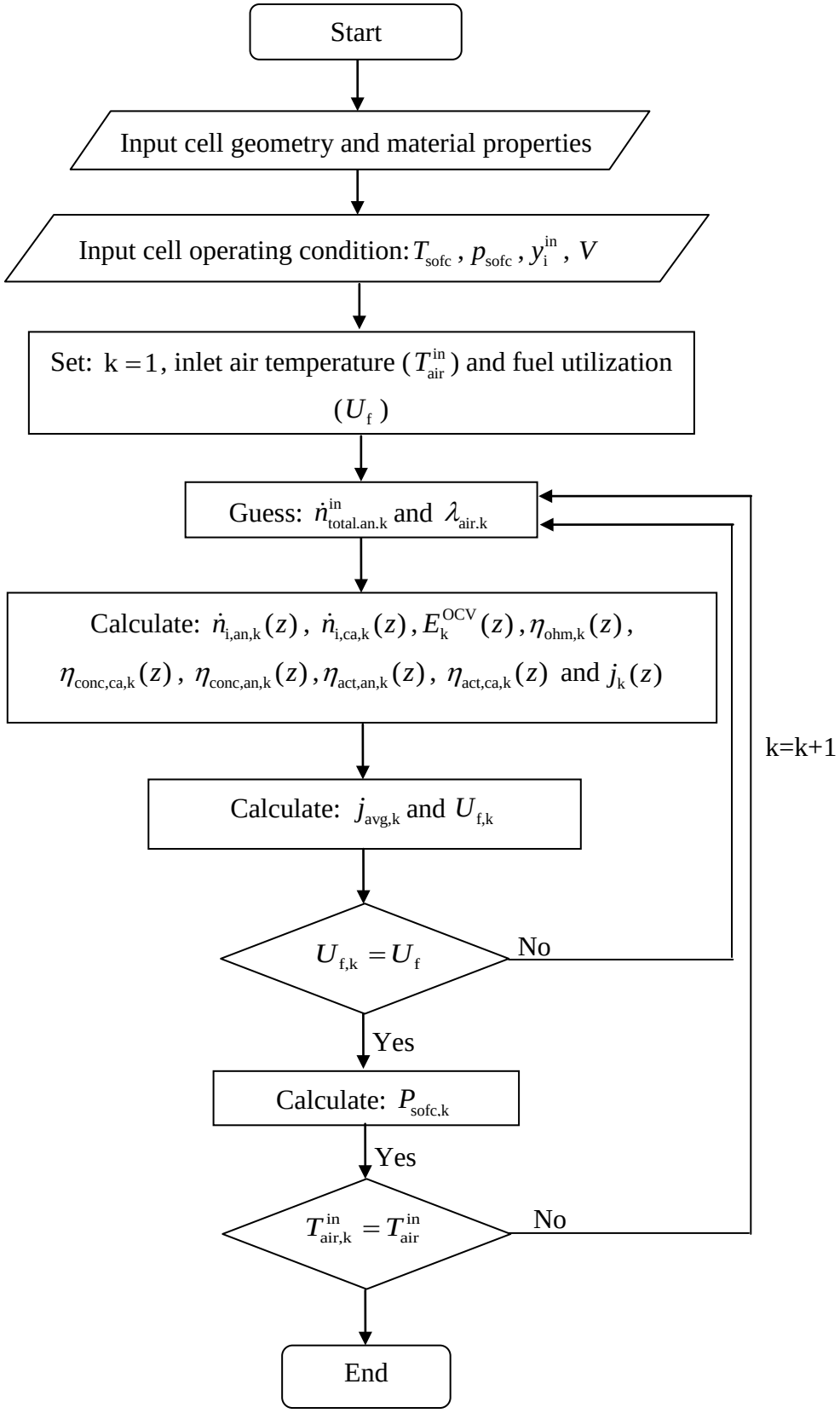


**Figure 4.4** Numerical solution of a one-dimensional model of SOFC

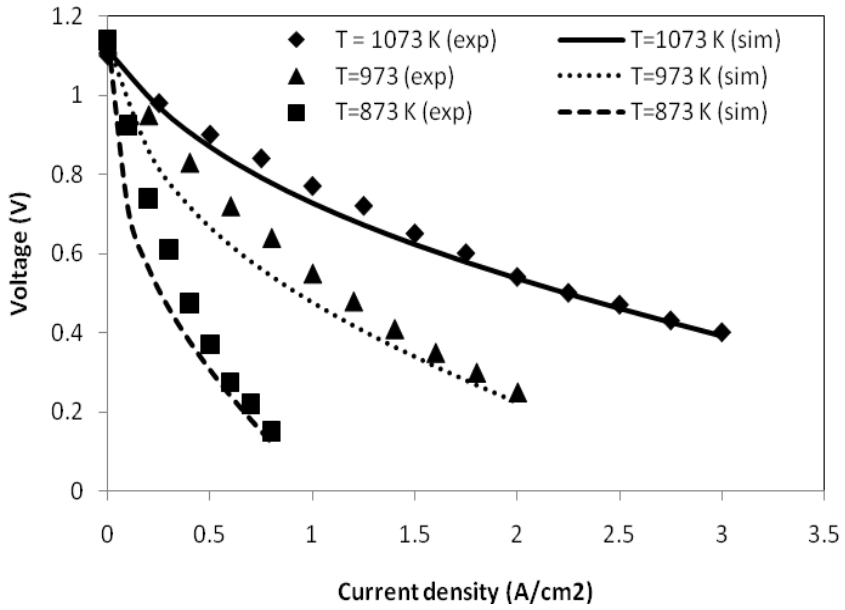


**Figure 4.5** Comparison between the model predictions and experimental results of Zhao and Virkar (2005).

**Table 4.6** Input parameters used in model validation (Zhao and Virkar, 2005).

| | |
|---|---|
| Operating temperature, $T_{sofc}$ (K) | 873, 973, 1073 |
| Operating pressure, $P_{sofc}$ (bar) | 1 |
| Air composition | 21% $O_2$, 79% $N_2$ |
| Fuel composition | 97% $H_2$, 3 % $H_2O$ |
| Cell length, $L$ (m) | 0.4 |
| Cell width, $W$ (m) | 0.1 |
| Fuel channel height, $h_f$ (mm) | 1 |
| Air channel height, $h_a$ (mm) | 1 |
| Anode thickness, $\tau_{anode}$ ($\mu$m) | 1000 |
| Cathode thickness, $\tau_{cathode}$ ($\mu$m) | 20 |
| Electrolyte thickness, $\tau_{electrolyte}$ ($\mu$m) | 8 |

## 4.2 Fuel processor

### 4.2.1 Conventional fuel processor: Thermodynamic analysis

In this study, a thermodynamic analysis of ethanol reforming systems is performed by using a stoichiometric approach to compute the equilibrium composition of reformed products. In the ethanol steam reforming, the following reactions are considered (Freni et al., 1996).

$$C_2H_5OH + H_2O \leftrightarrow 4H_2 + 2CO \tag{4.61}$$

$$CO + H_2O \leftrightarrow H_2 + CO_2 \tag{4.62}$$

$$CO + 3H_2 \leftrightarrow CH_4 + H_2O \tag{4.63}$$

The equilibrium compositions of synthesis gas obtained from the fuel processor can be determined by using a stoichiometric approach. The fuel professor is assumed to operate at isothermal condition so as to simplify the calculations. The equilibrium constants of each reaction (4.61)-(4.63) can be written as:

$$K_{\text{eq,SE}} = \frac{p_{\text{CO,r}}^2 p_{\text{H}_2\text{,r}}^4}{p_{\text{C}_2\text{H}_5\text{OH,r}} p_{\text{H}_2\text{O,r}}} \tag{4.64}$$

$$K_{\text{eq,WGS}} = \frac{p_{\text{CO}_2\text{,r}} p_{\text{H}_2\text{,r}}}{p_{\text{CO,r}} p_{\text{H}_2\text{O,r}}} \tag{4.65}$$

$$K_{\text{eq,MR}} = \frac{p_{\text{CH}_4\text{,r}} p_{\text{H}_2\text{O,r}}}{p_{\text{CO,r}} p_{\text{H}_2\text{,r}}^3} \tag{4.66}$$

where $K_{\text{eq,j}}$ represents the equilibrium constants associated to the reaction $j$ and $p_{\text{i,r}}$ is the partial pressures of the component $i$ in steam reformer.

The molar flow rates of each component for reactions in the ethanol steam reforming are given by the following expressions:

$$n_{\text{EtOH,r}}^{\text{out}} = a - x_{1,\text{r}} \tag{4.67}$$

$$n_{\text{H}_2\text{O,r}}^{\text{out}} = b - x_{1,\text{r}} - x_{2,\text{r}} + x_{3,\text{r}} \tag{4.68}$$

$$n_{\text{H}_2\text{,r}}^{\text{out}} = d + 4x_{1,\text{r}} + x_{2,\text{r}} - 3x_{3,\text{r}} \tag{4.69}$$

$$n_{\text{CO,r}}^{\text{out}} = g + 2x_{1,\text{r}} - x_{2,\text{r}} - x_{3,\text{r}} \tag{4.70}$$

$$n_{\text{CH}_4\text{,r}}^{\text{out}} = m + x_{3,\text{r}} \tag{4.71}$$

$$n_{\mathrm{CO_2,r}}^{\mathrm{out}} = e + x_{2,\mathrm{r}} \tag{4.72}$$

$$n_{\mathrm{total,r}}^{\mathrm{out}} = \sum_{i-1}^{6} n_i = a + b + d + e + g + m + 4x_{1,\mathrm{r}} - 3x_{2,\mathrm{r}} \tag{4.73}$$

where $x_{1,\mathrm{r}}$, $x_{2,\mathrm{r}}$ and $x_{3,\mathrm{r}}$ are the extent of ethanol steam reforming, water gas shift and methanation reactions in Equation (4.61)–(4.63), respectively. In case of non-recycling the anode exhaust gas, $a$ and $b$ represent the inlet moles of ethanol and water of steam reformer, respectively. For recycling the anode exhaust gas, $a$ represents the inlet moles of ethanol and $b$, $d$, $e$, $g$, $m$ represent the inlet moles of water, hydrogen, carbon dioxide, carbon monoxide, methane of steam reformer in which are recycled from SOFC anode exhaust gas, respectively.

The ethanol steam reforming is the endothermic reaction which requiring for supplying this unit. In analysis of energy used in system, the heat used in reformer for ethanol steam reforming reaction can be found from energy balance equation given as:

$$Q_{SR,r} = (\sum_{o} \dot{n}_{\mathrm{i,r}}^{\mathrm{out}} \dot{h}_{\mathrm{i,r}}^{\mathrm{out}}) - (\sum_{i} \dot{n}_{\mathrm{i,r}}^{\mathrm{in}} \dot{h}_{\mathrm{i,r}}^{\mathrm{in}}) \tag{4.74}$$

### 4.2.2 Membrane and $CO_2$ adsorption: Thermodynamic analysis

In an adsorption-membrane hybrid system of ethanol steam reforming, carbon dioxide adsorbent is mixed with steam reforming catalyst in a membrane reactor; carbon dioxide is removed from the reaction zone by adsorbent whereas hydrogen is separated from the reaction zone by membrane, as demonstrated in Figure 4.6.

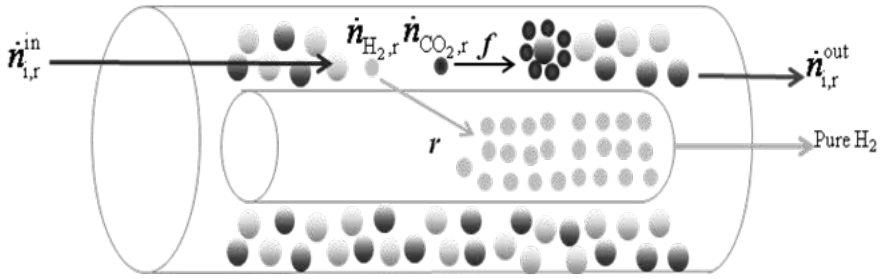


**Figure 4.6** Schematic of adsorption-membrane hybrid system

Considering the carbon dioxide adsorption and the hydrogen separation in the ethanol steam reforming process, the molar flow of carbon dioxide and hydrogen are expressed as:

$$n_{\mathrm{CO_2,r}}^{\mathrm{out}} = x_{2,\mathrm{r}} - fx_{2,\mathrm{r}} \tag{4.75}$$

$$n_{\mathrm{H_2,r}}^{\mathrm{out}} = 4x_{1,\mathrm{r}} + x_{2,\mathrm{r}} - 3x_{3,\mathrm{r}} - r(4x_{1,\mathrm{r}} + x_{2,\mathrm{r}} - 3x_{3,\mathrm{r}}) \tag{4.76}$$

where $f$ is the fraction of carbon dioxide that is removed by adsorption and $r$ is the fraction of hydrogen that is removed through membrane. As a result, the total moles of all species in the gas phase are decreased as shown below:

$$n_{\mathrm{total,r}} = \sum_{i-1}^{6} n_i = a + b + 4x_1 - 3x_2 - fx_2 - r(4x_1 + x_2 - 3x_3) \tag{4.77}$$

It is noted that for an adsorptive reactor, the composition of gases produced can be computed by setting the fraction of hydrogen removal through membrane to be zero. On the contrary, the fraction of carbon dioxide removal by adsorption equals to zero when a membrane reactor is applied to ethanol steam reforming.

### 4.2.3 Boundary of carbon formation

For carbon formation in reformer, three reactions are the most possible reactions that can lead to the formation of carbon in the ethanol reforming system, i.e., Boudouard reaction (Equation (4.78)), methane cracking reaction (Equation (4.79)), and CO reduction (Equation (4.80)), as follows:

$$2\mathrm{CO} \rightleftharpoons \mathrm{CO_2} + \mathrm{C} \tag{4.78}$$

$$\mathrm{CH_4} \rightleftharpoons 2\mathrm{H_2} + \mathrm{C} \tag{4.79}$$

$$\mathrm{CO} + \mathrm{H_2} \rightleftharpoons \mathrm{H_2O} + \mathrm{C} \tag{4.80}$$

In the calculation of the boundary of carbon formation, the thermodynamic analysis of carbon formation is examined by considering the Boudouard reaction since it shows the lowest value of Gibbs free energy. The possibility of carbon formation is calculated from the value of carbon activity as defined:

$$a_{\mathrm{c}} = \frac{K_{\mathrm{b}} p_{\mathrm{CO,r}}^2}{p_{\mathrm{CO_2,r}}} \tag{4.81}$$

where $a_c$ is activity coefficient of carbon and $K_b$ represents equilibrium constant for Boudouard reaction. If the carbon activity is greater than unity, the system is not in equilibrium and the carbon formation is present. In case of the carbon activity equals to unity, the system is in equilibrium. Finally, when the carbon activity is less than unity, the carbon formation is thermodynamically impossible to occur in system. It is noted that the carbon activity is only indicator for determining the presence of carbon in system and thus, an amount of carbon formation cannot be examined.

### 4.3 Gas turbine

For analysis of gas turbine in this work, the gas turbine model covers the linked compressor and the turbine with a shaft a mechanical manner. The turbine and compressor model are based on perfect gas and isentropic efficiency.

#### 4.3.1 Compressor

The ambient air is pressurized by compressor so as to feed into air channel of SOFC**.** The consumed power from compressor can be considered from the total change across the compressor from first law of thermodynamics, as follows:

$$P_c = \sum_i (\dot{n}_{i,c}^{in} \dot{h}_{i,c}^{in})_{out} - \sum_i (\dot{n}_{i,c}^{in} \dot{h}_{i,c}^{in})_{in} \tag{4.82}$$

where $\dot{n}_{i,c}$ is the inlet and outlet molar flow rate of species $i$ through compressor, $\dot{h}_{i,c}$ is the specific enthalpy of inlet and outlet flue gas through the compressor.

The compressor operates under an isotropic process. Therefore, the temperature ratio can be related to the pressure ratio using the relation in Equation (4.83):

$$\frac{T_{c,is}^{out}}{T_c^{in}} = \left( \frac{p_c^{out}}{p_c^{in}} \right)^{\frac{\gamma-1}{\gamma}} \tag{4.83}$$

where $p_c$ is the inlet and outlet pressure of compressor, $T_{c,is}^{out}$ is the temperature of the exhaust gas leaving the compressor if the compression were isentropic. However, the compressor process in the fact is not isentropic so the compressor isentropic efficiency defined as

$$\eta_{\mathrm{c}} = \frac{T_{\mathrm{c,is}}^{\mathrm{out}} - T_{\mathrm{c}}^{\mathrm{in}}}{T_{\mathrm{c}}^{\mathrm{out}} - T_{\mathrm{c}}^{\mathrm{in}}} \tag{4.84}$$

The exit temperature of compressor can be expressed from the isentropic efficiency, pressure ratio and the inlet temperature as defined:

$$T_{\mathrm{c}}^{\mathrm{out}} = T_{\mathrm{c}}^{\mathrm{in}} \left( 1 + \frac{1}{\eta_c} \left( \left( \frac{p_{\mathrm{c}}^{\mathrm{out}}}{p_{\mathrm{c}}^{\mathrm{in}}} \right)^{\frac{\gamma-1}{\gamma}} - 1 \right) \right) \tag{4.85}$$

### 4.3.2 Turbine

The exhaust gas from combustor is fed in to gas turbine in order to increase the produced system power. The generated power from turbine can be considered from the total change across the turbine from first law of thermodynamics, as follows:

$$P_{\mathrm{t}} = \sum_i (\dot{n}_{\mathrm{i,t}}^{\mathrm{in}} \dot{h}_{\mathrm{i,t}}^{\mathrm{in}}) - \sum_i (\dot{n}_{\mathrm{i,t}}^{\mathrm{out}} \dot{h}_{\mathrm{i,t}}^{\mathrm{out}}) \tag{4.86}$$

where $\dot{n}_i$ is the inlet and outlet molar flow rate of species $i$ through turbine, $\dot{h}_i$ is the specific enthalpy of inlet and outlet flue gas through the turbine.

The relation of isentropic outlet temperature and pressure ratio for turbine can express as

$$\frac{T_{\mathrm{t}}^{\mathrm{in}}}{T_{\mathrm{t,is}}^{\mathrm{out}}} = \left( \frac{p_{\mathrm{t}}^{\mathrm{in}}}{p_{\mathrm{t}}^{\mathrm{out}}} \right)^{\frac{\gamma-1}{\gamma}} \tag{4.87}$$

where $p_t$ is the inlet and outlet pressure of turbine, $\gamma$ is the ratio of the constant pressure specific heat over the constant volume specific heat. $T_{\mathrm{t,is}}^{\mathrm{out}}$ is the temperature of the exhaust gas leaving the turbine if the expansion were isentropic.

For an isotropic efficiency of gas turbine, as follows:

$$\eta_t = \frac{T_{\mathrm{t}}^{\mathrm{in}} - T_{\mathrm{t}}^{\mathrm{out}}}{T_{\mathrm{t}}^{\mathrm{in}} - T_{\mathrm{t,is}}^{\mathrm{out}}} \tag{4.88}$$

The outlet gas temperature from turbine can be explained from isentropic efficiency. Therefore, the outlet gas temperature of gas turbine and compressor can be given, respectively, as follows:

$$T_{\mathrm{i,t}}^{\mathrm{out}} = T_{\mathrm{i,t}}^{\mathrm{in}} \left( 1 - \eta_t \left( 1 - \left( \frac{p_{\mathrm{t}}^{\mathrm{out}}}{p_{\mathrm{t}}^{\mathrm{in}}} \right)^{\frac{\gamma-1}{\gamma}} \right) \right) \tag{4.89}$$

For total gas turbine power produced, the partial power of turbine is consumed for driving compressor so the net electrical power output of gas turbine section can be expressed as

$$P_{\mathrm{gt}} = (P_{\mathrm{t}} - P_{\mathrm{c}})\eta_{\mathrm{m}}\eta_{\mathrm{g}} \tag{4.90}$$

where $\eta_{\mathrm{m}}$ and $\eta_{\mathrm{g}}$ are mechanical and generator efficiencies, respectively.

## 4.4 Auxiliary units

### 4.4.1 Pump

The pump is used to increase the mechanical energy of ethanol and water before feeding to mixer. The power work can be expressed from Bernoulli equation. The following equations were obtained:

$$W_{\mathrm{i,pum}} = \frac{(p_{\mathrm{i,pum}}^{\mathrm{out}} - p_{\mathrm{i,pum}}^{\mathrm{in}}) \times \dot{n}_{\mathrm{i,\,pum}}^{\mathrm{in}}}{\eta_{\mathrm{p}}\rho_{\mathrm{i}}} \tag{4.91}$$

where $p_{\mathrm{i,pum}}^{\mathrm{in}}$ is the inlet pressure of ethanol and water, $p_{\mathrm{i,pum}}^{\mathrm{out}}$ is the required outlet pressure of ethanol and water, $\dot{n}_{\mathrm{i,\,pum}}^{\mathrm{in}}$ is inlet and outlet molar flow rate of ethanol and water through pump, $\rho_{\mathrm{i}}$ is the density of ethanol and water, and $\eta_{\mathrm{p}}$ is the pump efficiency which is defined to be 75 % in this study**.**

### 4.4.2 Vaporizer

Ethanol was selected to be fuel for supplying in system in this work. Moreover, water is used in reagent for steam reformer. The both are liquid phase which is changed from liquid to gas phase in the vaporizer.

The requiring heat for both of vaporizer is expressed as

$$Q_{\mathrm{i,vap}} = \dot{n}_{\mathrm{i,vap}}^{\mathrm{in}} \left[ (\dot{h}_{\mathrm{i,vap}}^{\mathrm{bt}} - \dot{h}_{\mathrm{i,vap}}^{\mathrm{in}}) + \dot{\lambda}_i + (\dot{h}_{\mathrm{i,vap}}^{\mathrm{out}} - \dot{h}_{\mathrm{i,vap}}^{\mathrm{bt}}) \right] \tag{4.92}$$

where $\dot{\lambda}_i$ is a specific latent heat of ethanol and water.

Normally, ethanol and water as liquid state transform to vapour state at boiling temperature of 78.1 and 100 $^{\circ}C$ operated at atmospheric pressure. In case of vaporizer operated at higher atmospheric pressure, the boiling temperature of ethanol and water will change. The boiling temperature at the pressurized system can be computed by Antoine's equation, as in Equation (4.93).

$$\ln(p_{\mathrm{i}}) = a + \frac{b}{(T+c)} + d\ln(T) + eT^{f} \tag{4.93}$$

Additionally, enthalpy of vaporization of ethanol and water can be defined in Equation (4.94).

$$H_{\mathrm{i}}^{\mathrm{Vap}} = A\left(1 - \frac{T}{T_{\mathrm{C}}}\right)^{n} \tag{4.94}$$

where $T_{\mathrm{C}}$ is critical temperature at of ethanol and water.

### 4.4.3 Pre-heater

The SOFC system has pre-heaters to preheat the feed stream of ethanol and steam, the synthesis gas obtained from the reformer and the air fed to the SOFC. The heat required for these pre-heaters can be determined by the following equations:

$$Q_{\mathrm{ph}} = \sum_{o}(\dot{n}_{\mathrm{i,ph}}^{\mathrm{out}}\dot{h}_{\mathrm{i,ph}}^{\mathrm{out}}) - (\sum_{i}\dot{n}_{\mathrm{i,ph}}^{\mathrm{in}}\dot{h}_{\mathrm{i,ph}}^{\mathrm{in}}) \tag{4.95}$$

where $\dot{n}_{\mathrm{i,ph}}$ is inlet and outlet molar flow rate of species $i$ through pre-heaters, $\dot{h}_{\mathrm{i,ph}}$ is the inlet and outlet enthalpy of formation of species $i$ through pre-heaters.

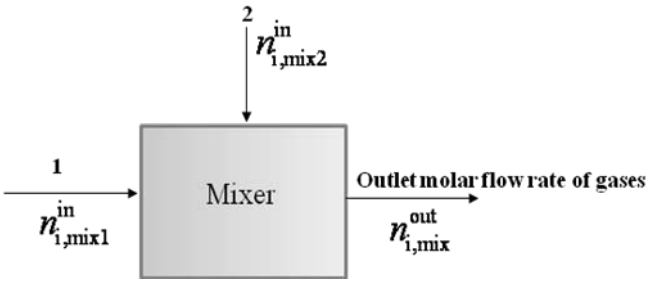


**Figure 4.7** Schematic of the mixer with inlet and outlet flows.

### 4.4.4 Mixer

In conventional system of this work, mixer is used to mix ethanol and water before pre-heater and feeding into system. For the SOFC system with recycling the anode exhaust gas, the recirculated gas stream is mixed with the fresh fuel feed in a mixer**.** Further, it was used to mix the cathode exhaust gas with fresh air in the SOFC system with the cathode exhaust gas recirculation before feeding gases to cathode channel. The inlet and outlet flows through the mixer are presented in Figure 4.7.

The mixer outlet molar flow rate can be defined from mass balance equations, as below:

$$\dot{n}_{i,mix}^{out} = \dot{n}_{\mathrm{i,mix1}}^{\mathrm{in}} + \dot{n}_{\mathrm{i,mix2}}^{\mathrm{in}} \tag{4.96}$$

where $\dot{n}_{\mathrm{i,mix1}}^{\mathrm{in}}$ and $\dot{n}_{\mathrm{i,mix2}}^{\mathrm{in}}$ are the mixer inlet molar flow rate of gas species i in stream 1 and stream 2 respectively.

The outlet temperature at mixer can be calculated from energy balance equation as given by:

$$(\sum_{i} \dot{n}_{\mathrm{i,mix1}}^{\mathrm{in}} \dot{h}_{\mathrm{i,mix1}}^{\mathrm{in}}) + (\sum_{i} \dot{n}_{\mathrm{i,mix2}}^{\mathrm{in}} \dot{h}_{\mathrm{i,mix2}}^{\mathrm{in}}) = (\sum_{o} \dot{n}_{\mathrm{i,mix}}^{\mathrm{out}} \dot{h}_{\mathrm{i,mix}}^{\mathrm{out}}) \tag{4.97}$$

### 4.4.5 Combustor

The residue flue gas of anode outlet stream and unused oxidant gas from the cathode are mixed and burnt in combustor. Moreover, the fresh fuel and air are added in combustor so as to adjust the combustor outlet gas temperature. The mass balance of the combustor can be described in Figure 4.8.

The combustion reactions occurred in combustor can be written as follows:

Hydrogen combustion: $H_2 + 0.5O_2 \rightarrow H_2O$ (4.98)

Carbon monoxide combustion: $CO + 0.5O_2 \rightarrow CO_2$ (4.99)

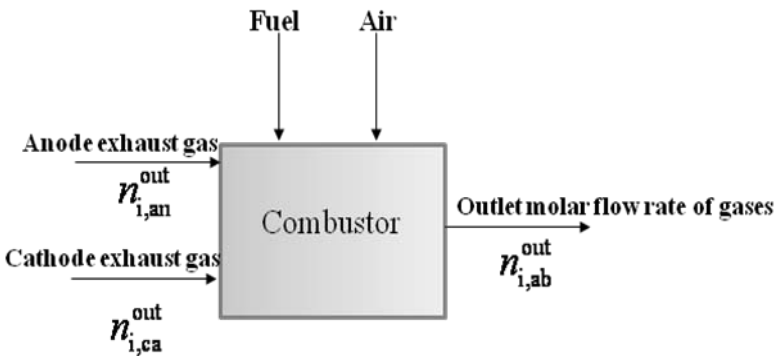


**Figure 4.8** Schematic of the combustor with inlet and outlet flows.

The combustion efficiency was set at conservatively 98% in this work (Akkaya et al., 2009). The combustor exit gas composition can be written based on molar mass balance equations given as follows:

$$n_{H_2,cb}^{out} = n_{H_2,an}^{out} - \dot{k}_{1,cb} \tag{4.100}$$

$$n_{CO,cb}^{out} = n_{CO,an}^{out} - k_{2,cb} \tag{4.101}$$

$$n_{CH_4,cb}^{out} = n_{CH_4,an}^{out} \tag{4.102}$$

$$n_{CO_2,cb}^{out} = n_{CO_2,an}^{out} + \dot{k}_{2,cb} \tag{4.103}$$

$$n_{H_2O,cb}^{out} = n_{H_2O,an}^{out} + \dot{k}_{1,cb} \tag{4.104}$$

$$n_{O_2,cb}^{out} = n_{O_2,ca}^{out} - 0.5\dot{k}_{1,cb} - 0.5\dot{k}_{2,cb} \tag{4.105}$$

$$n_{N_2,cb}^{out} = n_{N_2,ca}^{out} \tag{4.106}$$

where $n_{i,cb}^{out}$ is the outlet molar flow rate of combustor of species $i$, $\dot{k}_{1,cb}$ and $\dot{k}_{2,cb}$ are taken into consideration as molar flow rates of consumed hydrogen and carbon monoxide in combustor respectively.

The exit temperature of combustor can be calculated on basis of energy balance on combustor control volume, as shown below:

$$(\sum_i \dot{n}_{i,an}^{out}\dot{h}_{i,an}^{out}) + (\sum_i \dot{n}_{i,ca}^{out}\dot{h}_{i,ca}^{out}) + (\sum_i \dot{n}_{fuel,cb}^{in}\dot{h}_{fuel,cb}^{in}) + (\sum_i \dot{n}_{air,cb}^{in}\dot{h}_{air,cb}^{in}) = (\sum_o \dot{n}_{i,cb}^{out}\dot{h}_{i,cb}^{out}) \tag{4.107}$$

where $\dot{h}_{i,cb}$ is the combustor inlet and outlet enthalpy of formation of species $i$.

### 4.4.6 Recuperator and heat exchanger

The recuperator and heat exchanger used in system to heat recovery from turbine exhaust gas for preheating air before feeding into SOFC. The calculation of recuperator and heat exchanger use the similar method. The cool and hot stream fed through recuperator can be described in Figure 4.9.

In SOFC-GT hybrid system, the compressed air as cool stream is enhanced temperature by using heat exchanger so as to exchange heat with turbine outlet gas as hot stream before feeding into cell. The outlet cool gas temperature leaving the heat exchanger can be specified through heat exchanger effectiveness given as follows:

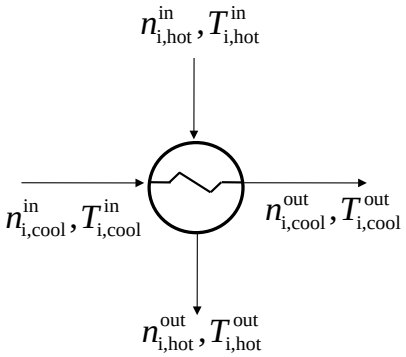


**Figure 4.9** Schematic of the recuperator with inlet and outlet flows.

$$\varepsilon_{\text{REC}} = \frac{T^{\text{out}}_{\text{cool}} - T^{\text{in}}_{\text{cool}}}{T^{\text{in}}_{\text{hot}} - T^{\text{in}}_{\text{cool}}} \tag{4.108}$$

The outlet temperature of hot gas leaving the heat exchanger can be determined from energy balance which is expressed as

$$(\sum_{i} \dot{n}^{\text{in}}_{\text{i,cool}} \dot{h}^{\text{in}}_{\text{i,cool}}) + (\sum_{i} \dot{n}^{\text{in}}_{\text{i,hot}} \dot{h}^{\text{in}}_{\text{i,hot}}) - (\sum_{o} \dot{n}^{\text{out}}_{\text{i,cool}} \dot{h}^{\text{out}}_{\text{i,cool}}) - (\sum_{o} \dot{n}^{\text{out}}_{\text{i,hot}} \dot{h}^{\text{out}}_{\text{i,hot}}) = 0 \tag{4.109}$$

where $\dot{n}_{\text{i,cool}}$ is inlet and outlet molar flow rate of compressed air as cool stream. $\dot{n}_{\text{i,cool}}$ is inlet and outlet molar flow rate of hot stream which is turbine outlet gas in first heat exchanger or recupeartor and combustor outlet gas in second heat exchanger for SOFC-GT hybrid system with recuperative heat exchanger.

### 4.5 System performance parameters

The performance parameters of the SOFC system are considered from the SOFC electrical efficiency ($\eta_{\text{el,sofc}}$), the energetic electrical efficiency of hybrid system, system efficiency and system thermal efficiency ($\eta_{\text{th}}$) which are calculated as:

$$\eta_{\text{el,sofc}} = \frac{P_{\text{sofc}}}{\dot{n}_{C_2H_5OH} LHV_{C_2H_5OH}} \tag{4.110}$$

$$\eta_{\text{el, system}} = \frac{P_{\text{sofc}} + P_{\text{GT}} - P_{\text{pump}} - P_{\text{blower}}}{\dot{n}^{\text{in}}_{C_2H_5OH} LHV_{C_2H_5OH}} \tag{4.111}$$

$$\eta_{\text{system}} = \frac{P_{\text{sofc}} + P_{\text{GT}} - P_{\text{pump}} - P_{\text{blower}}}{(\dot{n}^{\text{in}}_{C_2H_5OH} LHV_{C_2H_5OH}) + Q^{\text{ex}}_{\text{use}}} \tag{4.112}$$

$$\eta_{\text{th}} = \frac{Q_{\text{rec}} - Q_{\text{use}}}{\dot{n}^{\text{in}}_{C_2H_5OH} LHV_{C_2H_5OH}} \tag{4.113}$$

where $\dot{n}_{C_2H_5OH}$ is inlet ethanol molar flow rate, $LHV_{C_2H_5OH}$ is lower heating value of ethanol, $Q_{\text{rec}}$ is the amount of thermal energy from the SOFC system which exhaust gas is converted to low-grade ($100^{o}$C) , $Q_{\text{use}}$ is total amount of thermal energy used in system and $Q^{\text{ex}}_{\text{use}}$ is total amount of external heat used in system.

# CHAPTER V

# COMPARISON OF HYDROGEN PRODUCTION FROM RENEWABLE FUELS FOR SOFC SYSTEM

This chapter presents the investigating suitability of ethanol as fuel for SOFC system which is compared with other renewable fuels; i.e., glycerol and biogas. The effect of operating condition for the hydrogen production via steam reforming reaction from these fuels was considered by employing the thermodynamic analysis. Then, the integrated system between SOFC system and steam reformer was investigated. The electrical and thermal efficiency are performance indicator to compare in each supplied fuel for SOFC system. Further, the amount of carbon dioxide released from each system was analyzed as well.

## 5.1 Introduction

Fuel cells can generate electricity via an electrochemical reaction by using hydrogen as fuel and oxygen as oxidant, so that hydrogen production technology has been developed together with fuel cell technology. In general, hydrogen is produced by reforming of methane derived from natural gas, which mostly comes from fossil resources. As fossil fuel is limited and causes environmental problems, the use of renewable fuel sources with environmental friendliness to produce hydrogen should be explored. Among the renewable fuels, ethanol, biogas and glycerol have been received considerable attention. Ethanol and biogas are derived from similar raw materials such as biomass, organic fraction of municipal solid waste or forestry residue materials but their production processes are different. Ethanol is produced through fermentation process, whereas biogas is generated by an anaerobic digestion process. Glycerol becomes an important fuel since it is a major by-product from the production of biodiesel, which its demand continuously increases. Regarding energy

demand and environmental problems, these renewable are considered a promising alternative fuels for hydrogen production.

Among the various types of fuel cell, the solid oxide fuel cell (SOFC) is the most promising fuel cell technology, which can be used in a wide range of commercial applications. The high temperature operation of SOFC leads to many advantages. For example, the high-temperature waste heat from SOFC can be recovered for use in other heat-requiring units of SOFC systems. In addition, it is flexible to use various fuel types (i.e., methane, methanol and ethanol) (Lai et al., 2007; Liu et al., 2007; Cheddie et al., 2010). Using a high-cost catalyst can be avoided as the electrochemical reaction is more pronounced at high temperatures (Cordiner et al., 2007).

There are a number of studies concerning about hydrogen production from renewable and the use of renewable fuels for SOFC system. In general, the most widely-used fuel processors for hydrogen production are steaming reforming, partial oxidation and auto-thermal processes. However, the steam reforming process provides a higher hydrogen yield and is suitable for hydrogen production from hydrocarbon fuels (Rabenstein & Hacker, 2008). Piroonlerkgul et al. (2008) found that steam is considered to be the most suitable reforming agent for using biogas as fuel for SOFC system because the steam-fed SOFC offers much higher power density than the air-fed SOFC although its electrical efficiency is slightly lower. Toonssen et al. (2010) investigated the SOFC/GT hybrid system integrated with a biomass gasification and showed that the gasification technology has slightly effect on the overall SOFC system performance. Farhad et al. (2010) studied a SOFC micro-combined heat and power system using biogas as a fuel. The heat generated from an afterburner was used to other heat-requiring units in the system, achieving the highest thermal efficiency and electrical efficiency of the system. However, the thermal and electrical efficiency of the SOFC system depend on type of fuels used. As the thermal management and performance of SOFC systems using different fuels is discrepant, a detailed analysis of the SOFC system should be considered so as to select the suitable fuel for different applications of the SOFC system.

The aim of this study is to analyze a SOFC system integrated with a steam reforming process. Various renewable resources such as biogas, ethanol and glycerol,

are considered for hydrogen production. Effects of operating condition on reformer performance are investigated. Finally, the performance of the SOFC integrated system for power generation is investigated.

## 5.2 Results and discussion

### 5.2.1 Hydrogen production from various fuels

The study of hydrogen production from various renewable fuels such as biogas, ethanol and glycerol are investigated with thermodynamic analysis in this section. Biogas is composed of 60 mol% methane and 40 mol% carbon dioxide. Hydrocarbon fuels are reformed to produce a synthesis gas via a steam reforming reaction. The final composition of the synthesis gas at the equilibrium condition is determined from the minimization of Gibbs free energy. The main products of each fuel processing system are hydrogen, methane, carbon dioxide, carbon monoxide and water. Their equilibrium composition depends on the operating temperature and pressure of the steam reformer. Equation (5.1) gives the total Gibbs free energy of the system:

$$G = \sum n_i G_i^0 + \mathrm{RT} \sum n_i \ln \frac{y_i \varphi_i \mathrm{P}}{\mathrm{P}^0} \tag{5.1}$$

where $G$ is the total Gibbs free energy, $n_i$ is the mole of species $i$, $G_i^0$ is the standard Gibbs free energy of species $i$, $R$ is the gas constant, $T$ is the reforming temperature, $P$ is the operating pressure of the reformer, $y_i$ is the mole fraction of species $i$ and $\varphi_i$ is the fugacity coefficient of a gas mixture obtained by Redlich-Kwong equation of state. The equilibrium compositions obtained from solving the minimization of Gibbs free energy have to satisfy the following constraints:

$$\sum_{i=1}^{N} a_{ji} n_i = A_j \qquad j = 1, \ldots, k \tag{5.2}$$

where $a_{ji}$ is the number of atoms of the $j$ element in the species $i$ and $A_j$ is the total atoms of the $j$ element in the feed stream.

Lagrange's method is applied for total Gibbs free energy minimization. The following equations need to be solved simultaneously:

$$\frac{\Delta G_{fi}^{\circ}}{RT} + \ln \frac{y_i \varphi_i P}{P^0} + \sum_j \frac{\lambda_j}{RT} a_{ji} = 0 \quad (5.3)$$

$$\sum_j y_j a_{ji} = \frac{A_j}{n} \quad (5.4)$$

$$\sum_j y_j = 1 \quad (5.5)$$

The tendency of carbon formation in reformer can consider from section 4.2.3 in chapter 4. The proposed model consists of a set of nonlinear algebraic equations and was coded and solved by using MATLAB.

The effect of operating temperature on hydrogen production from the steam reforming of biogas, ethanol and glycerol is shown Figure 5.1. The results show a similar trend even different fuels are utilized. An increase in the temperatures enhance hydrogen yield due to the endothermicity of the steam reforming reaction.

It is found that ethanol and glycerol provide higher hydrogen yield, compared to biogas. At atmospheric pressure, glycerol provides higher hydrogen yield than ethanol at the temperature below 973 K. When the reformer is operated at high pressure, the use of glycerol can produce more hydrogen than that of ethanol at the temperature below 1033 K. In addition, pressure is not influence on hydrogen yield at temperature over 1073 K.

Figure 5.2 shows the effect of steam-to-carbon (S/C) ratio on hydrogen yield at pressure of 1 bar. At low S/C ratio, glycerol provides higher hydrogen than ethanol. However, ethanol gives the highest hydrogen yield at a higher S/C ratio. The use of biogas provides the lowest yield of hydrogen at all operational range studied.

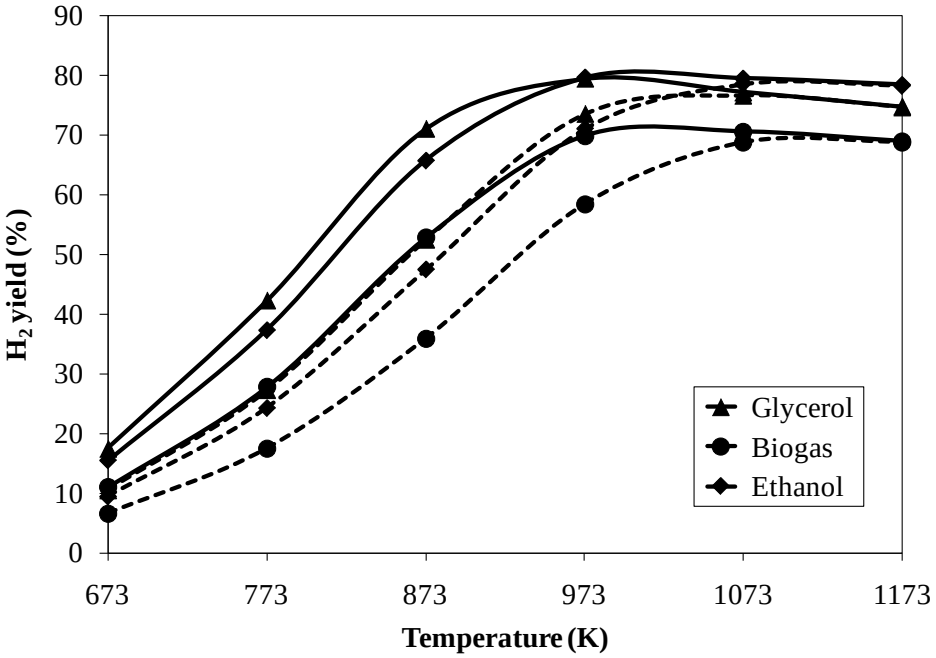


**Figure 5.1** Effect of reforming temperature on $H_2$ yield at S/C ratio = 2 and pressure of 1bar (solid line) and 3 bar (dash line).

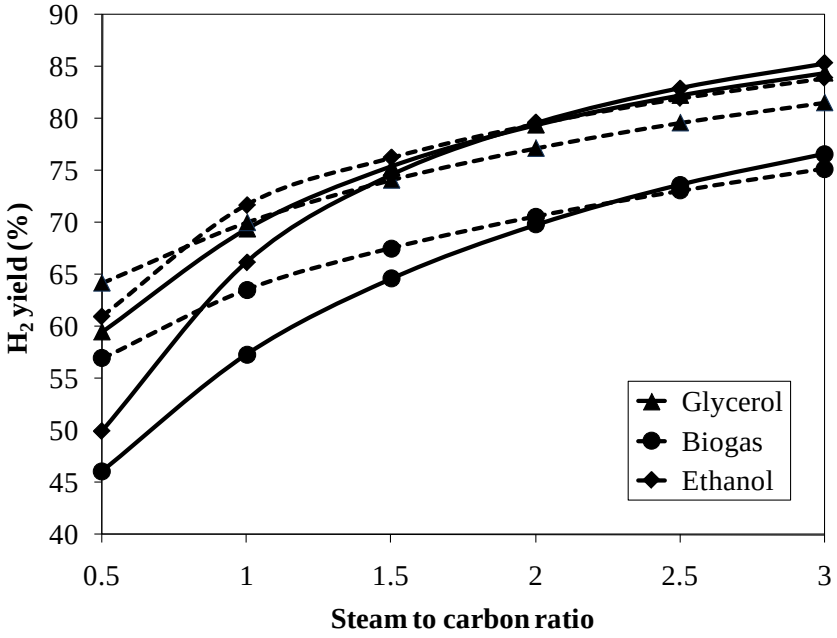


**Figure 5.2** Effect of steam-to-carbon ratio on $H_2$ yield ($P$ = 1 bar): $T$ = 973 K (solid line) and $T$ = 1073 K (dash line).

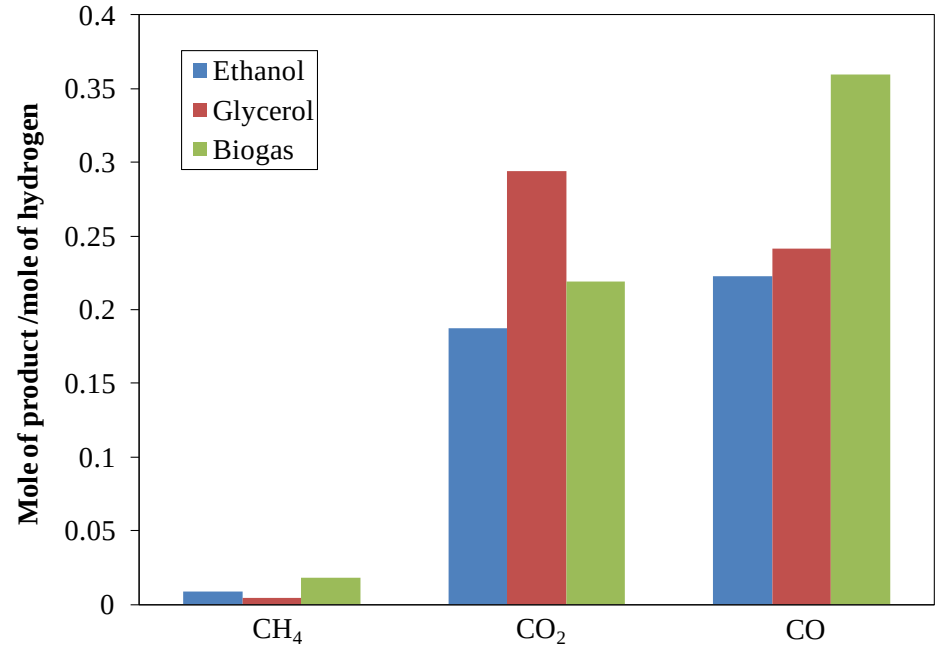


**Figure 5.3** Product distribution from steam reforming of glycerol, ethanol and biogas (*T* = 973 K and S/C ratio = 2).

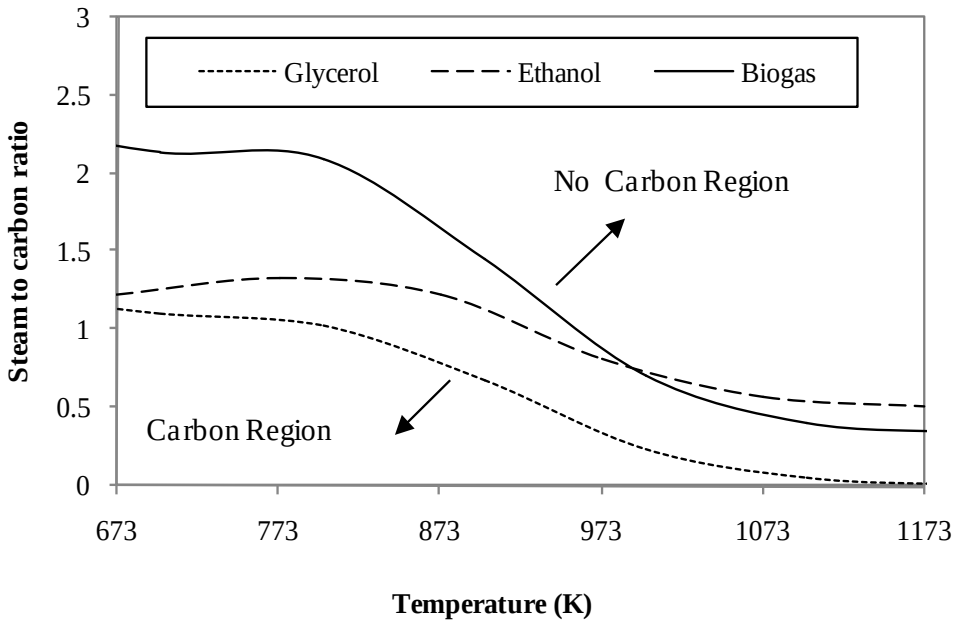


**Figure 5.4** Carbon boundary of various fuels.

Figure 5.5 shows carbon formation boundary of glycerol, ethanol and biogas as well as methane. It is found that the carbon formation tendency of all fuels reduce when operating temperature is higher. Comparing these fuels, biogas is most possible tendency of carbon formation in system. It can be noted that amount of produced carbon monoxide in system for biogas is more than glycerol and ethanol and consequently Boudouard reaction is diven forwardly. Although amount of carbon monoxide in steam reforming system supplying with ethanol is lower than that with glycerol, ethanol is higher tendency of carbon formation than that with glycerol. This reason is that glycerol molecule contains higher oxygen content and glycerol produce plentifully amount of carbon dioxide, resulting in reverse of Boudouard reaction (Slinn et al., 2008).

### 5.2.2 Comparing utilization of various fuels in SOFC system

In this section, the performance of SOFC fed by the synthesis gas obtained from the steam reforming of ethanol, glycerol and biogas is investigated**.** Figure 5.1 shows an external reformer and SOFC integrated system, which composes of evaporator, heat exchanger, fuel processor, SOFC and afterburner. The steam and fuel are mixed and then preheated at operating reforming temperatures. They are sent to the steam reformer where a synthesis gas (hydrogen-rich gas) is produced. The synthesis gas preheated at the desired temperature is fed to the SOFC. At the same time, air is compressed and preheated before entering the SOFC. SOFC produces electrical power and steam via an electrochemical reaction of hydrogen and oxygen in air. In general, SOFC cannot be operated at 100% fuel utilization, so that a residue fuel is combusted in an afterburner and then the heat generated from the afterburner is used for other heat-requiring units in the SOFC system such as preheators, which is shown red line in Figure 5.5.

To analyze the performance of the SOFC system, it was assumed that the system is run at steady-state condition and all gases behave as ideal-gases. Furthermore, heat losses from individual component in the SOFC system are negligible and the operating pressure and temperature of the reformer and the SOFC are kept constant.

The performance of the SOFC system with supply of various fuels is analyzed based on the SOFC system model mentioned in chapter 4. A planar SOFC is considered and a one-dimensional model is used to describe the SOFC, which is operated at a constant cell voltage along the cell coordinate. The SOFC system is designed for the net power output of 150 kW and the fuel utilization of 0.7 by varying the molar flow rate of fuel. Values of operating conditions for system under based condition are considered in Table 5.1 (Akkaya et al., 2008).

The performance of SOFC system can be considered from the cell-stack efficiency, electrical efficiency and thermal efficiency, given by

$$\eta_{\text{cell}} = \frac{P_{\text{cell}}}{(y^{\text{in}}_{\text{H}_2,\text{an}} LHV_{\text{H}_2} + y^{\text{in}}_{\text{CO,an}} LHV_{\text{CO}} + y^{\text{in}}_{\text{CH}_4,\text{an}} LHV_{\text{CH}_4}) \dot{n}^{\text{in}}_{\text{total,an}}} \tag{5.6}$$

$$\eta_{\text{elec}} = \frac{P_{\text{net}}}{\dot{n}^{\text{in}}_{\text{fuel}} LHV_{\text{fuel}}} \tag{5.7}$$

$$\eta_{th} = \frac{Q_{\text{rec}} - Q_{\text{use}}}{\dot{n}_{\text{fuel}} LHV_{\text{fuel}}} \tag{5.8}$$

where $\dot{n}_{\text{fuel}}$ is inlet molar flow rate of fuel, $LHV_{\text{fuel}}$ is lower heating value of fuel, $Q_{rec}$ is the amount of thermal energy from the SOFC system which exhaust gas is converted to low-grade (100$^{o}$C) , $Q_{use}$ is total amount of thermal energy used in system.

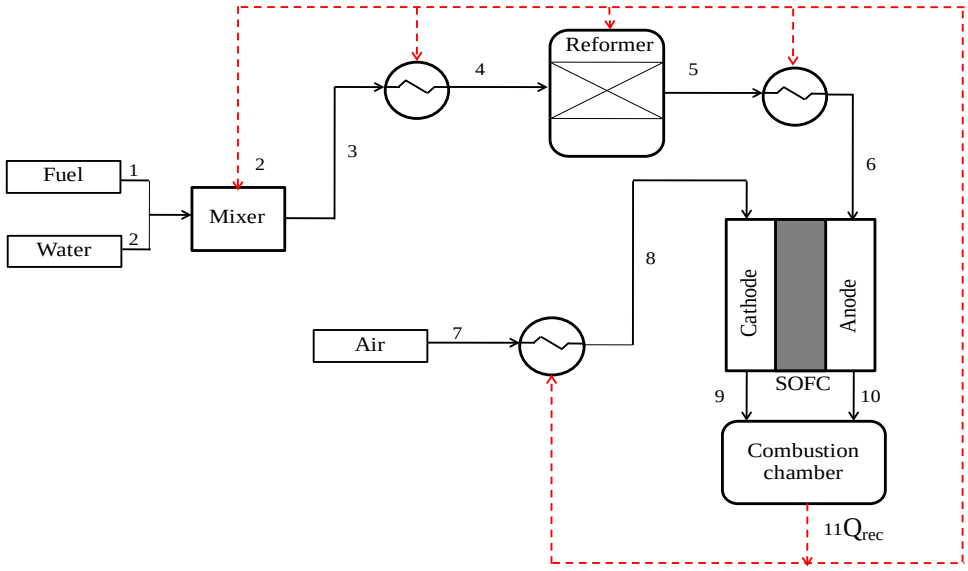


**Figure 5.5** Schematic of a SOFC system integrated with fuel processor.

**Table 5.1** Values of operating conditions for SOFC system under nominal condition

| **Parameter** | **Value** |
|---|---|
| *Reformer* | |
| Operating temperature (K) | 1073 |
| Operating pressure (bar) | 1 |
| Steam-to-carbon ratio | 1.5 |
| *Solid oxide fuel cell* | |
| Cell operating temperature (K) | 1173 |
| Cell operating pressure (bar) | 1 |
| Net power output (kW) | 150 |
| Cell fuel utilization factor (%) | 0.7 |
| Fuel cell active area ($m^2$) | 55.2 |
| Anode thickness, $\tau_{anode}$ ($\mu$m) | 500 |
| Cathode thickness, $\tau_{cathode}$ ($\mu$m) | 50 |
| Electrolyte thickness, $\tau_{electrolyte}$ ($\mu$m) | 20 |
| dc-ac inverter efficiency | 94 |
| *Afterburner* | |
| Afterburner combustion efficiency (%) | 98 |

The energy consumptions in each unit of the SOFC system fed by different fuels are shown in Figure 5.6. The results indicate that the SOFC system run on biogas requires the highest external energy supply, whereas the ethanol-fueled SOFC system shows the lowest requirement of energy. It is noticed the reforming of biogas needs high energy supply (77.9 kW). A high content of $CO_2$ in biogas increases a reverse water gas shift reaction, which is a endothermic reaction. Although the energy requirement of the glycerol steam reforming is lower, a higher heat is needed for the evaporator due to a high boiling point of glycerol (561.9 K).

Figure 5.7 shows the SOFC stack efficiency and the thermal efficiency and electrical efficiency of the SOFC system supplied by different fuels. As can be seen, the SOFC system fuelled by ethanol gives the best performance in terms of the SOFC stack efficiency, the electrical efficiency and the thermal efficiency. This results from a high performance of the ethanol steam reformer that gives the highest hydrogen production, compared to the reforming of other fuels. The ethanol fuelled SOFC system can achieve the electrical efficiency of 51 %, whereas that of the SOFC system supplied by glycerol and biogas is 49% and 32%, respectively. The use of biogas as a fuel for the SOFC system provides the minimum electrical efficiency since biogas mainly consists of carbon dioxide that dilutes the hydrogen fuel fed to the SOFC stack. This lowers the reversible cell voltage and increases the concentration and activation overpotentials in the SOFC. It is noted that the efficiency of the SOFC stack run on different fuel feeds is indifferent (42-43%). Considering the thermal efficiency, the results show that the SOFC system fed by biogas shows the lowest thermal efficiency since the desired power output of 150 kW. In addition, a lot of heat is lost to preheat carbon dioxide in biogas feed.

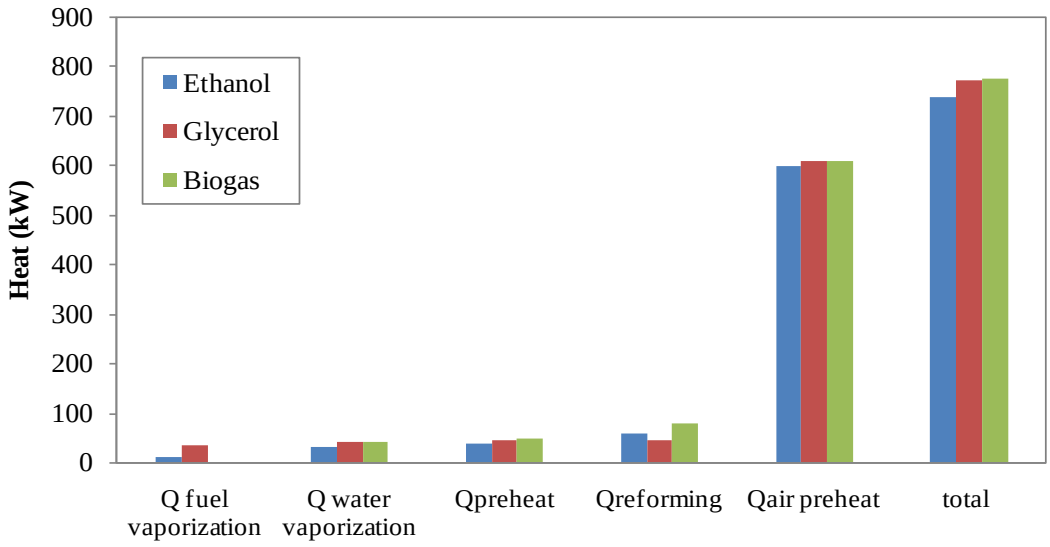


**Figure 5.6** Energy required in each unit of SOFC systems with different fuel feeds.

Figure 5.8 presents the amount of carbon dioxide released from the SOFC system at the power output of 150 kW. The SOFC system fed by ethanol minimizes the emission of carbon dioxide, whereas the glycerol-fuelled SOFC system shows the maximum. The carbon dioxide emission of the ethanol-fed SOFC system is less than other system by 21.76 % (glycerol) and 19.97 % (biogas).

The simulation study indicates that ethanol is the most suitable fuel for the SOFC system integrated with an external steam reformer. It provides not only the maximum SOFC stack efficiency, system electrical efficiency and thermal efficiency, but also the minimum of carbon dioxide emission. It is suggested that if biogas is used as a fuel for SOFC, a purification unit to remove carbon oxide from biogas is necessary. Therefore, ethanol is considered an attractive renewable fuel for the SOFC system.

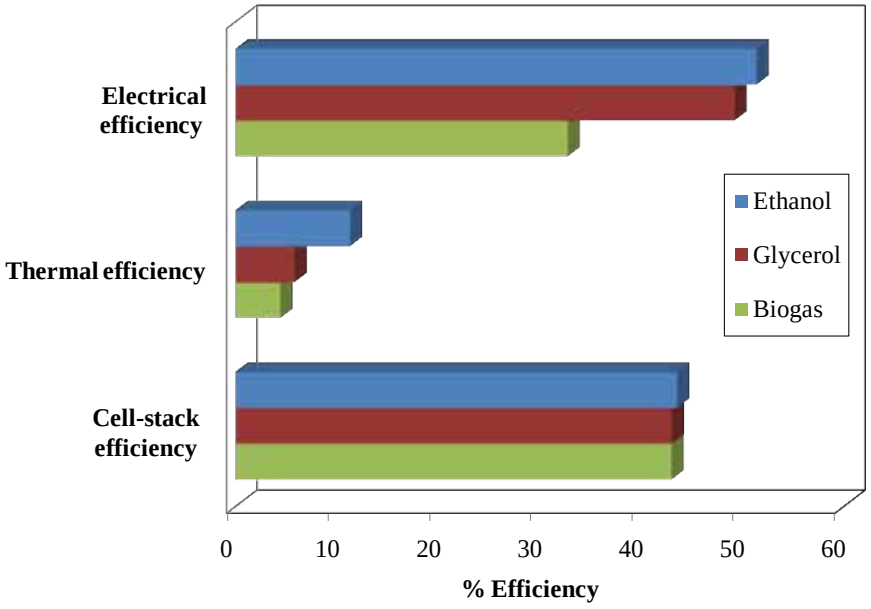


**Figure 5.7** Efficiencies of SOFC systems fuelled by different fuels.

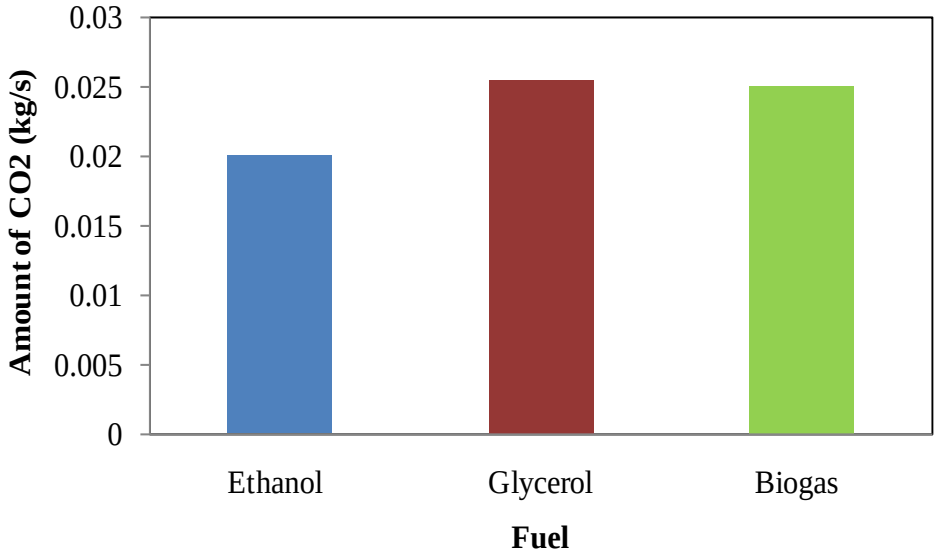


**Figure 5.8** $CO_2$ released from SOFC systems fuelled by different fuels.

### 5.4. Conclusions

This study presented a performance analysis of a steam reforming process and solid oxide fuel cell (SOFC) integrated system. Various renewable fuels, i.e., glycerol, ethanol and biogas, were used to generate hydrogen for SOFC. The results showed that the steam reforming of ethanol gives the highest hydrogen product at the operating temperature of 1073K. The use of glycerol to produce hydrogen from the steam reforming reaction shows less possibility of carbon formation, compared with other renewable fuels. The SOFC system supplied by biogas requires the highest energy and gives the lowest electrical and thermal efficiencies. The use of ethanol seems to be a promising fuel for the SOFC system as the highest electrical and thermal efficiencies can be achieved and in addition, the emission of carbon dioxide is less released.

# CHAPTER VI

# ADSORPTION-MEMBRANE HYBRID SYSTEM FOR ETHANOL STEAM REFORMING: THERMODYNAMIC ANALYSIS

This chapter presents a thermodynamic analysis of hydrogen production for ethanol steam reforming with hydrogen and/or carbon dioxide removal relying on membrane separation and carbon dioxide adsorption. The conventional hydrogen production of ethanol steam reforming at various operating conditions i.e. steam-to-carbon, temperature and pressure is firstly considered. Then, a comparison among a conventional reformer, membrane reactor, adsorptive reactor and adsorption-membrane hybrid system is performed to determine the suitable process of ethanol steam reforming. The boundary of possible carbon formation in ethanol steam reforming of all system is discussed in the end of this chapter.

## 6.1 Introduction

Hydrogen is a major fuel for electricity generation in fuel cells; however, its uses are still facing with several issues such as its economical production, storage and distribution (Vaidya and Rodrigues, 2006). In general, hydrogen can be derived from primary fuels such as natural gas, methanol, ethanol, gasoline, and coal via a fuel processor. Among all possible fuels, ethanol has been considered as an attractive green fuel since it can be produced renewably from the fermentation of various biomass sources, including energy plants, organic fraction of municipal solid waste, waste materials from ago-industries, or forestry residue materials (Comas et al., 2004a). Moreover, the use of ethanol for producing hydrogen offers some advantages as it is easy to store, handle, and transport in a safe way due to its lower toxicity and volatility (Arteaga et al., 2008; Arpornwichanop et al., 2009).

Considering a fuel processor, there are three main reactions (i.e., steaming reforming, dry reforming, and partial oxidation) used to reform ethanol into hydrogen-rich gas; however, the ethanol steam reforming provides a higher hydrogen yield, compared to the other reforming processes (Rabenstein and Hacker, 2008). Ethanol steam reforming has been widely investigated based on thermodynamic (Comas et al., 2004a) and experimental studies (Comas et al., 2004b; Cavallaro et al., 2003). Thermodynamic studies indicated that at atmospheric pressure, the steam reforming of ethanol can achieve high hydrogen production at temperatures higher than 1000 K because it is limited by the thermodynamic equilibrium of the reversible reforming reaction. Furthermore, the operation of ethanol steam reforming consumes high energy and needs expensive alloy reformer tubes (Wang and Rodrigues, 2005). The problem on purifying hydrogen is another issue in hydrogen production. Consequently, a new concept for the production of hydrogen with lower operating and capital costs compared to a conventional reforming process is desired.

The use of membrane reactors for improving the ethanol steam reforming process is one of the interesting options to be considered due to the integration of two different processes (reaction and separation) in a single unit. For this purpose, hydrogen as a desired product is selectively removed through the membrane and thus, it is possible to overcome the thermodynamic limitation (Aparicio et al., 2005; Iulianelli et al., 2010). In addition, the increased reaction rate leads to a reduction in the operating temperature and consequently the energy requirement (Gallucci et al., 2007). However, hydrogen produced from the membrane reactor still contains substantial amount of undesired by-products and a treatment unit is also needed to remove such the undesired by-products before its subsequent use in fuel cell powered vehicles (Park, 2004).

An alternative way to enhance the hydrogen production is the addition of a carbon dioxide adsorbent in reforming reactors (Barelli et al., 2008; Chen et al., 2008; Florin & Harris, 2008; Harrison, 2009; Harale et al., 2010). A hybrid system of adsorption and membrane processes in a single unit is considered as a very promising technique for hydrogen production via steam reforming reaction. Carbon dioxide adsorbent is used to remove undesired carbon dioxide, whereas hydrogen is separated from the reforming reaction by a hydrogen selective membrane. Therefore, the

adsorption-membrane hybrid system shows good potential to obtain pure hydrogen without the requirement of shift reactors. This would result in a reduction in operating temperature, providing low operating and capital cost (Harrison, 2009).

In this chapter, a thermodynamic analysis of ethanol steam reforming with and without the presence of carbon dioxide adsorbent and hydrogen selective membrane is presented. A comparison among a conventional reformer, membrane reactor, adsorptive reactor and adsorption-membrane hybrid system is performed to determine the suitable process of ethanol steam reforming. The effect of operating conditions, i.e., temperature, steam-to-ethanol ratio, and fraction of carbon dioxide and/or hydrogen removal, on an equilibrium composition of the reforming products is investigated. In addition, the boundary of carbon formation in the ethanol steam reforming system is considered. It is noted that although the study on the adsorption-membrane hybrid system is performed based on a thermodynamic analysis, this would demonstrate the possibility of applying the adsorption-membrane hybrid system for hydrogen production from ethanol.

## 6.2 Results and discussion

### 6.2.1 Ethanol steam reforming without carbon dioxide adsorbent and hydrogen selective membrane

In this section, a thermodynamic analysis of ethanol steam reforming process without the removal of carbon dioxide by adsorption and hydrogen by membrane (referred to a conventional process) is presented. Method for thermodynamic analysis of ethanol steam reforming can consider from stoichiometric approach, which is described in section 4.2.1 in chapter 4. At the standard conditions, the inlet molar flow rate of ethanol is 1 mol/s and steam-to-ethanol ratio is 3.

Since the reformer temperature is identified as a key parameter having a significant effect on the hydrogen production, the distribution of the reformed products at different operating temperatures is analyzed as shown in Figure 6.1. The results indicate that the amount of hydrogen increases rapidly with increasing temperatures from 673 K to 973 K and reaches its maximum value at 1073 K, whereas the opposite trend is observed for methane. This is because the strong endothermic steam reforming reaction is favored at higher temperatures. Furthermore,

an increase in operating temperature strongly raises carbon monoxide as water gas shift reaction (Equation 4.62) is less pronounced. As can be seen in Figure 6.1, the content of carbon monoxide in the synthesis gas obtained is rather high. This would indicate that the hydrogen product with high carbon monoxide may not be suitable for direct use in low temperature fuel cell stack like PEMFC unless there is a carbon monoxide treatment unit.

Figure 6.2 shows the effect of steam-to-ethanol ratio on the equilibrium compositions of ethanol steam reforming at $T$ = 1073 K and $P$ = 1 bar. When more steam is added in the system, the water gas shift reaction (Equation 4.62) can be driven forwardly and thus, hydrogen is more produced whereas carbon monoxide shows the opposite trend. However, the unreacted steam may lead to the dilution effect of hydrogen so that the choice of the steam-to-ethanol ratio should be carefully considered. The effect of operating pressure on the ethanol steam reforming is shown in Figure 6.3. The simulation results show that increasing operating pressure leads to a decrease in hydrogen, carbon dioxide and carbon monoxide. For this reason, operation of the ethanol steam reforming in the conventional steam reformer at the atmospheric pressure is considered to be a suitable condition.

From the above results, it is indicated that both the steam-to-ethanol ratio and the temperature have significant effects on the hydrogen production. Figure 5.4 presents the influence of the steam-to-ethanol ratio at different operating temperatures on the hydrogen produced at atmosphere pressure. From Figure 6.4, it can be seen that the optimal condition of the ethanol steam reforming in the conventional reformer is at the temperature of 1073 K and the steam-to-ethanol feed ratio of 5. Due to the equilibrium reactions, the maximum hydrogen produced is 4.9 mol/s. According to the reaction stoichiometry, for the steam reforming process, one mole of ethanol can provide 6 moles of hydrogen product. In order to improve the performance of hydrogen production, the removal of carbon dioxide by an adsorption process and the separation of hydrogen by a membrane should be considered.

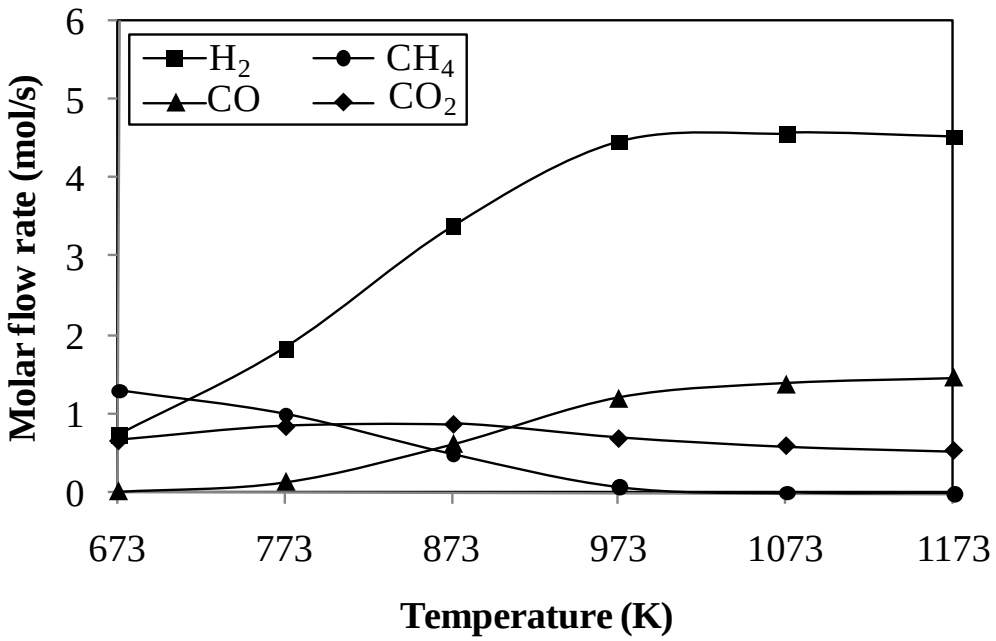


**Figure 6.1** Effect of temperature on equilibrium compositions in ethanol steam reforming (steam-to-ethanol ratio = 3 and atmospheric pressure).

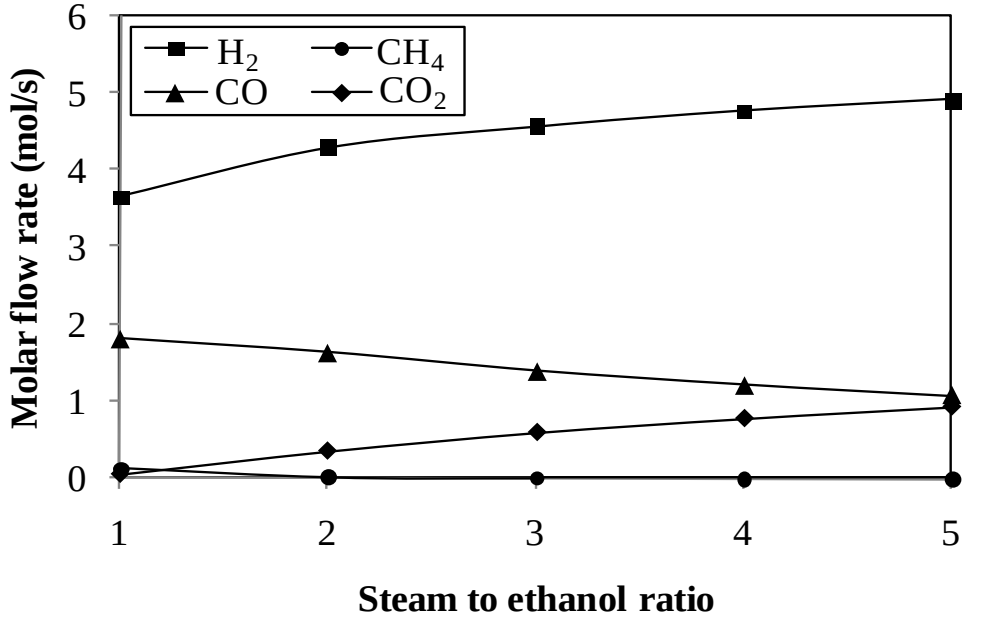


**Figure 6.2** Effect of the steam-to-ethanol ratio on equilibrium compositions in ethanol steam reforming ($T$ = 1073 K and atmospheric pressure).

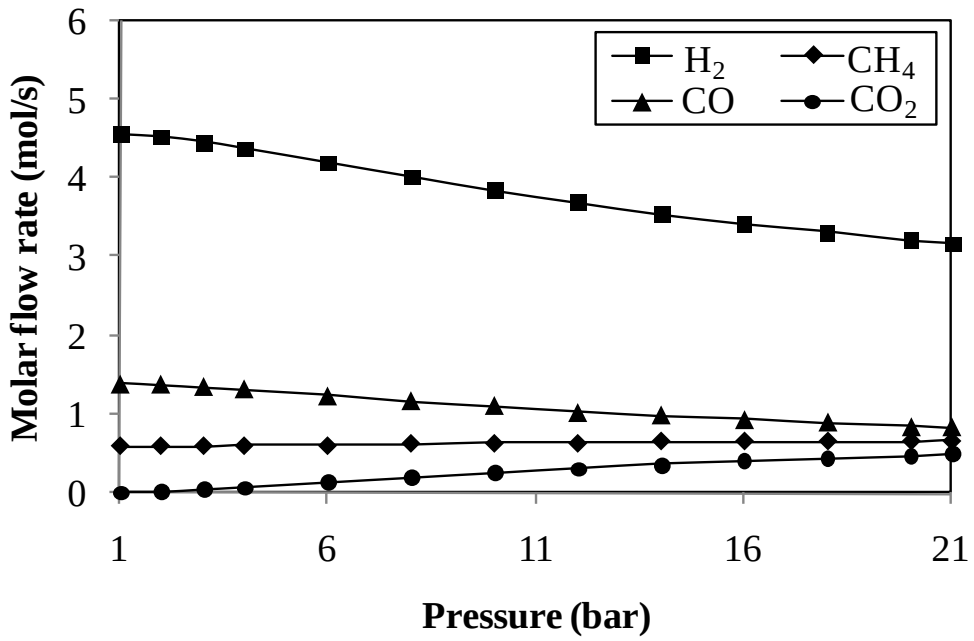


**Figure 6.3** Effect of pressure on equilibrium compositions in ethanol steam reforming at steam/ethanol ratio = 3 and $T$ = 1073 K.

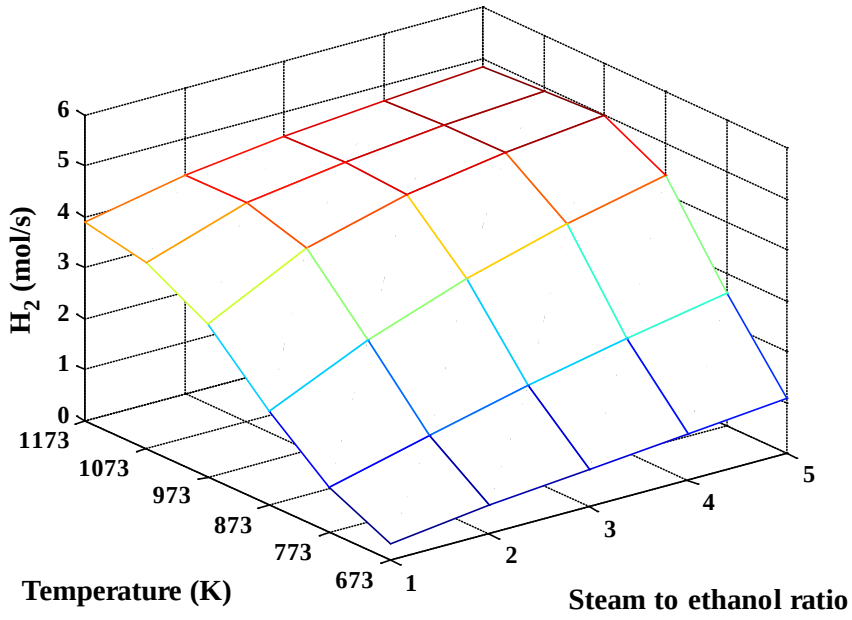


**Figure 6.4** Effects of temperature and steam-to-ethanol ratio on hydrogen production.

### 6.2.2 Ethanol steam reforming with carbon dioxide adsorbent and/or hydrogen selective membrane

Ethanol steam reforming process with the removal of carbon dioxide by adsorption and/or hydrogen by membrane is presented in this section. Method for thermodynamic analysis of ethanol steam reforming with the removal of carbon dioxide and/or hydrogen can consider from stoichiometric approach, which is described in section 4.2.2 in chapter 4.

#### 6.2.2.1 Effect of carbon dioxide removal

When carbon dioxide adsorbent is mixed with catalyst in an absorptive reactor, carbon dioxide, the undesired product produced in the ethanol steam reforming process, is removed by adsorption. Figure 6.5 demonstrates the effect of carbon dioxide removal from the steam reforming system on the equilibrium compositions of the reformed products. Increasing the fraction of carbon dioxide removal slightly promotes the water gas shift reaction, improving hydrogen production and reducing carbon monoxide in the system. The use of carbon dioxide absorbent also decreases the content of carbon dioxide remaining in the reforming system.

#### 6.2.2.2 Effect of hydrogen removal

The production of hydrogen from ethanol steam reforming is carried out in a membrane reactor. The effect of fraction of hydrogen removal on the performance of ethanol steam reforming is investigated as demonstrated in Figure 6.6. The results show that the content of hydrogen in the reformed product decreases with increasing the fraction of hydrogen removal. However, the total amount of hydrogen produced, sum of hydrogen in permeate and retentate streams, considerably increases. When hydrogen is increasingly removed from the system, the water gas shift and the reversed methanation reactions become more pronounced as observed from an increase in carbon dioxide and a decrease in methane.

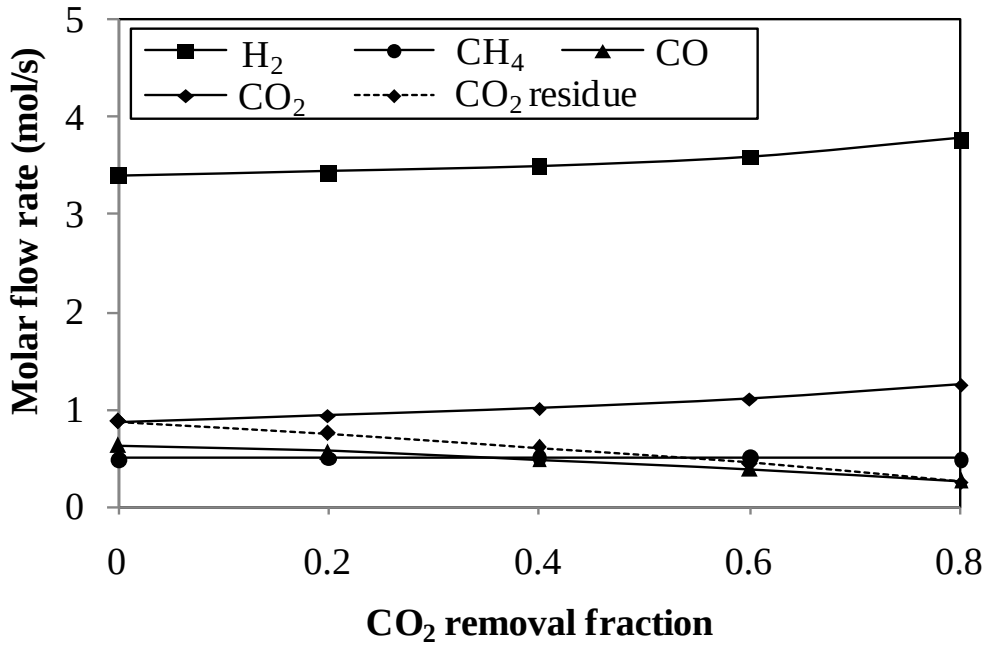


**Figure 6.5** Effect of fraction of carbon dioxide removal on ethanol steam reforming (*T* = 873 K, *P* = 1 bar, and ethanol to steam ratio = 3).

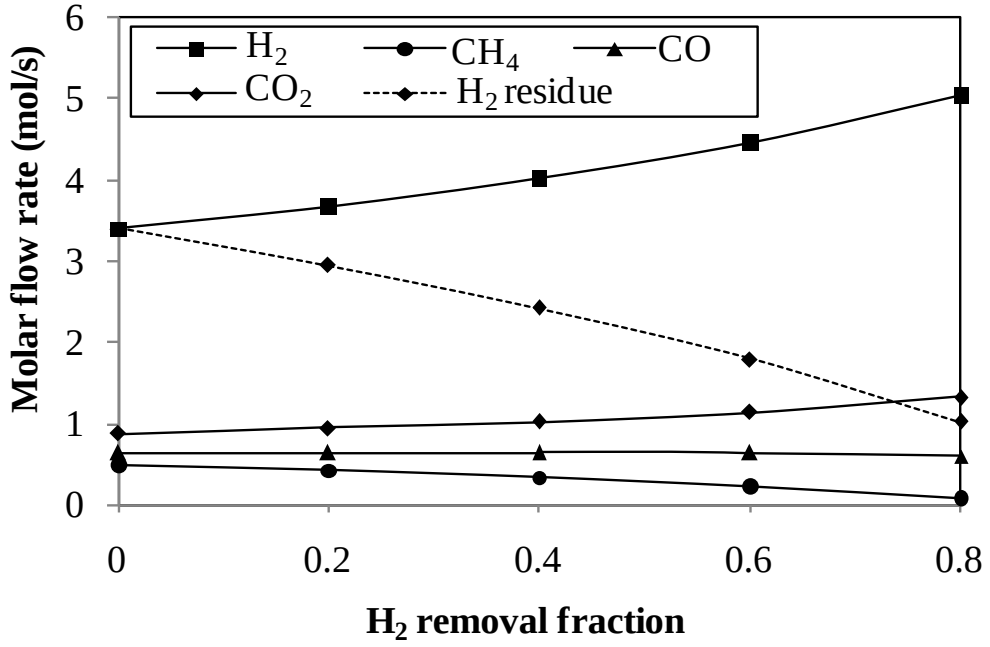


**Figure 6.6** Effect of fraction of hydrogen removal ethanol steam reforming (*T* = 873 K, *P* = 1 bar, and ethanol to steam ratio = 3)

Comparing with the case of carbon dioxide removal by the adsorption, it indicates that the selective separation of hydrogen via the membrane offers higher hydrogen production of the ethanol steam reforming. As the hydrogen is generated at higher content than the carbon dioxide, the removal of hydrogen has more effect on the ethanol reforming system. However, it is found that the amount of carbon monoxide becomes lower when the carbon dioxide absorbent is applied to the system. As a result, the fractions of hydrogen and carbon dioxide removal are key design parameters for the ethanol reforming process to obtain high purity of hydrogen with less carbon monoxide.

#### 6.2.2.3 Simultaneous removal of carbon dioxide and hydrogen

In this section, a thermodynamic analysis of ethanol steam reforming in an adsorption-membrane hybrid system is performed. Figures 6.7a-d show the effects of simultaneous removal of carbon dioxide and hydrogen on the equilibrium compositions of the reformed products, i.e., hydrogen, methane, carbon monoxide, and remaining carbon dioxide, respectively. As hydrogen separation is carried out along with carbon dioxide capture, the reversible reforming reactions are more driven to the product side, compared to the use of either an adsorptive or a membrane reactor. Increasing the fractions of hydrogen and carbon dioxide removal highly increases the amount of hydrogen, whereas the methane content deceases (Figures 6.7a-b). Figure 6.7c shows that the capture of carbon dioxide in the ethanol reforming system has strong effect on the content of carbon monoxide, compared to the removal of hydrogen. Moreover, it can be seen that the increased fraction of carbon dioxide removal leads to a reduced carbon dioxide content remaining in the reforming system, whereas increasing the hydrogen removal fraction gives an increased trend as shown in Figure. 6.7d. Therefore, addition of carbon dioxide adsorbent in the membrane reactor results in further purifying hydrogen in the reaction zone due to a decrease in the amount of carbon dioxide and carbon monoxide.

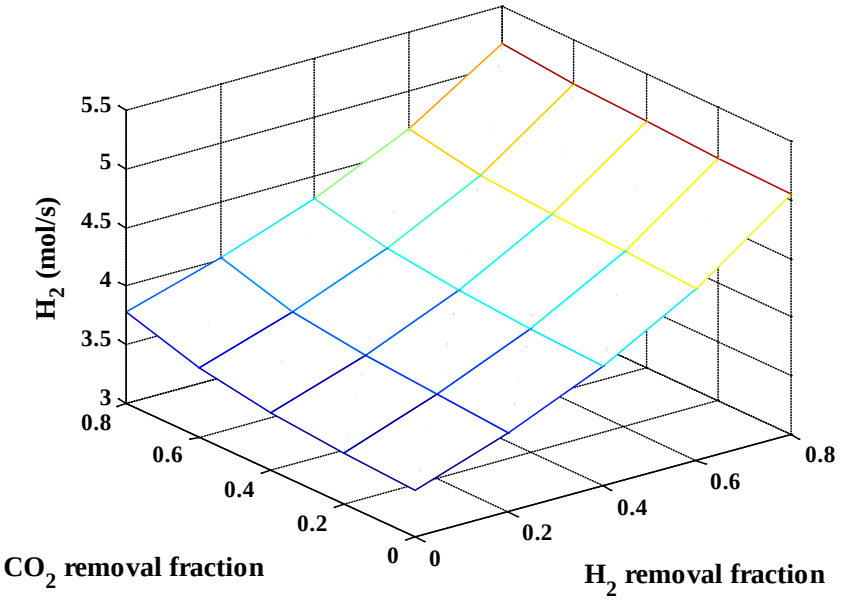
5.5
5
4.5
4
3.5
3
H2 (mol/s)
0.8
0.6
0.4
0.2
0
CO2 removal fraction
0
0.2
0.4
0.6
0.8
H2 removal fraction

(a)

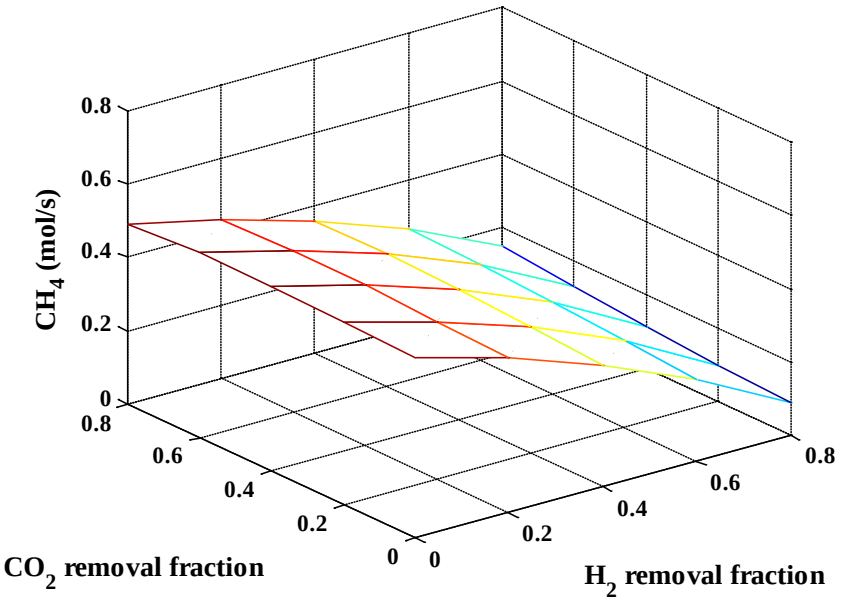
0.8
0.6
0.4
0.2
0
CH4 (mol/s)
0.8
0.6
0.4
0.2
0
CO2 removal fraction
0
0.2
0.4
0.6
0.8
H2 removal fraction

(b)

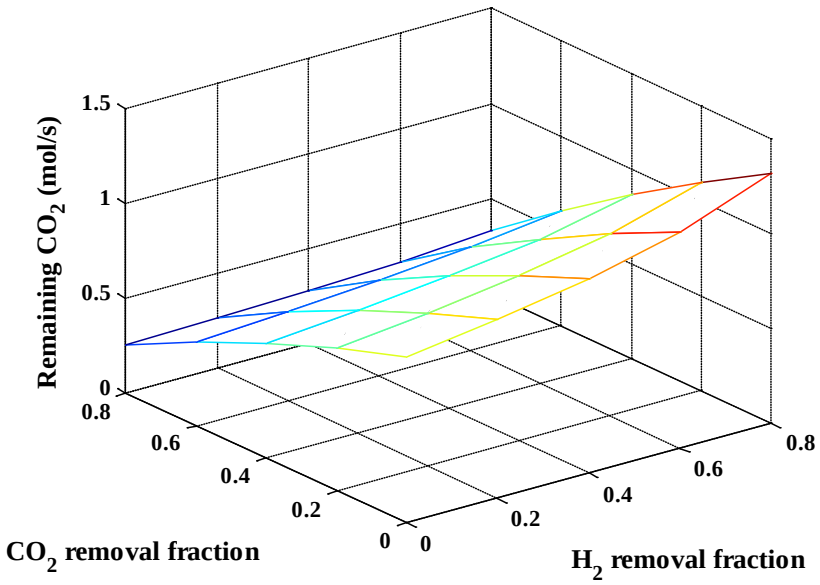


(c)

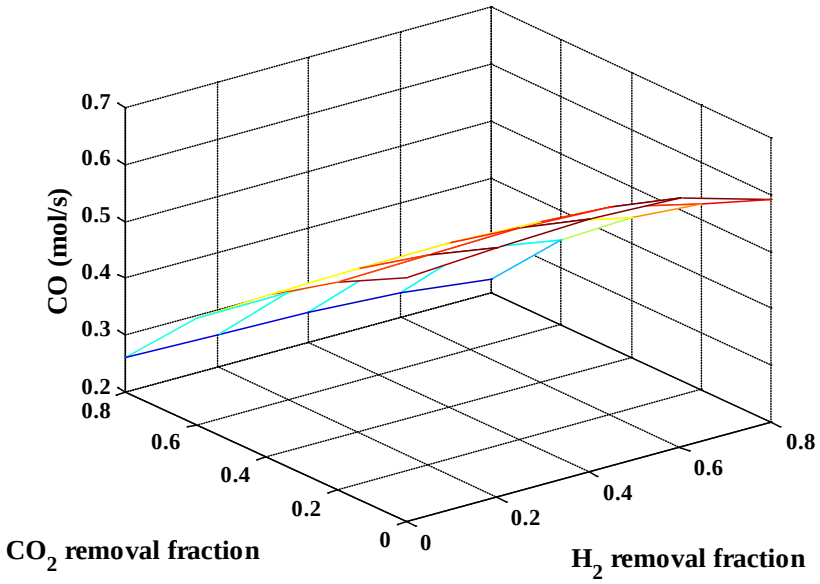


(d)

**Figure 6.7** Effect of the removal fraction of carbon dioxide and hydrogen in the adsorption-membrane hybrid system ($T$ = 873 K, $P$ = 1 bar, and ethanol to steam ratio = 3): (a) hydrogen, (b) methane, (c) carbon monoxide, and (d) remaining carbon dioxide.

### 6.3 Carbon formation in ethanol steam reforming systems

Figure 6.8 shows the requirement of inlet steam-to-ethanol ratio as a function of operating temperatures for the adsorption-membrane hybrid system of ethanol steam reforming. The region on the left side under the boundary line is the area where carbon formation may occur. It is found that at the fixed fraction of carbon dioxide removal ($f$ = 0.8), the possibility of carbon formation is more pronounced even the fraction of hydrogen removal is slightly increased ($r$ = 0→ $r$ = 0.2). On the other hand, the tendency of carbon formation in the adsorption-membrane hybrid system with a less removal of carbon dioxide ($r$ = 0.8, $f$ = 0.2) at a low temperature range (500-800 K) decreases when compared with the reforming system using only a membrane ($r$ = 0.8, $f$ = 0). As a result, it can be concluded that addition of carbon dioxide adsorbent in the membrane reactor alleviates the occurrence of carbon. Considering the amount of steam required for this system, increasing the fraction of carbon dioxide adsorption in the membrane reactor ($r$ = 0.8, $f$ = 0.8) results in a significant reduction in the requirement of steam fed to the system at low temperature of 500-800 K. However, when the operating temperature is higher than 850 K, the boundary of carbon formation of the adsorption-membrane hybrid system is greater than the use of the hydrogen selective membrane reactor.

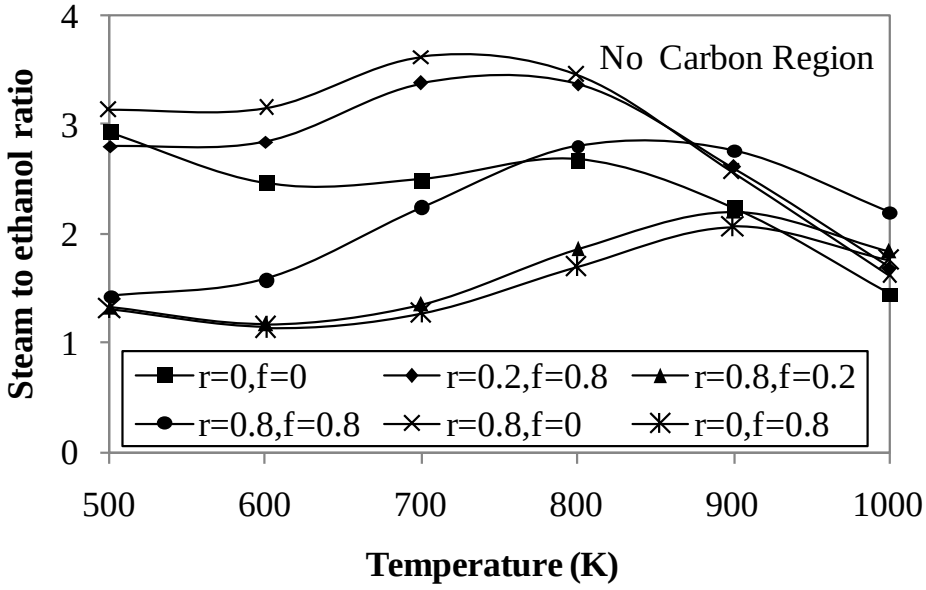


**Figure 6.8** Effect of fraction of carbon dioxide and hydrogen removal on the requirement of inlet steam-to-ethanol ratio at different operating temperatures.

## 6.4 Conclusions

This study presented the thermodynamic analysis of ethanol steam reforming in the adsorption-membrane hybrid system in which carbon dioxide adsorbent is used to remove undesired carbon dioxide and membrane is applied for hydrogen separation. Effects of operating conditions, i.e., temperature and steam-to-ethanol ratio, on hydrogen production were investigated. The results showed that at atmospheric pressure, the production of hydrogen from the ethanol steam reforming is favored at high steam-to-ethanol ratio and temperature. Considering the adsorption-membrane hybrid system, it was found that hydrogen removal by membrane separation has more impact on the reactor performance than carbon dioxide removal by adsorption. However, the boundary of carbon formation is likely to decrease when carbon dioxide adsorption is considered. The use of the adsorption-membrane hybrid system in ethanol steam reforming process does not only provide the highest hydrogen yield but also obtain pure hydrogen product.

# CHAPTER VII

# ANALYSIS OF AN ETHANOL-FULLED SOFC SYSTEM USING WITH PARTIAL ANODE EXHAUST GAS RECIRCULATION

This chapter presents the performance analysis of SOFC system integrated with ethanol steam reforming process with recycling partial anode gas. The system performance and energy management of both SOFC systems with non-recycling and recycling the anode exhaust gas were initially compared. Then, the impacts of using anode exhaust gas to ethanol steam reforming process on reformer performance namely components of synthesis gas product and boundary of carbon formation are investigated. The effects of recirculation ratio and fuel utilization of anode exhaust gas on SOFC performance are also considered. Finally, a variation of reformer and SOFC operating temperature at diverse recirculation ratio on system performance are studied. The SOFC electrical and system thermal efficiency is indicator for system performance in this chapter.

## 7.1 Introduction

When considering the operating parameters of SOFC systems, it has been reported that the fuel utilization is the most important parameter affecting the performance of SOFC. A SOFC operated at high fuel utilization can provide high electrical efficiency. However, at high fuel utilization, more hydrogen is consumed by the electrochemical reactions, and the fuel stream at the SOFC fuel channel is thus diluted by steam (Aguiar et al., 2004). A hydrogen deficiency due to the unbalanced fuel flowing through the SOFC causes a larger buildup of nickel oxide (Nehter, 2007) as well as corrosion on the carbon plate (Nishikawa et al., 2008). Therefore, it is reasonable to operate the SOFC at a moderate fuel utilization. Under this condition,

the SOFC can produce electrical power together with a high-temperature exhaust gas that contains useful remaining fuel (i.e., hydrogen and carbon monoxide). Typically, the exhaust gases from fuel and air channels are burnt in an afterburner to produce more heat, which is used to preheat the fuel stream and supplied to the steam reformer. Although the combustion of exhaust gases can increase the thermal efficiency of the SOFC system, the fuel stream is utilized inefficiently. To improve the overall SOFC performance, a SOFC system with anode exhaust gas recycling has been proposed in the literatures (Granovskii et al., 2007; Shekhawat et al., 2007). A portion of anode exhaust gas containing useful fuels, i.e., hydrogen and carbon monoxide, is recirculated to mix with the inlet fuel before it is fed to the reformer, whereas the rest of the anode exhaust gas is burnt with the cathode exhaust gas in the afterburner. Interestingly, it is noteworthy that the steam produced by the electrochemical reaction in the anode exhaust gas can be further used as a reagent for steam reforming and thus the requirement for fresh steam can be reduced (Peter et al., 2002). Shekhawat et al. (2007) demonstrated that the utilization of the anode exhaust gas in the SOFC system integrated with the catalytic partial oxidation of diesel can reduce the carbon formation and increase the hydrogen concentration in the reformate gas. Although the SOFC system with anode exhaust gas recycling was previously studied as mentioned above, there are few studies that investigate in detail the effect of utilizing the anode exhaust gas on the reforming process and the SOFC system performance. This understanding allows for the improvement of the overall SOFC system efficiency.

In this study, the performance of a SOFC system fuelled by synthesis gas derived from an ethanol reforming process with non-recycling and recycling of the anode exhaust gas is investigated based on a thermodynamic analysis. The optimal design of the SOFC system is determined by considering the electrical and thermal efficiencies. In addition, the influences of the fuel utilization and recirculation ratio of the anode exhaust gas on the carbon formation in the ethanol steam reformer and on the system efficiency are investigated to justify the benefit of using the anode exhaust gas recycling.

## 7.2 Configuration of SOFC system

Figures 7.1a and 7.1b show schematics of the ethanol steam reformer and the SOFC integrated system with and without the recycle of the anode exhaust gas, respectively. Both the SOFC systems consist of a vaporizer, heat exchanger, fuel processor, SOFC stack and afterburner. First, ethanol and water are separately fed into the vaporizer and then sent to the heat exchanger to be preheated to the desired operating temperature of the reformer. The ethanol and steam then undergo the steam reforming reaction at the reformer to produce a synthesis gas. The obtained synthesis gas is preheated before being fed to the SOFC stack where the hydrogen in the synthesis gas reacts with oxygen in air to produce electrical power via an electrochemical reaction. The residue fuel in the SOFC outlet stream is combusted in the afterburner and the heat thus generated can be used for the heat-requiring units in the SOFC system. In the case where the anode exhaust gas is recycled (Figure 7.1b), a portion of the anode exhaust gas is recycled to the reformer. The steam generated by the electrochemical reaction can be used as a reforming reagent, whereas the residue of carbon monoxide in the anode exhaust gas can further react with steam via the water gas-shift reaction to produce more hydrogen in the steam reformer.

The following assumptions have been made for modeling the ethanol steam reforming and SOFC integrated system: (i) heat losses from each unit in the SOFC system are negligible, (ii) all gases behave as ideal gases, (iii) the temperatures of the system are kept constant, (iv) the distributions of pressure and temperature are negligible in reformer and SOFC, and (v) the anode temperature is equal to cathode one.

The performance of SOFC system with and without the recycle of the anode exhaust gas is evaluated from system model proposed in chapter 4. The values of operating conditions for system under based condition are given in Table 7.1. For the simulation of SOFC system with the recycle of the anode exhaust gas, the analysis methodology is rather complex due to the interaction of relation among the components in system. The flow chart of simulation of SOFC system with recycling anode exhaust gas is shown in Figure 7.2. The recycle stream (i.e., the composition of the anode exhaust gas) is assumed to be variable. The calculation begins from the specification of input parameters i.e. operating pressure and temperature of reformer,

inlet ethanol molar flow rate and reformer and recirculation ratio of anode exhaust gas as well as guess of the molar flow rate of methane, carbon dioxide, carbon monoxide, water and hydrogen in recycle stream and the extent of reaction in ethanol steam reforming ($x_1, x_2, x_3$), which are initial value for reformer. The molar flow rate of reformer outlet gases is calculated under constraint, which the extent of reaction is over zero. Subsequently, the molar flow rate of reformer outlet gases is used to be the initial molar flow rate of fuel for SOFC. The details of evaluation for anode outlet molar flow rate and SOFC performance are shown in chapter 4. The new values of recycled molar flow rate of each species are determined and it will be the new initial value of molar flow rate in recycle stream fed to reformer in next loop. The procedure of evaluation for all gas compositions of anode exhaust gas in recycle stream must be iterative until the equal values between guess and outlet of all gas compositions of anode exhaust gas in recycle stream in same loop. This procedure is based on the sequential solution method, which is the increase of iteration loop to reduce the possibility of convergence. This procedure is repeated until the difference in the values of the assumed and calculated variables satisfies a desired accuracy ($10^{-6}$). The real value of recycled gas compositions of anode exhaust gas is evaluated and then the system performance such as current density, voltage, the electrical and thermal efficiency are determined.

$$\eta_{\text{el,sofc}} = \frac{P_{\text{sofc}}}{\dot{n}_{\text{C}_2\text{H}_5\text{OH}} LHV_{C_2H_5OH}} \tag{7.1}$$

$$\eta_{\text{th}} = \frac{Q_{\text{rec}} - Q_{\text{use}}}{\dot{n}^{\text{in}}_{\text{C}_2\text{H}_5\text{OH}} LHV_{\text{C}_2\text{H}_5\text{OH}}} \tag{7.2}$$

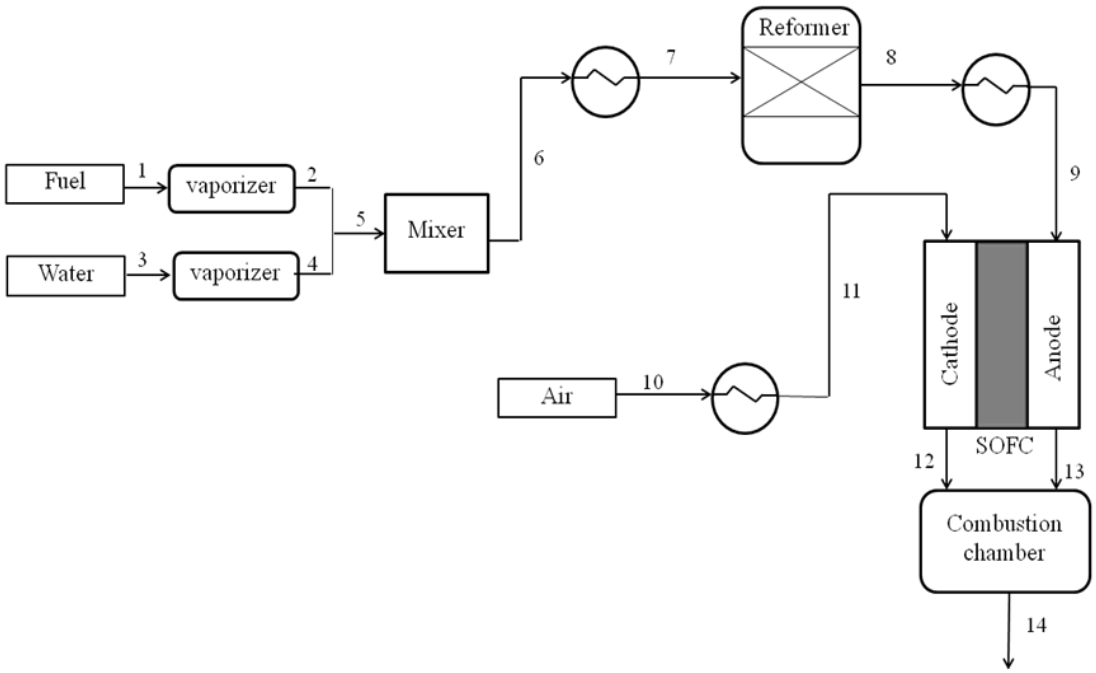


(a)

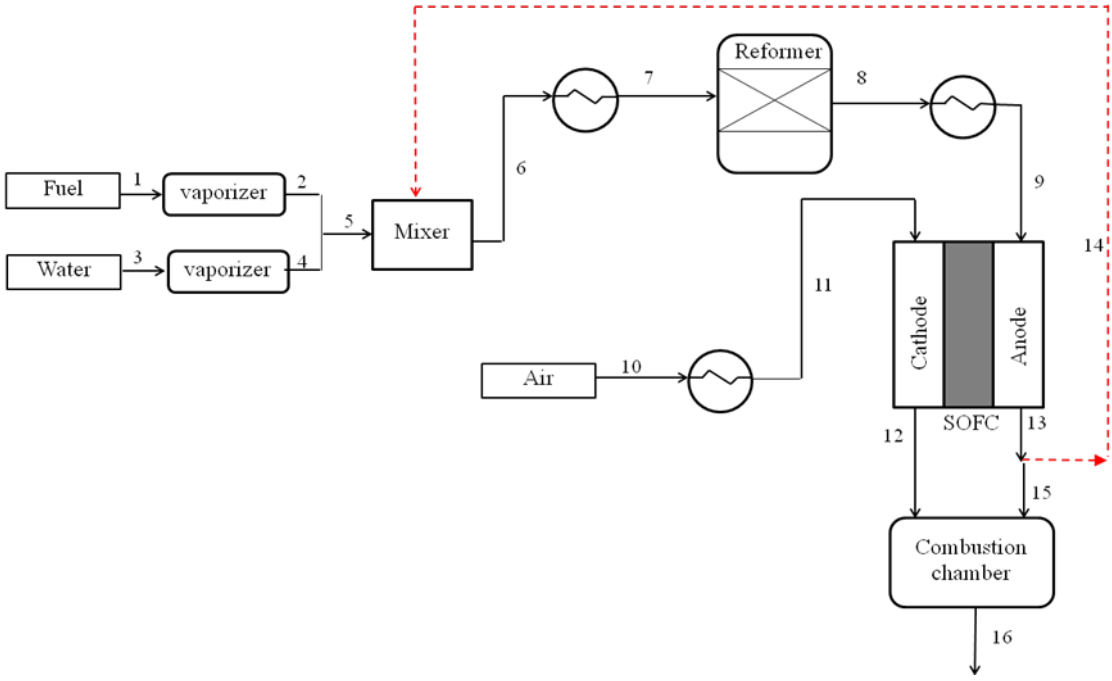


(b)

**Figure 7.1** Schematic of the SOFC systems integrated with an external ethanol steam reformer: (a) no recirculation and (b) anode exhaust gas recirculation.

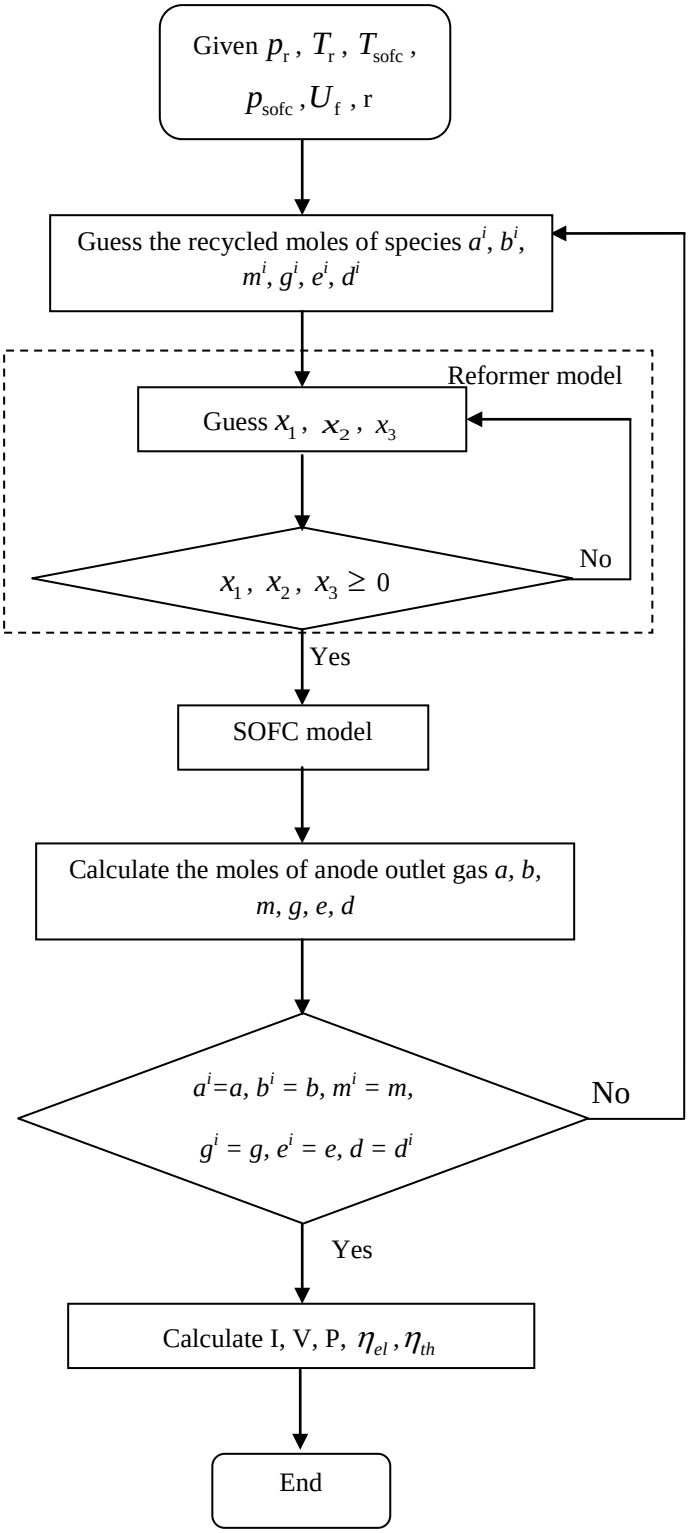


**Figure 7.2** Numerical algorithm for simulation of SOFC systems with anode exhaust gas recirculation.

**Table 7.1** Values of the operating conditions for the SOFC system under nominal conditions

| **Parameters** | **Value** |
|---|---|
| *Pre-reformer unit* | |
| Operating temperature, $T_r$ (K) | 973 K |
| Operating pressure, $P_r$ (bar) | 1 |
| Molar flow of ethanol (mol/s) | 1 |
| *Solid oxide fuel cell unit* | |
| Operating temperature, $T_{sofc}$ (K) | 1073 |
| Operating pressure, $P_{sofc}$ (bar) | 1 |
| Air composition | 21% $O_2$, 79% $N_2$ |
| Fuel utilization | 0.7 |
| Excess air ratio | 8.5 |
| SOFC pressure drop (%) | 2 |

## 7.3 Results and discussion

### 7.3.1 Comparison of SOFC systems with and without anode exhaust gas recycling

The performances of the SOFC system with and without recycling the anode exhaust gas are first analyzed under nominal conditions. The steam and ethanol fed to the ethanol steam reformer are fixed at the ratio of 3. Table 7.2 shows the heat duty needed in each unit of both SOFC systems. The energy requirements for the ethanol processor section of the SOFC system with and without the anode exhaust gas recirculation are 397.10 and 634.18 kW, respectively. The recirculation of the anode gas reduces the energy required by the fuel processor (37.4% reduction). In addition, it is observed that all of the steam required for the steam reformer is recovered by the anode exhaust gas recirculation (the recirculation ratio = 0.6), and this can save the energy supplied to the water vaporizer. However, the total energy requirements of the two SOFC systems are not different. The SOFC with anode gas recirculation can produce more electrical power and thus requires a high air supply to maintain the temperature of the SOFC. This results in high energy consumption in the air pre-

heater. It is noted that since the power required to drive the blower for the anode exhaust gas recycling has slight effect on the SOFC system, it is negligible in calculating the electrical efficiency of the SOFC system.

Figure 7.3 shows a comparison of the SOFC system performance when not recycling and recycling the anode exhaust gas at different steam-to-ethanol feed ratios. The simulation results clearly show that the SOFC system with anode exhaust gas recycling provides higher electrical and thermal efficiencies than that without recycling the anode exhaust gas. In the case of the SOFC system with anode exhaust gas recirculation, it is found that the molar flow rates of hydrogen and carbon monoxide in the SOFC feed stream increase. As a result, the current density generated by the SOFC is more produced, resulting in higher electrical and thermal efficiencies.

Considering the effect of the steam-to-ethanol feed ratio, the electrical performance of both SOFC systems decreases when increasing the steam-to-ethanol feed ratio. This can be explained by a dilution of the hydrogen fed to the SOFC. Unlike the electrical efficiency, when more steam is added, the thermal efficiency of the SOFC system operated with a recycle of the anode exhaust gas slightly increases because the load of steam generation is reduced. In addition, the high-temperature recycling gas reduces the external heat load for the SOFC feed pre-heater. In contrast, for the conventional SOFC system, an increase in the steam-to-ethanol ratio leads to a higher energy requirement for evaporating and preheating feed the steam, and thus the thermal efficiency is significantly decreased.

**Table 7.2** Heat duty of each unit in the SOFC systems with and without anode exhaust gas recirculation

| **Heat exchangers** | **Heat duty (kW)** | |
|---|---|---|
| | **SOFC System without recycling the anode-exhaust gas** | **SOFC System with recycling the anode-exhaust gas** |
| Ethanol vaporizer | 49.12 | 49.12 |
| Water vaporizer | 167.88 | - |
| Pre-heating gas before reformer | 152.04 | 33.18 |
| Pre-heating gas before SOFC | 30.44 | 47.61 |
| Reformer | 234.70 | 267.19 |
| Air pre-heater | 1503.94 | 1731.53 |
| Total | 2138.1 | 2128.63 |

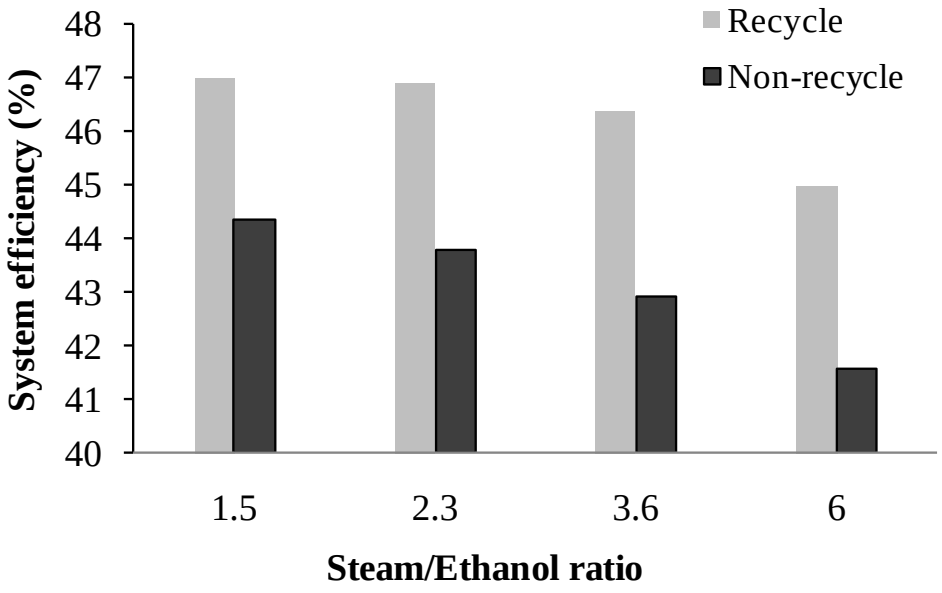


(a)

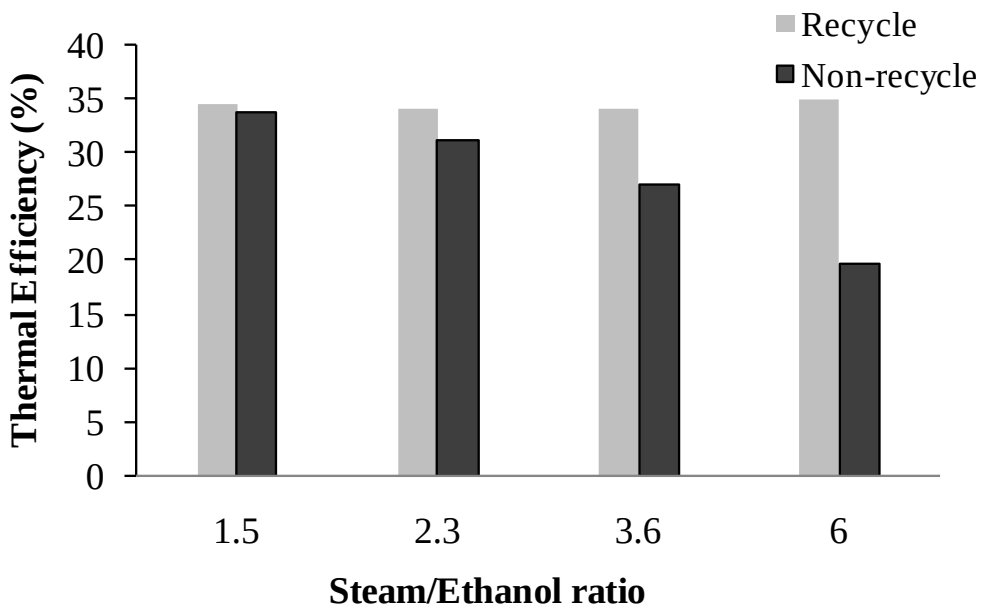


(b)

**Figure 7.3** Performance of the SOFC systems with and without recycling the anode exhaust gas at different steam-to-ethanol ratios: (a) electrical efficiency and (b) thermal efficiency.

### 7.3.2 Effects of recirculation ratio and fuel utilization

It is well known that a crucial problem of ethanol steam reforming is caused by the formation of carbon (graphite), which could lead to the deactivation of the catalyst and increased pressure drops in the reformer. To avoid carbon formation, the suitable operating temperature and steam-to-carbon ratio should be determined. In general, a steam reforming reaction needs to be fed with excess steam to increase hydrogen production and to reduce the carbon monoxide. The presence of carbon monoxide will promote carbon formation via the Boudouard reaction (Eq. (4.78). Furthermore, the tendency of carbon formation decreases as the reforming temperature increases due to the exothermic nature of the Boudouard reaction. However, operation of the steam reformer at a high temperature with more steam addition results in a high operating cost.

Figure 7.4 presents the effect of the recirculation ratio of the anode exhaust gas on the reformer temperature and steam-to-carbon ratio required to avoid carbon formation at different fuel utilizations. It is noted that the fuel utilization affects the

gaseous composition of the residual gas exiting from the SOFC anode, whereas the recirculation ratio indicates the amount of the steam, which is generated by the electrochemical reaction, that is recycled to the ethanol steam reforming section.

As seen in Figure 7.4a, the reforming temperature required to suppress the tendency of carbon formation is reduced when the SOFC is operated at the higher recirculation ratio and fuel utilization. The higher recirculation ratio increases the recycle of the steam to the ethanol reformer. Furthermore, at high fuel utilization, more steam is also generated from the SOFC stack. These factors lead to an increase in the steam-to-carbon ratio of the reformer feed (Figure 7.4b). From the simulation result, when the SOFC system with anode exhaust gas recycling is operated at a low fuel utilization of 0.6 and recirculation ratio of 0.4, the reforming temperature should be higher than 970 K to prevent the formation of carbon in the ethanol reformer.

Figure 7.5a-e shows the molar flow rates of hydrogen, carbon monoxide, carbon dioxide, steam and methane at the outlet of the ethanol reformer as functions of the recirculation ratio and fuel utilization. As expected, the amount of hydrogen and carbon monoxide decreases as the fuel utilization of the SOFC increases, whereas carbon dioxide and steam increase because the electrochemical and water gas shift reactions in the SOFC are more pronounced. The results show that an increase in the recirculation ratio increases the flow rates of the steam, carbon dioxide, carbon monoxide and hydrogen. However, at high fuel utilization, the carbon monoxide flow rate decreases when the recirculation ratio increases. At these conditions, more steam is recycled to the reformer, promoting the water gas shift reaction. It is noted that when the SOFC is operated at a high fuel utilization and recirculation ratio, a higher steam content in the anode exhaust gas and also a decrease in the content of methane at the reformer outlet is observed due to an increase in the reverse methanation reaction.

The influences of the fuel utilization and recirculation ratio on the current density, cell voltage, power density and electrical and thermal efficiencies are shown in Figure 7.6 It can be seen that increasing the fuel utilization and the recirculation ratio cause the SOFC to generate more current density (Figure 7.6a). When the SOFC is operated at higher fuel utilization, more hydrogen is consumed to produce electricity, while increasing the recirculation ratio of the anode exhaust gas leads to an

increase in the molar flow rate of fuel to the SOFC. However, it is found that the operating cell voltage decreases with the increments of fuel utilization and recirculation ratio (Figure 7.6b). This is mainly due to a significant increase of steam in the anode exhaust gas as the fuel utilization and recirculation ratio increase. Although a higher amount of steam promotes the ethanol reforming reaction, an excess of steam results in a dilution of the hydrogen required for the electrochemical reaction. This leads to a significant decrease in the open-circuit voltage and an increase in the concentration loss.

Figure 7.6c and d show that at low fuel utilization (0.5-0.6), the power density and electrical efficiency of SOFC increase with the increasing recirculation ratio. As the anode exhaust gas consists of a higher unreacted fuel content due to the low fuel utilization, an increase in the recirculation ratio results in an increase in hydrogen at the SOFC anode inlet, improving the SOFC performance in terms of current density, power density and electrical efficiency. However, the power density and the SOFC electrical efficiency decrease when increasing the recirculation ratio at high fuel utilization. Even though an increase in the fuel utilization results in more current density generated, the increased recirculation ratio causes a significant decrease in the fuel cell voltage. This implies that at high fuel utilization, the decrease in the fuel cell voltage has a strong impact on the power density and electrical efficiency, compared with an increase in the current density.

Considering the thermal efficiency of the SOFC system (Figure 7.6e), when the SOFC is operated at low fuel utilization, an increase in the recirculation ratio decreases the thermal efficiency. Operation of the SOFC at a high recirculation ratio lowers the amount of the exhaust gas sent to the afterburner; therefore, the heat generated from the afterburner for use in the SOFC system will decrease. However, the thermal efficiency can be enhanced when the SOFC system is operated at a higher recirculation ratio and higher fuel utilization. This is mainly because the significant increase of steam recycled to the ethanol reformer reduces the demand of energy for generating steam and preheating fuel stream.

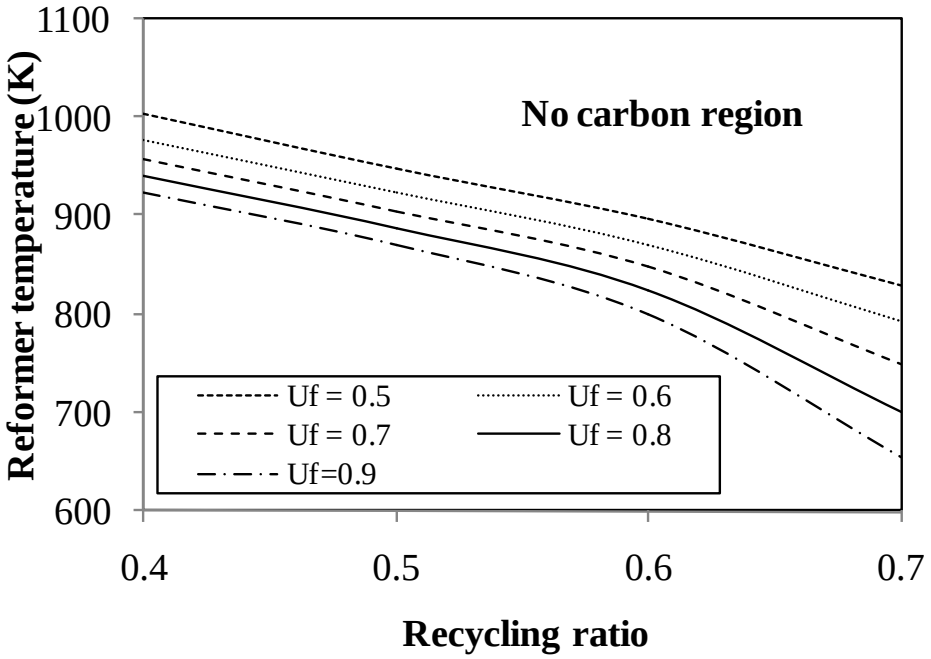


(a)

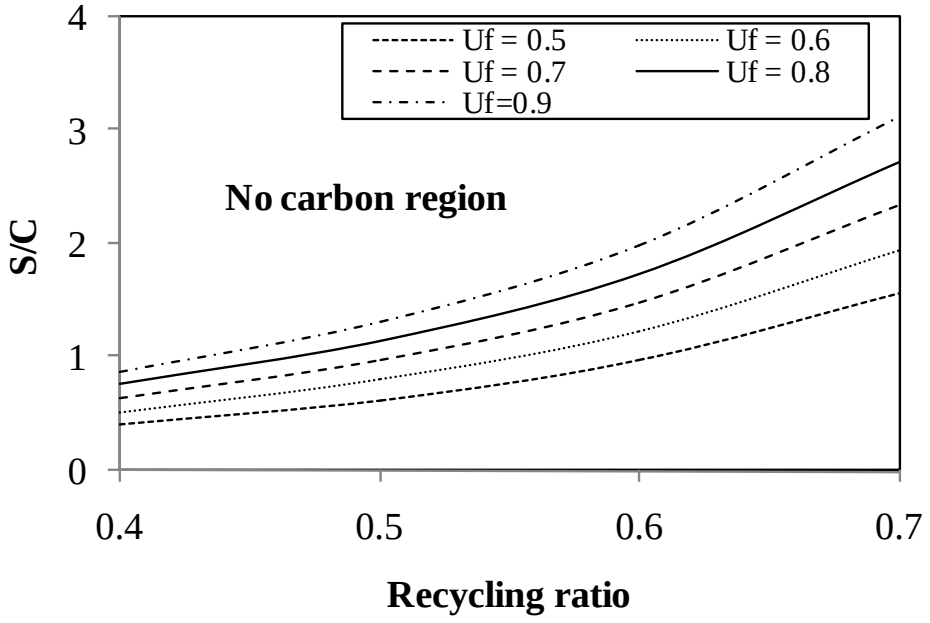


(b)

**Figure 7.4** Effect of the recirculation ratio of the anode exhaust gas at different fuel utilizations on the requirement of (a) the reformer temperature and (b) the steam-to-carbon ratio, to avoid a carbon formation.

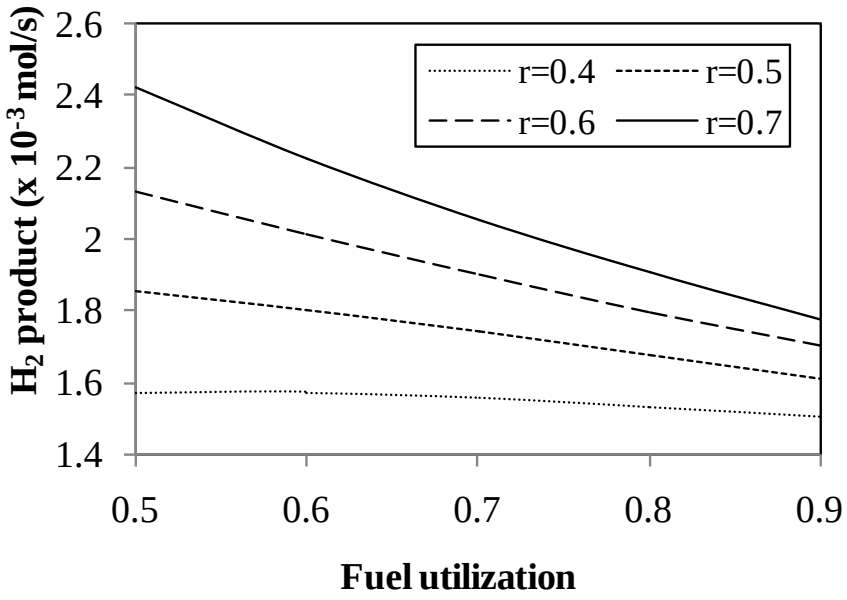
2.6
2.4
2.2
2
1.8
1.6
1.4
H2 product (x 10-3 mol/s)
r=0.4
r=0.5
r=0.6
r=0.7
0.5
0.6
0.7
0.8
0.9
Fuel utilization

(a)

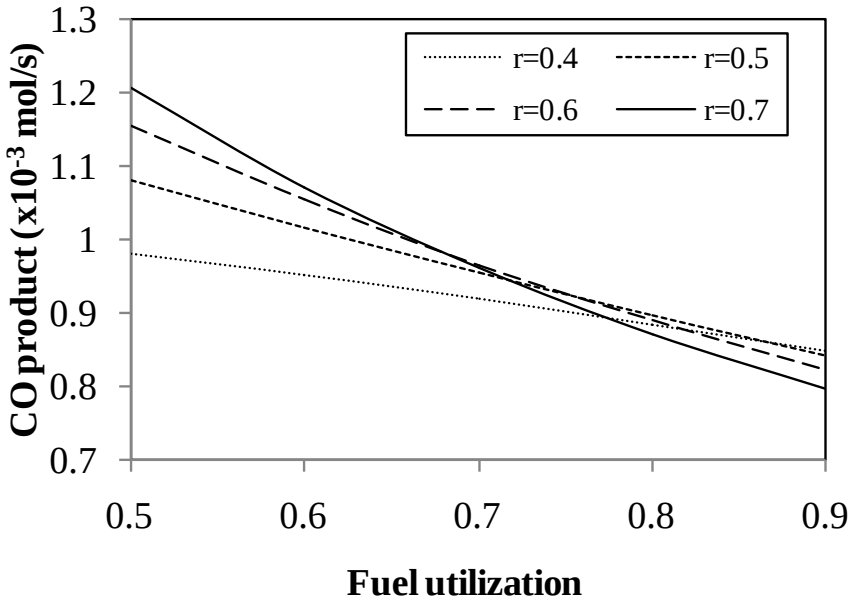
1.3
1.2
1.1
1
0.9
0.8
0.7
CO product (x10-3 mol/s)
r=0.4
r=0.5
r=0.6
r=0.7
0.5
0.6
0.7
0.8
0.9
Fuel utilization

(b)

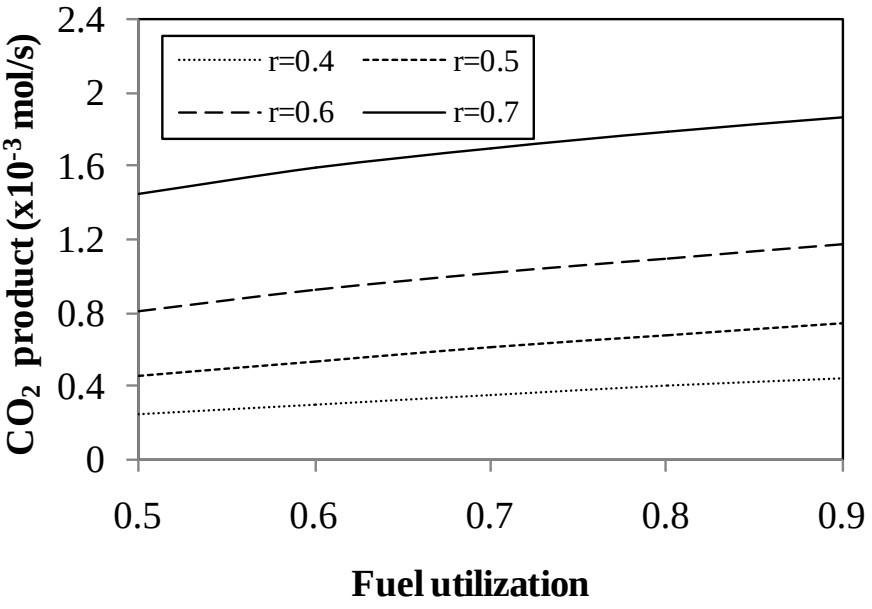
2.4
2
1.6
1.2
0.8
0.4
0
r=0.4
r=0.5
r=0.6
r=0.7
CO2 product (x10-3 mol/s)
0.5
0.6
0.7
0.8
0.9
Fuel utilization

(c)

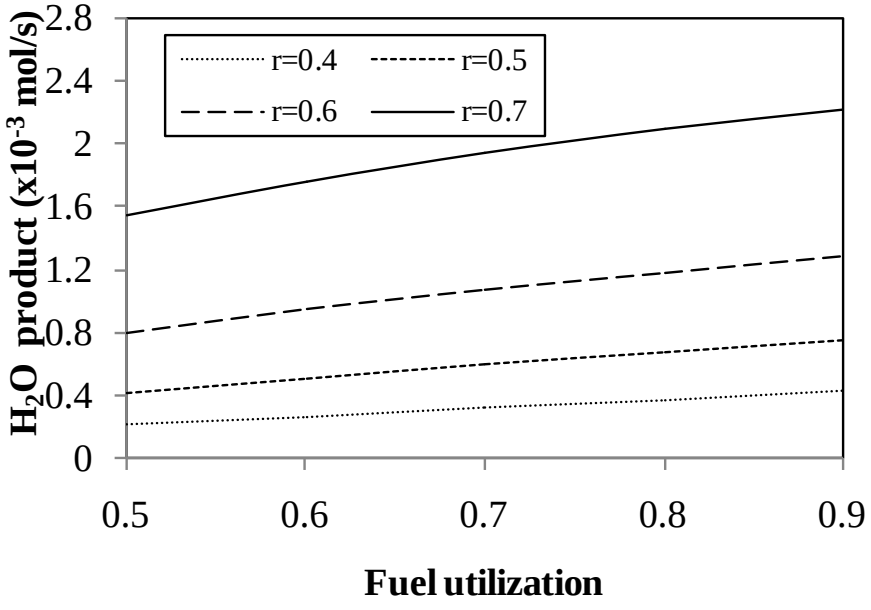
2.8
2.4
2
1.6
1.2
0.8
0.4
0
r=0.4
r=0.5
r=0.6
r=0.7
H2O product (x10-3 mol/s)
0.5
0.6
0.7
0.8
0.9
Fuel utilization

(d)

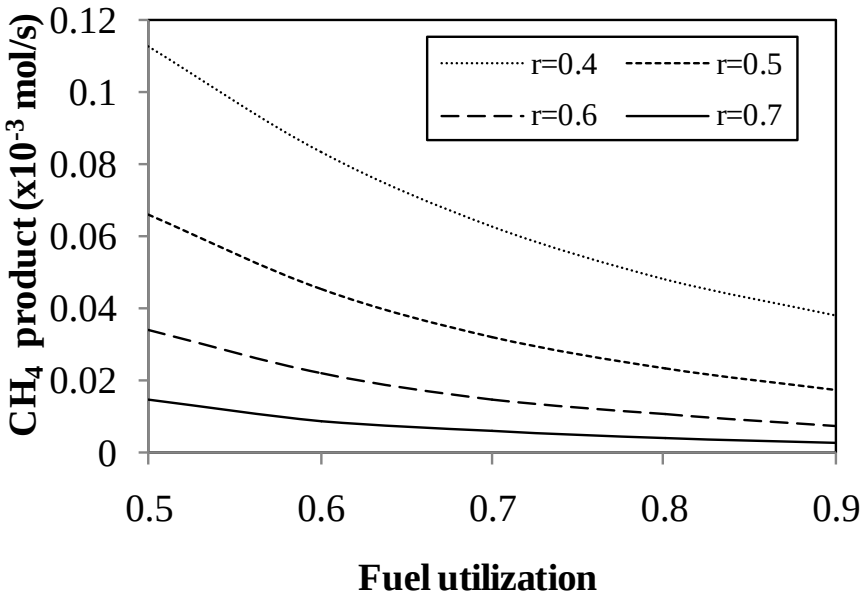


(e)

**Figure 7.5** Effect of fuel utilization on the composition of the synthesis gas obtained from the ethanol steam reformer at different recirculation ratios.

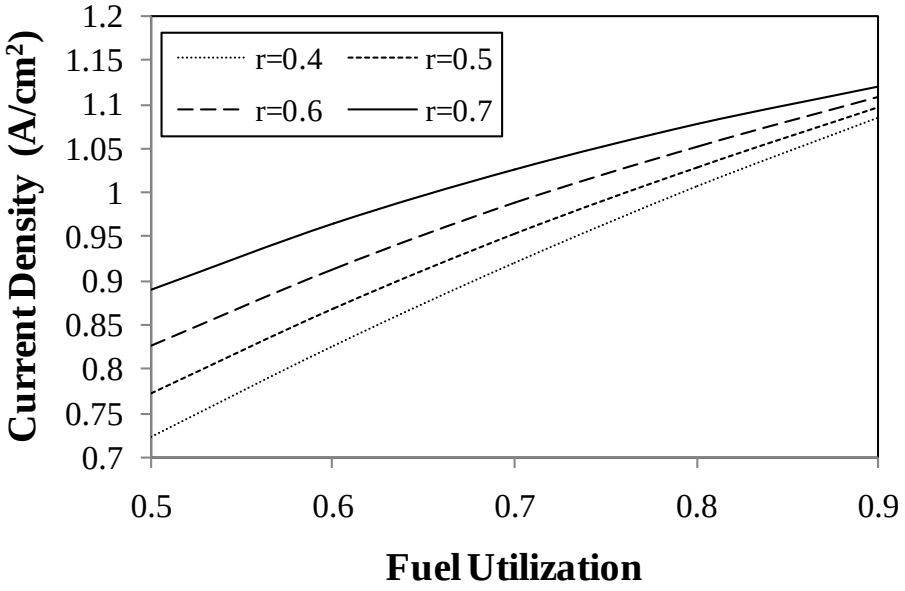


(a)

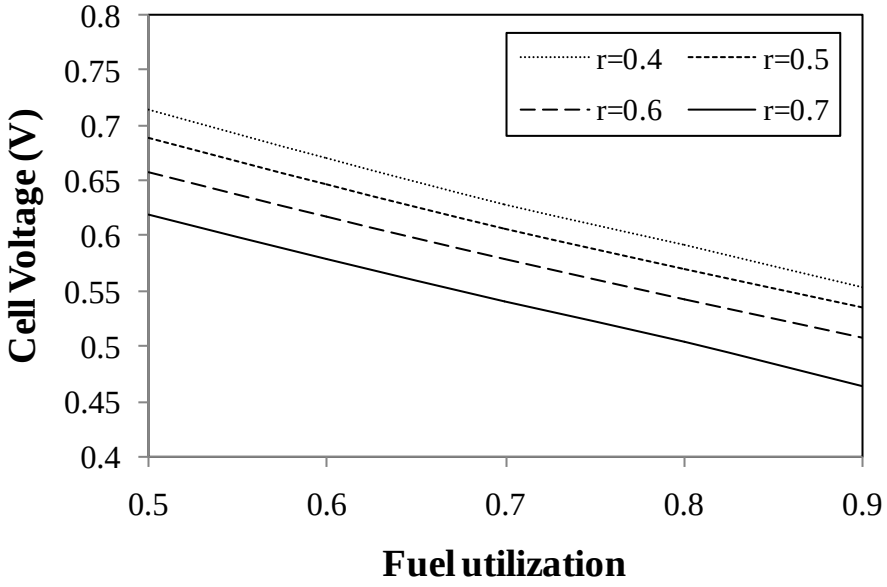
0.8
0.75
0.7
0.65
0.6
0.55
0.5
0.45
0.4
Cell Voltage (V)
r=0.4
r=0.5
r=0.6
r=0.7
0.5
0.6
0.7
0.8
0.9
Fuel utilization

(b)

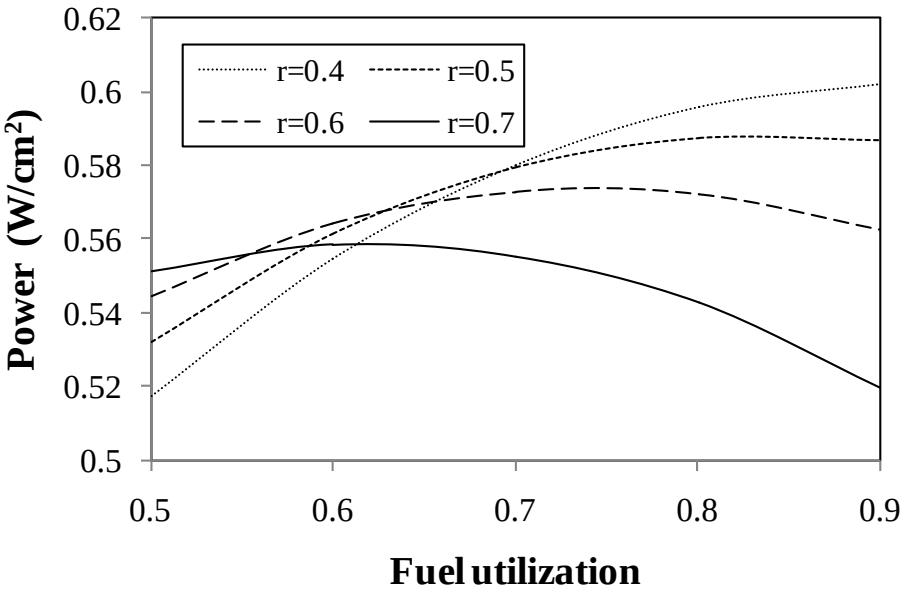
0.62
0.6
0.58
0.56
0.54
0.52
0.5
Power (W/cm2)
r=0.4
r=0.5
r=0.6
r=0.7
0.5
0.6
0.7
0.8
0.9
Fuel utilization

(c)

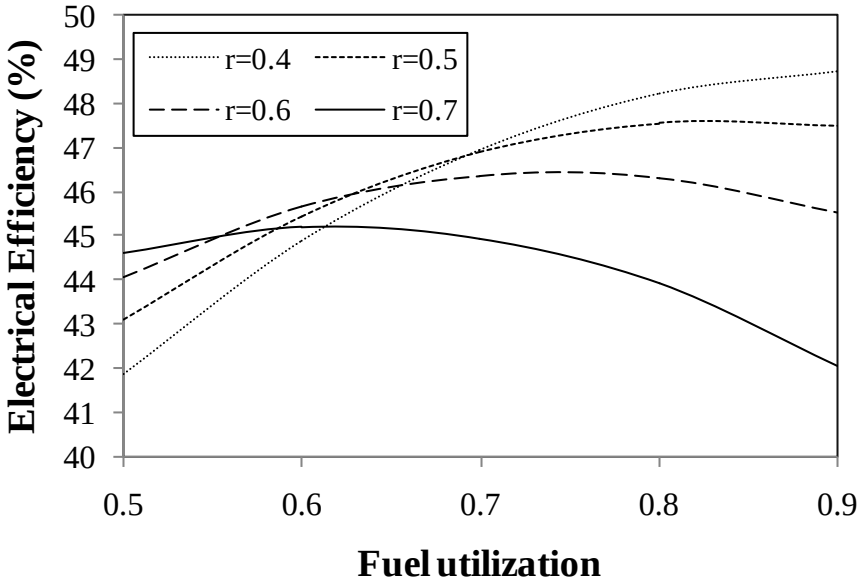


(d)

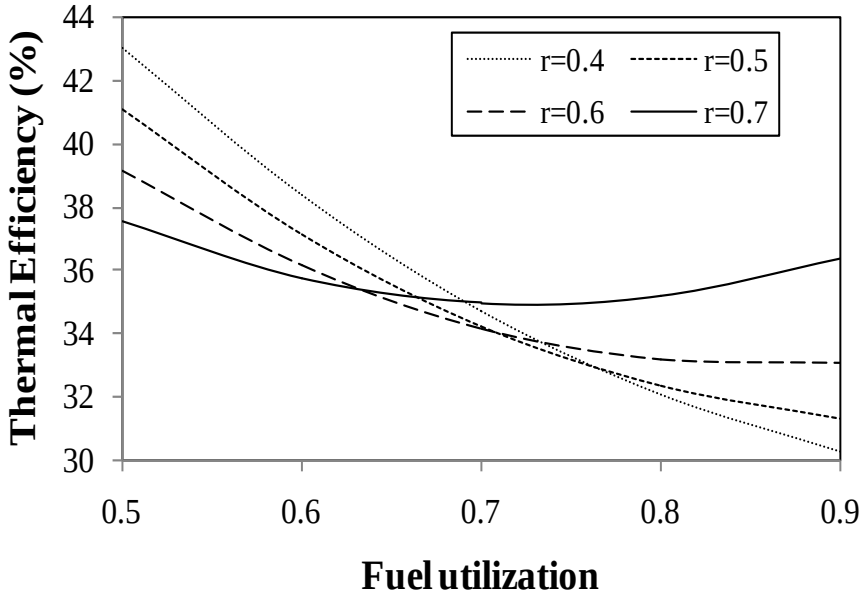


(e)

**Figure 7.6** Effect of fuel utilization on the SOFC system performance at different recirculation ratios: (a) current density, (b) fuel cell voltage, (c) power density, (d) electrical efficiency, and (e) thermal efficiency.

### 7.3.3 Effects of reformer and SOFC operating temperature

The effect of the reformer temperatures on the electrical efficiency when the SOFC is operated at temperature of 1073 K is shown in Figure 7.7. The electrical efficiency of the SOFC system with the anode gas recirculation considerably increases when increasing the reformer temperature. As the ethanol steam reforming is favored in operation at high temperatures, the increase in produced hydrogen promotes the electrochemical reaction in the SOFC stack, and thus, the electrical efficiency of SOFC is enhanced. However, an increase in the recirculation ratio results in a lower SOFC electrical efficiency. The degradation of the SOFC performance is obviously noticed when the reformer is operated at unsuitable temperatures. This lowers the production of hydrogen fuel for the SOFC. In addition, at a high recirculation of the anode exhaust gas, more steam is added to the SOFC, thereby decreasing the fuel cell voltage and the electrical efficiency.

Figure 7.8 presents the electrical efficiency of the SOFC system as a function of the SOFC operating temperatures when the reformer is operated at temperature of 973 K. It can be seen that the electrical efficiency increases as the operating temperature of SOFC increases. An increase in the SOFC operating temperature can improve its performance because the rate of the electrochemical reaction is more pronounced. In addition, at elevated temperatures, the ohmic and activation losses are also reduced. Therefore, the more current density is generated, leading to the increased electrical efficiency.

### 7.3.4 Effect of excess air ratio

The influence of the excess air ratio on the system's electrical and thermal efficiencies at different recirculation ratios is presented in Figures 7.9a and 7.9b, respectively. The excess air ratio has a slight effect on the system electrical efficiency but a larger effect on the system thermal efficiency. The thermal efficiency sharply drops when the SOFC system is operated at a high excess air ratio owing to an increased requirement of the heat duty of the air pre-heater.

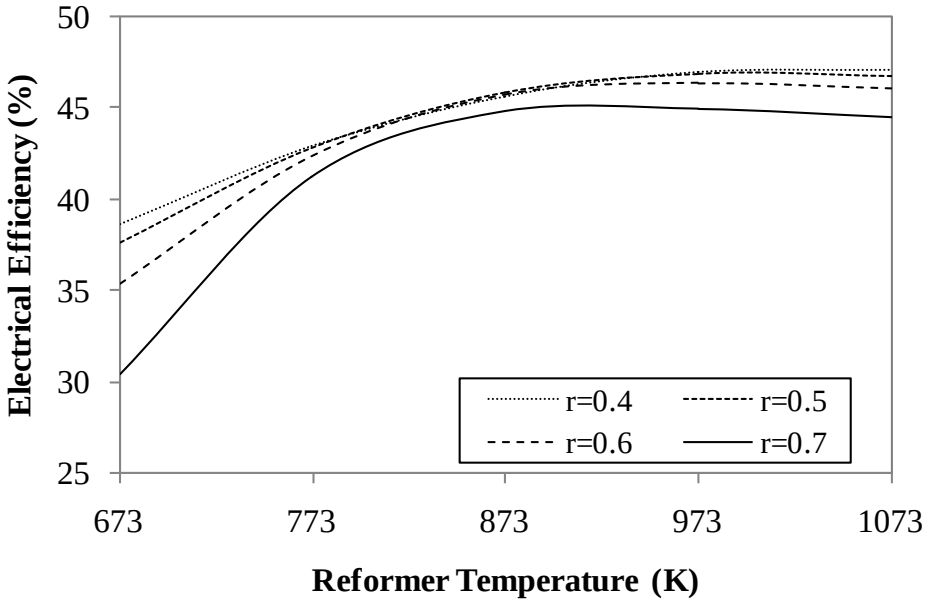


**Figure 7.7** Effect of the reformer operating temperature on the electrical efficiency of the SOFC system at different recirculation ratio

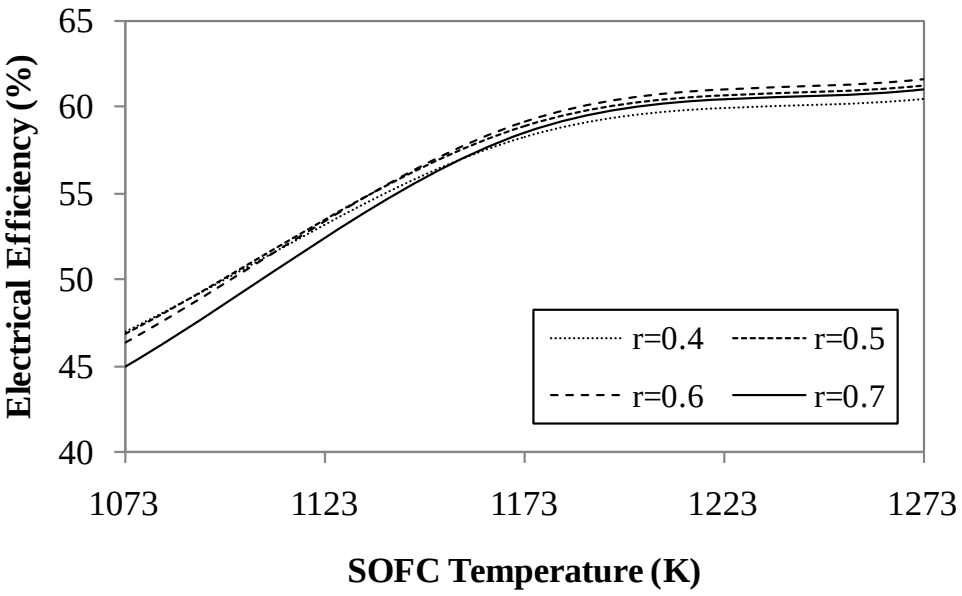


**Figure 7.8** Effect of the SOFC operating temperature on the electrical efficiency of the SOFC system at different recirculation ratios**.**

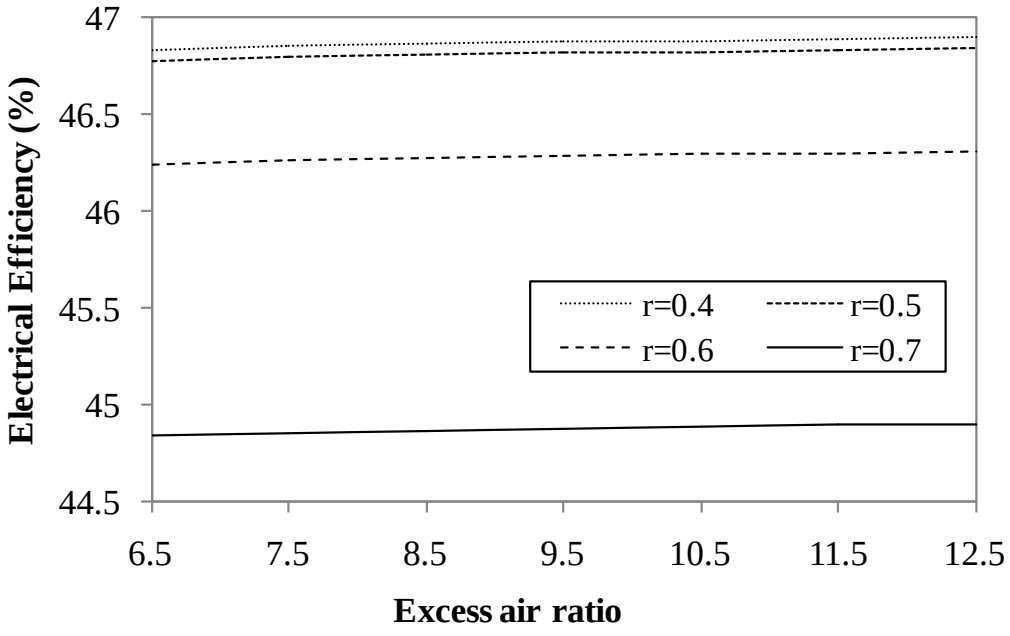


(a)

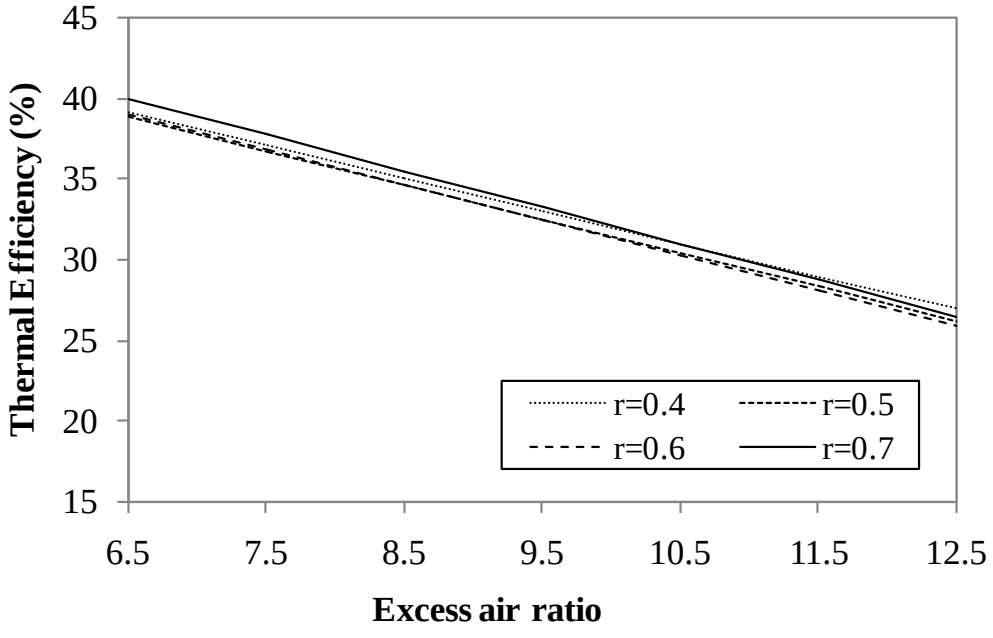


(b)

**Figure 7.9** Effect of the excess air ratio on (a) the electrical efficiency and (b) the thermal efficiency of the SOFC system at different recirculation ratios**.**

## 7.4 Conclusions

The performance analysis of a SOFC system fuelled by ethanol is presented in this work. An electrochemical model of the SOFC and an equilibrium model of ethanol steam reforming are employed to simulate the SOFC system. The performance of two SOFC systems with and without anode exhaust gas recirculation is compared. The results indicate that the SOFC system with anode exhaust gas recycling provides higher electrical and thermal efficiencies than that of a non-recycling SOFC system. It is found that the tendency of carbon formation in the ethanol steam reformer decreases with an increasing recirculation ratio and fuel utilization in the SOFC stack. At low fuel utilization, the electrical efficiency of the SOFC system increases with the increasing recirculation ratio while the thermal efficiency decreases. The performances of the SOFC system show an opposite trend at high fuel utilization operation. Therefore, the recirculation ratio must be carefully selected. Furthermore, the electrical efficiency of the SOFC system can be enhanced when the ethanol reformer and SOFC stack are operated at high temperatures.

# CHAPTER VIII

# DESIGN OF A PRESSURIZED SOFC-GAS TURBINE HYBRID SYSTEM WITH CATHODE GAS RECIRCULATION

In this chapter, the integration of SOFC system and gas turbine was studied. The electrical efficiency and self-sustaining energy in system are considered as performance indicator of hybrid system between solid oxide fuel cell and gas turbine. Firstly, the impact of operating pressure on performance of the pressurized SOFC-GT hybrid system was investigated. The energy management within the pressurized SOFC-GT hybrid system was also considered. Then, the pressurized SOFC-GT hybrid system with recycling a portion of cathode exhaust gas back to use in solid oxide fuel cell was proposed to reduce external energy. The impact of cathode exhaust gas recirculation on performance of solid oxide fuel cell, gas turbine and overall system was presented in this chapter.

## 8.1 Introduction

SOFC is operated at high temperatures so that the exhaust gas from the SOFC can be used as a heat source for other heat-requiring units in the SOFC system resulting in the improvement of the system thermal efficiency. Moreover, SOFC can be integrated with a gas turbine to generate more electricity. At present, the power generation of a SOFC-gas turbine hybrid system (SOFC-GT) has been increasingly received much attention because of its high system efficiency.

In general, a SOFC-GT hybrid system can be run at either atmospheric (non pressurized system) or high pressure (pressurized system) conditions. In the non-pressurized SOFC-GT hybrid system, a gas turbine operation does not depend directly on the SOFC leading to a simple cycle system. Nevertheless, heat exchangers in the

system have to be operated at very high temperature and pressure differences, thereby requiring a high effective material (Traverso et al., 2010; Burbank et al., 2009). At present, the pressurized SOFC-GT hybrid system has attracted more attention because it can achieve higher system efficiency (Park et al., 2007). A number of investigations on the pressurized SOFC-GT system have been carried out in various aspects. Some researchers studied the effect of parameters on the SOFC system performance by performing energy and exergy analyses to determine the optimum parameters for the systems that are operated under full and partial loads (Calise et al, 2006; Akkaya et al., 2008; Haseli et al, 2008; Motahar and Alemrajabi, 2009). In addition, a design of the pressurized SOFC-GT system was proposed in order to improve the system efficiency. Yang et al. (2006) considered the effect of operating temperatures on the performance of the pressurized SOFC-GT hybrid system that is designed by supplying the additional air or fuel to a combustor of the gas turbine system. Prapan et al. (2003) developed the pressurized SOFC-GT system fuelled by a natural gas. Heat in the exhaust gas of the gas turbine was recuperated and used for steam generation. This generated steam is injected into GT combustion chamber in order to increase GT power and the system efficiency. Park et al. (2009) analyzed the influence of steam generation by using the gas turbine exhaust gas on the performance of both the non-pressurized and pressurized SOFC-GT hybrid system.

Apart from the electrical efficiency, a heat management of the SOFC system should also be considered. Braun et al. (2006) focused on a design of the SOFC system for a residential application taking into account a combined heat and power (CHP). Jia et al. (2011) investigated the SOFC power system with cathode gas recycling. The results showed that the efficiency of the SOFC system using a cathode gas recirculation can be improved by a reduction of the energy supplied to the air pre-heater. The SOFC-GT hybrid system with cathode exhaust gas recycling is the interesting and potential power system that minimizes the system heat requirement and maximizes the system efficiency. However, there are few studies that perform a detailed analysis of such a system. An understanding of the effect of the cathode gas recirculation on both the SOFC and gas turbine performances would lead to an optimal design of the SOFC-GT system.

The aim of this study is to analyze the performance of a pressurized SOFC-GT hybrid system with and without a cathode gas recirculation. Ethanol is used as a fuel for hydrogen production via a steam reforming process. An energy management of the SOFC-GT system is considered to achieve the highest electrical generation and thermal energy usage. Effect of the recirculation ratio of cathode exhaust gas on the system efficiency is also investigated.

**8.2 Configuration of SOFC system**

The schematic diagram of a pressurized SOFC-GT hybrid system is illustrated in Figure 8.1a. The system consists of a pump, evaporator, heat exchanger, fuel processor, SOFC, combustor, gas turbine and compressor. The steam and ethanol are pumped and then vaporized in the evaporator. The mixture of ethanol and steam is preheated to the desired temperature and converted into a synthesis gas in the steam reformer. The synthesis gas is preheated and fed into the SOFC. Hydrogen in the synthesis gas reacts with oxygen in the compressed air to produce the electrical power and steam via the electrochemical reaction. In general, SOFC cannot be operated at the full utilization of fuel. As a result, the residue fuel in the SOFC outlet stream is combusted in the combustor and the obtained exhaust gas is then fed into the gas turbine to generate more electricity. Due to its high temperature, the gas turbine outlet can be used as a heat source for other heat-requiring units. The heat management of the SOFC system can reduce the requirement of an external heat. Figure 8.1b shows the SOFC-GT hybrid system in which a portion of the cathode exhaust gas is recycled to mix with the compressed fresh air. The retrofitted SOFC-GT hybrid system would minimize the energy requirement of the air pre-heater.

Modeling of the SOFC-GT system is based on the following assumptions: (i) the system is operated at steady state, (ii) heat losses in each unit of the system is negligible, (iii) all gases behave as ideal gases, (iv) the pressure and temperatures of the system are constant, and (v) the SOFC operating voltage is constant along the cell coordinate. In evaluation of pressurized SOFC-GT hybrid system with non-recycling and recycling cathode exhaust gas, the current density and fuel utilization are specified 0.4 $A/cm^2$ and 0.7, respectively. Additionally, the constraint of analysis in these systems is that the different temperature across fuel cell is not over value of 100

K and the values of operating conditions used for simulation of the SOFC system under nominal conditions are given in Table 8.1.

For the SOFC-GT system with cathode exhaust gas recycling, the numerical solution of the SOFC system model is quite complicated due to the interaction among the units in the SOFC system. The calculation procedure in SOFC-GT hybrid system with recycling exhaust gas is shown in Figure 8.2. Firstly, the desired value of operating temperature and pressure of both reformer and SOFC, the current density, fuel utilization, steam-to-carbon ratio, different temperature across cell and recirculation ratio of cathode exhaust gas are input into the model, as well as the inlet fuel and air molar flow rate fed into system and voltage are guessed because of unknown value at the beginning and the outlet cathode exhaust gas. The anode and cathode outlet molar flow rate, the recycled cathode molar flow rate are calculated and then the calculated value of recycled cathode molar flow rate is the new guess value of recycled cathode molar flow rate in the next loop. This procedure is iterative until the difference in the values of the assumed and calculated variables satisfies a desired accuracy ($10^{-4}$). Finally, the SOFC and GT power and energy within system are determined. To evaluate the SOFC system performance, the SOFC electrical efficiency and the net electrical efficiency of the system are defined as:

$$\text{SOFC electrical efficiency} = \frac{P_{\text{sofc}}}{\dot{n}_{C_2H_5OH} LHV_{C_2H_5OH}} \tag{8.1}$$

$$\text{System electrical efficiency} = \frac{P_{\text{out,SOFC}} + P_{\text{GT}} - P_{H_2O,\text{pump}} - P_{C_2H_5OH,\text{pump}}}{\dot{n}_{C_2H_5OH} LHV_{C_2H_5OH}} \tag{8.2}$$

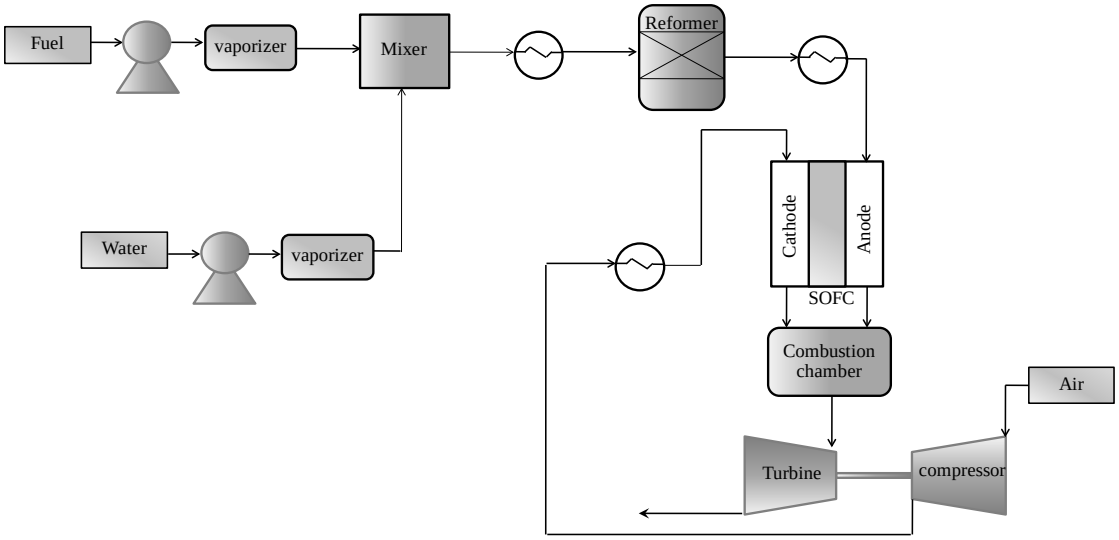


(a)

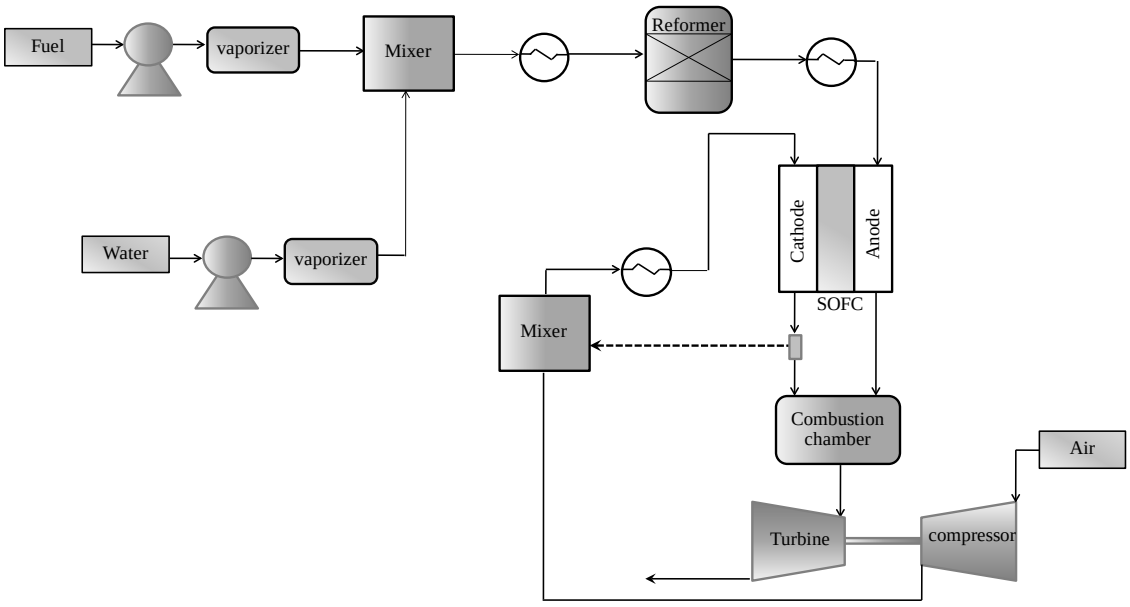


(b)

**Figure 8.1** Schematic diagram of an ethanol-fuelled SOFC system integrated with gas turbine: (a) a conventional SOFC-GT system and (b) a SOFC-GT system with cathode gas recirculation.

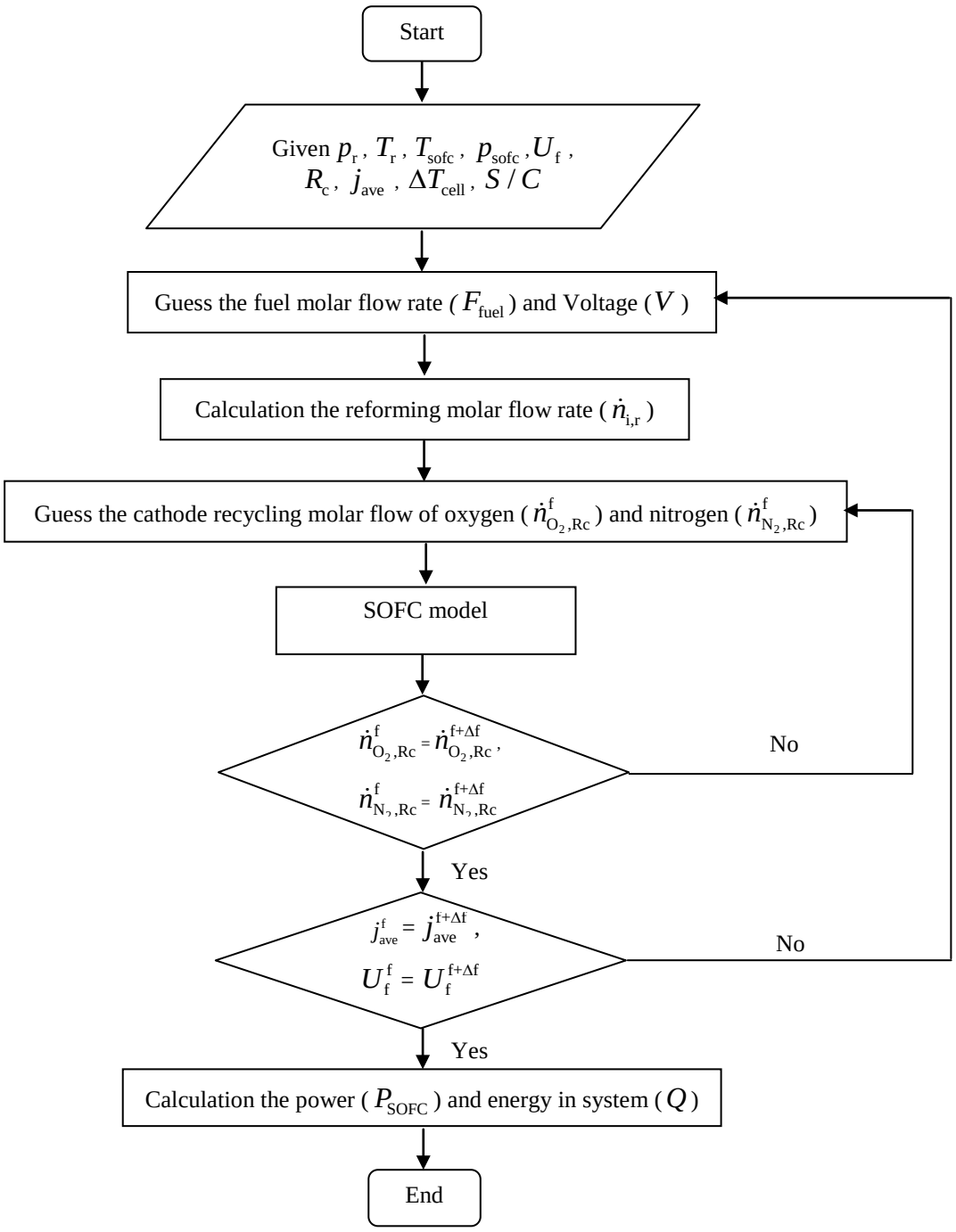


**Figure 8.2** Numerical algorithm for simulation of SOFC systems with cathode exhaust gas recirculation.

**Table 8.1** Value of operating conditions used for simulation of the SOFC-GT system under nominal conditions.

| | |
|---|---|
| Pre-reformer unit | |
| - Operating temperature, (K) | 973 |
| - Steam-to-carbon ratio | 1.5 |
| Solid oxide fuel cell unit | |
| - Operating temperature, (K) | 1073 |
| - Average current density ($A/cm^2$) | 0.4 |
| - Air composition | 21% $O_2$, 79% $N_2$ |
| - Fuel utilization | 0.7 |
| - SOFC pressure loss (%) | 2 |
| - dc-ac inverter efficiency | 94 |
| - Combustor pressure loss (%) | 3 |
| - Combustor efficiency (%) | 98 |
| Gas turbine | |
| - Turbine isentropic efficiency (%) | 82 |
| - Compressor isentropic efficiency (%) | 78 |
| - Generator mechanical efficiency (%) | 94 |
| - Pump efficiency (%) | 80 |

## 8.3 Results and discussion

### 8.3.1. A pressurized SOFC-GT system

Firstly, the performance of a pressurized SOFC-GT hybrid system is analyzed. Figure 8.3a shows the effect of the operating pressure on the electrical efficiency of the SOFC-GT system, whereas its effect on the SOFC electrical efficiency and the power ratio of gas turbine to SOFC (PGT/PSOFC) is given in Figure 8.3b. It can be seen that the system efficiency is considerably improved when increasing the operating pressure from 2 to 4 bar. This is because the SOFC and GT can generate more electrical power; the PGT/PSOFC ratio increases with increasing the operating pressure (Figure 8.3b). The increased pressure increases the partial pressure of $H_2$ in the fuel channel and $O_2$ in the air channel. In addition, the transport of gases to the

electrolyte-electrode interfaces is improved, thereby reducing the concentration losses. These factors lead to the improvement of fuel cell performance. However, it is found that the system efficiency decreases when the operating pressure is higher than 6 bar. This is caused by that the compressor consumes more power at the high pressure operation, while the power produced by the GT slightly increases. As a result, the pressurized SOFC-GT hybrid system should not be operated at a higher pressure. Moreover, the high pressure operation of the SOFC system causes a faster fuel cell degradation and higher capital cost. From Figure 8.3a, the SOFC-GT system gives the maximum electrical efficiency of 78.27 % when operated at the pressure of 6 bar. The SOFC generates the power output at 60-75 % of the overall power produced by the SOFC-GT system.

When considering the GT operation, although the temperature of the GT outlet gas will decrease, it is still high enough and is considered a useful heat source for supplying to other heat-requiring units within the SOFC system. Figure 8.4a shows the effect of the operating pressure of the SOFC system on the thermal energy of the GT outlet gas, which is calculated based on the reference temperature of 100 $^{o}$C. It is found that the thermal energy of the GT outlet gas reduces when the SOFC system is operated at a higher pressure. This thermal energy depends on the inlet gas flow to the GT, the GT inlet temperature and the operating pressure of the GT. Figure 8.4b shows the relation of the operating pressure to the GT outlet temperature and the excess air ratio. The results indicate that the temperature of the GT outlet decreases with increasing the operating pressure. Furthermore, the excess air needed for supplying to the SOFC is lower when the SOFC system is run at a higher pressure, leading to a decrease in the flow rate of gas fed into the GT.

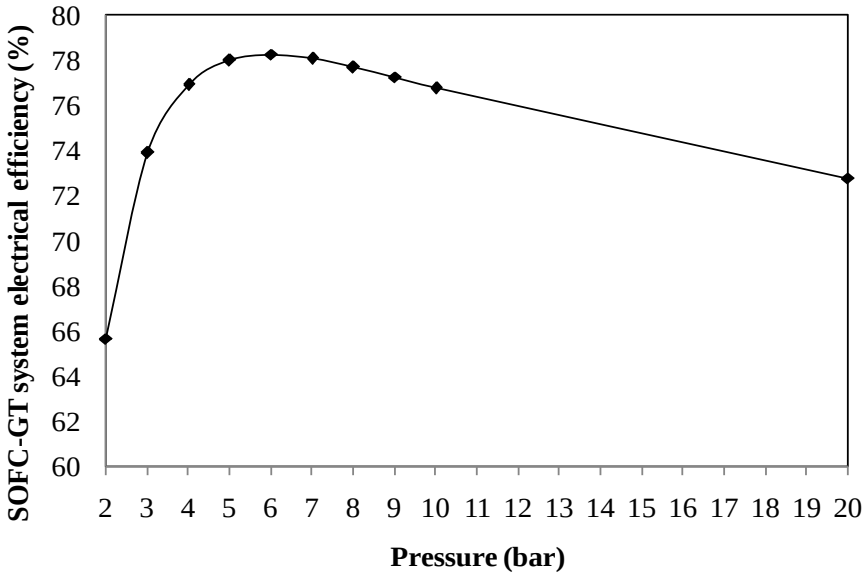


(a)

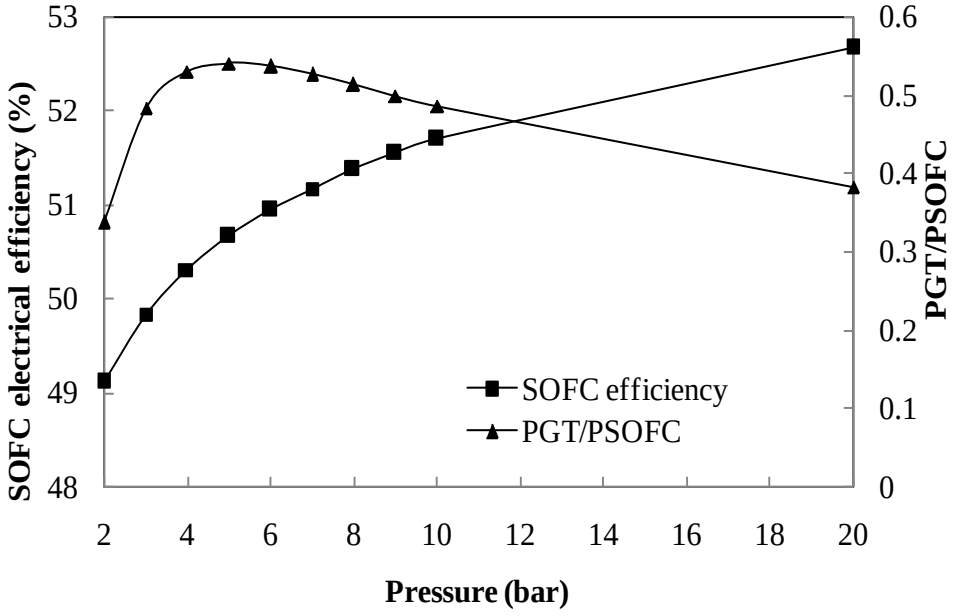


(b)

**Figure 8.3** Effect of operating pressure on the conventional SOFC-GT hybrid system: (a) system electrical efficiency and (b) SOFC electrical efficiency and power ratio of GT to SOFC.

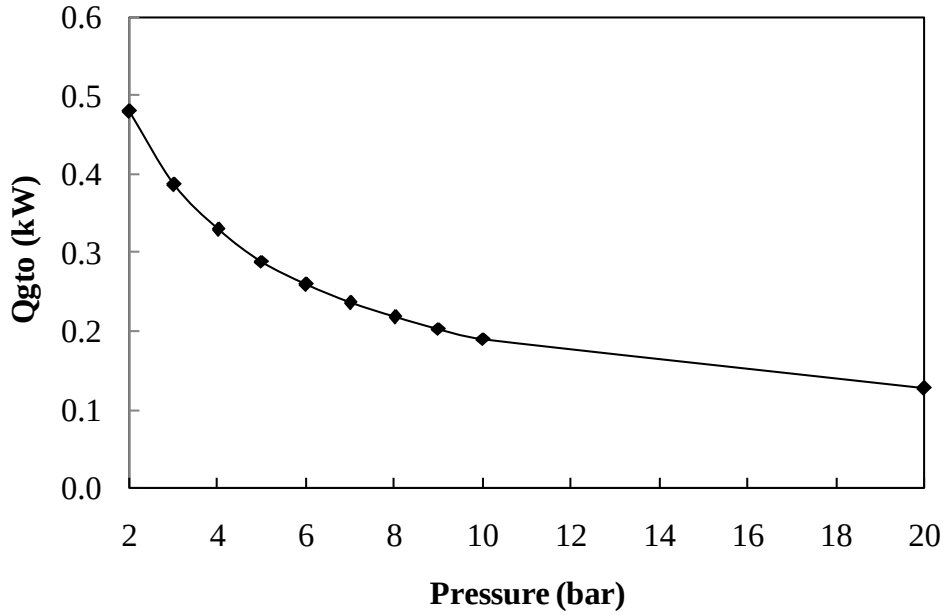


(a)

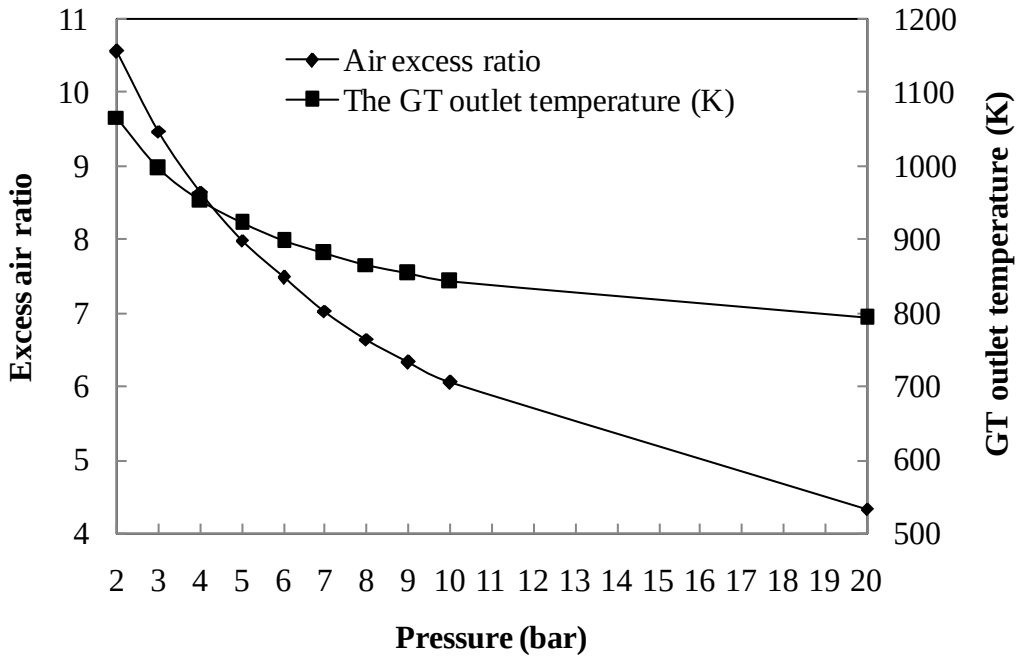


(b)

**Figure 8.4** Effect of operating pressure on (a) thermal energy of the GT outlet gas (Qgto) and (b) excess air ratio and GT outlet temperature (the conventional SOFC-GT hybrid system).

Regarding the energy management of the SOFC-GT hybrid system, the thermal energy in the turbine exhaust gas is generally utilized for pre-heating air fed to the SOFC. However, this study focuses on the use of this remaining thermal energy for supplying to all other heat-requiring units in order to reduce the requirement of the external heat at least. Figure 8.5 shows the impact of the operating pressure on the residual energy calculated from the thermal energy of the GT exhaust gas subtracted by the system heat requirement. The negative value of the residual energy indicates that the thermal energy from the GT outlet gas is insufficient to supply the SOFC system and thus the external heat is needed. It is found that an increase in the operating pressure reduces the external heat requirement because the ethanol steam reformer needs less energy. It is noted that when operated at the pressure of 20 bar, the SOFC-GT system can be operated at the self-sustainable condition where the external heat is unnecessary; however, at high pressure operation, a low system electrical efficiency is obtained.

Figure 8.6 shows the energy requirement in each part of the pressurized SOFC-GT hybrid system. It can be divided into three parts, namely the energy used for pre-heating air, pre-heating fuel and water and ethanol steam reformer. The air pre-heating unit consumes the highest energy; it takes about 65-74% of the overall energy consumption of the SOFC-GT system. Therefore, if the energy used for the air pre-heater operation can be reduced, the requirement of the external heat for supplying to the SOFC system would be minimized and the energy management of the system would probably better.

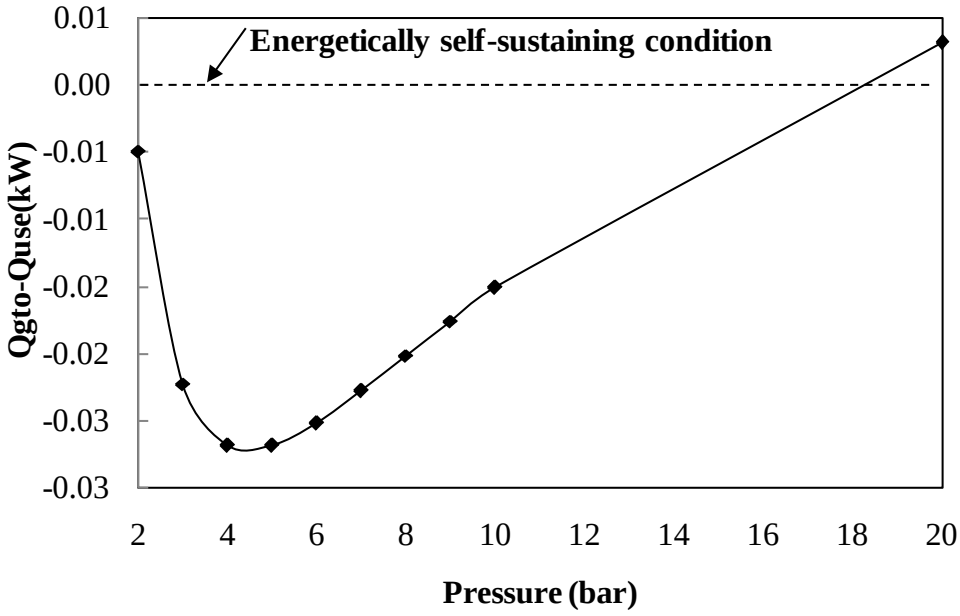


**Figure 8.5** Effect of operating pressure on the remaining energy of the GT exhaust gas (the conventional SOFC-GT hybrid system).

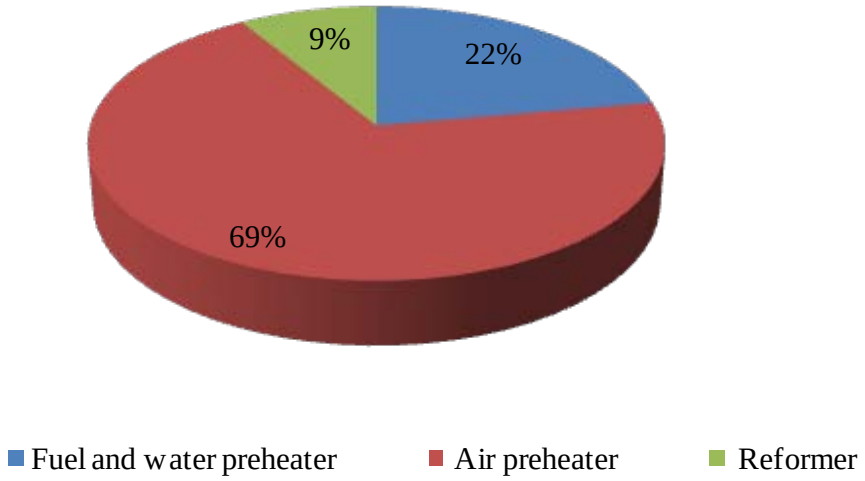


**Figure 8.6** Distribution of heat used in the conventional SOFC-GT hybrid system (*P* = 6 bar).

### 8.3.2 A pressurized SOFC/GT system with cathode gas recirculation

In the previous section, it is found that most thermal energy consumption in the SOFC system is caused by the air pre-heater. To improve the system performance, a portion of the cathode exhaust gas is recycled and then mixed with a fresh air feed to reduce a heat duty of the air pre-heater. Regarding the system electrical efficiency, the pressurized SOFC-GT hybrid system is studied under a pressure range of 2-8 bar. The influence of a recirculation ratio of the cathode exhaust gas at different operating pressures on the system electrical efficiency, SOFC electrical efficiency and the PGT/PSOFC ratio is illustrated in Figures 8.7a-c, respectively. The system electrical efficiency decreases with increasing the recirculation ratio of the cathode exhaust gas at all the operating pressure considered, and system electrical efficiency and the PGT/PSOFC ratio show similar trends. The results also indicate that the recirculation ratio has impact on the performance of the GT more than the SOFC. The electrical efficiency of the SOFC slightly declines with increasing the recirculation ratio of the cathode exhaust gas of 0.1-0.7; nevertheless, the decrement of SOFC electrical efficiency is obviously at the recirculation ratio of the cathode exhaust gas above 0.7. This is because the oxygen feed is diluted when increasing the recirculation ratio and consequently, a larger concentration loss in the SOFC appears. An increase in the cathode gas recycle also decreases the PGT/PSOFC ratio as the gas inlet flow to the GT drop and thus the GT power is less generated.

Figure 8.8 shows the variations in the GT inlet temperature and the thermal energy of the GT outlet gas as a function of the recirculation ratio of the cathode gases at different operating pressures. An increase in the cathode gas recycle results in the elevated temperature of the GT inlet because the air stream fed to the combustor decreases while the fuel in the anode exhaust gas is still constant. It is noted that the fuel utilization of the SOFC is kept constant at 70% in all case studies. Although the increased temperature of the GT inlet enhances the performance of the GT, the GT inlet temperature should not exceed the endurance limit of GT materials. In general, the maximum GT inlet temperature is 1400 K (Cheddie, 2010). Taking this constraint into consideration, the cathode recirculation ratio should not be higher than 0.50-0.68, depending on the operating pressure (Figure 8.8a). When considering the thermal

energy of the GT exhaust gas (Figure 8.8b), it decreases with the increased recirculation ratio because a decrease in the GT inlet feed flow has more effect on the thermal energy of the GT outlet gas than an increase in the GT inlet temperature.

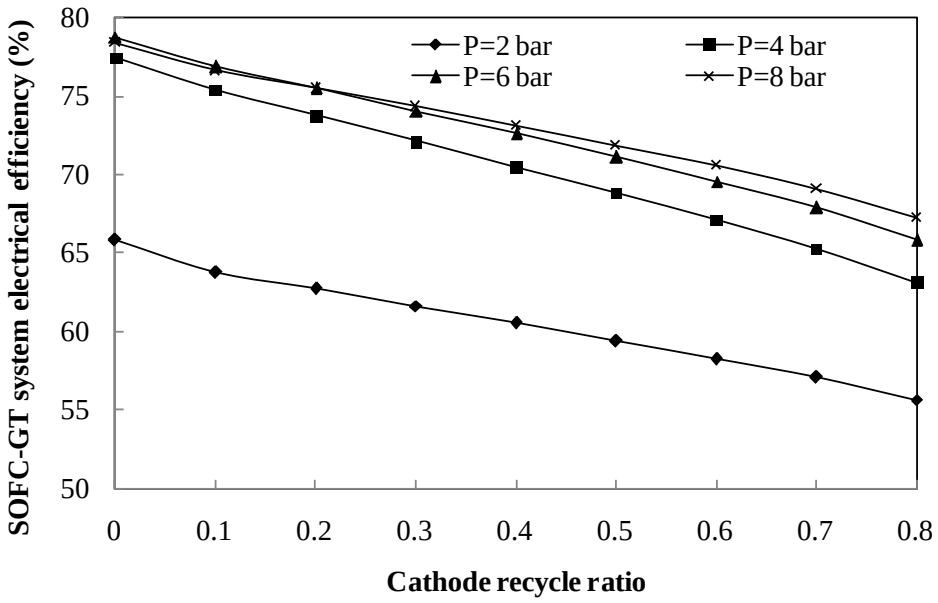


(a)

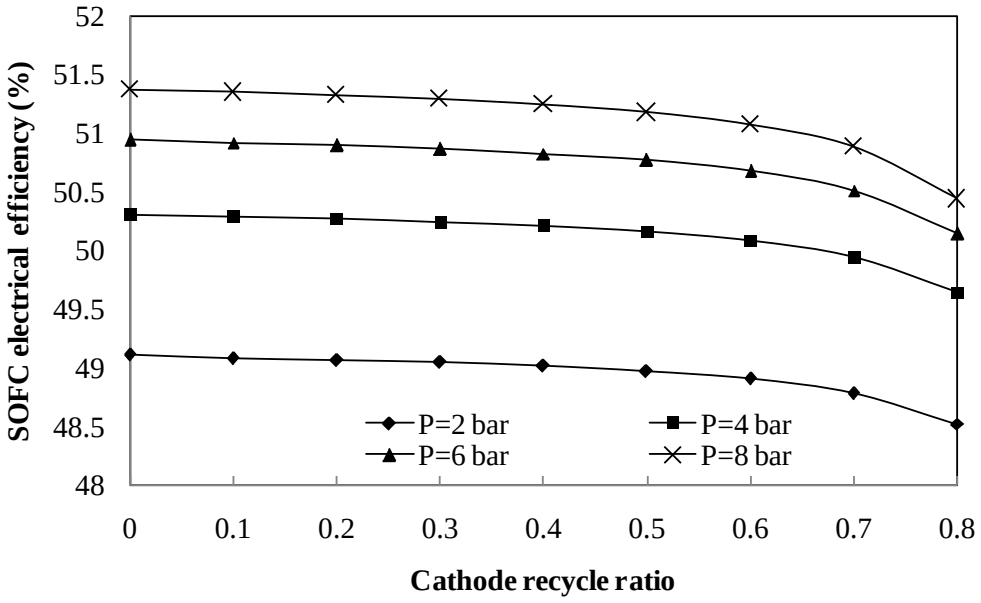


(b)

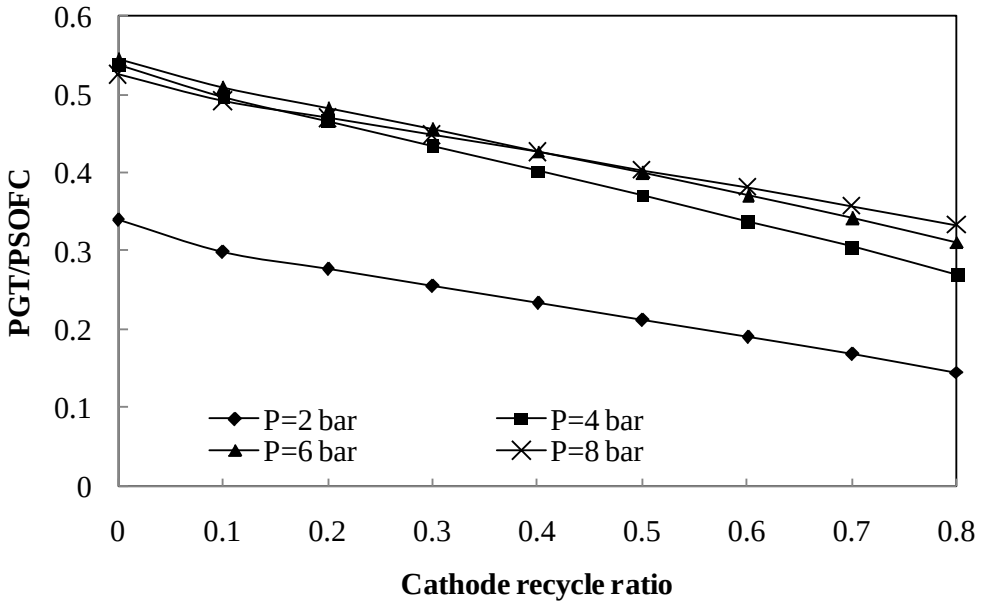


(c)

**Figure 8.7** Effect of recirculation ratio of cathode gas on the SOFC-GT hybrid system with cathode gas recirculation at different operating pressure: (a) system electrical efficiency, (b) SOFC electrical efficiency and (c) power ratio of GT to SOFC.

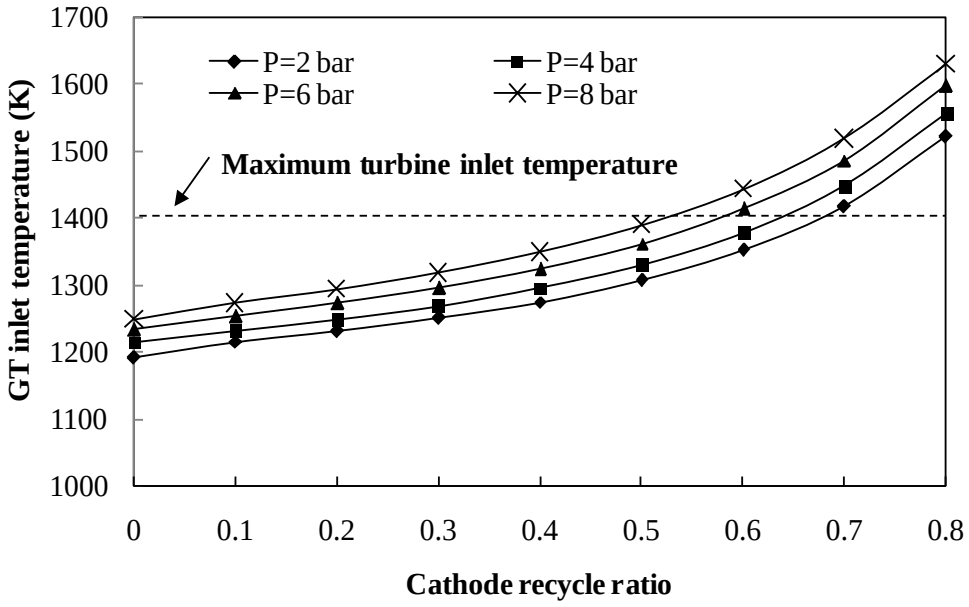


(a)

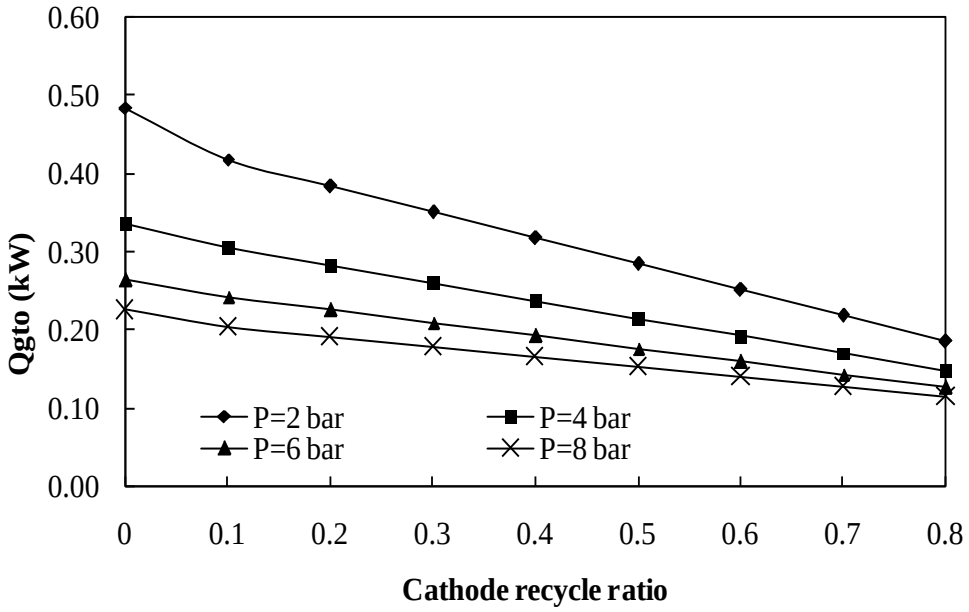


(b)

**Figure 8.8** Effect of recirculation ratio of cathode gas on (a) the GT inlet temperature and (b) the thermal energy of the GT outlet gas (the SOFC-GT hybrid system with cathode gas recirculation).

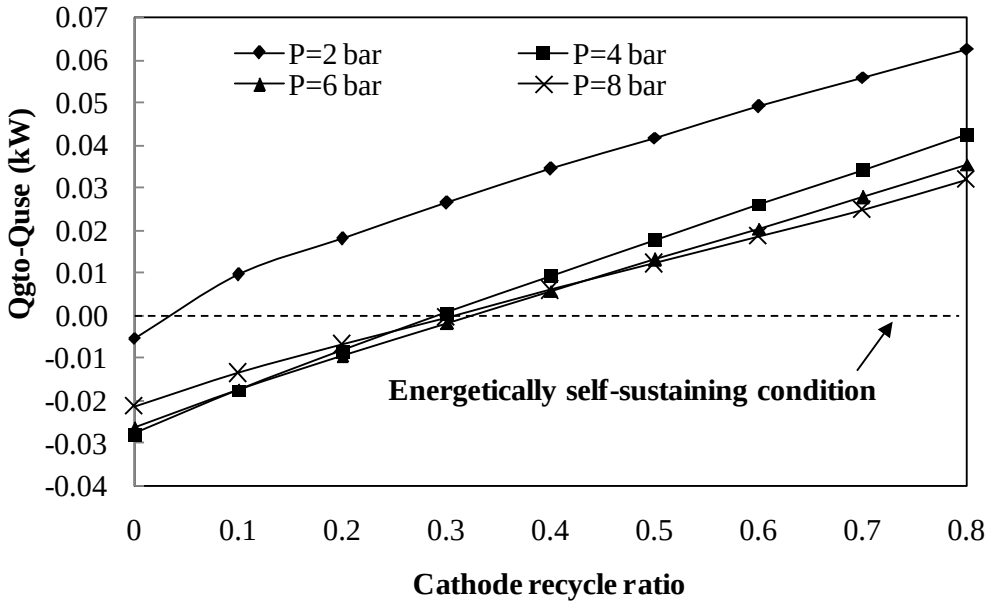


**Figure 8.9** Effect of recirculation ratio of cathode-off gas on the residual energy from the outlet GT energy (the SOFC-GT hybrid system with cathode gas recirculation).

Figure 8.9 shows the effect of the cathode gas recirculation on the residual thermal energy of the SOFC-GT system. When the system is operated at a higher recirculation of the cathode gas, it is found that the SOFC system generates the thermal energy higher than its consumption. This result indicates a possibility of the SOFC-GT system with cathode gas recirculation to be operated at the self-sustainable condition. At high recirculation ratio of the cathode exhaust gas, the requirement of the fresh air fed to the SOFC reduces, resulting in the decreased heat duty of the air pre-heater. Because the recirculation of the cathode gas has a positive effect on the thermal management of the pressurized SOFC-GT hybrid system but decreases the system electrical efficiency. Therefore, the recirculation ratio of the cathode exhaust gas should be carefully selected. In this study, it is found that the pressurized SOFC-GT hybrid system should be operated at pressure of 6 bar because the highest electrical efficiency can be achieved and the cathode gas recirculation ratio of 0.3 is selected. At this condition, the SOFC system can self-sustainable and the system electrical efficiency slightly decreases (3 %).

## 8.4 Conclusions

A pressurized solid oxide fuel cell and gas turbine hybrid system (SOFC-GT) fed by ethanol is studied. The performance of the SOFC system in terms of electrical efficiency and thermal management is analyzed with respect to the operating pressure and recycle ratio of a cathode exhaust gas. The simulation results show that the optimal operating pressure of the pressurized SOFC system is in a range of 4-6 bar. Under this condition, the system can achieve the highest electrical efficiency, whereas the recuperation of the waste heat from the GT exhaust gas is minimized. The recirculation of the cathode exhaust gas in the SOFC system can reduce the external heat requirement of an air pre-heater. However, the electrical efficiency of the SOFC system with cathode gas recycling is lower than the conventional SOFC system. In addition, it is found that the SOFC system with cathode gas recycling can be operated at a self-sustainable condition.

# CHAPTER IX

# DESIGNS OF HEAT RECOVERY FOR A PRESSURIZED SOFC-GT HYBRID SYSTEM

The objective of this chapter is to design and the suitable configuration of a pressurized SOFC-GT hybrid system. Two configurations of heat recovery for the air preheating unit within the system are considered, i.e., uses of recuperative heat exchangers and cathode exhaust gas recirculation. The energy management and heat recovery of both the systems are firstly analyzed. The effect of operating parameters, i.e., pressure, fuel utilization, current density and the tubomachinery efficiency, on the recuperated heat in the system and the system performance of both the SOFC-GT hybrid systems are also present in this chapter.

## 9.1 Introduction

As mentioned earlier, the external reforming is higher molar flow rate of required air for cooling cell than the internal reforming fuel cell. This is because a directly reforming within SOFC can reduce the molar flow rate of supplied air to system from cooling cell with the endothermic reaction in cell (Liese and Gemmen, 2005). Additionally, the high temperature and energy input are needed to preheat air before feeding to SOFC so as to control an acceptably cell temperature, which requires more excess air fed to system and results in more use of energy for preheating air. From previous mention, the increment of molar flow rate of air for system makes an adverse impact on the system efficiency. Thus, the application of an external steam reformer to produce hydrogen for the SOFC-GT hybrid system would be a potential solution. A design of cycle scheme in the SOFC-GT hybrid system is important technologies on the improvement of system efficiency. A number of design options for SOFC-GT hybrid system have been available. Park et al. (2006) investigated the ambient pressure and pressurized SOFC-GT hybrid system. Their results indicated that the pressurized system exhibits a better efficiency due to more

effective utilization of gas turbine. Yang et al. (2006) analyzed two configurations of hybrid system with internal and external reforming by examining the effect of matching between the fuel cell and turbine temperature on the hybrid system performance. Further, several literatures have proposed various possible schemes for hybrid SOFC-GT plant in order to enhance system efficiency i.e., SOFC-GT hybrid system with retrofitting system by steam injection (Motahar et al., 2009; Kuchonthara et al., 2003), SOFC combined with multi-stage of GT (Chan et al., 2003; Musa et al., 2008; Haseli et al., 2008) and SOFC-GT hybrid system with inter-cooling of air compressor (Yi et al., 2004).

The most common design of the SOFC-GT hybrid system is that recuperated heat from turbine exhaust gas with recuperator to preheat air in order to feed SOFC. Nonetheless, the air preheating unit fed into SOFC requires the abundantly energy. In some operating condition of the pressurized SOFC-GT hybrid system, there is a only recuperator for preheating air before feeding to SOFC that is not able to provide all of the heat necessary to preheat the cathode flow to the desired temperature (Bove and Ubertini, 2008). Although increase of heat for preheating air can increase with addition of fuel into combustor, this method causes to higher inlet turbine temperature that is not suitable for the hybrid system with a small turbine. The addition of high-temperature heat exchanger (or recuperative heat exchanger) combined with recuperator as alternative design option can enhance efficiency for heat transfer from the exhaust gas of turbine (Song et al., 2006; Calise et al., 2006; Park et al., 2007; Akkaya et al., 2008); however, the high-temperature heat exchanger is expensive cost. Moreover, the SOFC system with recycling cathode gas is able to improve the efficiency due to reduction of air preheating (Jia et al., 2011). The method of cathode exhaust gas recirculation adopted in SOFC-GT hybrid system integrated external steam reformer is possible to enhancing the system efficiency.

In this work, the design and heat recovery of a pressurized SOFC-GT hybrid system integrated with the external reformer of ethanol steam reformer are mainly focused. Two configurations of pressurized SOFC-GT hybrid system were considered, which are different the cycle scheme for air preheating in system namely the SOFC-GT hybrid system with recuperative heat exchanger and cathode exhaust gas recirculation. The analysis of suitable energy management and heat recovery

within both systems for the required heat unit such as the external reformer, preheating air and fuel based on standard condition under the constraint are firstly investigated. Moreover, the effect of important operating parameters such as operating pressure, fuel utilization, current density and the turbomachinery efficiency on the recuperated heat in system and the system performance are studied.

### 9.2 Configurations of SOFC-GT hybrid system

In this chapter, there are two schematic configurations of the SOFC-GT system with recuperative heat exchanger and cathode exhaust gas recirculation considered as shown in Figure 9.1a-b. These systems are different in heat recovery methods for air preheating. For SOFC-GT system with recuperative heat exchanger, the exhaust gas from combustor is through the high-temperature heat exchanger before feeding to gas turbine. The hot gas is expanded in turbine and produces the electricity. Compressed air from compressor is heated at inlet temperature of SOFC by recuperator and high-temperature heat exchanger. Air is preheated with the exchange of heat from turbine exhaust gas in recuperator and then it is exchanged the heat with combustor outlet gas in high-temperature heat exchanger before feeding to cell, which is presented in Figure 9.1a.

For SOFC-GT hybrid system with cathode exhaust gas recirculation, there is a recuperator used to exchange the heat between turbine exhaust gas and air, which is similar the hybrid system with recuperative heat exchanger. However, they are different at position of air pre-heater before feeding into cathode. A portion of cathode exhaust gas is recycled and mixed with fresh air heated with recuperator, which is illustrated in Figure 9.1b. This system requires blower to overcome the pressure losses of recycled gas before feeding to the air mixer. A residual oxidant gas from cathode exhaust gas passes through the external reformer to be exchanged heat for ethanol steam reformer. Afterwards, it is mixed with anode exhaust-gas combustor and combusted in combustor. Then, the combusted gas from combustor is sent to turbine.

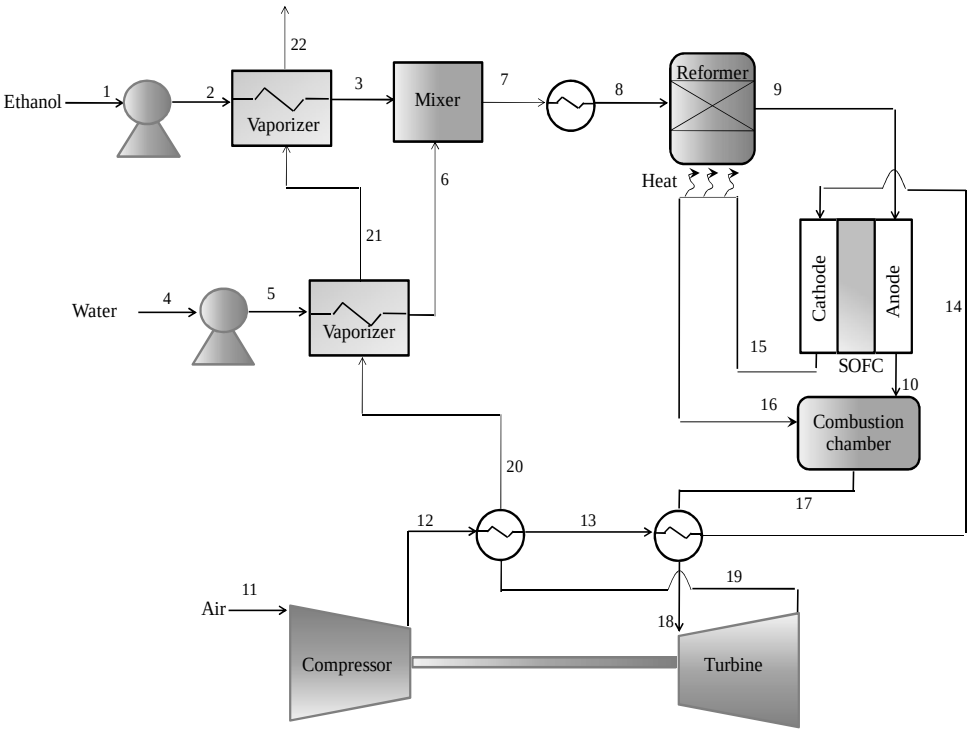


(a)

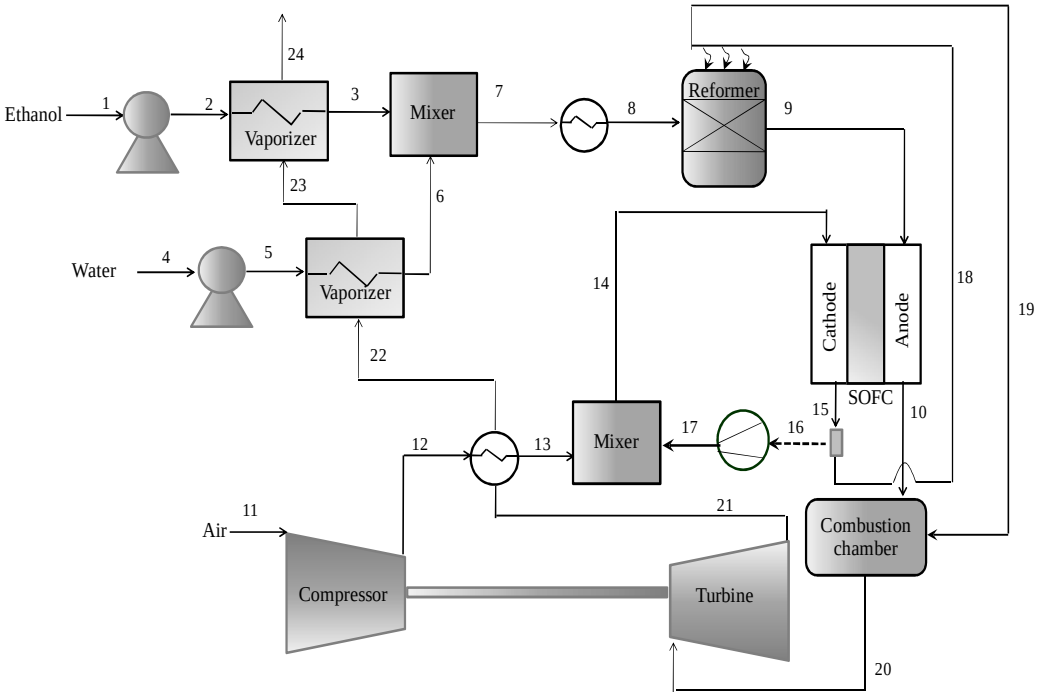


(b)

**Figure 9.1** Pressurized SOFC-GT hybrid system with (a) recuperative heat exchanger and (b) cathode exhaust gas recirculation.

The ethanol steam reformer under nominal conditions is operated at temperature of 973K and steam to carbon of 1.5 which are suitable operating condition for ethanol steam reforming (Saebea et al., 2011) as well as the data of other units are taken from the publication (Park et al., 2007; Akkaya et al., 2008; Santin et al., 2009).The input parameter under nominal conditions are given in Table 9.1.

Performance analysis of the SOFC-GT hybrid system is considered from modeling in chapter 4. In the evaluation, fuel and air molar flow rate are adjusted until the required values of average current density, fuel utilization and the different temperature across fuel cell**.** For consideration of heat recovery in the both schematic configurations, the recuperator effectiveness has the same value of 0.9. Turbine inlet temperature (TIT), turbine outlet temperature (TOT), heat exchanger effectiveness for the SOFC-GT hybrid system with recuperative heat exchanger and cathode recirculation ratio for the SOFC-GT hybrid system with cathode exhaust gas recirculation are considered as dependent variables of design parameters.

The comparison of both the 500 kW power systems between SOFC-GT hybrid systems with recuperative heat exchanger and cathode exhaust gas recirculation was studied by designing system under constraint condition. Considering the 500 kW power of SOFC-GT hybrid system, the range of produced power from gas turbine should be in 40-200 kW. Therefore, the small metallic radial turbines are generally used in the SOFC-GT hybrid system in this range power. A constraint of this turbine inlet temperature should not over 1223 K due to uncooled turbine blade (Costamagna et al., 2001). Further, the efficiency and the hot gas inlet temperature of heat exchanger at position after combustor in SOFC-GT hybrid system with recuperative heat exchanger is limited at a maximum of 55% and 1273 K (Santin et al., 2009).

The performance of hybrid system can be considered from overall system efficiency. The system efficiency of SOFC-GT hybrid system depends on net power output and the amount of heat fed for system which is obtained as:

$$\eta_{sys} = \frac{P_{out,SOFC} + P_{GT} - P_{H_2O,pump} - P_{C_2H_5OH,pump} - P_{blower}}{\dot{n}_{C_2H_5OH} LHV_{C_2H_5OH} + Q_{ex}} \tag{8.1}$$

The net power output estimates from total output power deducted from input power used for auxiliary units in system. $\dot{n}_{C_2H_5OH}$ is overall fuel molar flow rate used in system. $Q_{ex}$ is external heat and $LHV_{C_2H_5OH}$ is lower heating value of ethanol.

## 9.3 Results and discussion

### 9.3.1 Analysis of SOFC-GT system performance

The SOFC-GT hybrid system with recuperative heat exchanger and cathode exhaust gas recirculation under nominal conditions are analyzed by considering design constraints. The aim of this analysis is to insight of energy management within both systems. Considering a 500 kW class hybrid systems, both systems are specified the average current density of 0.4 A/cm$^2$ and fuel utilization of 0.675. The inlet molar flow rate of air is adjusted in order to control the air inlet temperature before feeding into SOFC by following temperature different across fuel cell of 100 K. The states along the flow stream of SOFC-GT hybrid system with recuperative heat exchanger and cathode exhaust gas recirculation from model simulation are showed in Table 9.2 and 9.3, respectively. These results show that the molar flow rate at anode outlet of SOFC of node 10 increase while the molar flow rate at cathode outlet of node 15 decrease. This reason is oxygen at cathode side transformed to oxygen ion through electrolyte and then reacted with hydrogen at anode by the electrochemical reaction.

The results of heat duty in each unit within the both systems are shown in Table 9.4. The ethanol steam reforming reaction is strongly endothermic which require the heat input to reformer. In system designs of this work, the cathode exhaust gas passes through reformer so as to supply heat for external reformer before being fed to combustor to combust with residual fuel from anode exhaust gas. The use of heat from cathode exhaust gas for supplying in reformer not only reduces the external heat for reformer but it also reduces combustor outlet temperature because high combustor temperature needs high cost alloy materials of heat exchanger at downstream. Further, it reduces turbine inlet temperature which is important constraint for a small turbine. In SOFC-GT with recuperative heat exchanger, the cathode outlet exhaust gas is used for supplying heat in reformer about 97.75 kW.

**Table 9.1** Values of operating conditions for system under norminal conditions

| | | | |
|---|---|---|---|
| Pre-reformer unit | | GT unit | |
| Operating temperature, $T_r$ (K) | 973 K | Turbine isentropic efficiency (%) | 82 |
| Steam-to- carbon ratio | 1.5 | Compressor isentropic efficiency (%) | 78 |
| SOFC unit | | Generator mechanical efficiency (%) | 94 |
| Operating temperature, $T_{sofc}$ (K) | 1073 | Compressor pressure ratio (bar) | 4 |
| Air temperature increase across cathode (K) | 100 | Blower | |
| Average current density (A/cm$^2$) | 0.4 | Blower isentropic efficiency (%) | 70 |
| Air composition | 21% $O_2$, 79% $N_2$ | Recuperator | |
| Fuel utilization | 0.675 | Recuperator effectiveness (%) | 90 |
| SOFC pressure loss (%) | 2 | Recuperator pressure loss of cool stream (%) | 1.5 |
| dc-ac inverter efficiency | 94 | Recuperator pressure loss of hot stream (%) | 2.5 |
| Combustor | | Fuel manifold | |
| Combustor combustion efficiency (%) | 98 | Fuel composition | 100% $C_2H_5OH$ |
| Combustor pressure loss (%) | 3 | Fuel temperature at system inlet (K) | 298.15 |
| Pump efficiency | 0.75 | Air temperature at system inlet (K) | 298.15 |

The cathode outlet temperature is down from 1073 K at node 15 to 1013.5 K at node 16 and consequently combustor outlet temperature is at 1193.3K while it is at1244.7 K for case of the heat from cathode exhaust gas not used for reformer.

In the hybrid system with cathode exhaust gas recirculation, combustor outlet temperature is considerably increased, resulting from reduction of air flow into combustor. Combustor outlet temperature is high about 1339.1 K in case of not use heat for reformer and thus the heat from the recycled cathode exhaust gas in this system should be used for fuel processor more than system with recuperative heat exchanger in order to reduce turbine inlet temperature under constraints of design. In this case, fuel processor requires a total of 180.64 kW which is used 82.64 kW for pre-heating fuel before reformer and 98 kW for endothermic reaction. The exit temperature of combustor is able to be low at 1183.8 K.

Both systems are different heat recovery for pre-heating air so the recuperator effectiveness of both systems is fixed same value of 90% to compare system efficiency. To control air inlet temperature before feeding to cell, recuperative heat exchanger effectiveness of 51.03 % for the heat exchanger between outlet combustor and air from recuperator require in the hybrid system with recuperative heat exchanger while the hybrid system with cathode exhaust gas recirculation need to the recirculation ratio of cathode exhaust gas of 0.435.

Considering fuel processor before reformer, heat duty for ethanol and water vaporizer unit in pressurized system require more than that in atmospheric system due to elevated boiling point temperature when it is operated at high operating pressure. The boiling point temperature of ethanol and water when system operating pressure operates at 4 bar are 390.7 K and 416.78 K, respectively, as well as heat duty of ethanol and water vaporizer are 86.76 kW and 30.67 kW for hybrid system with recuperative heat exchanger and 30.78 kW and 87.07 kW for hybrid system with cathode exhaust gas recirculation. However, the amount of heat and outlet gas temperature from recuperator are 264.48 kW and 532.3 K for the system with recuperative heat exchanger, and 241.09 kW and 611.08 K for the system with cathode exhaust gas recirculation which is still high energy enough to heat recovery for ethanol and water vaporizer unit.

**Table 9.2** Stream data of the SOFC-GT hybrid system with recuperative heat exchanger

| Node | T(K) | P(bar) | $\dot{m}$ | Molar fraction (%) | | | | | | | |
|---|---|---|---|---|---|---|---|---|---|---|---|
| | | | (mol/s) | $C_2H_5OH$ | $CH_4$ | CO | $CO_2$ | $H_2$ | $H_2O$ | $O_2$ | $N_2$ |
| 1 | 298.15 | 1.013 | 0.6241 | 1 | 0 | 0 | 0 | 0 | 0 | 0 | 0 |
| 2 | 298.15 | 4 | 0.6241 | 1 | 0 | 0 | 0 | 0 | 0 | 0 | 0 |
| 3 | 390.70 | 4 | 0.6241 | 1 | 0 | 0 | 0 | 0 | 0 | 0 | 0 |
| 4 | 298.15 | 1.013 | 1.8724 | 0 | 0 | 0 | 0 | 0 | 1 | 0 | 0 |
| 5 | 298.15 | 4 | 1.8724 | 0 | 0 | 0 | 0 | 0 | 1 | 0 | 0 |
| 6 | 416.78 | 4 | 1.8724 | 0 | 0 | 0 | 0 | 0 | 1 | 0 | 0 |
| 7 | 404.77 | 4 | 2.4965 | 0.25 | 0 | 0 | 0 | 0 | 0.75 | 0 | 0 |
| 8 | 973.15 | 4 | 2.4965 | 0.25 | 0 | 0 | 0 | 0 | 0.75 | 0 | 0 |
| 9 | 973.15 | 4 | 4.4838 | 0 | 0.0568 | 0.1176 | 0.1040 | 0.4905 | 0.2311 | 0 | 0 |
| 10 | 1073.15 | 3.92 | 5.0821 | 0 | 0 | 0.0622 | 0.1878 | 0.1905 | 0.5595 | 0 | 0 |
| 11 | 298.15 | 1.013 | 51.4569 | 0 | 0 | 0 | 0 | 0 | 0 | 0.21 | 0.79 |
| 12 | 479.39 | 4 | 51.4569 | 0 | 0 | 0 | 0 | 0 | 0 | 0.21 | 0.79 |
| 13 | 743.46 | 3.94 | 51.4569 | 0 | 0 | 0 | 0 | 0 | 0 | 0.21 | 0.79 |
| 14 | 973.15 | 3.94 | 51.4569 | 0 | 0 | 0 | 0 | 0 | 0 | 0.21 | 0.79 |
| 15 | 1073.15 | 3.86 | 50.3254 | 0 | 0 | 0 | 0 | 0 | 0 | 0.1902 | 0.8098 |
| 16 | 1013.45 | 3.86 | 50.3254 | 0 | 0 | 0 | 0 | 0 | 0 | 0.1902 | 0.8098 |
| 17 | 1193.34 | 3.7738 | 54.7783 | 0 | 0 | 0.0001 | 0.0231 | 0.0004 | 0.0692 | 0.1632 | 0.7440 |
| 18 | 991.75 | 3.7738 | 54.7783 | 0 | 0 | 0.0001 | 0.0231 | 0.0004 | 0.0692 | 0.1632 | 0.7440 |
| 19 | 772.79 | 1.094 | 54.7783 | 0 | 0 | 0.0001 | 0.0231 | 0.0004 | 0.0692 | 0.1632 | 0.7440 |
| 20 | 532.45 | 1.067 | 54.7783 | 0 | 0 | 0.0001 | 0.0231 | 0.0004 | 0.0692 | 0.1632 | 0.7440 |
| 21 | 480.65 | 1.067 | 54.7783 | 0 | 0 | 0.0001 | 0.0231 | 0.0004 | 0.0692 | 0.1632 | 0.7440 |
| 22 | 462.23 | 1.067 | 54.7783 | 0 | 0 | 0.0001 | 0.0231 | 0.0004 | 0.0692 | 0.1632 | 0.7440 |

**Table 9.3** Stream data of the SOFC-GT hybrid system with cathode recirculation ratio

| Node | T(K) | P(bar) | $\dot{m}$ (mol/s) | Molar fraction (%) | | | | | | | |
|---|---|---|---|---|---|---|---|---|---|---|---|
| | | | | $C_2H_5OH$ | $CH_4$ | CO | $CO_2$ | $H_2$ | $H_2O$ | $O_2$ | $N_2$ |
| 1 | 298.15 | 1.013 | 0.6263 | 1 | 0 | 0 | 0 | 0 | 0 | 0 | 0 |
| 2 | 298.15 | 4 | 0.6263 | 1 | 0 | 0 | 0 | 0 | 0 | 0 | 0 |
| 3 | 390.70 | 4 | 0.6263 | 1 | 0 | 0 | 0 | 0 | 0 | 0 | 0 |
| 4 | 298.15 | 1.013 | 1.8790 | 0 | 0 | 0 | 0 | 0 | 1 | 0 | 0 |
| 5 | 298.15 | 4 | 1.8790 | 0 | 0 | 0 | 0 | 0 | 1 | 0 | 0 |
| 6 | 416.78 | 4 | 1.8790 | 0 | 0 | 0 | 0 | 0 | 1 | 0 | 0 |
| 7 | 404.77 | 4 | 2.5054 | 0.25 | 0 | 0 | 0 | 0 | 0.75 | 0 | 0 |
| 8 | 973.15 | 4 | 2.5054 | 0.25 | 0 | 0 | 0 | 0 | 0.75 | 0 | 0 |
| 9 | 973.15 | 4 | 4.4998 | 0 | 0.0568 | 0.1176 | 0.1040 | 0.4905 | 0.2311 | 0 | 0 |
| 10 | 1073.15 | 3.92 | 5.0108 | 0 | 0 | 0.0600 | 0.1900 | 0.1838 | 0.5662 | 0 | 0 |
| 11 | 298.15 | 1.013 | 29.6093 | 0 | 0 | 0 | 0 | 0 | 0 | 0.21 | 0.79 |
| 12 | 479.39 | 4 | 29.6093 | 0 | 0 | 0 | 0 | 0 | 0 | 0.21 | 0.79 |
| 13 | 887.96 | 3.94 | 29.6093 | 0 | 0 | 0 | 0 | 0 | 0 | 0.21 | 0.79 |
| 14 | 973.15 | 3.94 | 51.3975 | 0 | 0 | 0 | 0 | 0 | 0 | 0.1950 | 0.8050 |
| 15 | 1073.15 | 3.8612 | 50.1292 | 0 | 0 | 0 | 0 | 0 | 0 | 0.1747 | 0.8253 |
| 16 | 1073.15 | 3.8612 | 21.7912 | 0 | 0 | 0 | 0 | 0 | 0 | 0.1747 | 0.8253 |
| 17 | 1080.89 | 3.94 | 21.7912 | 0 | 0 | 0 | 0 | 0 | 0 | 0.1747 | 0.8253 |
| 18 | 1073.15 | 3.8612 | 28.3380 | 0 | 0 | 0 | 0 | 0 | 0 | 0.1747 | 0.8253 |
| 19 | 875.17 | 3.8612 | 28.3380 | 0 | 0 | 0 | 0 | 0 | 0 | 0.1747 | 0.8253 |
| 20 | 1183.80 | 3.7739 | 32.7503 | 0 | 0 | 0.0002 | 0.0381 | 0.0005 | 0.1142 | 0.1328 | 0.7142 |
| 21 | 933.36 | 1.094 | 32.7503 | 0 | 0 | 0.0002 | 0.0381 | 0.0005 | 0.1142 | 0.1328 | 0.7142 |
| 22 | 611.08 | 1.067 | 32.7503 | 0 | 0 | 0.0002 | 0.0381 | 0.0005 | 0.1142 | 0.1328 | 0.7142 |
| 23 | 526.36 | 1.067 | 32.7503 | 0 | 0 | 0.0002 | 0.0381 | 0.0005 | 0.1142 | 0.1328 | 0.7142 |
| 24 | 496.066 | 1.067 | 32.7503 | 0 | 0 | 0.0002 | 0.0381 | 0.0005 | 0.1142 | 0.1328 | 0.7142 |

**Table 9.4** Required heat input in each unit of the 500kW SOFC-GT hybrid system

| | Recuperative heat exchanger (System 1) | Cathode exhaust gas recirculation (System 2) |
|---|---|---|
| Ethanol vaporizer (kW) | 30.68 | 30.79 |
| Water vaporizer (kW) | 86.76 | 87.07 |
| pre-heater | 82.35 | 82.64 |
| Steam reformer (kW) | 97.75 | 98.10 |
| Total input heat energy (kW) | 297.54 | 298.6 |

**Table 9.5** System performance based on design point condition

| | Recuperative heat exchanger (System 1) | Cathode exhaust gas recirculation (System 2) |
|---|---|---|
| Input fuel (LHV) (kW) | 879.74 | 800.22 |
| SOFC power (kW) | 388.28 | 388.27 |
| Net GT power (kW) | 111.9 | 117.39 |
| SOFC efficiency (%) | 43.86 | 43.70 |
| System efficiency (%) | 56.85 | 62.48 |
| Specific work (kJ/kg) | 334.70 | 581.50 |
| GT to SOFC power ratio | 0.2882 | 0.3023 |

The energy management of the both systems at the same condition found that the hybrid system with recuperative heat exchanger require the external heat about 82.35 kW for supplying system; on the contrary the hybrid system with cathode exhaust gas recirculation does not need the additional fuel to use other units, leading to achieve higher system efficiency than the hybrid system with recuperative heat exchanger. The system performance of the both systems under nominal condition is presented in Table 9.5. The SOFC-GT hybrid system with recuperative heat exchanger achieves the system efficiency of 56.85% while the SOFC-GT hybrid system with cathode exhaust gas achieves the system efficiency of 63.48%. Moreover, the specific work in the SOFC-GT hybrid system with cathode exhaust gas recirculation is higher than another system due to reduce in the supplied air to system. In this section, the operating condition of both systems is specified as same. However, the suitable operation and the effect of operating parameter on efficiency of both systems may be different. Thus, the influence of operating parameters on SOFC efficiency and system performance was studied on the next section.

### 9.3.2 Effect of operating pressure

The influences of operating pressure on system performance i.e. system efficiency, SOFC electrical efficiency, GT to SOFC power ratio, heat exchanger effectiveness and cathode recirculation ratio are showed in Figure 9.2a-f, respectively. As seen in Figure 9.2a, SOFC electrical efficiency increases with increasing operating pressure ratio of compressor from 3 to 8 bar. The increment of SOFC performance as operating pressure raised is due to enhancing the cell open circuit voltage and subsiding concentration overpotentials.

Although SOFC electrical efficiency of the hybrid system with recuperative heat exchanger is minor higher than system with cathode exhaust gas recirculation and higher as increasing operating pressure, the system efficiency of hybrid system with recuperative heat exchanger is lower when operating pressure is higher, as seen in Figure 9.2b. It is noted be that the most of energy input fed to turbine transform to electricity when system is operated at high pressure, which results in diminishing the heat quantity from turbine exhaust gas used to preheat air before feeding cathode side, and consequently the requirement of heat exchanger effectiveness for the hybrid

system with recuperative heat exchanger have to increase (Figure 9.2e). In increment of heat exchanger effectiveness so as to exchange heat between the combustor outlet gas with cathode inlet air before entering cell with increase in operating pressure, turbine inlet temperature was lowered (Figure 9.2d) and it cause to reduce the turbine performance, which can observe from GT to SOFC power ratio, as shown in Figure 9.3e. This reason leads to lower system efficiency of the hybrid system with recuperative heat exchanger.

Considering the hybrid system with cathode exhaust gas recirculation, the system efficiency of SOFC-GT hybrid system with recirculation ratio is distinctively increasing with increasing pressure from 3 to 5 bar, contrasting with the hybrid system with recuperative heat exchanger, as can be seen in Figure 9.2b. From Figure 9.2d, the turbine inlet temperature in the hybrid system with cathode exhaust gas recirculation positively correlated with the operating pressure due to increase in the combustor outlet temperature and reduction of the input heat supplied for reformer unit as operating pressure of system raised. Thus, the turbine performance of the hybrid system with cathode exhaust gas recirculation is elevated (Figure 9.2c), arising from the increment of turbine inlet temperature when operating pressure increases. Nonetheless, the operating pressure of the hybrid system with cathode exhaust gas recirculation should not over 6 bar when fuel utilization of a SOFC is operated at 0.675 since the turbine inlet temperature exceed the constraint condition of inlet temperature for small turbine. Moreover, the increase in operating pressure has slightly impact on the reduction of SOFC electrical efficiency in the hybrid system with cathode exhaust gas recirculation as compared with SOFC electrical efficiency in the hybrid system with recuperative heat exchanger. To control the air inlet temperature before feeding cathode side, the recirculation ratio of cathode exhaust gas is higher with increasing operating pressure, that affect on the higher dilution of oxygen in cathode side and SOFC electrical efficiency a insignificant decrease.

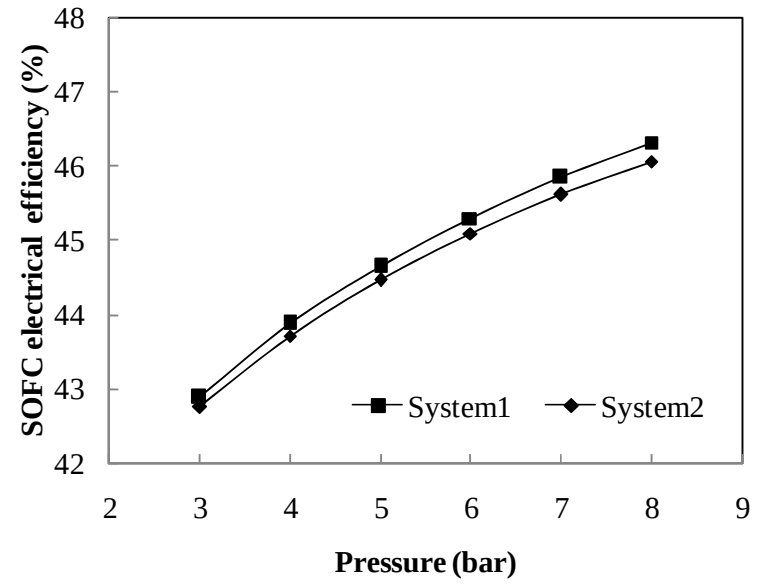
SOFC electrical efficiency (%)
48
47
46
45
44
43
42
2
3
4
5
6
7
8
9
Pressure (bar)
System1
System2

(a)

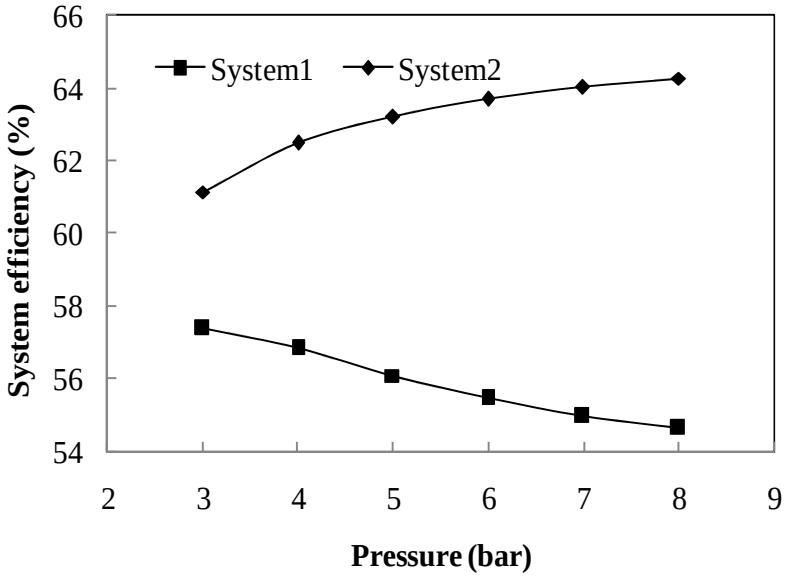
System efficiency (%)
66
64
62
60
58
56
54
2
3
4
5
6
7
8
9
Pressure (bar)
System1
System2

(b)

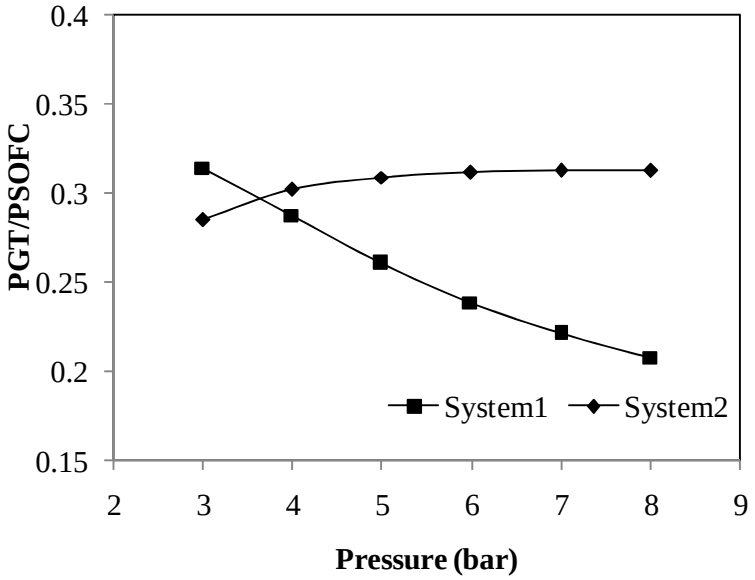
0.4
0.35
0.3
0.25
0.2
0.15
PGT/PSOFC
System1
System2
2
3
4
5
6
7
8
9
Pressure (bar)

(c)

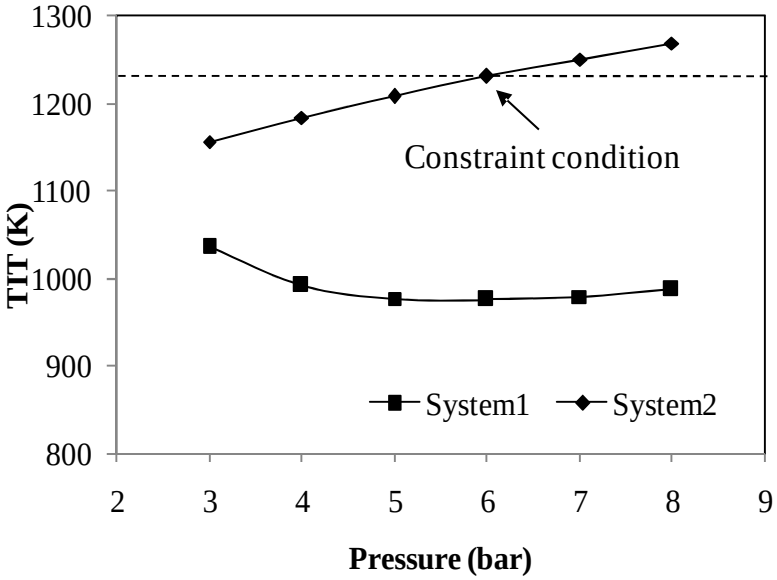
1300
1200
1100
1000
900
800
TIT (K)
Constraint condition
System1
System2
2
3
4
5
6
7
8
9
Pressure (bar)

(d)

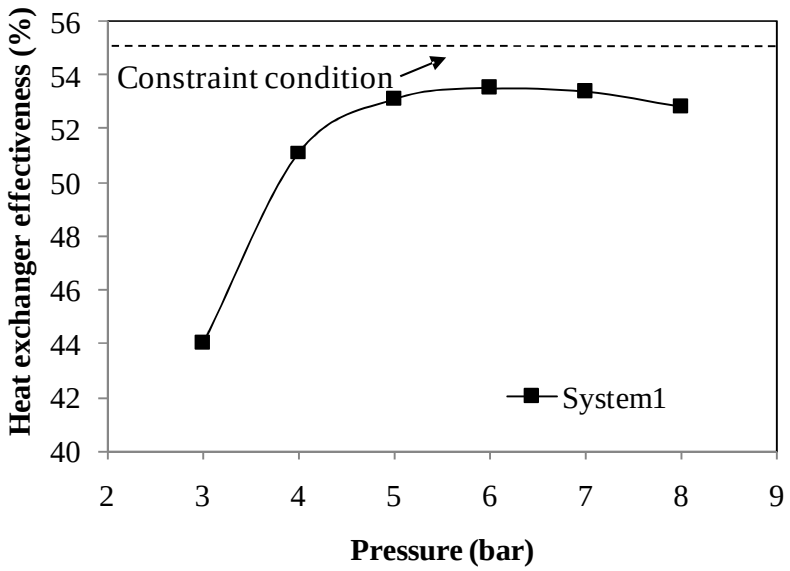


(e)

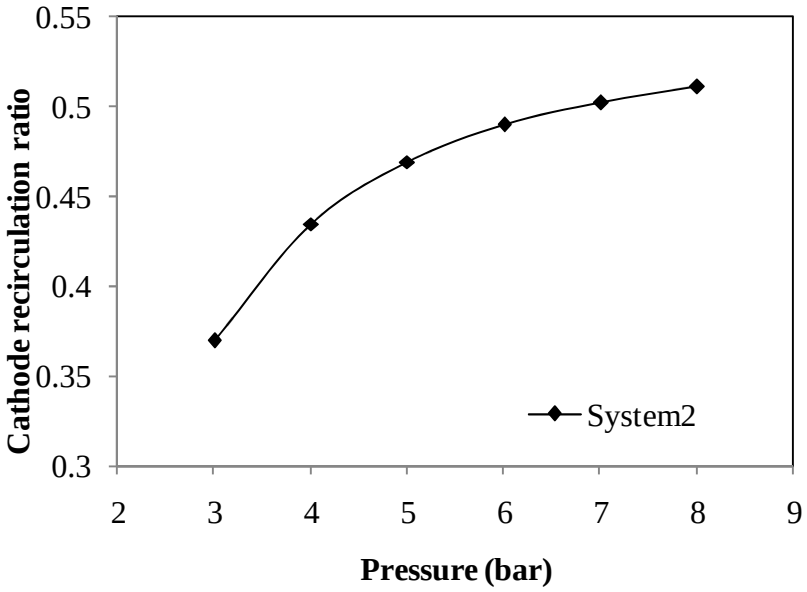


(f)

**Figure 9.2** Effect of operating pressure on (a) SOFC electrical efficiency (b) system efficiency (c) GT to SOFC power ratio (d) Turbine inlet temperature (e) Heat exchanger effectiveness and (f) cathode recirculation ratio of the SOFC hybrid system with recuperative heat exchanger (System1) and cathode exhaust gas recirculation (System2).

### 9.3.3 Effect of SOFC operating parameters

#### 9.3.3.1 Effect of fuel utilization

The influence of fuel utilization is abundantly important on heat recovery and system performance of SOFC-GT hybrid system, as been presented in Figure 9.3. The SOFC electrical efficiency in term of fuel utilization is shown Figure 9.3a. It can be found that the elevated fuel utilization improves the SOFC electrical efficiency of both systems. It can be explained that the amount of hydrogen converted to produce electricity in cell by electrochemical reaction increases when the fuel utilization of cell is higher.

In consideration of the effect of fuel utilization on GT performance and heat recovery in system, the residue fuel used in combustor is lower when SOFC operates at higher fuel utilization and then the energy used to turbine reduce. Figure 9.3c and 9.3d present that the turbine inlet temperature and GT to SOFC power were lowered as fuel utilization increased. The increase in operation of fuel utilization has more impact on the decrement of turbine performance in the hybrid system with recuperative heat exchanger than that in that hybrid system with cathode exhaust gas recirculation, and thus it also affect on decrease in system efficiency of the hybrid system with recuperative heat exchanger even though SOFC electrical efficiency enhance with increase in fuel utilization, on the other hand; the system efficiency of hybrid system with cathode exhaust gas recirculation would be raised as fuel utilization increased thanks to more impact of increase in SOFC efficiency on system efficiency than the decrement of turbine performance, as seen in Figure 9.3b.

Figure 9.3e and f show the effect of fuel utilization on the requirement of heat exchanger effectiveness for the hybrid system with recuperative heat exchanger and recirculation ratio of cathode exhaust gas for cathode exhaust gas recirculation to control inlet air temperature. The results indicate that the requirement of heat exchanger effectiveness for the hybrid system with recuperative heat exchanger and the recirculation ratio of cathode exhaust gas increased with raising the operation of fuel utilization. This reason is that the heat recovery from combustor to supply for preheating other units required energy input after SOFC unit will be drop when SOFC is operated at the high fuel utilization. Additionally, the fuel utilization of SOFC operation in the hybrid system with recuperative heat exchanger should not be over

than 0.7 as system operating pressure of 4 bar since it is extremely than the capacity of present technology for high-temperature heat exchanger.

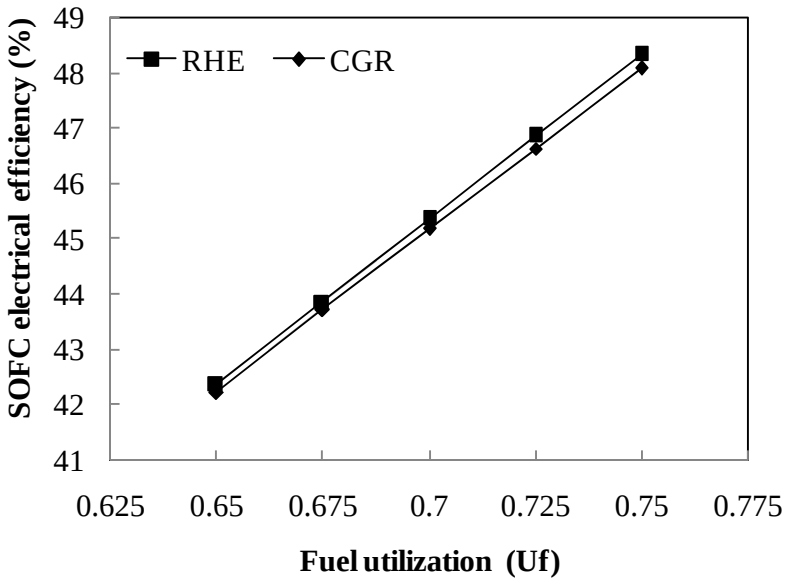


(a)

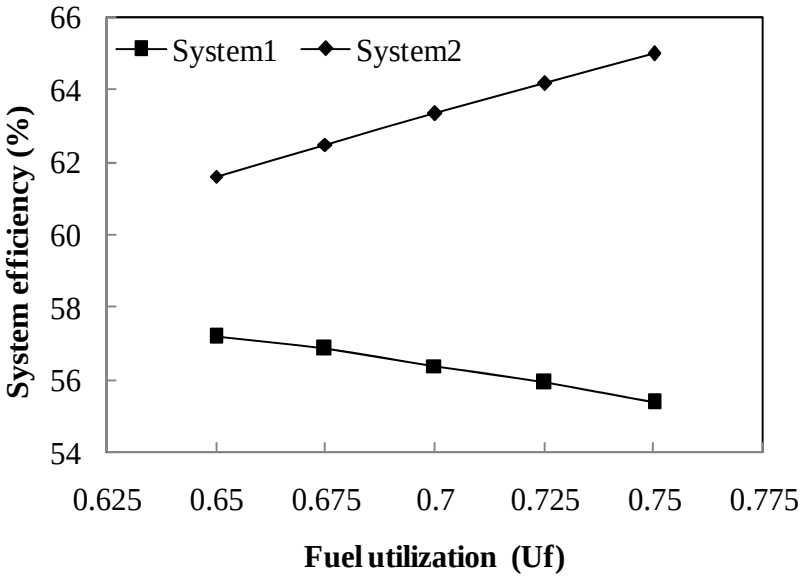


(b)

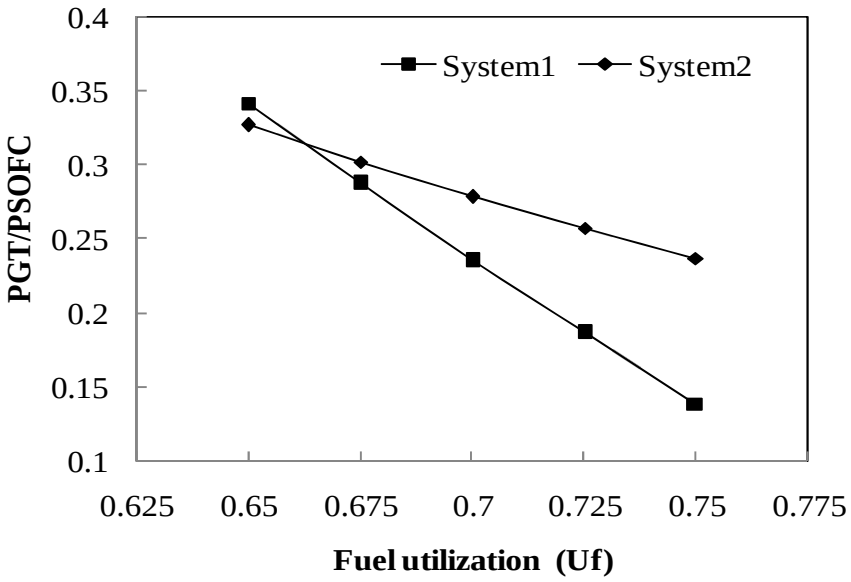
0.4
0.35
0.3
0.25
0.2
0.15
0.1
PGT/PSOFC
System1
System2
0.625
0.65
0.675
0.7
0.725
0.75
0.775
Fuel utilization (Uf)

(c)

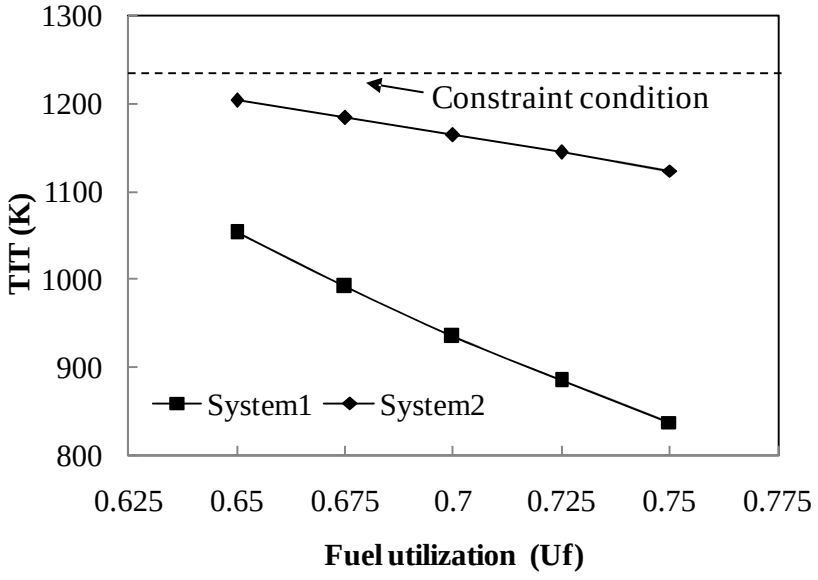
1300
1200
1100
1000
900
800
TIT (K)
Constraint condition
System1
System2
0.625
0.65
0.675
0.7
0.725
0.75
0.775
Fuel utilization (Uf)

(d)

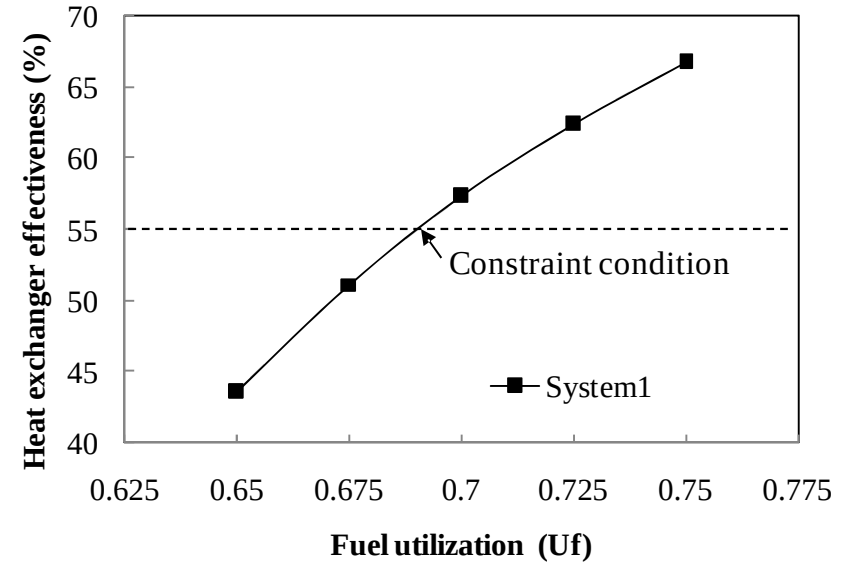


(e)

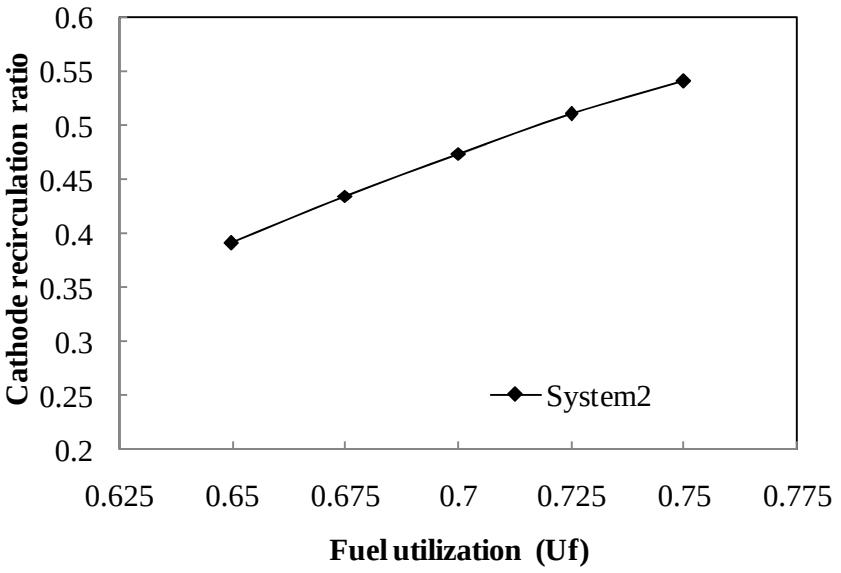


(f)

**Figure 9.3** Effect of fuel utilization on (a) SOFC electrical efficiency (b) system efficiency (c) GT to SOFC power ratio (d) Turbine inlet temperature (e) Heat exchanger effectiveness and (f) cathode recirculation ratio of the SOFC hybrid system with recuperative heat exchanger (System1) and cathode exhaust gas recirculation (System2).

#### 9.3.3.2 Effect of current density

The variant of load in SOFC-GT hybrid system is studied from the change of current density. The influence of variable current density on system performance when the fuel utilization is kept constant is illustrated in Figure 9.4. Figure 9.4a shows the effect of current density on SOFC electrical efficiency of both systems. It can be seen that the SOFC electrical efficiency are negatively correlated with raising current density. This is expected that voltage losses from the irreversible SOFC cell resistance enhance with increase in current density, as resulting in lower SOFC electrical efficiency. From Figure 9.4b, the system efficiency of both systems is lower when current density of cell operation is higher.

The released heat from the electrochemical reaction is elevated when the current density of cell operation is higher, and consequently the amount of air required to cool cell enhances in order to control cell temperature, resulting in increase of the heat duty for preheating air part. Therefore, the combustor outlet temperature is reduced with the higher current density. This affects the turbine inlet temperature decrease (Figure 9.4d). The turbine inlet temperature of the hybrid system with recuperative heat exchanger is lower than the hybrid system with cathode exhaust gas recirculation. This reason is that the requirement of heat exchanger effectiveness for the hybrid system with recuperative heat exchanger has to be increased (Figure 9.4e) while recirculation ratio of cathode exhaust air increase with increasing the current density (Figure 9.4f).

Considering the turbine performance with enhancing the current density, it slightly reduces in the hybrid system with recuperative heat exchanger. Meanwhile, turbine performance of the hybrid system with cathode exhaust recirculation increases due to the increment of air molar flow rate to turbine, as shown in Figure 9.4c.

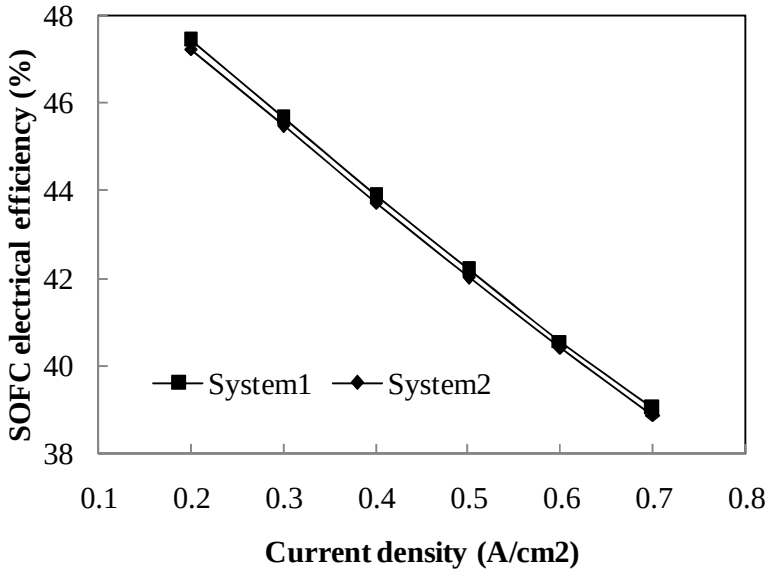
48
46
44
42
40
38
SOFC electrical efficiency (%)
System1
System2
0.1
0.2
0.3
0.4
0.5
0.6
0.7
0.8
Current density (A/cm2)

(a)

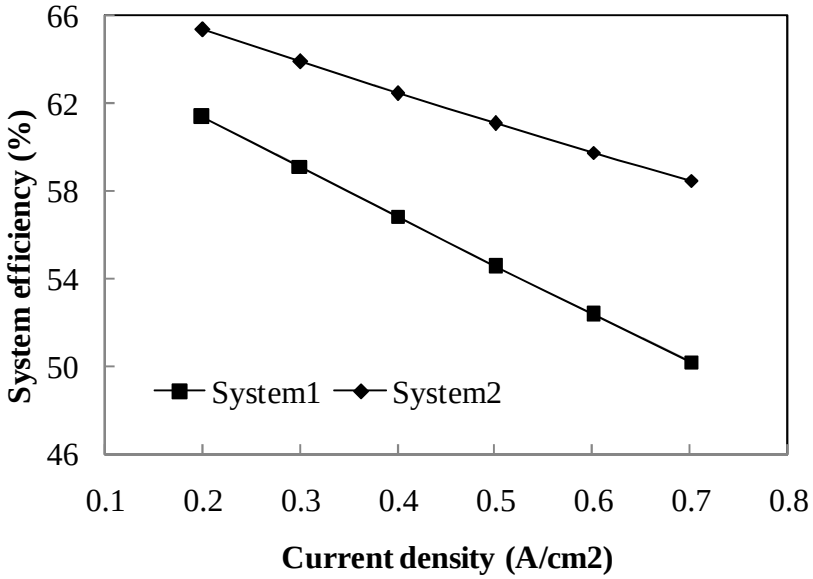
66
62
58
54
50
46
System efficiency (%)
System1
System2
0.1
0.2
0.3
0.4
0.5
0.6
0.7
0.8
Current density (A/cm2)

(b)

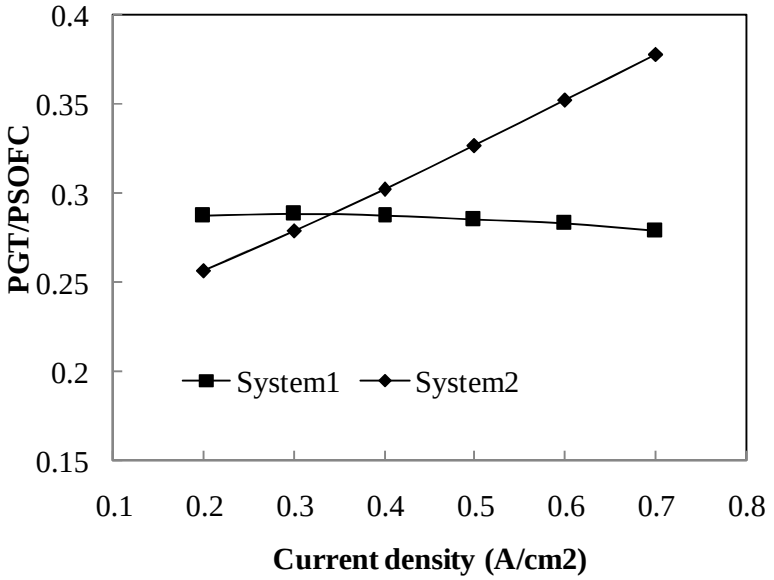
0.4
0.35
0.3
0.25
0.2
0.15
PGT/PSOFC
System1
System2
0.1
0.2
0.3
0.4
0.5
0.6
0.7
0.8
Current density (A/cm2)

(c)

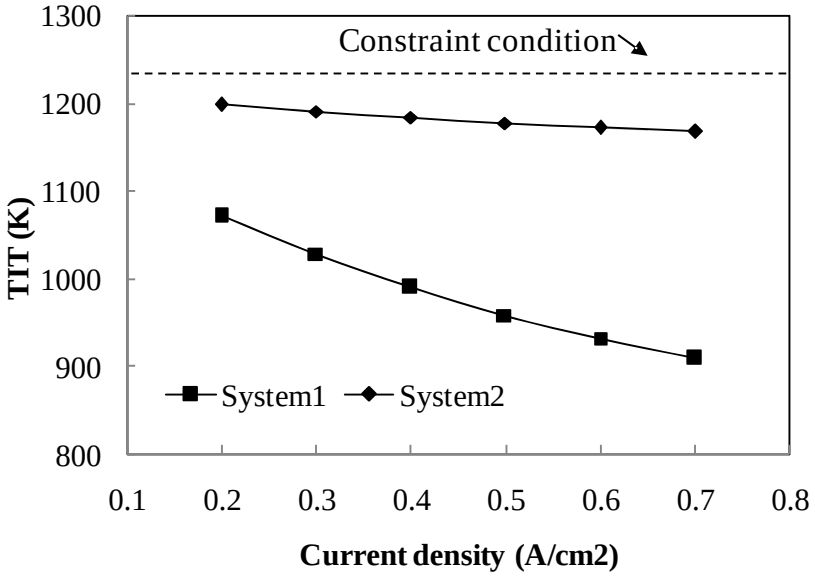
1300
1200
1100
1000
900
800
TIT (K)
Constraint condition
System1
System2
0.1
0.2
0.3
0.4
0.5
0.6
0.7
0.8
Current density (A/cm2)

(d)

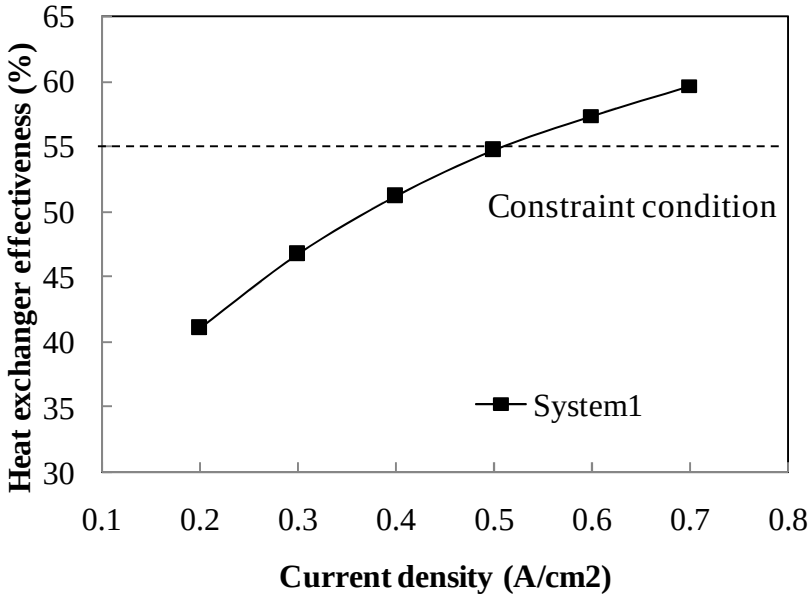


(e)

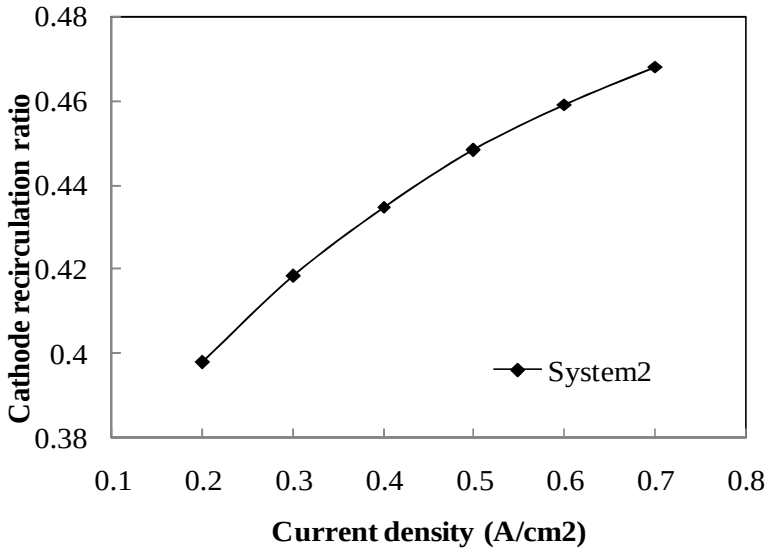


(f)

**Figure 9.4** Effect of current density on (a) SOFC electrical efficiency (b) system efficiency (c) GT to SOFC power ratio (d) Turbine inlet temperature (e) Heat exchanger effectiveness and (f) cathode recirculation ratio of the SOFC hybrid system with recuperative heat exchanger (System1) and cathode exhaust gas recirculation (System2).

### 9.3.4 Effect of turbine operating parameters

The impact of turbomachinery efficiency on system performance namely the recuperator effectiveness, turbine efficiency, and compressor efficiency are investigated in this section. The turbomachinery efficiency has a effcet on turbine performance and heat recovery in system. However, it has less impact on SOFC electrical efficiency. Therefore, the influence of turbomachinery efficiency was presented only on system efficiency and turbine performance.

#### 9.3.4.1 Effect of recuperator effectiveness

Figure 9.5 shows the recuperative heat exchanger effectiveness on the system performance of both systems. From Figure6a, the increment of recuperator effectiveness affects on higher the system efficiency of both systems, which is more the impact on the system efficiency of the hybrid system with recuperative heat exchanger than the system efficiency with cathode exhaust gas recirculation. For increase in recuperator effectiveness of 7.5%, the system efficiency in the hybrid system with recuperative heat exchanger is able to raise about 2.2% while that in the hybrid system with cathode exhaust gas could increase about 1.1%.In increase of recuperator effectiveness, the compressed air is able to more exchange heat with the turbine outlet exhaust gas. The air outlet temperature from recuperator decreases and it cause to reduce the requirement of heat exchanger effectiveness for the hybrid system with recuperative heat exchanger, leading to increase turbine inlet temperature and consequently turbine performance raise, which can observe from the GT to SOFC power ratio as shown in Figure 6b; on the other hand, the recuperator air outlet temperature increase in the hybrid system with cathode exhaust gas, resulting in reducing turbine inlet temperature because the recirculation ratio of cathode exhaust gas reduce while the requirement of fresh air increase and combustor outlet temperature is lower.

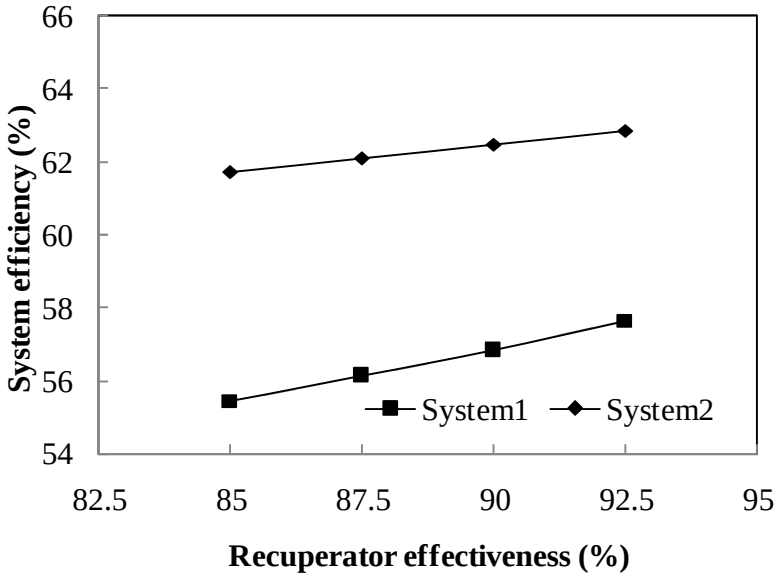


(a)

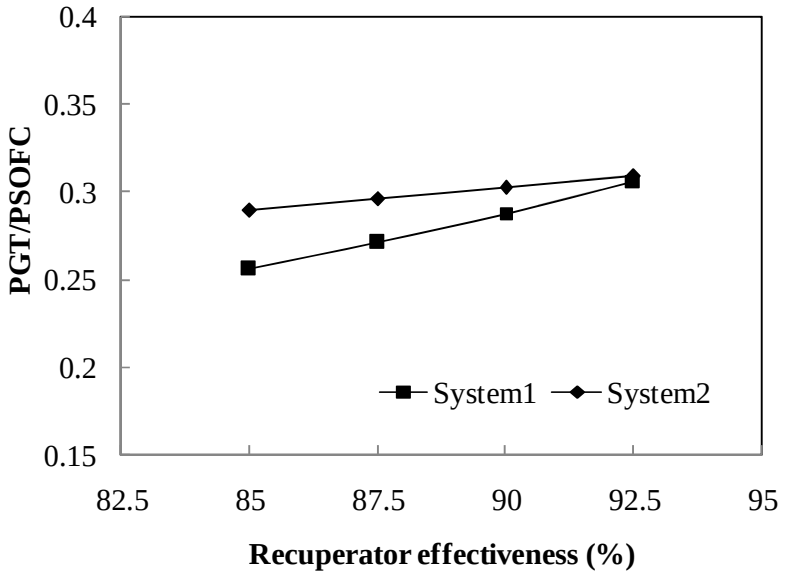


(b)

**Figure 9.5** Effect of recuperator effectiveness on (a) system efficiency (b) GT to SOFC power ratio of the SOFC hybrid system with recuperative heat exchanger (System1) and cathode exhaust gas recirculation (System 2).

### 9.3.4.2 Effect of compressor and turbine efficiency

The influence of the compressor efficiency on the system efficiency of both systems is presented in Figure 9.6a. This can seen that the increment of compressor efficiency by 10% leads to increase the system efficiency of 3.445% for the hybrid system with recuperative heat exchanger and 2.45% for the hybrid system with cathode exhaust gas recirculation. In increment of compressor efficiency, work used for compressing air reduces so the net output work of gas turbine part increase, as shown in Figure 9.6b. The increase in the compressor efficiency on the system efficiency of the hybrid system with cathode exhaust gas recirculation is lower than that of the hybrid system with recuperative heat exchanger since the requirement of air fed to the hybrid system with recuperative heat exchanger is more than the hybrid system with cathode exhaust gas recirculation about 42.4%, as a consequence of more reduced work for air compressor.

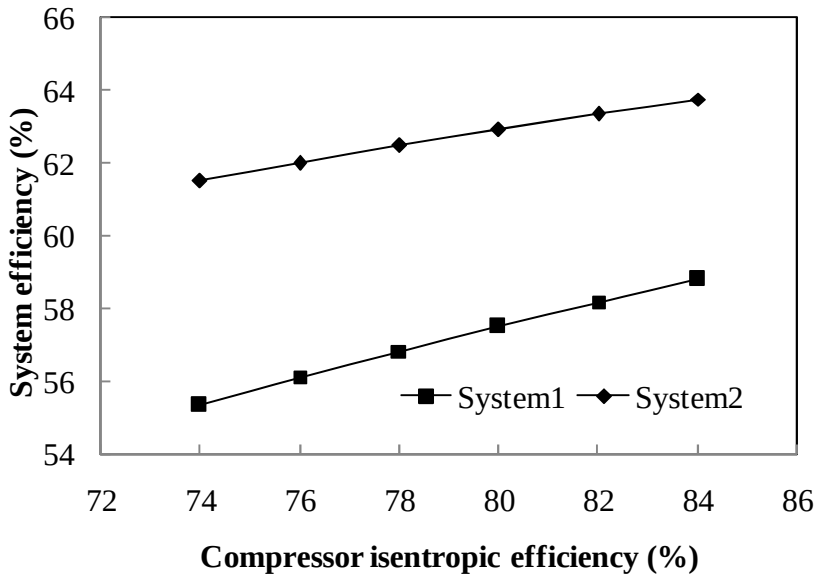


(a)

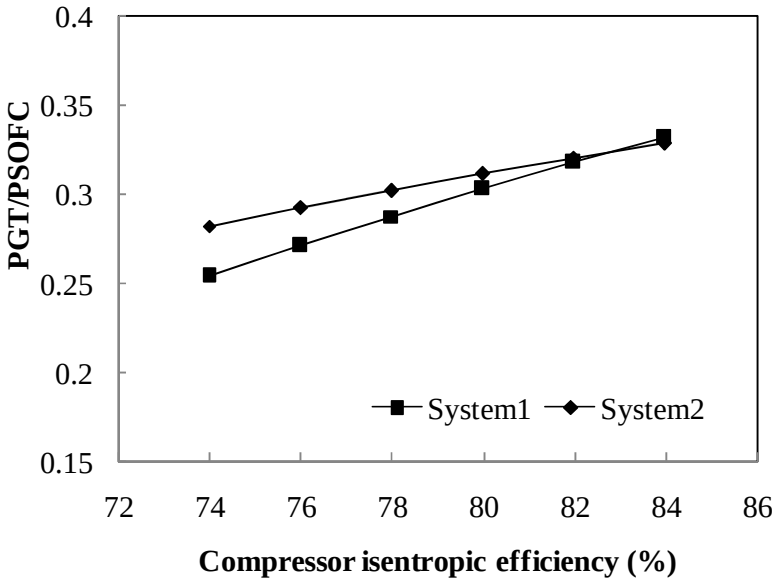


(b)

**Figure 9.6** Effect of compressor isentropic efficiency on (a) system efficiency (b) GT to SOFC power ratio of the SOFC hybrid system with recuperative heat exchanger (System1) and cathode exhaust gas recirculation (System2).

Figure 9.7a and 9.7b show the effect of turbine efficiency on the system efficiency and the GT to SOFC power ratio of both systems. The results show that the system efficiency of both systems is elevated with increasing turbine efficiency. The influence of raise in the turbine efficiency on the system efficiency of the cathode exhaust gas recirculation is more than on that of hybrid system with recuperative heat exchanger, which is greater than 1.2% by the turbine efficiency increased 10%. This reason is that there is the reduction of turbine outlet temperature in both systems with increasing turbine efficiency. For the hybrid system with recuperative heat exchanger, the lower turbine outlet temperature causes the reduction of turbine inlet temperature owing to increase in heat exchanger effectiveness; on the contrary the decrease of turbine outlet temperature in the hybrid system with cathode exhaust gas recirculation leads to increase of turbine inlet temperature because the increase in recirculation ratio of cathode exhaust gas results in less fresh air fed to system and then the combustor outlet temperature increase.

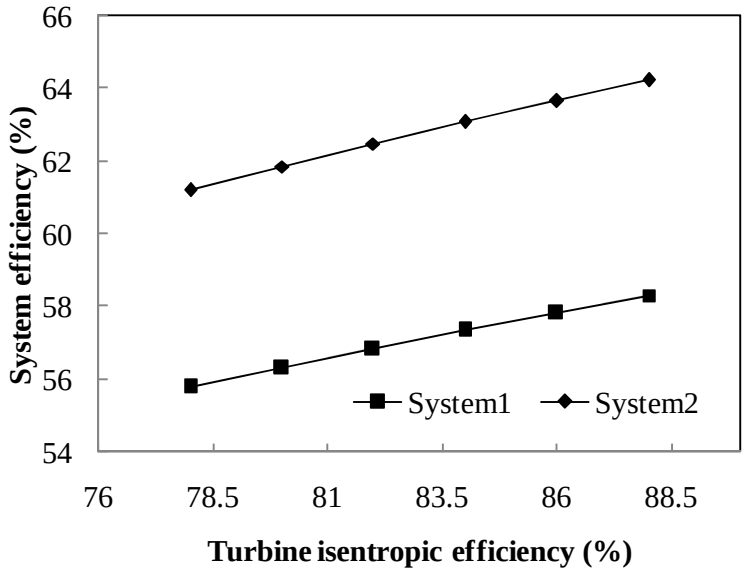


(a)

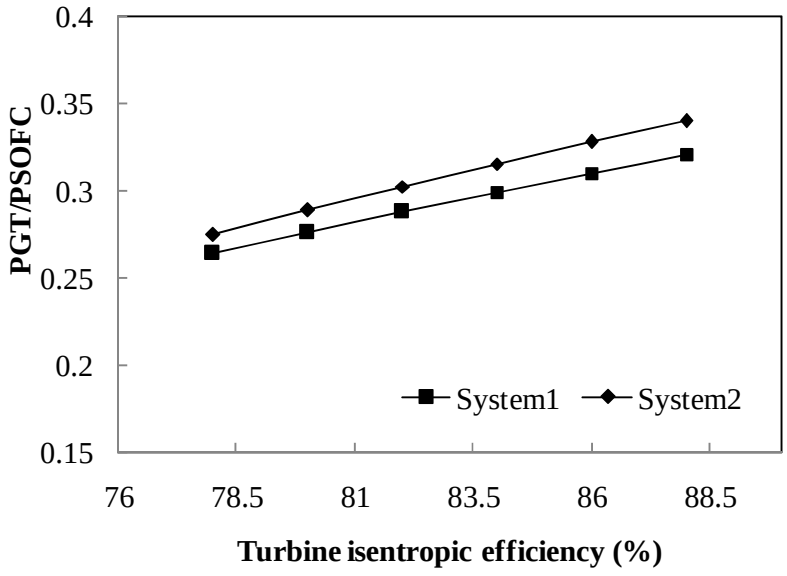


(b)

**Figure 9.7** Effect of turbine isentropic efficiency on (a) system efficiency (b) GT to SOFC power ratio of the SOFC hybrid system with recuperative heat exchanger (System1) and cathode exhaust gas recirculation (System2).

## 9.4 Conclusions

The heat recovery in the pressurized SOFC-GT hybrid system was studied in this paper, which focus on two systems namely the hybrid system with recuperative heat exchanger and the hybrid system with cathode exhaust gas recirculation. The both systems are different in schematic configuration of heat recovery for preheating air in the SOFC-GT hybrid system. In first section, the both systems were analyzed and compared based on nominal condition under the constraint of the 500 kW SOFC-GT hybrid system. The simulation results showed that downstream of the hybrid system with cathode exhaust gas recirculation could recovery heat enough to supply both fuel processor and air pre-heater fed to SOFC while the hybrid system with recuperative heat exchanger require the external heat for fuel processor, and consequently the hybrid system with cathode exhaust gas achieve the system efficiency more than another system. Further, it is also the high value of specific work due to less requirement of air flow fed to system.

The effects of variant operating pressure, fuel utilization, current density and turbomachinery efficiency on system performance have been investigated. It was found that the increment of operating pressure and fuel utilization affect on higher the SOFC electrical efficiency of both system. However, the effects of these parameters on the system performance of both systems are opposed. The system efficiency of the hybrid system with cathode exhaust gas recirculation is raised whereas that of the hybrid system with recuperative heat exchanger is subsided when operating pressure and fuel utilization increase. Main point of reduction of system efficiency in the hybrid system with recuperative heat exchanger is that increase in theses parameters cause to higher air flow to system for controlling cell temperature and higher the requirement of heat exchanger effectiveness and consequently turbine inlet temperature reduce. For the influence of current density, high current density results in low SOFC electrical efficiency and the system efficiency of in both systems but it is more impact on decrease in system efficiency of the hybrid system with recuperative heat exchanger. Moreover, the higher level of recuperator effectiveness and compressor efficiency has enormous on the higher system efficiency of the hybrid system with recuperative heat exchanger whereas the turbine efficiency make strong

effect on the increment of system efficiency in the hybrid system with cathode exhaust gas recirculation.

# CHAPTER X

# CONCLUSIONS AND RECOMMENDATION

## 10.1 Conclusions

The aims of this research are to analyze the performance and design configuration of solid oxide fuel cell system fed with ethanol in order to improve both thermal and electrical efficiency of system. The SOFC system consists of three main parts: (1) an external reformer, occurring ethanol steam reforming, (2) the SOFC stack, producing both electrical power and the useful gas, and (3) the afterburner, burning the anode and cathode exhaust gases to produce additional heat and power. In evaluation of SOFC performance, the model simulation was employed by simulation and validation with the results with experiment data in literatures. In this study, the main issues were divided into five major sections; i.e., the investigation of the suitable ethanol for SOFC system with comparing other renewable, the improvement of ethanol steam reforming with principal of adsorption and membrane technologies, the integration of solid oxide fuel cell and ethanol steam reformer with/ without the recycling anode exhaust gas, the analysis of the pressurized SOFC-GT hybrid system with/ without the recycling cathode exhaust gas and the investigation of two configurations that are different air preheating by considering heat recovery in the pressurized SOFC-GT hybrid system. Each issue is summarized as in following subsections.

### **10.1.1** SOFC system fueled by ethanol and other renewable fuels

A suitable use of ethanol for SOFC system was studied in this section with comparing with other alternative renewable fuel; i.e., glycerol and biogas. In consideration of hydrogen production in steam reforming process with supplying these fuels, the effects of temperature, steam to carbon and carbon formation were investigated. The results show that ethanol and glycerol provide higher hydrogen yield, compared to biogas and glycerol steam reforming reaction is at least the

possibility of carbon formation. The optimal condition of steam reforming process for these fuels are evaluated operating temperature about 973-1073 K and steam-to-carbon ratio above 1.5 to prevent occurrence of carbon formation. For consideration of steam reformer process integrated with SOFC system, the system supplying by glycerol requires the highest energy used in system because of its high boiling point. In system supplying by biogas showed that the both electrical and thermal efficiency is lowest. The use of ethanol seems to be a promising fuel for the SOFC system owing to achieve the highest electrical and thermal efficiencies. Additionally, the emission of carbon dioxide is less released.

### 10.1.2 Ethanol steam reforming with adsorption and membrane separations

The thermodynamic analysis of ethanol steam reforming with adsorption and membrane technologies was investigated in this section. A comparison among a conventional reformer, membrane reactor, adsorptive reactor and adsorption-membrane hybrid system is performed to determine the suitable process of ethanol steam reforming. The adsorption-membrane hybrid system in which carbon dioxide adsorbent is used to remove undesired carbon dioxide and membrane is applied for hydrogen separation. The results showed that the conventional reformer of the ethanol steam reforming is favored at high steam to ethanol ratio and temperature when it is operated at atmospheric pressure. For synthesis gas production of ethanol steam reforming with adsorption and/or membrane technologies, it was found that hydrogen removal from system with principal of membrane separation has more impact on the reactor performance than carbon dioxide removal with principal of adsorption. Nonetheless, the boundary of carbon formation is likely to decrease when carbon dioxide adsorption is considered. The use of the adsorption-membrane hybrid system in ethanol steam reforming process does not only provide the highest hydrogen yield but also obtain pure hydrogen product.

### 10.1.3 SOFC system with partial anode exhaust gas recirculation

In this section, the combination of operation between ethanol steam reformer and SOFC was studied. The combined system with recycling anode exhaust gas to ethanol steam reformer was proposed to improve the combined system efficiency. In

comparison of two schematics of SOFC system with non-recycling and recycling the SOFC anode exhaust gas, an equilibrium model of ethanol steam reforming and an electrochemical model of SOFC employed to investigate the operating condition. The simulation results indicated that the SOFC system with recycling anode exhaust gas is higher electrical and thermal efficiencies than that with non-recycling SOFC system owing to reusing the residue fuel to SOFC system and reducing the energy requirements for the ethanol processors.

Before the performance of SOFC system with recycling anode exhaust gas was analyzed, the effect of the operating conditions of the reformer with using SOFC anode exhaust gas as reagent (i.e., reformer temperature and steam to ethanol ratio) on the boundary of carbon formation was investigated at different recirculation ratio and fuel utilization. The results showed that the tendency of carbon formation in ethanol reformer, in which the recycled anode exhaust gas is used as reagent, decreases with increasing recirculation ratio and fuel utilization. This would result in decrease in the required reformer temperature as well as increase in the steam-to-carbon ratio at the inlet of reformer. Further, the influences of the operating conditions of the SOFC on SOFC performance were studied. It was found that the increases of fuel utilization and recirculation ratio can improve the current density of SOFC. Nevertheless, the increment of recirculation ratio is too extravagant; it has an adverse impact on electrical efficiency of system. The electrical and thermal efficiencies depend on different range of fuel utilization. At low fuel utilization, the electrical efficiency increases with increasing recirculation ratio while the thermal efficiency decreases. On the other hand, at high fuel utilization, the electrical efficiency is reduced with increasing recirculation ratio whereas thermal efficiency shows an opposite trend. It is noted that the electrical efficiency relates to current density and cell voltage. The increase of recirculation ratio has effect on increasing the cell current density as well as decreasing cell voltage. Therefore, the value of recirculation ratio has to be carefully selected from a wider range of fuel utilization. Additionally, the effects of reformer and SOFC temperatures on electrical efficiency also were examined. The results showed that the electrical efficiency can be enhanced with increasing reformer and SOFC temperatures.

### 10.1.4 Pressurized SOFC-GT hybrid system with cathode recycling

A pressurized solid oxide fuel cell-gas turbine hybrid system (SOFC-GT system) fuelled by ethanol was analyzed in this section. Further, the recirculation of a cathode exhaust gas to recover heat for the air heater in the pressurized SOFC-GT system was proposed to reduce the external heat required for the system. Therefore, this section aims to analyze the pressurized SOFC-GT hybrid system fed by ethanol with non-recycling and recycling of cathode exhaust gas. The important operating parameters on the system performance of SOFC-GT system in terms of the electrical efficiency and the heat management were firstly investigated. The results indicate that an increase in the operating pressure dramatically improves the system electrical efficiency. The suitable pressure is in a range of 4-6 bar, achieving the highest system electrical efficiency and the lowest recuperation energy from the waste heat of the GT exhaust gas. In addition, it is found that the waste heat obtained from the GT is higher than the heat required for the system, leading to a possibility of the SOFC-GT system to be operated at a self-sustainable condition. Under a high pressure operation, the SOFC-GT system requires a high recirculation of the cathode exhaust gas to maintain the system without supplying the external heat; however, the increased recirculation ratio of the cathode exhaust gas reduces the system electrical efficiency.

### 10.1.5 Heat recovery of a pressurized SOFC-GT hybrid system

The design and heat recovery of a SOFC-GT system under the constraint of the 500 kW are mainly focused in this section. Considering design of SOFC-GT hybrid system for 500 kW power, a crucial constraint for small turbine is that inlet GT temperature should not high over a limited temperature of 1223 K due to uncooled turbine blade. Two pressurized SOFC-GT systems with recuperative heat exchanger and cathode exhaust gas recirculation under isothermal condition are considered, which are different in heat recovery methods for air preheating. The simulation results showed that the downstream of SOFC-GT hybrid system with recuperative heat exchanger require the external heat for fuel processor and air pre-heater unit. In contrast, the downstream of SOFC-GT hybrid system with cathode exhaust gas recirculation can supply enough to requiring heat unit in system due to less amount of air used to maintain the SOFC stack temperature; therefore, this system achieves

higher the system efficiency and specific work. Moreover, important operating parameters (e.g., operating pressure, fuel utilization, current density and turbomachinery efficiency) in designing the SOFC-GT hybrid system for 500 kW power generations were investigated. In operation of the SOFC-GT hybrid system at higher operating pressure and fuel utilization, SOFC performance improves the in terms of electrical efficiencies. The effects of these parameters on both system efficiencies are contrast. System efficiencies of the SOFC-GT hybrid system with recuperative heat exchanger declines whereas that of the SOFC-GT hybrid system with cathode exhaust gas recirculation enhances with raising the operating pressure and fuel utilization. For the influence of current density, the increase in current density has more adverse effect on the system efficiency with hybrid system with recuperative heat exchanger than that of the hybrid system with cathode exhaust gas recirculation. Considering the turbomachinery efficiency, the hybrid system with recuperative heat exchanger require highly amount of supplied air to feed to system; thus, higher level of recuperator effectiveness and compressor efficiency has enormous on the higher system efficiency with recuperative heat exchanger. Nevertheless, the turbine efficiency makes strong effect on the increment of system efficiency in the hybrid system with cathode exhaust gas recirculation.

## 10.2 Recommendations

(1) Effect of operational parameters such as hydrogen flux, the rate of carbon dioxide adsorption, on hydrogen and carbon dioxide separations should be considered.

(2) For a SOFC-GT hybrid system, there are different configurations of system integration for air preheating. The different operating temperature of each component relates to energy loss within each unit in the system. To clarify on this point, an exergy analysis should be performed.

# REFERNCES


Achenbach, E., Riensche, E., Methane/steam reforming kinetics for solid oxide fuel cells. Journal of Power Sources 52 (1994): 283-288.

Agnew, G.D., Bernardi, D., Collins, R.D., Cunningham, R.H., An internal reformer for a pressurised SOFC system. Journal of Power Sources 157 (2006): 832–836.

Aguiar, P., Adjiman, C.S., and Brandon, N.P., Anode-supported intermediate-temperature direct internal reforming solid oxide fuel cell. I: Model-based steady-state performance. Journal of Power Sources 138 (2004): 120-136.

Ahmad, H.S., Soroush, M., Dynamics and control of a tubular solid-oxide fuel cell. Industrial & Engineering Chemistry 48 (2009): 6112– 25.

Akande, A., Aboudheir, A., Idem, R., Dalai, A., Kinetic modeling of hydrogen production by the catalytic reforming of crude ethanol over a co-precipitated Ni-$Al_2O_3$ catalyst in a packed bed tubular reactor. International Journal of Hydrogen Energy 31 (2006): 1707-1715.

Akkaya, A.V., Sahin, B., Erdern, H.H., An analysis of SOFC/GT CHP system based on exergetic performance criteria. International journal of hydrogen energy 33 (2008): 2566-2577.

Akkaya, A.V., Sahin, B., Erdem, H.H., Thermodynamic model for exergetic performance of a tubular SOFC module, Renewable Energy 34 (2009): 1863-1870.

Aloui, T., Halouani, K., Analytical modeling of polarizations in a solid oxide fuel cell using biomass syngas product as fuel. Applied Thermal Engineering 27 (2007): 731–737.

Andres, M.B., Boyd, T., Grace, J.R., Lim, C.J., Gulamhusein, A., Wan, B., Kurokawa, H., Shirasaki, Y., In-situ $CO_2$ capture in a pilot-scale fluidized-bed membrane reformer for ultra-pure hydrogen production. International Journal of Hydrogen Energy 36 (2011): 4038-4055.

Angrist, S.W., Direct Energy Conversion, Allyn and Bacon, New York, U.S.A, 1997.

Arpornwichanop, A., Chalermpanchai, N., Patcharavorachot, Y., Assabumrungrat, S., Tade, M., Performance of an anode-supported solid oxide fuel cell with direct-

internal reforming of ethanol. International Journal of Hydrogen Energy 34 (2009): 7780-7788.

Arteaga, L.E., Peralta, L.M., Kafarov, V., Casas, Y., Gonzales, E., Bioethanol steam reforming for ecological syngas and electricity production using a fuel cell SOFC system. Chemical Engineering Journal 136 (2008): 256–266.

Arteaga-Perez, L.E., Peralta, L.M., Kafarov, V., Casas, Y. and Gonzales, E., Bioethanol steam reforming for ecological syngas and electricity production using a fuel cell SOFC system. Chemical Engineering Journal 136 (2008): 256-266.

Arteaga-Perez, L.E., Casas, Y., Peralta, L.M., Kafarov, V., Dewulf, J., Giunta, P., An auto-sustainable solid oxide fuel cell system fueled by bio-ethanol Process simulation and heat exchanger network synthesis. Chemical Engineering Journal 150 (2009): 242–251.

Aparicio, P.F., Benito, M., Kouachi, K., Menad, S., Catalysis in membrane reformers: a high-performance catalytic system for hydrogen production from methane. Applied Catalysis 231 (2005): 331–343.

Barelli, L., Bidini, G., Gallorini, F., Servili, S., Hydrogen production through sorption-enhanced steam methane reforming and membrane technology: A review. Energy 33 (2008): 554–570.

Belyaev, V.D., Politova, T.I., Marina, O.A., Sobyanin, V.A., Internal steam reforming of methane over Ni-based electrode in solid oxide fuel cells. Applied Catalysis 133 (1995):47-57.

Bessette, N.F., Modeling and simulation for solid oxide fuel cell power systems, Ph.D. Thesis, Georgia Institute of Technology, 1994.

Biswas, P., Kunzru, D., Steam reforming of ethanol for production of hydrogen over $Ni/CeO_2–ZrO_2$ catalyst: Effect of support and metal loading. International Journal of Hydrogen Energy 32 (2007): 969 – 980.

Blum, L., Steinberger-Wilckens, R., Meulenberg, W.A., Nabielek, H., SOFC worldwide-technology development stutus and early application. Full Cell Technologies: State and Perspectives 202 (2005): 107-122.

Bove, R., Ubertini, S., Modeling solid oxide fuel cells: Methods, Procedures and Techniques, Springer, Cleveland, USA, 2008.

Bove, R., Ubertini, S., Modeling solid oxide fuel cell operation: Approaches, techniques and results. Journal of Power Sources 159 (2006): 543–559.

Braun, R. J., Klein, S.A. Reindl, D.T., Evaluation of system configurations for solid oxide fuel cell-based micro-combined heat and power generators in residential applications. Journal of Power Sources 158 (2006): 1290-1305.

Brouwer, J., On the role of fuel cells and hydrogen in a more sustainable and renewable energy future. Current Applied Physics 10 (2010): S9–S17.

Cai, W., Wang, F., Veen, A.V., Descorme, C., Schuurman, Y., Shen, W., Mirodatos, C., Hydrogen production from ethanol steam reforming in a micro-channel reactor. International Journal of Hydrogen Energy 35 (2010): 1152-1159.

Cali, M., Santarelli, M.G.L., Leone, P., Design of experiments for fitting regression models on the tubular SOFC CHP100kWe: Screening test, response surface analysis and optimization. International Journal of Hydrogen Energy 32 (2007): 343 – 358.

Cali, M., Santarelli, M.G.L., Leone, P., Computer experimental analysis of the CHP performance of a 100kWe SOFC Field Unit by a factorial design. Journal of Power Sources 156 (2006): 400–413.

Calise, F., Dentice d'Accadia, M., Palombo, A., Vanoli, L., Simulation and exergy analysis of a hybrid Solid Oxide Fuel Cell (SOFC)–Gas Turbine System. Energy 31 (2006): 3278–3299.

Calise, F., Palombo, A., Vanoli, L., Design and partial load exergy analysis of hybrid SOFC–GT power plant. Journal of Power Sources 158 (2006): 225–244.

Cavallaro, S., Ethanol Steam Reforming on Rh/Al2O3 Catalysts. Energy & Fuels 14 (2000): 1195-1199.

Cavallaro, S., Chiodo, V., Freni, S., Mondello, N., Frusteri, F., Performance of $Rh/Al_2O_3$ catalyst in the steam reforming of ethanol: $H_2$ production for MCFC. Applied Catalysis A: General 249 (2003): 119–128.

Chan, S.H., Ho, H.K., Tian, Y., Multi-level modeling of SOFC–gas turbine hybrid system. International Journal of Hydrogen Energy 28 (2003): 889-900.

Chan, S.H., Khor, K.A., Xia, Z.T., A complete polarization model of a solid oxide fuel cell and its sensitivity to the change of cell component thickness. Journal of Power Sources 93 (2001): 130-140.

Cheddie, D.F., Integration of A Solid Oxide Fuel Cell into A 10 MW Gas Turbine Power Plant. Energies 3 (2010): 754-769.

Chen, H., Zhang, T., Dou, B., Dupont, V., Williams, P., Ghadiri, M., Ding, Y., Thermodynamic analyses of adsorption-enhanced steam reforming of glycerol for hydrogen production. International Journal of Hydrogen Energy 34 (2009): 7208-7222.

Chen, Y., Wang, Y., Xu, H., Xiong, G., Efficient production of hydrogen from natural gas steam reforming in palladium membrane reactor. Applied Catalysis B: Environmental 80 (2008): 283-294.

Chen, Z., Po, F., Grace, J.R., Lim, C.J., Elnashaie, S., Mahecha-Botero, A., Rakib, M., Shirasaki, Y., Yasuda, I., Sorbent-enhanced/membrane-assisted steam-methane reforming. Chemical Engineering Science 63 (2008): 170-182.

Cocco, D., Tola, V., Externally reformed Solid oxide fuel cell-micro-gas turbine (SOFC-MGT) hybrid system fueled by methanol and di-methyl-ether (DME). Energy 34 (2008): 2124-2130.

Colantoni, A., Giuseppina1, M., Buccarella, M., Cividino, S., Vello, M., Economical Analysis of SOFC System for Power Production. Computational Science and ITS Applications 6785 (2011): 270-276.

Colpan, C.O., Dincer, I., Hamdullahpur, F.,Thermodynamic modeling of direct internal reforming solid oxide fuel cells operating with syngas. International Journal of Hydrogen Energy 32 (2007): 787 – 795.

Cordiner, S., Feola, M., Mulone, V., Romanelli, F., Analysis of a SOFC energy generation system fuelled with biomass reformate. Applied Thermal Engineering 27 (2007): 738–747.

Comas, J., Laborde, M., Amadeo, N., Thermodynamic analysis of hydrogen production from ethanol using CaO as a $CO_2$ sorbent. Journal of Power Sources 138 (2004a): 61–67.

Comas, J., Marino, F., Laborde, M., Amadeo, N., Bio-ethanol steam reforming on $Ni/Al_2O_3$ catalyst. Chemical Engineering Journal 98 (2004b): 61-68.

Cormos, C.C., Starr, F., Tzimas, E., Peteves, S., Innovative concepts for hydrogen production processes based on coal gasification with CO2 capture. Hydrogen energy 33 (2008): 1286-1294.

Costamagna, P., Magistri, L., Massardo, A.F., Design and part-load performance of a hybrid system based on a solid oxide fuel cell reactor and a micro gas turbine. Journal Power Sources 96 (2001): 352-368.

Ding, Y., Alpay, E., Adsorption-enhanced steam-methane reforming. Chemical Engineering Science 55 (2000): 3929-3940.

Douvartzides, S.L., Coutelieris, F.A., Demin, A.K., Tsiakaras, P.E., Electricity from ethanol fed SOFCs: the expectations for sustainable development and technological benefits. International Journal of Hydrogen Energy 29 (2004): 375 – 379.

Douvartzides, S.L., Coutelieris, F.A., Tsiakaras, P.E., On the systematic of ethanol fed SOFC-based electricity generating system in terms of energy and exergy. Journal of Power Sources 114 (2003): 203-212.

Eguchi, K., Kojo, H., Takeguchi, T., Kikuchi, R., Sasaki, K., Fuel flexibility in power generation by solid oxide fuel cells. Solid State Ionics 152 (2002): 411 – 416.

Falco, M.D., Ethanol membrane reformer and PEMFC system for automotive application. Fuel 90 (2011): 739-747.

Farhad, S., Hamdullahpur, F., Yoo, Y., Performance evaluation of different configurations of biogas-fuelled SOFC micro-CHP systems for residential applications. Internaltional Journal of Hydrogen Energy 35 (2010): 3758-3768.

Fatsikostas, A.N., Verykios, X.E., Reaction network of steam reforming of ethanol over Ni-based catalysts. Journal of Catalysis 225 (2004): 439–452.

Ferguson, J.R., Fiard, J.M., Herbin, R., Three-dimensional numerical simulation for various geometries of solid oxide fuel cells. Journal of Power Sources 58 (1996): 109–122.

Florin, N.F., Harris, A.T., Enhanced hydrogen production from biomass with in situ carbon dioxide capture using calcium oxide sorbents. Chemical Engineering Science 63 (2008): 287-316.

Franzoni, A., Magistri, L., Traverso, A., Massardo, A.F., Thermoeconomic analysis of pressurized hybrid SOFC systems with $CO_2$ separation. Energy 33 (2008) 311–320.

Freni, S., Maggio, G., Cavallaro, S., Ethanol steam reforming in a molten carbonate fuel cell: a thermodynamic approach. Journal of Power Sources 62 (1996): 67-73.

Gallucci, F., Basile, A., Pd–Ag membrane reactor for steam reforming reactions:A comparison between different fuels. International Journal of Hydrogen Energy 33 (2008): 1671 – 1687.

Gallucci, F., Basile, A., Tosti, S., Iulianelli, A., Drioli, E., Methanol and ethanol steam reforming in membrane reactors: An experimental study. International Journal of Hydrogen Energy 32 (2007): 1201 – 1210.

Garcia, E., Laborde, M.A., Hydrogen product by the steam reforming of ethanol: Thermodynamic analysis. Hydrogen Energy 16 (1991): 307-312.

George R.A., Status of tubular SOFC field unit demonstrations. Journal of Power Sources 86 (2000): 134-139.

Goula, M.A., Kontou, S.K., Tsiakaras, P.E., Hydrogen production by ethanol steam reforming over a commercial Pd/$\gamma$-$Al_2O_3$ catalyst. Applied Catalysis B: Environmental 49 (2004): 135-144.

Granovskii, M., Dincer, I., Rosen, M.A., Performance comparison of two combined SOFC-gas turbine systems. Journal of Power Sources 165 (2007): 307-314.

Haberman, B.A., Young, J.B., Three-dimensional simulation of chemically reacting gas flows in the porous support structure of an integrated-planar solid oxide fuel cell. International of Journal Heat Mass Transfer 47 (2004): 3617-29.

Hajimolana, A.S., Azlan Hussain, M., Daud, A.W.W.M., Soroush, M., Shamiri, A., Mathematical modeling of solid oxide fuel cells: A review. Renewable and Sustainable Energy Reviews 15 (2011): 1893–1917.

Harale, A., Hwang, H.T., Liu, P.K.T., Sahimi, M., Tsotsis, T.T., Design aspects of the cyclic hybrid adsorbent-membrane reactor (HAMR) system for hydrogen production. Chemical Engineering Science 65 (2010): 427-435.

Harale, A., Hwanga, H.Y., Liu, P.K.T., Sahimia, M., Tsotsis, T.T., Experimental studies of a hybrid adsorbent-membrane reactor (HAMR) system for hydrogen production. Chemical Engineering Science 62 (2007): 4126 – 4137.

Harrison, D.P., Calcium enhanced hydrogen production with $CO_2$ capture. Energy Procedia 1 (2009): 675-681.

Haseli, Y., Dincer, I., Naterer, G.F., Thermodynamic analysis of a combined gas turbine power system with a solid oxide fuel cell through exergy. Thermochimica Acta 480 (2008): 1–9.

Haseli, Y., Dincer, I., Naterer, Thermodynamic modeling of a gas turbine cycle combined with a solid oxide fuel cell. International Journal of Hydrogen Energy 33 (2008): 5811-5822.

Haynes, C., Wepfer, W. J., 'Design for power' of a commercial grade tubular solid oxide fuel cell. Energy Conversion and Management 41 (2000): 1123-1139.

Henne, R., Solid Oxide Fuel Cells: A Challenge for Plasma Deposition Processes. Journal of Thermal Spray Technology 16 (2007): 381-403.

Hernandez, L., Kafarov, V., Use of bioethanol for sustainable electrical energy production. International Journal of Hydrogen Energy 34 (2009): 7041-7050.

Hernandez-Pacheco, E., Singh, D., Hutton, P.N., Patel, N., Mann, M.D., A macro-level model for determining the performance characteristics of solid oxide fuel cells. Journal of Power Sources 138 (2004): 174–186.

Holtappels, P., Vinke, I.C., de Haart, L.G.J., Stimming, U., Reaction of hydrogen/water mixtures on nickel-zirconia cermet electrodes II. AC polarization characteristics. Journal of Electrochemical Society 146 (1999): 2976-2982.

Hotza, D., Diniz da Costa, J.C., Fuel cells development and hydrogen production from renewable resources in Brazil. International Journal of Hydrogen Energy 33 (2008): 4915-4935.

Hu, Q., Wang, S., Wen, T.L., Analysis of processes in planar solid oxide fuel cells. Solid State Ionics 179 (2008): 1579–1587.

Iora, P., Aguiar, P., Adjiman, C.S., Brandon, N.P., Comparison of two IT DIR-SOFC models: Impact ofv ariable thermodynamic, physical, and flow properties. Steady-state and dynamic analysis. Chemical Engineering Science 60 (2005): 2963 – 2975.

Iulianelli, A., Liguori, S., Longo, T., Tosti, S., Pinacci, P., Basile, A., An experimental study on bio-ethanol steam reforming in a catalytic membrane reactor. Part II: Reaction pressure, sweep factor and WHSV effects. International Journal of Hydrogen Energy 35 (2010): 3159-3164.

Jamsak, W., Assabumrungrat, S., Douglas, P.L., Laosiripojana, N., Suwanwarangkul, R., Charojrochkul, S., Croiset, E., Performance of ethanol-fuelled solid oxide fuel cells: Proton and oxygen ion conductors. Chemical Engineering Journal 133 (2007): 187–194.

Ji, Y., Yuan, K., Chung, J.N., Chen, Y.C., Effects of transport scale on heat/mass transfer and performance optimization for solid oxide fuel cells. Journal of Power Sources 161 (2006): 380–391.

Jia, J., Li, Q., Luo, M., Wei, L., Abudul, A., Effects of gas recycle on performance of solid oxide fuel cell power systems. Energy 36 (2011): 1068-1075.

Jiang, S.P., Badwal, S.P.S., An electrode kinetics study of $H_2$ oxidation on Ni/$Y_2O_3$-$ZrO_2$ cermet electrode of the solid oxide fuel cell. Solid State Ionics 123 (1999): 209–224.

Jiang, W., Fang, R., Khan, J.A., Dougal, R.A., Parameter setting and analysis of a dynamic tubular SOFC model. Journal of Power Sources 162 (2006): 316–326.

Johnsen, K., Grace, J.R., High-temperature attrition of sorbents and a catalyst for sorption-enhanced steam methane reforming in a fluidized bed environment. Powder Technology 173 (2007): 200–202.

Kandepu, R., Imsland, L., Foss, B.A., Stiller, C., Thorud, B., Bolland, O., Modeling and control of a SOFC-GT-based autonomous power system. Energy 32 (2007): 406-417.

Kakac, S., Pramuanjaroenkij, A., Zhou, X.Y., A review of numerical modeling of solid oxide fuel cells. International Journal of Hydrogen Energy 32 (2007): 761-786.

Kanga,Y.W., Li, G., Cao, G.Y., Tu, H.Y., Li, J., Yang, J., A reduced 1D dynamic model of a planar direct internal reforming solid oxide fuel cell for system research. Journal of Power Sources 188 (2009): 170–176.

Kendall, K., Singhal, S.C., High-temperature solid oxide fuel cells: Fundamentals, design and applications, Elsevier, New York, U.S.A, 2003.

Khaleel, M.A, Lin, Z., Singh, P., Surdoval, W., Collin, D.A., Finite element analysis modeling tool for solid oxide fuel cell development: coupled electrochemistry, thermal and flow analysis in MARC. Journal of Power Sources 130 (2004): 136–48.

Kim, J., Virkar, A.V., Fung, K., Mehta, K., Singhal, S.C., Polarization effects in intermediate temperature, anode-supported solid oxide fuel cells. Journal of Electrochemical Society 146 (1999): 69–78.

Kuchonthara, P., Bhattacharya, S., Tsutsumi, A., Combinations of solid oxide fuel cell and several enhanced gas turbine cycles. Journal of Power Sources 124 (2003): 65–75.

Kuchonthara, P., Tsutsumi, A., Energy recuperation in solid oxide fuel cell (SOFC) and gas turbine (GT) combined system. Journal of Power Sources 117 (2003): 7-13.

Lai, W.H., Hsiao, C.A., Lee, C.H., Chyou, Y.P., Tsai, Y.C., Experimental simulation on the integration of solid oxide fuel cell and micro-turbine generation system. Journal of Power sources 171 (2007): 130-139.

Laosiripojana, N., Assabumrungrat, S., Catalytic steam reforming of methane, methanol, and ethanol over Ni/YSZ: The possible use of these. Journal of Power Sources 163 (2007): 943–951.

Leucht, F., Bessler, W.G., Kallo, J., Friedrich, K.A., Müller-Steinhagen, H., Fuel cell system modeling for solid oxide fuel cell/gas turbine hybrid power plants, Part I: Modeling and simulation framework. Journal of Power Sources 196 (2011): 1205–1215.

Levin, D.B., Chahine, R., Challenges for renewable hydrogen production from biomass. International Journal of Hydrogen Energy 35 (2010): 4962-4969.

Li, P.W., Suzuki, K., Numerical modeling and performance study of a tubular SOFC. Journal of the Electrochemical Society 151 (2004): 548–557.

Liese, E.A., Gemmen, R.S., Performance comparison of internal reforming against external refroming in a solid oxide fuel cell, gas turbine hybrid system. Proc. of ASME Turbo Expo, Reno, USA (2005) ASME Paper GT2005-127.

Liguras, D.K., Kondarides, D.I., Verykios, X.E., Production of hydrogen for fuel cells by steam reforming of ethanol over supported noble metal catalysts. Applied Catalysis B: Environmental 43 (2003): 345–354.

Lim, T.H., Song, R.H., Shin, D.R., Yang, D.R., Jung, J. Jung, H., Vinke, I.C., Yang, S.S. Operating characteristics of a 5 kW class anode-supported planar SOFC stack for a fuel cell/gas turbine hybrid system. International Journal of Hydrogen Energy 33 (2007): 1076-1083.

Lisbona, P., Romeo, L.M., Enhanced coal gasification heated by unmixed combustion integrated with an hybrid system of SOFC/GT. International Journal of Hydrogen Energy 33 (2008): 5755-5764.

Liu, H.C., Lee, C.H., Shiu, Y.H., Lee, R.Y., Yan, W.M., Performance simulation for an anode-supported SOFC using Star-CD code. Journal of Power Sources 167 (2007): 406–412.

Litzinger, K.P., Veyo, S.E., Shockling, L.A., Lundberg, L., Comparative evaluation of SOFC/Gas turbine hybrid system options, Proc. of ASME Turbo Expo, Reno, USA (2005) ASME paper GT2005-68909.

Mahcene, H., Moussa, H.B., Bouguettaia, H., Bechki, D., Babay, S., Meftah, M., Study of species, temperature distributions and the solid oxide fuel cells performance in a 2-D model. International Journal of Hydrogen Energy 36 (2011): 4244-4252.

Martavaltzi, C.S., Lemonidou, A.A., Hydrogen production via sorption enhanced reforming of methane: Development of a novel hybrid material-reforming catalyst and CO2 sorbent. Chemical Engineering Science 65 (2010): 4134–4140.

Monteverde, M., Cardone, P., Saarinen, J., A Review on solid oxide fuel cell models. International Journal of Hydrogen Energy 36 (2011): 7212-7228.

Motahar, S., Alemrajabi, A.A., Exergy based performance analysis of a solid oxide fuel cell and steam injected gas turbine hybrid power system. International Journal of Hydrogen Energy 34 (2009): 2396 -2407.

Motahar, S., Alemrajabi, A.A., Exergy based performance analysis of a solid oxide fuel cell and steam injected gas turbine hybrid power system. International Journal of Hydrogen Energy 34 (2009): 2396-2407.

Motloch, C.G., Thermochemical modeling and performance of a methane reforming solid oxide fuel cell, Ph.D. Thesis, Idaho State University, January 1998.

Moussa, H.B., Zitouni, B., Oulmi, K., Mahmah, B., Belhamel, M., Mandin, P., Hydrogen consumption and power density in a co-flow planar SOFC. International Journal of Hydrogen Energy 34 (2009): 5022-5031.

Musa, A., Paepe, M.D., Performance of combined internally reformed intermediate/high temperature SOFC cycle compared to internally reformed two-staged intermediate temperature SOFC cycle. International Journal of Hydrogen Energy 33 (2008): 4665-4672.

Nehter, P., A high fuel utilizing solid oxide fuel cell cycle with regard to the formation of nickel oxide and power density. Journal of Power Sources 164 (2007): 252–259.

Ni, M., Leung, D.Y.C., Leung, M.K.H., A review on reforming bio-ethanol for hydrogen production. International Journal of Hydrogen Energy 32 (2007): 3238 – 3247.

Ni, M., Leung, D.Y.C., Leung, M.K.H., Thermodynamic analysis of ammonia fed solid oxide fuel cells: Comparison between proton-conducting electrolyte and oxygen ion-conducting electrolyte, Journal of Power Sources 183 (2008): 682–686.

Ni, M., Leung, D.Y.C., Leung, M.K.L., Electrochemical modeling and parametric study of methane fed solid oxide fuel cells. Energy Conversion and Management 50 (2009): 268–278.

Nishikawa, H., Sasou, H., Kurihara, R., Nakamura, S., Kano, A., Tanaka, K., Aoki, T., Ogami, Y., High fuel utilization operation of pure hydrogen fuel cells. International Journal of Hydrogen Energy 33 (2008): 6262–6269.

Palsson, J., Selimovic, A., Sjunnesson, L., Combined solid oxide fuel cell and gas turbine systems for efficient power and heat generation. Journal of Power Sources 86 (2000) 442-448.

Papadias, D.D., Lee, H.D.L., Ferrandon, M., Ahmed**, S.,** An analytical and experimental investigation of high-pressure catalytic steam reforming of ethanol in a hydrogen selective membrane reactor. International Journal of Hydrogen Energy 35 (2010): 2004- 2017.

Park, B.G., A hybrid adsorbent-membrane reactor (HAMR) system for hydrogen production. Korean Journal of Chemical Engineering 21(4) (2004): 782-792.

Park, S. K., Kim, T.S., Comparison between pressurized design and ambient pressure design of hybrid solid oxide fuel cell–gas turbine systems. Journal of Power Sources 163 (2006):490-499.

Park, S.K., Kim, T.S., Sohn, J.L., Influence of steam injection through exhaust heat recovery on the design performance of solid oxide fuel cell - gas turbine hybrid systems. Journal of Mechanical Science and Technology 23 (2009): 550-558.

Park, S.K., Oh, K.S., Kim, T.S., Analysis of the design of a pressurized SOFC hybrid system using a fixed gas turbine design. Journal of Power Sources 170 (2007): 130-139.

Park, S.K., Kim, T.S., Sohn, J.L., Influence of steam injection through exhaust heat recovery on the design performance of solid oxide fuel cell — gas turbine hybrid systems. Journal of Mechanical Science and Technology 23 (2009): 550-558.

Patcharavorachot, Y., Arpornwichanop, A., Chuachuensuk, A., Electrochemical study of a planar solid oxide fuel cell: Role of support structures. Journal of Power Sources 177 (2008): 254–261.

Patcharavorachot, Y., Paengjuntuek, W., Assabumrungrat, S., Arpornwichanop, A., Performance evaluation of combined solid oxide fuel cells with different electrolytes. International Journal of Hydrogen Energy 35 (2010): 4301-4310.

Peter, R., Dahl, R., Kluttgen, U., Plam, C., Stolten, D., Internal reforming of methane in Solid oxide fuel cell systems. Journal of Power Sources 106 (2002): 238-244.

Petruzzi, L., Cocchi, S., Fineschi, F., A global thermo-electrochemical model for SOFC systems design and engineering. Journal of Power Sources 118 (2003): 96–107.

Piroonlerkgul, P., Assabumrungrat, S., Laosiripojana, N., Adesina, A.A., Selection of appropriate fuel processor for biogas-fuelled SOFC system. Chemical Engineering Journal 140 (2008): 341–351.

Poullikkas, A., An overview of current and future sustainable gas turbine technologies. Renewable and Sustainable Energy Reviews 9 (2005): 409–443.

Pramuanjaroenkij, A., Kakac, S., Zhou, X.Y., Mathematical analysis of planar solid oxide fuel cells. International Journal of Hydrogen Energy 33 (2008): 2547 – 2565.

Qi, Y., Huang, B., Chuang, K., Dynamic modeling of solid oxide fuel cell: the effect of diffusion and inherent impedance. Journal of Power Sources 150 (2005): 32–47.

Rabensteinl, G., Hacker, V., Hydrogen for fuel cells from ethanol by steam-reforming, partial-oxidation and combined auto-thermal reforming: A thermodynamic analysis. Journal of Power Sources 185 (2008): 1293–1304.

Rahimpour, M.R., Lotfinejad, M., A comparison of co-current and counter-current modes of operation for a dual-type industrial methanol reactor. Chemical Engineering and Processing 47 (2008): 1819–1830.

Rokni, M., Plant characteristics of an integrated solid oxide fuel cell cycle and a steam cycle. Energy 35 (2010): 4691-4699.

Rokni, M., Thermodynamic analysis of an integrated solid oxide fuel cell cycle with a rankine cycle. Energy Conversion and Management 51 (2010): 2724–2732.

Roy, S., Cox, T.B.G., Adriss, T. A.M., Prudent, B.B., Economics and simulation of fluidized bed membrane reforming. International Journal of Hydrogen Energy 23 (1998): 745-752.

Sammes, N.M., Bove, R., Pusz, J., Fuel Cell Technology: Reaching Towards Commercialization, Springering, London, UK, 2006.

Samuelsen, S., Fuel cell/Gas Turbine Hybrid system. Proc. of ASME Turbo Expo, Reno, USA (2005) ASME Paper 2004-GT-3350.

Sangtongkitcharoen, W., Vivanpatarakij, S., Laosiripojana, N., Performance analysis of methanol-fueled solid oxides fuel cell system incorporated with palladium membrane reactor. Chemical Engineering Journal 138 (2008): 436-441.

Santin, M., Traverso, A., Magistri, L., Massardo, A., Liquid fuel utilization in SOFC hybrid system. Applied Energy 86 (2009): 2204-2212.

Santin, M., Traverso, A., Magistri, L., Massardo, A., Thermoeconimic analysis of SOFC-GT hybrid systems fed by liquid fuels. Energy 35 (2010): 1077-1083.

Shekhawat, D., Berry, D.A., Gardner, T.H., Haynes, D.J., Spivey, J.J., Effects of fuel cell anode recycle on catalytic fuel reforming. Journal of Power Sources 168 (2007): 447-483.

Silva, A.L., Malfatti, C.F., Muller, I.L., Thermodynamic analysis of ethanol steam reforming using Gibbs energy minimization method: A detailed study of the conditions of carbon deposition. International Journal of Hydrogen Energy 34 (2009): 4321-4330.

Slinn, M., Kendall, K., Mallon, C., Andrews, J., Steam reforming of biodiesel by-product to make renewable hydrogen. Bioresource Technology 99 (2008): 5851–5858.

Song, T.W., Sohn, J.L., Kim, J.H., Kim, T.S., Ro, S.T., Suzuki, K., Performance analysis of a tubular solid oxide fuel cell/ micro gas turbine hybrid power system based on a quasi-two dimensional model. Journal of Power Sources 142 (2005): 30–42.

Song, T.W., Sohn, J.L., Kim, T.S., Ro, S.T., Performance characteristics of a MW-class SOFC/GT hybrid system based on a commercially available gas turbine. Journal of Power Sources 158 (2006): 361–367.

Suwanwarangkul, R., Croiset, E., Fowler, M.W., Douglas, P.L., Entchev, E., Douglas, M.A., Performance comparison of Fick's, dusty-gas and Stefan–Maxwell models to predict the concentration overpotential of a SOFC anode. Journal of Power Sources 122 (2003): 9–18.

Stolten, D., Hydrogen and Fuel Cells: Fundamentals, Technologies and Applications, Wiley-VCH Verlag GmbH, Germany, 2010.

Takeguchi, T., Kani, Y., Yano, T., Kikuchi, R., Eguchi, K., Tsujimoto, K., Uchida, Y., Ueno, A., Omoshiki, K., Aizawa, M., Study on steam reforming of $CH_4$ and $C_2$ hydrocarbons and carbon deposition on Ni-YSZ cermets. Journal of Power Sources 112 (2002): 588–595.

Tarun, C.B, Croiset, E., Douglas, P.L., Gupta, M., Chowdhury, M.H.M., Techno-economic study of $CO_2$ capture from natural gas based hydrogen plants. International Journal of Greenhouse Gas Control 1 (2007): 55-61.

Therdthianwong, A., Sakulkoakiet, T., Therdthianwong, S., Hydrogen Production by Catalytic Ethanol Steam Reforming. ScienceAsia 27 (2001): 193-198.

Tong, J., Matsumura, Y., Pure hydrogen production by methane steam reforming with hydrogen-permeable membrane reactor. Catalysis Today 111 (2006): 147–152.

Toonssen, R., Sollai, S., Aravind, P.V., Woudstra, N., Verkooijen, A.H.M., Alternative system designs of biomass gasi fication SOFC/GT hybrid system. International Journal of Hydrogen Energy 36 (2010): 1-12.

Tosti, S., Basile, A., Borgognoni, F., Capaldo, V., Cordiner, S., Cavec, S.D., Gallucci, F., Rizzello, C., Santucci, A., Traversa, E., Low-temperature ethanol steam reforming in a Pd–Ag membrane reactor Part 2. Pt-based and Ni-based catalysts and general comparison. Journal of Membrane Science 308 (2008): 258–263.

Tosti. S., Borgognoni. F., Santucci, A., Multi-tube Pd-Ag membrane reactor for pure hydrogen production. International Journal of Hydrogen Energy 35 (2010): 11470-11477.

Traverso, A., Magistri, L., Massardo, A.F., Turbomachinery for the air management and energy recovery in fuel cell gas turbine hybrid systems. Energy 35 (2010) 764–777.

Trimm, D.L., Coke formation and minimisation during steam reforming reactions. Catalysis Today 37 (1997): 233-238.

Tsiakaras, P., Athanasiou, C., Marnellos, G., Stoukides, M.E, Elshof, J., Bouwmeester, H.J.M., Applied Catalysis 169 (1998): 249-261.

Tsiakaras, P., Demic, A., Thermodynamic analysis of a solid oxide fuel cell system fuelled by ethanol. Journal of Power Sources 102 (2001): 210–217.

Vaidya, P.D., Rodrigue, A.E., Insight into steam reforming of ethanol to produce hydrogen for fuel cells. Chemical Engineering Journal 117 (2006): 39-49.

Vasudeva, K., Mitra, N., Umasankar, P., Dhingra, S.C., Steam reforming of ethanol for hydrogen production: Thermodynamic analysis. Hydrogen Energy 21 (1996): 13-18.

Veyo, S.E., Lundberg, W.L., Vora, S.D., Litzinger, K. P., Turbular SOFC hybrid power system status. Proc. of ASME Turbo Expo, Atlanta, USA (2003) AMSE Paper GT2003-38943.

Virkar, A.V., Chen, J., Tanner, C.W., Kim, J., The role of electrode microstructure on activation and concentration polarizations in solid oxide fuel cells. Solid State Ionics 131 (2000): 189–198.

Vivanpatarakij, S., Laosiripojan, N., Kiatkittipong, W., Arpornwichanop, A., Soottitantawat, A., Assabumrungrat, S., Simulation of solid oxide fuel cell systems integrated with sequential CaO–$CO_2$ capture unit. Chemical Engineering Journal 147 (2009): 336–341.

Wang, L., Zhang, H., Weng, S., Modeling and simulation of solid oxide fuel cell based on the volume–resistance characteristic modeling technique. Journal of Power Sources 177 (2008): 579–589.

Wang, Y., Chao, Z., Chen, D., Jakobsen, H.A., SE-SMR process performance in CFB reactors: Simulation of the $CO_2$ adsorption/desorption processes with CaO based sorbents. International Journal of Greenhouse Gas Control 5 (2010): 489-497.

Wang, Y.N., Rodrigues, A.E., Hydrogen production from steam methane reforming coupled with in situ $CO_2$ capture: Conceptual parametric study. Fuel 84 (2005): 1778-1789.

Wang, K., Hissel, D., Pera, M.C., Steiner, N., Marra, D., Sorrentino, M., Pianese, C., A Review on Solid oxide fuel cell models. International Journal of Hydrogen Energy 36 (2011): 7212-7228.

Winker, W., High-temperature solid oxide fuel cells: Fundamentals, design and applications: Chapter 3, Elsevier, New York, U.S.A, 2003.

Xi, H., Sun, J., Tsourapas, V., A control oriented low order dynamic model for planar SOFC using minimum Gibbs free energy method. Journal of Power Sources 165 (2007): 253–266.

Xue, X., Tang, J., Sammes, N., Du, Y., Dynamic modeling of single tubular SOFC combining heat/mass transfer and electrochemical reaction effects. Journal of Power Sources 142 (2005): 211–222.

Yang ,W.J., Park, S.K., Kim, T.S., Kim, J.H., Sohn, J.L., Ro, S.T., Design performance analysis of pressurized solid oxide fuel cell/gas turbine hybrid systems considering temperature constraints. Journal of Power Sources 160 (2006): 462–473.

Yi, Y., Rao, D.A., Brouwer, J., Samuelsen, G.S., Analysis and optimization of a solid oxide fuel cell and intercooled gas turbine (SOFC–ICGT) hybrid cycle. Journal of Power Sources 132 (2004): 77-85.

Yu, Z., Han, J., Cao, X., Chen, W., Zhang, B., Analysis of total energy system based on solid oxide fuel cell for combined cooling and power applications. International Journal of Hydrogen energy 35 (2009): 2703-2707.

Zhang, X., Chan, S.H., Li, G., Ho, H.K., Li, J., Feng, Z., A review of integration strategies for solid oxide fuel cells. Journal of Power Sources 195 (2010): 685–702.

Zhao, F., Virkar, A.F., Dependence of polarization in anode-supported solid oxide fuel cells on various cell parameters. Journal of Power Sources 141 (2005): 79–95

Zhe, Y., Qizhao, L., Zhu, B., Thermodynamic analysis of ITSOFC hybrid system for polygenerations. International Journal of Hydrogen Energy 35 (2009): 2824-2828.

# APPENDICES

# APPENDIX A

# SELECTED THERMODYNAMIC DATA

**Table A1** Heat capacities ($C_p$)

| Components | $Cp = a + bT + cT^2 + dT^3 + eT^4$ [J/mol.K] | | | | |
|---|---|---|---|---|---|
| | a | $b\times10^3$ | $c\times10^5$ | $d\times10^8$ | $e\times10^{12}$ |
| Ethanol | 27.091 | 110.55 | 10.957 | -15.046 | 46.601 |
| Carbon dioxide | 27.437 | 42.315 | -1.9555 | 39.968 | -29.872 |
| Carbon monoxide | 29.556 | -6.5807 | 2.0130 | -1.2227 | 2.2617 |
| Hydrogen | 25.399 | 20.178 | -3.8549 | 3.1880 | -8.7585 |
| Methane | 34.942 | -39.957 | 19.184 | -15.303 | 39.321 |
| Water | 33.933 | -8.4186 | 2.9906 | -1.7825 | 3.6934 |
| Oxygen | 29.526 | -8.8999 | 3.8083 | -3.2629 | 8.8607 |
| Nitrogen | 29.342 | -3.5395 | 1.0076 | -4.3116 | 2.5935 |

**Table A2** Heat of formation ($H_f$)

| Components | $H_f = a + bT + cT^2$ [kJ/mol] | | | $H_f{}^0$ at 298 K |
|---|---|---|---|---|
| | a | $b\times10^3$ | $c\times10^5$ | |
| Ethanol | -216.961 | -69.572 | 3.1744 | -234.81 |
| Carbon dioxide | -393.422 | 0.15913 | -0.13945 | -393.51 |
| Carbon monoxide | -112.190 | 8.1182 | -0.80425 | -110.54 |
| Hydrogen | - | - | - | - |
| Methane | -63.425 | -43.355 | 1.7220 | -74.85 |
| Water | -238.41 | -12.256 | 27.656 | -241.8 |

**Table A3** Heat of vaporization

| Components | $H_i^{Vap} = A\left(1-\frac{T}{T_C}\right)^n$ | | |
|---|---|---|---|
| | A | n | Tc |
| Ethanol | 43.122 | 0.079 | 516.25 |
| Water | 52.053 | 0.321 | 647.13 |

**Table A4** Antoine coefficient

| Components | $\ln(p_i) = a + \frac{b}{(T+c)} + d\ln(T) + eT^f$ | | | | | |
|---|---|---|---|---|---|---|
| | a | b | c | d | e | f |
| Ethanol | 8.6486 | $-7.9311\times10^{3}$ | 0 | -10.0250 | $6.3895\times10^{-12}$ | 2 |
| Water | 65.9278 | $-7.2275\times10^{3}$ | 0 | -7.1770 | $4.0313\times10^{-6}$ | 2 |

# APPENDIX B

# DETERMINING GIBBS ENERGY

# AND EQUILIBRIUM CONSTANT

**B1. Determining Gibbs energy (G) at any temperatures by equation following:**

$$G = H - TS \quad \text{(B1)}$$

$$dG = dH - d(TS) \quad \text{(B2)}$$

**Take integration to equation above:**

$$\int dG = \int dH - \int d(TS) \quad \text{(B3)}$$

$$G_T - G_{STD} = \int_{298}^{T} dH - \int_{298}^{T} d(TS) \quad \text{(B4)}$$

**Where** $$H = H(T) = a + bT + cT^2 \quad \text{(B5)}$$

$$S = S(T) = S^0 + \int_{298}^{T} C_p dT \quad \text{(B6)}$$

Where $T$ = The temperature range of 500 – 1,500 K

$S^0$= The entropy at standard state (298 K, 1 atm)

**B2. Determining the equilibrium constant (K) from thermochemical data**

The equilibrium constant (K) is defined as follows:

$$\ln K = -\frac{\Delta G_{rxn}}{RT} \tag{B7}$$

To calculate the temperature dependence of K, we wish to find

$$\frac{d \ln K}{dT} = -\frac{d\left(\frac{\Delta G_{rxn}}{RT}\right)}{dT} \tag{B8}$$

$$\frac{d \ln K}{dT} = \frac{\Delta G_{rxn}}{RT^2} - \frac{1}{RT}\frac{d\left(\Delta G_{rxn}\right)}{dT} \tag{B9}$$

# APPENDIX C

# LIST OF PUBLICATIONS

**International publications**

1. **Saebea, D**., Arpornwichanop, A., Patcharavorachot, Y. and Assabumrungrat, S. (2011). Adsorption-membrane hybrid system for ethanol steam reforming: Thermodynamic analysis. International Journal of Hydrogen Energy, 36, 14428-14434**.**
2. **Saebea, D.,** Patcharavorachot, Y. Arpornwichanop, A. (2012). Analysis of an Ethanol-Fuelled Solid Oxide Fuel Cell System Using Partial Anode Exhaust Gas Recirculation. Journal of Power Sources, 208, 120-130.

**International conferences**

1. **Saebea, D**, Patcharavorachot, Y., Assabumrungrat, S. and Arpornwichanop, A., A Thermodynamic Study on Adsorption-Membrane Hybrid System for Ethanol Steam Reforming. (CHEMECA 2010), Victoria 3600, Australia, September 26-29, 2010.
2. **Saebea, D,** Patcharavorachot, Y., Assabumrungrat, S. and Arpornwichanop, A., Design of a Solid Oxide Fuel Cell-Gas Turbine Hybrid Power System with Cathode Gas Recycling. Asia Pacific Chemical Reaction Engineering Symposium (APCRE'11)**,** Beijing, China, September 18-21, 2011 (The Excellent Poster Presentation Award).
3. **Saebea, D.,** Authayanun, S., Patcharavorachot, Y., .Paengjuntuek**,** W., Arpornwichanop, A., Performance Analysis of SOFC Systems Integrated with Steam Reforming of Different Renewable Fuels**.** International Conference on Renewable Energy and Power Quality (ICREPQ'12), Santiago de Compostela, Spain, March 28-30, 2012.

4. **Saebea, D.,** Magistri, L., Massardo, A., Arpornwichanop, Design and Heat Recovery of Pressurized SOFC/GT Hybrid Systems. Fuel cell 2012 Science & Technology Conference, Berlin, Germany, April 11-12, 2012.

**National conferences**

1. **Saebea, D**. and Arpornwichanop, A. (2010). Analysis of ethanol fuelled Solid oxide fuel cell system with partial anode off gas recycle. Commission on Higher Education Congress III: University Staff Development Consortium, Chonburi, Thailand, September 9-11, 2010.

# VITA

Miss Dang Saebea was born on April 14, 1984 in Bangkok, Thailand. She finished high school from Saipanya School, Bangkok in 2003. She received her Bachelor's Degree in Chemical Engineering, from the Department of Chemical Engineering, Srinakarinwirot University in April 2007. Afterward, she continued studying Doctoral degree of Chemical Engineering, Chulalongkorn University and received Ph.D. scholarship from the Thailand's Higher Education Commission under the program "Strategic Scholarships for Frontier Research Network for the Joint Ph.D. Program Thai Doctoral degree." During her Ph.D. study, she joined with the Thermochemical Power Group (TPG), University of Genoa, Italy, for eight months to do some parts of her research under the collaboratation with Professor Aristide F. Massardo and Assistant Professor Loredana Magistri.